



REFERENCE ONLY

UNIVERSITY OF LONDON THESIS

Degree *PhD*

Year *2005*

Name of Author *BANBOSA, F.C. d. M.*

COPYRIGHT

This is a thesis accepted for a Higher Degree of the University of London. It is an unpublished typescript and the copyright is held by the author. All persons consulting the thesis must read and abide by the Copyright Declaration below.

COPYRIGHT DECLARATION

I recognise that the copyright of the above-described thesis rests with the author and that no quotation from it or information derived from it may be published without the prior written consent of the author.

LOANS

Theses may not be lent to individuals, but the Senate House Library may lend a copy to approved libraries within the United Kingdom, for consultation solely on the premises of those libraries. Application should be made to: Inter-Library Loans, Senate House Library, Senate House, Malet Street, London WC1E 7HU.

REPRODUCTION

University of London theses may not be reproduced without explicit written permission from the Senate House Library. Enquiries should be addressed to the Theses Section of the Library. Regulations concerning reproduction vary according to the date of acceptance of the thesis and are listed below as guidelines.

- A. Before 1962. Permission granted only upon the prior written consent of the author. (The Senate House Library will provide addresses where possible).
- B. 1962 - 1974. In many cases the author has agreed to permit copying upon completion of a Copyright Declaration.
- C. 1975 - 1988. Most theses may be copied upon completion of a Copyright Declaration.
- D. 1989 onwards. Most theses may be copied.

This thesis comes within category D.



This copy has been deposited in the Library of *UCL*



This copy has been deposited in the Senate House Library, Senate House, Malet Street, London WC1E 7HU.

**REGULATION OF GASTRULATION MOVEMENTS
BY PLANAR CELL POLARITY GENES IN
ZEBRAFISH**

FILIPA CARREIRA DE AVELAR BARBOSA

In submission for the degree of Doctor of Philosophy

March 2005

UNIVERSITY COLLEGE LONDON
UNIVERSITY LONDON

UMI Number: U591648

All rights reserved

INFORMATION TO ALL USERS

The quality of this reproduction is dependent upon the quality of the copy submitted.

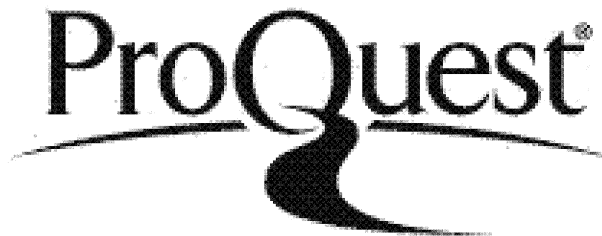
In the unlikely event that the author did not send a complete manuscript and there are missing pages, these will be noted. Also, if material had to be removed, a note will indicate the deletion.



UMI U591648

Published by ProQuest LLC 2013. Copyright in the Dissertation held by the Author.
Microform Edition © ProQuest LLC.

All rights reserved. This work is protected against
unauthorized copying under Title 17, United States Code.



ProQuest LLC
789 East Eisenhower Parkway
P.O. Box 1346
Ann Arbor, MI 48106-1346

ACKNOWLEDGEMENTS

Time as come to write what is the trickiest and surely most requested part of my thesis. Time to thank those who were by my side.

I am grateful to António Coutinho for the creation of the Programa Gulbenkian de Doutoramento em Biologia e Medicina (PGDBM) and to the Portuguese Foundation for Science and Technology (PRAXIS 2001), who have financed me throughout my PhD and chose me to be part of such honourable group of students.

I am deeply grateful to Lena and Avó Zé - my mother and grandmother - for always being there for me, in every sense of the word and for putting me before them.

I am very, very grateful to my supervisor Masazumi Tada that taught me almost everything that I know about Developmental Biology and for all the support over the years showing me there is always a better experiment to do. He also showed what a real scientist is made of, patience and determination. Thanks to Steve Wilson for making possible this project and for being a critical and knowledgeable scientist and a cool co-supervisor. Thanks as well to Jon Clarke for the all the comments and scientific advice.

During the time that I have studied and worked at UCL, in both Masa and Steve's labs, I had the good fortune to meet a lot of amazing people, some of which become my friends. I am afraid of missing people out, but thanks to Florencia, Silvia, Arantza, Richard, Marika, Jenny, Nina, Masa junior, KoKo, Emily, Jacquie, Paul, Will, Tom, Mathias, Claire, Isaac Lucas and Miguel for giving me courage when I was low, for believing in me and also for making me laugh and laughing with me at my silliness.

I also want to thank Carole and her team for taking care of the fish and keeping them in good shape. A special thanks For Diz for keeping Steve's lab sorted and going and also for being my "English mother". Another special thanks goes to Steve O'Connor for being such good DJ and a master in Macs. Thanks as well to Leonor Saúde for being with me in the

beginning and in the end of my Ph.D. Especial thanks goes to Nina for all the support in this “fight”.

My thoughts also go to all my friends in London and in Portugal, outside the lab, who transformed my life to a very pleasant time and contributed to my mental healthiness. Big thanks for all the girls and boys that were my flatmates (Sara, Silvy, Manuel, Rita, Rosarinho, Paulo, Celine and Madalena). Thanks also to Andrea and Isabel, who always knew the right thing to say. I am very grateful to Zé for all advice and help in my decisions about future, work, life and thesis. The Spanish and Greek community also helped in my sanity for having such lovely and nice parties.

I also want to thanks to all my friends far away (Duarte, Zainha, Joãozinha, Joana, Marta, Angela, Fernandinha, Alice, Leonor, Xico, Vasco e TD) and family (Aunt Janeca and Uncle Luís, cousins Maria and João and respective couples with their beautiful babies) back in Portugal for their encouragement, support and optimism.

Thanks particularly to the long-suffering Claudio for helping me with this thesis production and to be so patient with me and to support me when I needed, even in my grumpiest moments.

A special thanks to Maria Joao and Mariana, who become my “sisters in soul” in this adventure in London, they were always there in the bitter moments and in the most happy and sweet moments, even when I could not see!!!!

ABSTRACT

REGULATION OF GASTRULATION MOVEMENTS BY PLANAR CELL POLARITY GENES IN ZEBRAFISH

During vertebrate gastrulation, mesodermal and ectodermal cells undergo convergent extension (CE), a process characterised by cellular rearrangements in which polarised cells intercalate along the medio-lateral axis leading to elongation of the antero-posterior axis. This thesis aims to prove that genes which have been implicated in the establishment of planar cell polarity (PCP) in *Drosophila* are conserved in the non-canonical Wnt pathway that regulates CE in zebrafish during gastrulation. Firstly, I analyzed functions of Wnt5 and Wnt11 ligands and of Fz2 and Fz7 receptors in regulating CE movements. Here, I will show that *pipetail* (*ppt/wnt5*) mutant is required for regulating CE movements in posterior mesendoderm and ectoderm while its function in the anterior mesendoderm is redundant to *siberblick* (*slb/wnt11*). Based on gene expression analyses, loss of function and gain of function analyzes, the interaction between these Wnt ligands and Fz receptors is dependent on time, concentration and position of expression during gastrulation. Secondly, I will describe the isolation and functional characterisation of the zebrafish homologue of *Drosophila* *prickle* (*pk1*) during gastrulation. Zebrafish *pk1* functions together with Slb/Wnt11 and Ppt/Wnt5 to regulate CE movements due to abrogation of Pk1 function by morpholino that leads to defective CE movements, enhances the *slb/wnt11* and *ppt/wnt5* phenotypes and suppresses the ability of *wnt11* to rescue the *slb* phenotype. Gain-of-function of Pk1 also inhibits CE movements. Additionally, I found that Pk1 could destabilise Dsh and thereby block the ability of Fz to target Dsh to the cell membrane by down-regulating levels of Dsh protein. These results suggest that Pk1 acts in the non-canonical Wnt pathway to regulate CE, but it is unlikely to be a simply linear component of this pathway. I will describe the isolation of zebrafish *flamingo* (*fmi*) genes and characterise the expression pattern during gastrulation. I also describe functional characterisation of those genes during gastrulation. Initially, abrogation of Fmi function by morpholino leads to weakly defective CE movements enhances the *slb/wnt11* phenotype and defective epiboly phenotypes of the *offroad* (*ord*)/*fmi2* mutants. In contrast, a dominant negative approach with a mutant form of Fmi, led me to conclude that Fmi is involved in the regulation of CE movements. Together with analyses of Fmi protein, I will discuss how Fmi regulates different gastrulation movements, such as convergent extension and epiboly.

As minhas mães, Avó Zé e Lena

List of Figures:	9
CHAPTER 1.....	12
GENERAL INTRODUCTION	12
1.1.THE ZEBRAFISH (<i>Danio rerio</i>) AS A MODEL ORGANISM TO STUDY	
EARLY DEVELOPMENT	12
PART I	15
GASTRULATION MOVEMENTS	15
I.1.Gastrulation movements in the Animal Kingdom.....	15
I.1.2.Gastrulation movements in Zebrafish	17
I.1.2.1. Epiboly:.....	19
I.1.2.2. Internalization or involution:	23
I.1.2.3. Convergence and extension:	25
I.1.2.3.1.Celular mechanisms underlying convergent extension in <i>Xenopus</i>	27
I.1.2.3.2.Cellular mechanisms underlying convergent extension in zebrafish	
.....	31
PART II.....	37
Molecular Mechanisms	37
II.1.1. Wnt pathway.....	37
II.1.2. Non-canonical Wnt Pathway.....	38
II.1.2.1. Planar Cell Polarity in <i>Drosophila</i>	38
II.1.2.2. Non-Canonical Wnt Signalling in Vertebrates.....	46
II.1.2.2.1 Proposed non-canonical Wnt Pathway in Zebrafish	47
II.1.2.2.1.1 Possible downstream and upstream effectors	53
II.1.2.2.2. Mouse mutants with phenotypic defects due to defective CE.....	55
II.1.2.3. Calcium Pathway	56
II.1.2.4.Cell adhesion molecules.....	59
II.1.2.4.1.Protocadherins.....	59
II.1.2.4.2.Non classical Cadherins.....	60
II.1.2.4.3.Integrins and Fibronectin.....	62
II.1.3.Other Pathways:.....	62
II.1.3.1.PDGF/PI3K Pathway	62
II.1.3.2.JAK/STAT Pathway	64
II.1.3.3.Slit/Robo Pathway	65
1.2. THE PROJECT	65
CHAPTER 2.....	67
Material and Methods	67
2.1. Molecular Biology Techniques.....	67
2.1.1.Measurement of DNA/RNA concentration	67
2.1.2.Polymerase Chain Reaction (PCR)	67
2.1.3.Bacterial Plasmid DNA extraction.....	67
2.1.4.Basic DNA Manipulation	68
2.1.5.Ligation reactions.....	68
2.1.6.Agarose Gel Electrophoresis and DNA Extraction from Agarose.....	69
2.1.7.DNA sequencing	69
2.1.8.Extraction of Total RNA from tissues.....	69
2.1.9. Isolation of <i>fmi</i> genes.....	69
2.1.10.Screening of cDNA Libraries	70
2.1.10.1. Lambda Bacteriophage Library.....	70

2.1.10.2. Rescue of Phagemids from Bacteriophage.....	71
2.1.10.3. Micro-Arrayed cDNA Library	71
2.2. Embryological Techniques	71
2.2.1. Maintenance of zebrafish lines.....	71
2.2.2. Observation of live embryos.....	72
2.2.2.1. DIC microscopy.....	72
2.2.2.2 Confocal microscopy	72
2.2.3. RNA <i>in situ</i> hybridisation	72
2.2.3.1. Synthesis of antisense RNA probes for <i>in situ</i> hybridisation.....	72
2.2.3.2. Single whole -mount <i>in situ</i> hybridisation	73
2.2.3.3. cDNAs used for <i>in situ</i> hybridisation	74
2.2.4. RNA and morpholino antisense oligonucleotide (Mo) injection	74
2.2.4.1. <i>In vitro</i> transcription of mRNA synthesis.....	74
2.2.4.2. Morpholino Preparation	75
2.2.4.3. Injection of mRNA into early stage embryos.....	76
2.2.5. Analyses for sub-cellular protein localization	76
2.2.6. Cell transplantation.....	77
2.2.7. Production and Purification of Fmi2 antibody.....	77
2.2.8. Immunohistochemistry	78
2.2.8.1 Antibodies used	78
2.2.8.2. Whole-mount antibody staining	78
2.2.9. Polyacrylamide gel electrophoresis (Page) Western-blotting and Chemilluminuscent detection of proteins.....	79
CHAPTER 3.....	81
Possible role of Wnts and Fz receptors in regulating convergent extension (CE) movements	81
3.1.Introduction.....	81
3.2.Results	82
3.2.1.Possible interaction between <i>wnt11</i> and <i>wnt5</i>	82
3.2.2.Characterisation of receptors of the non-canonical Wnt pathway (Fz7 and Fz2)	87
3.2.3.Genetic interaction between <i>slb</i> mutants and Fz2 and Fz7 receptors.....	90
3.3.Discussion.....	94
3.3.1. Expression patterns of <i>wnt11</i> , <i>wnt5</i> , <i>fz2</i> and <i>fz7</i> and possible relations between these genes	94
3.3.2.Overexpression of Wnt ligands and Fz receptors on wild type and mutant background	95
3.3.3.Loss of function experiments to assess the specificity of the non-canonical pathway	96
3.4.Summary.....	98
CHAPTER 4.....	99
Prickle1 regulates cell movements during gastrulation in zebrafish	99
4.1.Introduction.....	99
4.2.Results	100
4.2.1. The expression patterns of zebrafish <i>prickle</i> genes.....	100
4.2.2. Interfering with Pk1 function disrupts CE during gastrulation.....	103
4.2.3. Pk1 regulates CE movements by modulating the Wnt/PCP pathway	108

4.2.4. Gain-of-function of <i>pk1</i> causes defective CE movements by modulating the Wnt/PCP pathway	112
4.2.5. <i>pk1</i> genetically interacts with <i>trilobite/strabismus</i>	115
4.3. Discussion.....	117
4.3.1. <i>pk1</i> regulates CE movements by modulating the non-canonical Wnt/PCP pathway	117
4.3.1.1. Loss of function experiments	117
4.3.1.2. Overexpression experiments	118
4.3.1.3. Sub-cellular localisation of components of this pathway	119
4.4. Summary.....	121
CHAPTER 5.....	122
Cloning and Characterisation of the expression pattern of the <i>fmi</i> genes during zebrafish gastrulation	122
5.1. Introduction.....	122
5.2. Results:	124
5.2.1. Cloning of the <i>fmi</i> genes	124
5.2.2. Expression pattern of the <i>fmi</i> genes.....	126
5.2.3. Functional analyses of <i>fmi</i> genes:.....	131
5.2.3.1. General approach with Morpholino (Mo):	131
5.2.3.1.1. Splice morpholinos	131
5.2.3.1.2. 5'- prime morpholinos.....	135
5.2.3.2. The dominant negative approach:	142
5.2.3.2.1. Genetic interactions of Fmi with <i>slb</i> mutants.....	147
5.2.3.2.2. Transplantation experiments	151
5.2.3.2.3. Localization of key regulators of the pathway using an <i>in vivo</i> imaging assay	153
5.2.3.3. Localization of Fmi protein.....	156
5.2.3.3.1. Purification and refinement of Fmi antibody	158
5.2.3.3.2. Possible localization of Fmi	158
5.3. Discussion.....	161
5.3.1. Expression patterns.....	161
5.3.2. Loss of function- Morpholino approach.....	162
5.3.3. Dominant negative approach	163
5.3.4. Possible mechanism of action of Fmi protein.....	165
5.4. Summary.....	167
Addendum	167
CHAPTER 6.....	169
General Discussion and future directions	169
6.1. Differences and similarities between the vertebrate system and the PCP in <i>Drosophila</i>	171
6.2. Fundamental characteristics of the function of the PCP proteins.....	173
6.3. Remaining and arising questions	174
Bibliography.....	176

List of Figures:

Figure 1.1	Stages of zebrafish development.....	13
Figure 1.2	Lateral view of a zebrafish embryo at 6 hours post fertilization showing the three kinds of gastrulation movements.....	18
Figure 1.3	Cell rearrangements during zebrafish gastrulation.....	20
Figure 1.4	Model for convergent extension in <i>Xenopus</i> compared with the model for convergent extension in Teleosts.....	29
Figure 1.5	Cell trajectories in the ventral, lateral and dorsal C&E domains.....	32
Figure 1.6	<i>Drosophila</i> wing and eye.....	40
Figure 1.7	Polarized subcellular distribution of PCP genes in wing and eye cells.....	43
Figure 1.8	Updated model for the Wnt non Canonical pathway regulating CE during gastrulation in vertebrates.....	52
Figure 1.9	The Wnt/Ca ²⁺ pathway.....	58
Figure 1.10	Structures of Flamingo and Prickle proteins.....	61
Figure 3.1	Expression pattern of <i>wnt5</i> during zebrafish gastrulation.....	83
Figure 3.2	Injection of <i>wnt11</i> and <i>wnt5</i> RNA rescues the <i>slb</i> ^{-/-} mutant phenotype.....	86
Figure 3.3	Expression patterns of <i>fz7</i> and <i>fz2</i> during gastrulation in wild type embryos.....	89
Figure 3.4	Injection <i>fz2</i> or <i>fz7</i> RNA in wild type embryos at pharyngula stage.....	91
Figure 3.5	<i>slb</i> embryos injected with <i>fz2</i> RNA at tail bud stage.....	92
Figure 3.6	Injection of wild type or <i>slb</i> embryos with <i>fz7</i> RNA.	93
Figure 4.1	Homology of Prickle proteins between zebrafish (Pk1, Pk2, Pk3) and <i>Xenopus</i>	101
Figure 4.2	<i>pk1</i> is expressed maternally and in migrating mesodermal precursors in zebrafish.....	102
Figure 4.3	<i>pk1</i> morphants exhibit defects in convergent extension movements.....	105
Figure 4.4	Control experiment for the specificity of <i>pk1</i> -Mo.....	106
Figure 4.5	Pk1 function does not alter AP patterning of the neural plate.....	107

Figure 4.6	Abrogation of Pk1 function enhances the <i>slb</i> phenotype and suppresses elevated Wnt11 activity.....	110
Figure 4.7	Abrogation of Pk1 function enhances the <i>pipetail</i> (<i>ppt</i>) phenotype.....	111
Figure 4.8	Over-expression of <i>pk1</i> causes defective morphogenetic movements and enhances the <i>silberblick</i> (<i>slb</i>) phenotype.....	114
Figure 4.9	<i>pk1</i> and <i>tri</i> show genetic interaction in regulating convergent extension.....	116
Figure 5.1	Schematic representation of the cloning strategy of <i>flamingo</i> genes.....	125
Figure 5.2	Expression pattern of <i>fmi1</i> during zebrafish development in wild type embryos during gastrulation.....	127
Figure 5.3	Expression pattern of <i>fmi2</i> during zebrafish development in wild type embryos during gastrulation.....	128
Figure 5.4	Dorsal expression of <i>fmi1</i> in the mesoendodermal layer and in the presumptive notochord.....	129
Figure 5.5	Expression of <i>fmi1</i> at 24hpf in the brain of wildtype embryos.....	130
Figure 5.6	Injection of splice Morpholinos (Mos) in wild type embryos.....	133
Figure 5.7	Injection of splice Mos and characterization at tail bud stage.....	134
Figure 5.8	Injection of 5'- prime Mos (Fmi1a + Fmi1b) in wild type embryos.....	137
Figure 5.9	Injection of WT embryos with the combination of Mos against Fmi1a and Fmi1b and characterization at tail bud stage.....	138
Figure 5.10	Injection of wild type embryos with 5'-prime Fmi1a and Fmi2 Mos	139
Figure 5.11	Injection of wild type embryos with 5'- prime Fmi1a and Fmi2 Mos and characterization at tail bud stage.....	140
Figure 5.12	Characterization of <i>off road</i> (<i>ord</i>) mutants and injection with Fmi1a+Fmi1b Mos at 80% epiboly and tail bud stage.....	141
Figure 5.13	Overexpression of Lyn-Fmi causes defective CE movements and is similar to <i>slb</i>	144
Figure 5.14	Wild type injected embryos with Lyn-Fmi have a lateral expansion of the head and presomitic mesoderm without affecting the D-V patterning.....	145
Figure 5.15	Overexpression of Lyn-Fmi causes a lateral expansion of the prospective telecephalon and reorganization of the eye field and prospective midbrain.	146

Figure 5.16	Genetic interactions of <i>fmi</i> with <i>slb</i> mutants.....	149
Figure 5.17	Overexpression of Lyn-Fmi RNA in <i>slb</i> embryos.....	150
Figure 5.18	Analysis of cell behaviour of cells expressing Lyn-Fmi in gastrulating embryos.....	152
Figure 5.19	Lyn-Fmi partially inhibits Fz7-dependent membrane localisation of Dsh...	154
Figure 5.20	Lyn-Fmi co-localizes with Dsh-GFP in the presence of Fz7.....	155
Figure 5.21	Specificity and purification of Fmi2 Antibody.....	157
Figure 5.22	Possible localization of Fmi protein.....	160

CHAPTER 1

GENERAL INTRODUCTION

The work described in this thesis aspires to understand the roles of core planar cell polarity genes like *flamingo* and *prickle*, during gastrulation in zebrafish embryo. Throughout I aim to explain how planar cell polarity genes function *in vivo*, as well as to increase our knowledge of their involvement in morphogenetic movements during gastrulation .

After a short introduction on the use of the zebrafish embryos as a model system in the study of early vertebrate development, this introduction will be divided in two parts. The first will describe gastrulation, and the second introduces possible molecular pathways that control the gastrulation movements. At the end of the chapter, I will introduce the experimental aims of my project.

1.1.THE ZEBRAFISH (*Danio rerio*) AS A MODEL ORGANISM TO STUDY EARLY DEVELOPMENT

Predominantly, the experiments in this thesis use zebrafish as a model for vertebrate development. The zebrafish (*Danio rerio*) has become increasingly popular as a model organism to study the cellular and molecular mechanisms that underlie vertebrate gastrulation movements.

Zebrafish are small and simple to keep in the laboratory. They achieve sexual maturity in three months and a female can lay over a hundred eggs at one time. Moreover, zebrafish embryos are fertilized *ex utero*, are transparent and undergo rapid embryonic development, making it easy to observe different structures in the embryo or even single cells, while manipulation is relatively straightforward. The different stages of development are well characterized and classified by Westerfield (Figure 1.1.) (Westerfield 1993) All these reasons make them ideally suited for an *in vivo* analysis of morphogenetic processes during early development.

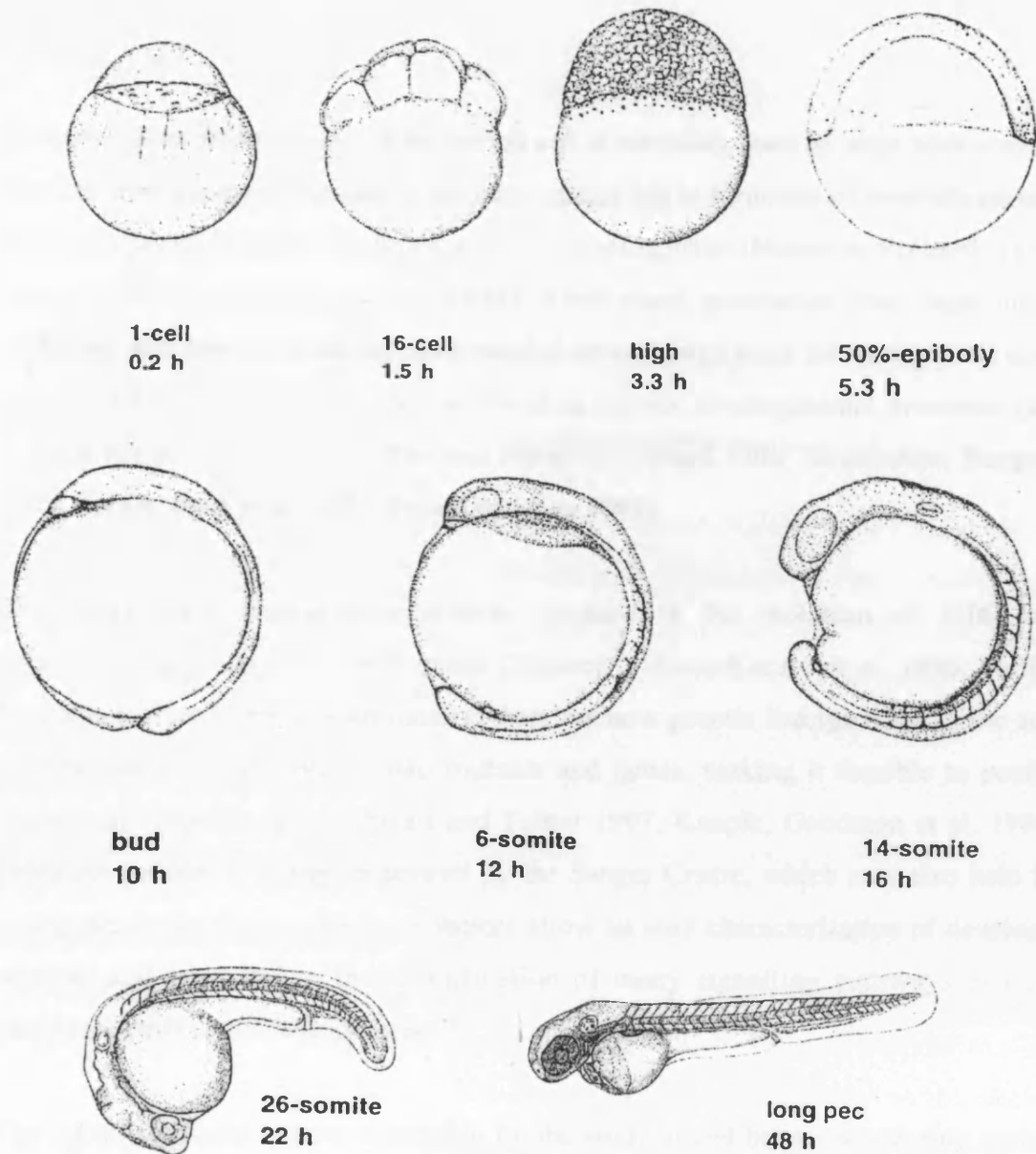


Figure 1.1. Stages of zebrafish development. Adapted from Westerfield, 1993 "the zebrafish Book" university of Oregon press

Several genetic approaches can be carried out in zebrafish, such as large scale mutagenesis screens, which are very similar to the ones carried out in a number of invertebrate and plant model organisms such as *Drosophila melanogaster* (Nusslein-Volhard 1980) and *Caenorhabditis elegans* (Brenner 1974). Their short generation time, high number of offspring, and ease of handling have enabled several large scale forward genetic screens to uncover a large number of genes involved in various developmental processes (Driever, Solnica-Krezel et al. 1996; Haffter and Nusslein-Volhard 1996; Amsterdam, Burgess et al. 1999; Farber, Pack et al. 2001; Patton and Zon 2001).

Two large-scale mutagenesis screens resulted in the isolation of 1500 mutants, corresponding to nearly to 600 genes (Driever, Solnica-Krezel et al. 1996; Haffter and Nusslein-Volhard 1996). Additionally, there are now genetic linkage maps of the zebrafish genome and it is possible to map mutants and genes, making it feasible to positionally clone many mutants (Postlethwait and Talbot 1997; Knapik, Goodman et al. 1998). The zebrafish genome is being sequenced by the Sanger Centre, which may also help identify new genes in the future. All these factors allow an easy characterization of developmental mutants and have led to the identification of many signalling pathways essential for vertebrate embryonic development.

The zebrafish model system is suitable for the study of cell behaviours during gastrulation because several homozygous/heterozygous mutants with gastrulation defects have been identified from the large scale screen. As well, it is possible to do different manipulations of the embryos, such as mRNA injections and cell transplantation assays. Lastly, their size and transparency makes possible the visualization of the embryo and its cells at high and low-resolution through the use of powerful microscopes, allowing for their study *in vivo*.

PART I

GASTRULATION MOVEMENTS

I.1.Gastrulation movements in the Animal Kingdom

One of the most puzzling questions in developmental biology is how a single layer of cells can give rise to a complex three-dimensional structure like the embryonic body. This is actually created by the action of gastrulation movements in the earliest stages of development. During this dynamic stage, the body plan of all of vertebrate embryos is established by a series of co-ordinated cell movements that transform an unstructured blastula into a three-layered gastrula. This highly-organized gastrula usually has the three germ layers - ectoderm, mesoderm and endoderm - that are created during gastrulation movements. The germ layers in the gastrula will be rearranged along both dorso-ventral axis and an anterior-posterior axis by the end of gastrulation. The process of gastrulation is conserved between vertebrates despite vast differences in morphology and most of our understanding comes from study of *Xenopus* and zebrafish (Keller, Davidson et al. 2000; Keller 2002).

Gastrulation movements employ different strategies at different periods and even between different species to generate the basic body axes. For instance, embryos use restricted cell behaviours, in different combinations, in distinct mechanical contexts and with different timings. As a result, diverse reproductive strategies such as different egg sizes, amount and proportions of yolk in the animal kingdom gave rise to a great diversity between species.

During gastrulation in Chordates, one particular structure, “the organizer structure” exists in the early embryo and serves as an embryonic centre where the some of the gastrulation cell movements occur to give shape to the embryo and enables cells to become induced in a certain fate, meaning that they will receive the correct signals at the right time. This structure has different names according the species like Spemann’s organizer (*Xenopus*), the shield (Teleosts), Hensen’s node (chick) or the node (mouse).

Some of the processes underlying gastrulation are also conserved in invertebrates, as in *Drosophila melanogaster*. In the fly, major features of gastrulation include invagination and the spreading of the ventral mesoderm. Also, nematode gastrulation offers an informative overview of gastrulation due to single cell ingression (Nance J 2002), but here this is driven by apical constriction of the kind that promotes migration of epithelial cell sheets (Lee and Goldstein 2003).

By comparing the gastrulation movements between avian, amphibian and teleosts, it can be said that frogs and fish gastrulation is a mass migration where tissues moves in a coordinated manner (Keller, Davidson et al. 2000). On the contrary, in chick the cell movements require the loss of cell-cell contacts as it involves the migration of single or small groups of cells through the extra-cellular matrix. Chick cells undergo a process of epithelial-mesenchymal transition (EMT) where they delaminate from the ectodermal layer and acquire migratory properties (Hay 1995). Also, in this situation, cells are under the influence of the node-inducing centre (Joubin and Stern 1999). The ingression movements and the fact that only a subset of cells become the definitive embryo are common features of gastrulation between chick and mouse (Sausedo and Schoenwolf 1994; Smith, Schoenwolf et al. 1994), accompanied by a high rate of proliferation and cell migration in a structure called the primitive streak that is derived from the node (Lawson, Meneses et al. 1991; Psychoyos and Stern 1996). Furthermore, processes of gastrulation in the Sea Urchin are also a useful parallel in the study the gastrulation movements. This model system reveals a mechanism of invagination of a monolayered epithelium in a two-step way (primary and secondary invagination) to give rise to a three dimensional embryo with the three germ layers. There is no “organizer“ structure; in this case the specification of blastodermal cells precedes the movements of gastrulation (reviewed in Kominami and Takata, 2004).

In summary, fundamental movements during gastrulation are conserved in many species across the animal kingdom. Variation exists in the combination of cell behaviors, the geometry, the timing and way the cell behaviors are orchestrated. However, current research seems to evaluate gastrulation in terms of genetic specific functions or molecular mechanisms involved.

I.1.2. Gastrulation movements in Zebrafish

Firstly, I will concentrate on the current status of knowledge about the cellular mechanisms that drive gastrulation movements in zebrafish embryos. Some comparisons with *Xenopus* gastrulation movements will be made.

In zebrafish there are three major kinds of gastrulation movements: epiboly, involution (or internalization), convergence and extension. I will explain the first two briefly and then I will concentrate on convergent and extension movements, which are the main focus of my Ph.D. (Figure 1.2.).

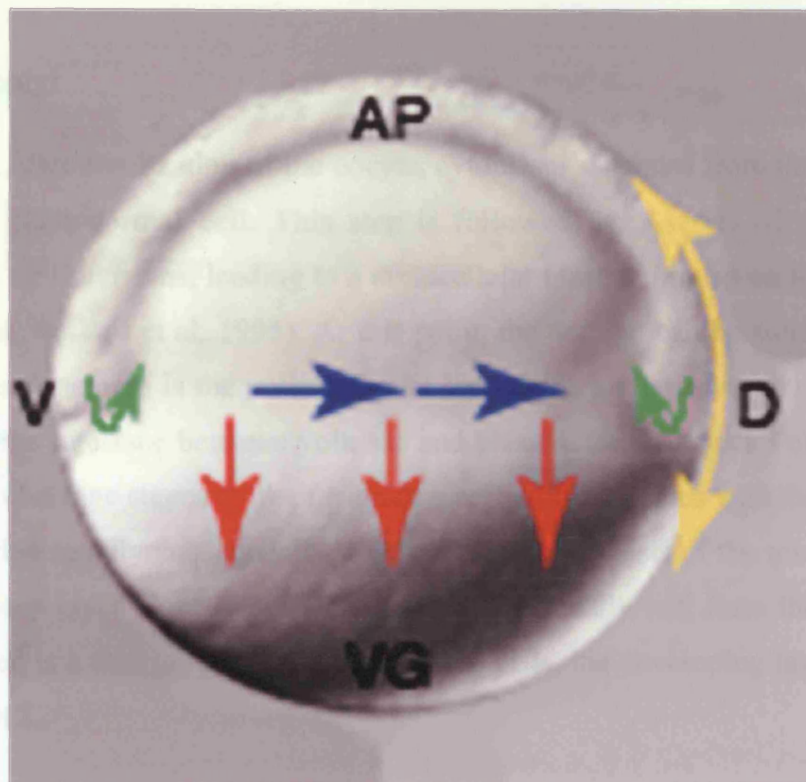


Figure 1.2. Lateral view of a zebrafish embryo at 6 hours post fertilization showing the three kinds of gastrulation movements. Epiboly movements are shown by the red arrows that spreads the the blatoderm until it covers all the yolk cell. Involution movements are shown by the the green arrows. Convergent movements are shown in blue arrows and extesion movements are shown in yellow arrows. AP, animal pole; D, dorsal; VG, vegetal pole; V, ventral. Adapted from Myers *et al.* (2002)

I.1.2.1. Epiboly:

In zebrafish, after fertilization of the oocyte, cytoplasm separates from the yolk giving rise to the first blastodermal cell. This step is followed by a series of rapid and highly synchronous cell divisions, leading to a multicellular blastoderm cap on top of a large yolk cell (Kimmel, Ballard et al. 1995). At this point, the embryo can be subdivided into three distinct areas. One area is the yolk syncytial layer (YSL). A syncytium of multiple nuclei localized at the interface between yolk sac and blastoderm. The nuclei of the YSL appear during early cleavage stages by the fusion of marginal blastomeres with the underlying yolk cell, and divide rapidly subsequently. The second area consists of the rounded and loosely associated deep layer blastomeres (DEL), which eventually will form the proper embryo. The third area is a thin layer of extra-embryonic cells, the enveloping layer (EVL), which covers the DEL.

The real epibolic process is when the blastoderm tissue flattens medially and spreads out in all lateral directions (Figure 1.3. A, D). Initially, a thinning of the blastoderm happens and there is an overall movement of the EVL, the DEL blastomeres and the nuclei of the YSL from animal or equatorial regions towards the vegetal pole. By the end of gastrulation (bud stage), the yolk cell is entirely covered by the blastoderm layer and EVL (Figure 1.3. A-C; (Warga and Kimmel 1990).

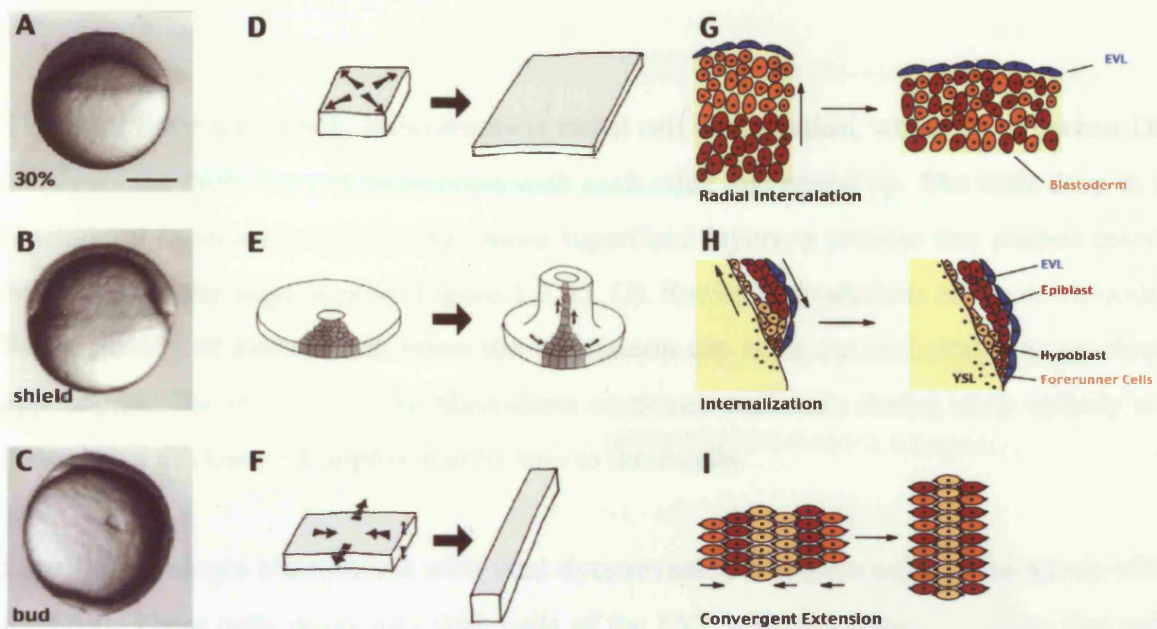


Figure 1.3. Cell rearrangements during zebrafish gastrulation. (A – C) DIC images of wildtype embryos at 30% epiboly (A), 60% epiboly or shield stage (B) and bud stage (C). Lateral views with animal to the top and dorsal (B,C) to the right. Scale bar = 250 μm . (D – F) Drawings illustrating the principles of the tissue rearrangements at the stages depicted in (A – C). The orientations in (A – C) and (D – F) are the same. (D) Epiboly. The tissue flattens and spreads outwards, away from the center. (E) Mesendodermal progenitor cell internalization. The tissue leaves its original plane and folds into a direction perpendicular to the original plane. (F) Convergent extension. The tissue narrows medio-laterally (convergence) and lengthens into the perpendicular direction (extension). (G – I) Schematic views of the main cellular rearrangements at the stages depicted in (A – C). (G) Radial intercalations flatten the blastodermal cells flatten the tissue during epiboly and push cells towards the side. (H) Internalization. Hypoblast cells move towards the animal pole in a direction opposite to that of the overlying epiblast, EVL and forerunner cells. (I) Convergent extension. Mediolateral intercalations of cells lead to the extension of the tissue in anterior-posterior direction. The orientations in (A – B) and (G – H) are the same; (I) shows a dorsal view on the cells instead of a lateral view in (C). In (G – I), black dots indicate the cell nuclei. YSL = yolk syncytial layer. Adapted from Montero and Heisenberg (2004); Kimmel *et al.* (1995) and Keller *et al.* (2000)

The main force for epiboly movements is radial cell intercalation, which occurs when DEL cells become more loosely associated with each other and round up. The cells deep in the blastoderm intercalate radially into more superficial layers, a process that pushes epiblast cells towards the vegetal pole (Figure 1.3. D, G). Radial intercalations are most obvious at the beginning of gastrulation when the blastoderm cap thins out and attains a cup-shaped appearance. The thinning of the blastoderm continues uniformly during early epiboly until it reaches a thickness of approximately two to three cells.

Labelling of single blastomeres with vital dyes revealed extensive cell intercalations within the DEL. These cells never mix with cells of the EVL and vice versa, revealing that radial intercalation movements are restricted to the cells within one tissue (Warga and Kimmel 1990). In *Xenopus*, epiboly is also known to occur by radial cell intercalation, in which cells at different depths in the blastoderm intercalate, creating the thinning process (Keller 1980).

In *Xenopus*, epiboly involves spreading and division of superficial cells and radial intercalation of several layers of deep cells to produce less layers of larger area (Keller 1980). In the 1980, Keller proposed that an active push of several layers of deep cells between one another during radial intercalation drives epiboly while the overlying epithelial cells are just stretched by the spreading deep region. Amplified affinity or adhesion between the undersides of the epithelial cells and the juxtaposed surfaces of the intercalating deep cells would operate as a “boundary capture” mechanism, making sure that any deep cell that intercalated between others and made contact with this favorable adhesion site would probably stay there (Keller, Danilchik et al. 1985).

Additionally, in *Xenopus* compared to zebrafish, there are two types of radial intercalation. The first happens early during epiboly, and is independent of cell-fibronectin interactions. The second occurs later and results in extension, and is dependent on cell-matrix interactions. The second process is an active, force producing process (Keller and Danilchik 1988) but it is not known if of the same kind of the early epibolic process.

In fish, the yolk cell also plays a crucial role in directing epiboly movements. Specifically, the nuclei of the YSL have epibolic movements similar to the movements of overlying blastodermal cells, meaning that the movements of these two domains are regulated in a similar way (D'Amico and Cooper 2001). A tight co-ordination of the movements between the blastodermal cells and the YSL nuclei appears to be important, especially as YSL serves as an source for mesoderm inducing signals (Chen and Kimelman 2000; Kimelman and Griffin 2000; Schier 2001). In addition, it has been suggested that the YSL nuclei are pulled over the yolk cell towards the vegetal pole by a microtubule-dependent mechanism . Furthermore, the movements of the YSL could reflect the mitotic movements of the YSL nuclei, which divide many times during the course of gastrulation (Kane and Adams 2002).

There is also a possible contractile force responsible for epiboly. This could be either mediated by an actin-rich cytoskeletal network formed around a subset of YSL nuclei at the blastoderm margin or, alternatively, by EVL cells close to the blastoderm margin that form an actin-rich 'purse string' at their vegetally oriented sides around the circumference of the germ ring (D'Amico and Cooper 2001; Kane and Adams 2002; Cheng, Miller et al. 2004).

EVL cells may also contribute to epibolic movements as they are passively pulled over the embryo by their interaction with the YSL nuclei (Kimmel, Ballard et al. 1995; Kane and Adams 2002). But the movement of EVL cells towards the vegetal pole could also be driven by active migration (Zalik, Lewandowski et al. 1999). These cells also exhibit cell intercalations contributing to the epibolic movements of the EVL (Keller and Trinkaus 1987; Fink and Cooper 1996).

In zebrafish mutants exhibiting defective epiboly movements and in embryos in which the microtubule cytoskeleton is disrupted, the epibolic movements of the DEL, YSL and EVL cells can be uncoupled from one another (Kane, Hammerschmidt et al. 1996; Solnica-Krezel, Stemple et al. 1996). The vegetal expansion of the EVL and YSL takes place, but the epiboly of the DEL cells is arrested, indicating that the movement of those cells is specifically affected. Among these mutants, *half-baked (hab)*, *avalanche (ava)*, *lawine (law)*, and *weg* are mapped to a single locus, and they are considered alleles (Kane and Adams 2002). As a result, these movements appear to be autonomously regulated. In spite of this, these movements might still be highly synchronized with each other. Actually, DEL

cells extend protrusions both along the YSL surface and towards the EVL layer (Kane, Hammerschmidt et al. 1996; Kane and Adams 2002; Ulrich, Concha et al. 2003), indicating that there is an extensive intercellular communication between these cell layers during epiboly.

For these reasons, the molecular mechanism of epiboly is not completely understood. As already mentioned, two microtubule arrays have been detected in the zebrafish embryo during epiboly: one intercrossing the YSL and the other extending along the animal-vegetal axis in the yolk cell (Solnica-Krezel and Driever 1994). Impairment of the microtubule arrays by ultraviolet irradiation or treatment with a microtubule-destabilizing agent, nocodazole, disrupts epiboly (Solnica-Krezel and Driever 1994). Additionally, ring-like F-actin-based structures observed in the edges of the EVL and DEL cells, support a role for microfilaments in the epiboly of the EVL, DEL cells, and YSL (Cheng, Miller et al. 2004). Furthermore, epiboly is thought to disturb convergence and extension (Solnica-Krezel and Cooper 2002). Most recently, the *hab* locus has been positional cloned to encode E-cadherin and which is required for normal radial intercalation during epiboly (Kane, McFarland et al. 2005; Montero, Carvalho et al. 2005).

I.1.2.2. Internalization or involution:

Involution consists of the rolling of tissue over an inflection point, or around a lip or even back on itself. The internalization of mesendodermal cells is a key point in gastrulation. During this process, cells separate from ectodermal precursors, giving rise to the establishment of the three germ layers: ectoderm, mesoderm and endoderm. Precursor cells are also brought into their crucial positions from where they can develop into more specific tissues (Warga and Kimmel 1990; Kimmel, Ballard et al. 1995; Kane and Adams 2002).

In zebrafish, internalization of mesendodermal progenitors is observed at 50% epiboly, when the blastoderm has covered half of the yolk sac. It becomes obvious by a local thickening at the blastoderm margin, which from thereafter is called as the ‘germ ring’ (Figure 1.3. B). During formation of the germ ring, epibolic movements slow down but continue towards the vegetal pole after the first mesendodermal progenitors have internalized (Kimmel, Ballard et al. 1995; Kane and Adams 2002). At the beginning of

internalization, DEL blastomeres within the germ ring start moving towards the yolk and, after reaching the yolk cell surface, turn around and move towards the animal pole in a direction opposite to their overlying (not internalized) cells. Prospective mesendodermal cells that internalize later do not turn towards the animal pole but instead move towards the vegetal pole (Warga and Kimmel 1990). The internalization of mesendodermal progenitors forms an internal cell layer, the hypoblast, which is located beneath an outer layer of non-internalized cells, the epiblast. The epiblast gives rise to ectodermal tissues, but early internalizing hypoblast cells will form endodermal and mesodermal tissues, while later internalized cells become mesodermal tissues (Figure 1.3. E, H.). In contrast, EVL cells are never internalized (Warga and Kimmel 1990).

While cells can internalize at the entire margin of the blastoderm, only the two most marginal rows of cells seem to directly take part in this process (Warga and Kimmel 1990; Kane and Adams 2002). Two main types of cellular movements have been proposed to drive mesendodermal cell internalization: involution of a sheet of blastoderm cells immediately at the margin of the germ ring and ingression of single blastodermal cells close to the germ ring margin. Recent reports suggest that in zebrafish, blastodermal cells at the margin of the germ ring primarily involute synchronously as a uniform sheet of cells and then, once they have reached the yolk cell surface, undergo an epithelial to mesenchymal transition (EMT) and start to move as individuals, reminiscent of single cell ingression (D'Amico and Cooper 1997; Kane and Adams 2002). However, there is evidence that wild type single cells can internalise in the MZOne-eye pinhead mutant embryos that lack internalisation process (Carmany-Rampey and Schier 2001).

The next crucial step of gastrulation happens around 50%-55% of epiboly where there is the formation of the embryonic organizer or the so-called shield, a dorsal thickening of the germ ring, in this region the internalized cells that reach the yolk cell surface turn around and migrate towards the animal pole (Figure 1.3. B). The embryonic shield is the equivalent of the dorsal blastopore lip of the amphibian. Cells from the lateral regions of the germ ring margin migrate as loosely associated mesenchymal cells, while cells ingressing in the region of the shield are tightly clustered together and move as an epithelial-like sheet of cells, that will give rise to the prechordal plate. It is possible that the movement of early internalized mesendodermal cells towards the animal pole drags adhering cells in more

superficial blastodermal layers passively towards the yolk cell surface, leading to the internalization of those cells. Additionally, YSL nuclei that move simultaneously with the first internalizing cells towards the animal pole might dynamically modify the plasma membrane of the yolk cell. This would generate a force which is capable to pull more superficially located mesendodermal progenitors that adhere to the plasma membrane of the yolk cell towards the yolk cell surface (Kane and Adams 2002).

To finalize in *Xenopus* both the epithelial cell sheet and the deep mesenchymal cell layers involute together. The epithelial layer maintains its consistency, but details of cell movements in the deep region are unknown. In fish, a single layer of cells, the epiblast cells, that it is not a tight-junctioned sheet of cells, undergo involution-like movements that exhibit an ingression behaviour (Shih and Fraser 1995; Trinkaus 1996; Glickman, Kimmel et al. 2003). One of the major differences in zebrafish and *Xenopus* is that in *Xenopus* the different rates of extension that exist in the several layers of cells could also drive involution. On the other hand, in fish the passage of cells over the lip shows ingression behaviour because the cells do not leave the epiblast in a sequential fashion.

I.1.2.3. Convergence and extension:

Convergent extension movements, along with epiboly and the continuous internalization of mesendodermal precursor cells, lead to the formation of an embryonic body axis with distinct anterior-posterior and dorsal-ventral polarity from the initially spherical gastrula. Tissue explants experiments in *Xenopus* provided a lot of our knowledge about convergent extension (Keller, Davidson et al. 2000).

First of all, a point that needs to be clarified is the definition of concepts. When I talk about convergence and extension (C&E) this is the overall process of medio-lateral narrowing and antero-posterior elongation of the embryonic body. When I use the term convergent extension (CE), it means the process of medio-lateral narrowing and antero-posterior elongation of embryonic tissues, which may or may not be simultaneous and interdependent. The most studied example has been the mediolaterally or dorsally-oriented cell intercalation in *Xenopus* gastrulae (Keller, Shih et al. 1992). In another words, I define

convergent extension as the synchronized narrowing and lengthening of a tissue, no matter what the primary cellular mechanism is. Indeed, convergent extension (CE) is accomplished by different cellular mechanisms in different animals and in different tissues.

There are both similarities and differences between convergence and extension in fish and frog, both at level of cellular mechanisms and tissue organization. Both frogs and fish engage in CE, in frog embryos only cell rearrangement (where cells move relatively to each other) where implicated in CE, while both models use cell rearrangement and directed migration. This could explain why some gastrulation movements occur independently of one another in fish gastrulae. In contrast to frog, even strong obliteration of CE does not interfere with mesendoderm internalization and epiboly (Solnica-Krezel, Stemple et al. 1996). Studies in *Fundulus heteroclitus* (killifish) suggest that the dorsal migration of lateral mesoderm cells give rises to mediolateral narrowing and dorsal accumulation of tissue without associated extension (Trinkaus, Trinkaus et al. 1992). Furthermore, studies of zebrafish *no-tail* and *somitabun* mutants, in which convergence defects occur, although extension continues relatively normally. These observations indicate that extension in the fish gastrula does not depend only on convergence (Myers, Sepich et al. 2002; Glickman, Kimmel et al. 2003). These suggest that a consequence of the separation of CE movements in fish embryos is that the cellular mechanisms underlying these processes are likely to differ from those employed in *Xenopus* gastrulae.

As a result, in zebrafish, we can separate the convergence that narrows the embryo mediolaterally, from extension that lengthens the tissue into the anterior-posterior direction (Figure 1.3. C, F, I). Although it appears the mechanisms may differ, the process of C&E movements is an essential and conserved principle in many species (Sausedo and Schoenwolf 1993; Sausedo and Schoenwolf 1994; Keller, Davidson et al. 2000; Munro and Odell 2002; Myers, Sepich et al. 2002; Glickman, Kimmel et al. 2003). The extent to which convergence and extension movements are coordinated with each other varies between different species and in specific domains within the gastrula (Keller, Davidson et al. 2000).

I.1.2.3.1. Cellular mechanisms underlying convergent extension in *Xenopus*

The cellular mechanisms underlying CE have been intensively studied in *Xenopus*, mainly in the posterior mesoderm (notochord and somites), and neuroectoderm (spinal cord and hindbrain) (Keller, Davidson et al. 2000). A large proportion of the CE studies have taken advantage of autonomous movements of explanted *Xenopus* tissue (reviewed in (Keller, Shih et al. 1992; Keller, Davidson et al. 2000)). From these experiments and time lapse experiments in the mesoderm it is possible to conclude that there is tissue-autonomous activity that leads cells to become highly aligned along the major embryonic axes. Additionally, it is also possible to conclude that the mesoderm cells intercalate between one another along the mediolateral axis to provide the elongation of a tissue also along the anterior posterior axis (Shih and Keller 1992). Studies of intact embryos confirmed the mediolateral arrangement and intercalation of these cells, therefore supporting the explant experiments (Keller, Cooper et al. 1989; Keller and Tibbetts 1989).

Cell tracing and time-lapse data of cells with epi-illumination (Keller, Danilchik et al. 1985; Keller, Cooper et al. 1989; Wilson, Oster et al. 1989; Wilson and Keller 1991), or fluorescently-labeled cells (Keller, Cooper et al. 1989; Shih and Keller 1992; Shih and Keller 1992) showed that CE involves two types of cell intercalation. To begin with, deep cells intercalate along the radius of the embryo, radial intercalation, to create fewer layers, thinning, of greater length, extension, and then these same cells intercalate mediolaterally, mediolateral intercalation, to produce a narrower and longer array, convergent extension. Radial intercalation prevails in the first half of gastrulation and mediolateral intercalation predominates in the second half of gastrulation and then throughout neurulation in both the dorsal mesodermal tissue and in the prospective posterior neural tissue (spinal cord and hindbrain) (reviewed in (Keller, Davidson et al. 2003)).

Within the mesoderm at the beginning of gastrulation, all cells display random protrusive activity that develops predominantly into a bipolar, medio–laterally oriented protrusive activity, resulting in medio–lateral cell intercalation (Shih and Keller 1992; Shih and Keller 1992)(Figure 1.4A). These stable protrusions could generate the traction force required for

the mediolateral intercalation (Keller, Davidson et al. 2000). If these protrusions are somehow disturbed, CE movements are affected (Wallingford, Rowning et al. 2000).

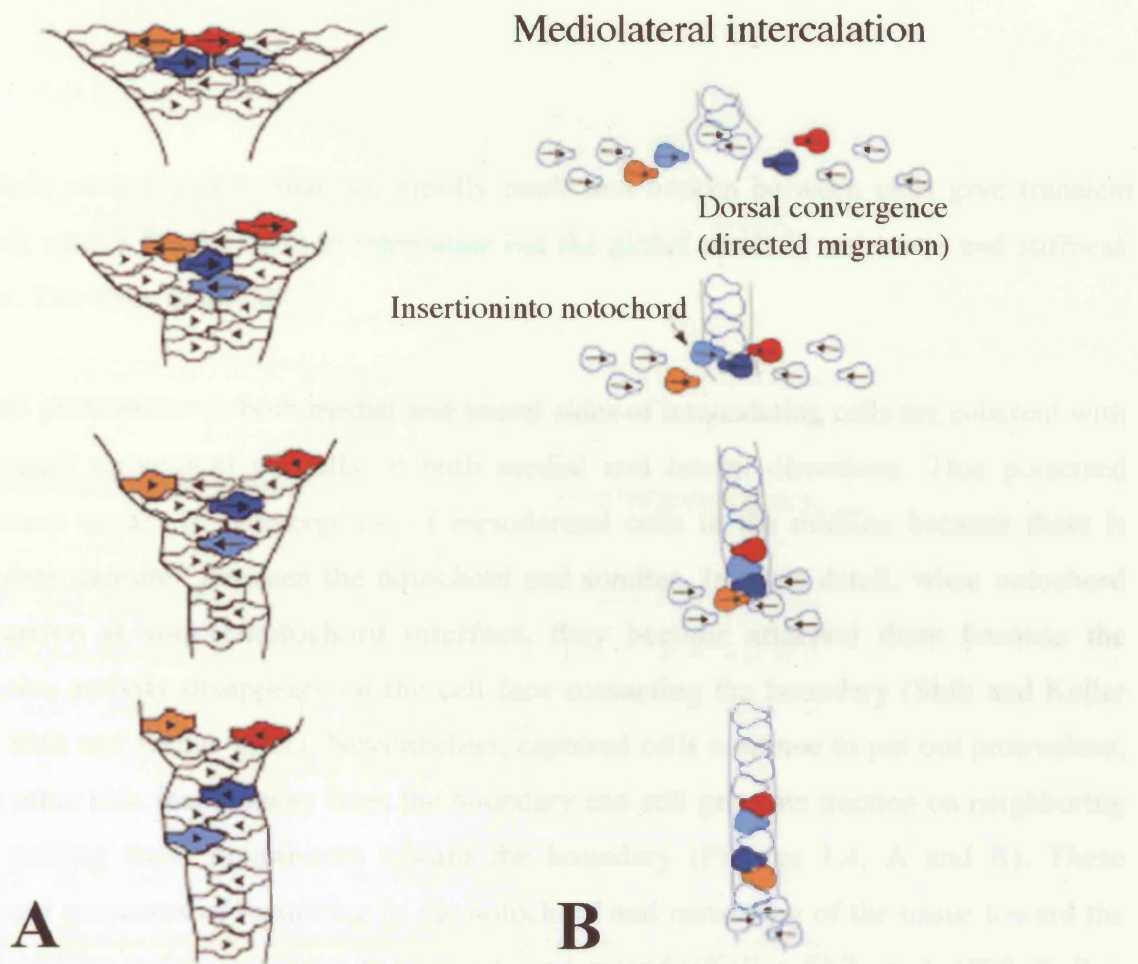


Figure 1.4. Model for convergent extension in *Xenopus* (A) compared with the Model for convergent extension in Teleosts (B). A- Arrows show the direction of movement of each cell; arrowheads show the medially directed traction of boundary captured cells. The direction of movement of the cells is biased mediolaterally. The blue cells move medially at first, then pass each other and diverge laterally until they reach a boundary. The brown and orange cells diverge laterally from the outset, yet are then brought closer as the boundaries converge. B - Arrows show the direction of cell movement. Lateral cells migrate dorsally and are not firmly packed and do not rearrange. Upon arrival to the midline cells insert into the notochord and make contact with other cells. Intercalation origins a repacking (e.g., when the blue and orange cells reach the midline, they become separated by other cells). In fish axis elongation demands intercalation at the midline and dorsal directed migration of lateral cells. Adapted from Wallingford *et al.* (2002)

Multiple contact points that are rapidly made and broken between cells give transient opening spaces for the cells to intercalate but the global result is resistance and stiffness (Keller, Davidson et al. 2000).

The cell protrusions on both medial and lateral sides of intercalating cells are coherent with the overall movement of cells in both medial and lateral directions. This polarized movement results in convergence of mesodermal cells to the midline because there is “boundary capture” between the notochord and somites. In more detail, when notochord cells arrive at somite/notochord interface, they become attached there because the protrusive activity disappears on the cell face contacting the boundary (Shih and Keller 1992; Shih and Keller 1992). Nevertheless, captured cells continue to put out protrusions, on the other side facing away from the boundary and still generate traction on neighboring cells, pulling these neighbours toward the boundary (Figures 1.4. A and B). These continued processes of repacking in the notochord and narrowing of the tissue toward the dorsal midline makes the tissue to converge and extend ((Keller, Shih et al. 1992; Keller, Davidson et al. 2000).

Within the neural plate there are also convergent extension movements, confirmed by explant experiments (Keller and Danilchik 1988). This neural convergent extension is driven by cell intercalation (Keller, Shih et al. 1992), but in this case, time-lapse analysis reveals that it involves a monopolar lateral-to-medially directed protrusive activity that depends on signalling from the underlying mesoderm, and which results in medio-lateral cell intercalation and elongation of the neural plate along the anterior-posterior axis (Keller, Shih et al. 1992; Elul, Koehl et al. 1997; Elul and Keller 2000). It also implicates the boundary capture at the border between the neural plate and notoplate (Elul, Koehl et al. 1997; Elul and Keller 2000). Deep neural explants at late gastrula deprived of further contact with underlying notochord and midline tissues (notoplate/floorplate) do not develop. In their absence the deep neural cells have a bipolar protrusive activity. Nevertheless, when explanted with underlying mesoderm they acquire monopolar protrusive activity. It is still an open question, why the ectoderm and mesoderm can choose between monopolar and bipolar cellular organization, and these issues have yet to be resolved.

I.1.2.3.2. Cellular mechanisms underlying convergent extension in zebrafish

In zebrafish, both layers, epiblast and hypoblast, converge towards the dorsal side, where there is an accumulation of blastodermal cells, that leads to the formation of the embryonic organizer called the shield (Figure 1.2; (Kimmel, Ballard et al. 1995). At later stages, this results in an almost complete compaction of all embryonic cells on the dorsal side, where the axis forms, and an associated depletion of cells on the ventral side of the embryo (Figure 1.2). Hypoblast (future mesendodermal) cells that exhibit CE movements migrate as loosely-associated mesenchymal cells on the yolk cell surface, while epiblast (future ectodermal) cells move like a sheet of epithelial cells towards the dorsal side (Kimmel, Ballard et al. 1995; Concha and Adams 1998).

Cell tracing experiments in zebrafish demonstrated that as mesodermal and ectodermal clones reach the dorsal midline, they form antero-posteriorly elongated strings of labeled and unlabeled cells (Warga and Kimmel 1990; Kimmel, Warga et al. 1994). Based on these observations, a model for teleost gastrulation was proposed whereby the most first converge dorsally by directed migration, and then intercalate to extend the axis (Figure 1.4.B).

Tracking dorsal translocation (convergence) or anteroposterior elongation (extension) of cell groups labeled with either lipophilic or photoactivated dyes reveal the presence of three C&E movement domains in the gastrula (Figure 1.5.). Dependent on their position within the embryo during gastrulation, cells seem to have three different levels of CE movements. (Kimmel, Warga et al. 1990; Kimmel, Ballard et al. 1995; Myers, Sepich et al. 2002) (Figure 1.5.). First, cells on the prospective ventral side of the embryo do not contribute to convergence or extension of the body axis. Alternatively, they migrate over the vegetal half of the yolk towards the vegetal pole, where they later become part of the tail. Such cell behavior occurs in the “no convergence, no extension zone” (NCEZ). (Sepich, Myers et al. 2000; Myers, Sepich et al. 2002).

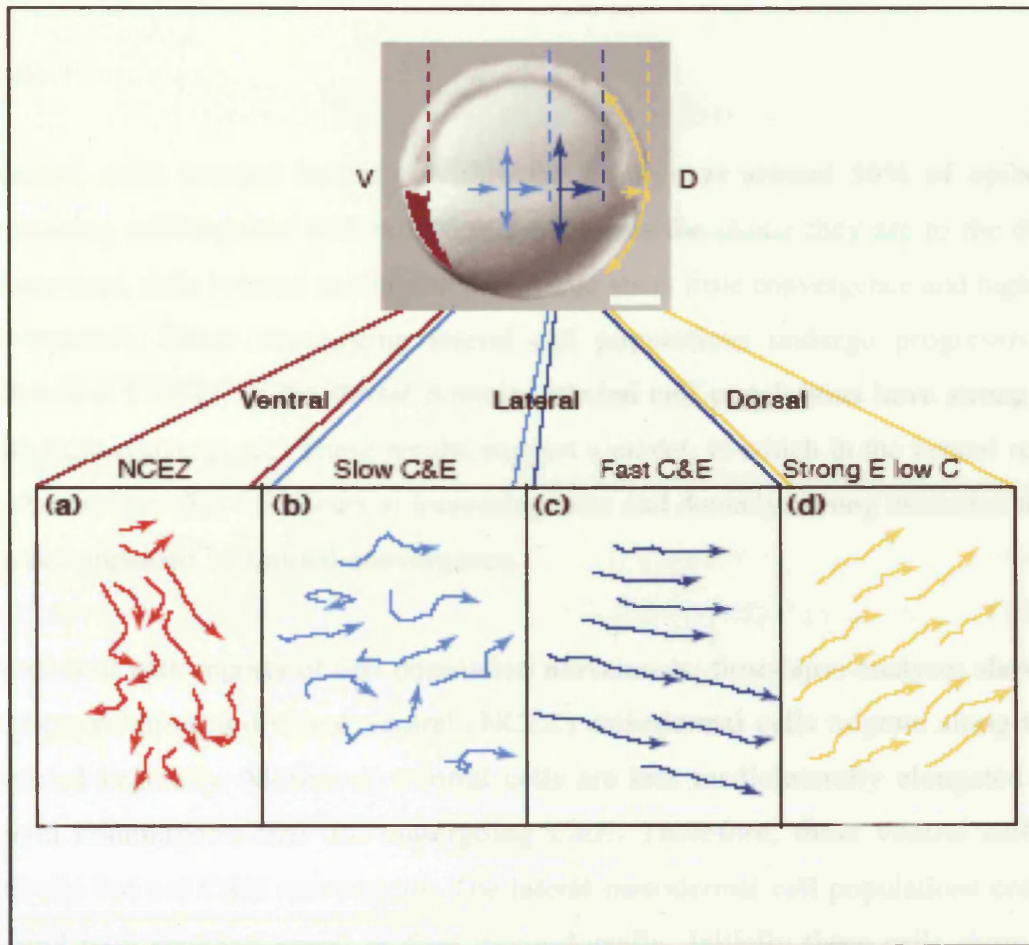


Figure 1.5 Cell trajectories in the ventral, lateral and dorsal C&E domains. Time-lapse analyses at late gastrula stages was used to calculate the trajectories movement. (a) Cells in the no convergence no extension zone (NCEZ, red) travel in zig-zag path. (b) Lateral cells undergoing slow C&E still have a zig-zag pattern but not so severe (c) Lateral cells undergoing fast C&E move in straight trajectories. (d) The paths of dorsal cells are oriented dorsally and biased towards anterior or posterior.

Abbreviations: D, dorsal; V, ventral.

Adapted from Myers et al. (2002)

Second, cells located laterally within the embryo at around 50% of epiboly, show increasing convergence and extension movements the closer they are to the dorsal side. Meanwhile, cells located near to the dorsal side show little convergence and high extension movements. These converging lateral cell populations undergo progressively faster extension. Finally, in the dorsal domain, labeled cell populations have strong extension with little convergence. These results support a model, in which in the ventral region C&E is absent; laterally, CE occurs at increasing rates and dorsally, strong extension movements are accompanied by limited convergence.

Consistent with reports of cell population movements, time-lapse analyses showed that at mid-gastrulation, individual ventral (NCEZ) mesodermal cells migrate along trajectories directed vegetally. Moreover, ventral cells are less mediolaterally elongated than their dorsal counterparts that are undergoing C&E. Therefore, these ventral cells undergo epibolic but not C&E movements. The lateral mesodermal cell populations converge and extend with growing speed as they move dorsally. Initially these cells show amoeboid morphology and take dorsally oriented zig-zagging paths, getting a slow net dorsal speed (the sum of the velocity and persistence of the movements of cells). As these cells move dorsally, their trajectories become more directed and, as a result, net dorsal speed increases (Myers, Sepich et al. 2002).

At the cellular level, the stability and persistence of the trajectories of these movements corresponds to which cells undergo CE movements. These cells will elongate along their medio-lateral axes, and this elongation appears to be required for the velocity and persistence of CE movements (Topczewski, Sepich et al. 2001; Marlow, Topczewski et al. 2002). These cells also create pseudopodial and filopodial protrusions, projecting towards the yolk and on to neighbouring cells. Whether this protrusive activity is necessary to stabilize cell movements or to directly mediate them is not yet known (Kilian, Mansukoski et al. 2003; Ulrich, Concha et al. 2003).

In addition, the cell behaviors observed in the posterior mesoderm and neuroectoderm of zebrafish suggest that medio-lateral cell intercalation contributes greatly to convergent extension movements. Epiblast cells elongate along the medio-lateral axis while showing

autonomous protrusive activities (Concha and Adams 1998). This behaviour occurs simultaneously with medio–lateral cell intercalation and anterior–posterior extension of the neural plate (Warga and Kimmel 1990; Kimmel, Warga et al. 1994; Concha and Adams 1998).

To sum up, neurectodermal cells display CE movements using mediolateral intercalations. The entire process starts at shield stage, when non-internalizing epiblast cells in the blastoderm margin, in addition to their vegetally directed epibolic movements, converge to the dorsal midline in a persistent fashion. During gastrulation, cells that are more animally situated relative to the blastoderm margin also start to converge on the way to the dorsal midline. At the same time, epiblast cells are more compact, so that by mid-gastrulation the whole epiblast moves as a sheet of cells. Cells that become elongated and extend projections in a medio-lateral direction, may facilitate medio-lateral intercalation at the dorsal midline. Though, it is not yet completely clear to what extent convergence and extension movements in the epiblast are connected by mediolateral intercalation (Concha and Adams 1998).

In the mesoderm, cells also become elongated along the medio–lateral axis (Topczewski, Sepich et al. 2001) while undergoing medio–lateral cell intercalation (Warga and Kimmel 1990). These data suggest that there are similarities in cell behavior between zebrafish and *Xenopus*. Therefore, during late gastrula or early segmentation stages, a large fraction of ectodermal and mesodermal cells in this region are mediolaterally elongated (Concha and Adams 1998; Topczewski, Sepich et al. 2001; Myers, Sepich et al. 2002). Furthermore, confocal time-lapse analyses of dorsal (notochord and paraxial somitic) mesoderm have shown that cell exchanges are extremely oriented. In detail, cell “gains” occurs mainly in the mediolateral axis, while losses are antero-posteriorly biased, as expected from mediolateral intercalation behaviour (Glickman and Yelon 2002). These results imply that in the dorsal region of the zebrafish, as in the frog gastrula, mediolateral intercalation of mesodermal cells results in simultaneous C&E. On the other hand, as extension in dorsal mesoderm does not depend only on convergence (Glickman and Yelon 2002), suggesting that mediolateral intercalation cannot be the only cell behavior involved. Although mediolateral intercalation can be observed in both of these tissues (notochord and paraxial somatic), the rate of convergence is not always linked to the rate of extension (as it would

be the case in *Xenopus*), indicating that there are other mechanisms driving CE movements. This is evident in *no tail (ntl)* mutants, where the embryonic axis can still extend even in the near-complete absence of convergence movements within the paraxial mesendoderm (Glickman, Kimmel et al. 2003).

Radial intercalations of mesendodermal cells might also contribute to the anterior-posterior extension of the new embryonic axis. This idea is substantiated by the analysis of the *volcano* mutant, which shows that defects in epibolic cell movements at the beginning of gastrulation are followed by reduced CE movements. This suggests that these different movements might be regulated by a common cellular mechanism (Solnica-Krezel, Stemple et al. 1996).

In more anterior regions of the embryo, extension of axial mesendodermal tissues, like the prechordal plate is mediated mostly by the directed migration of single cells or groups of cells in the direction of the animal pole, while mediolateral cell intercalation looks to be limited to paraxial mesendodermal tissues (Miguel Concha, Masa Tada, Carl –Philipp Heisenberg, Steve Wilson, Richard Adams, unpublished observations). Also, the analysis that different signalling molecules are necessary to lead CE movements in anterior and posterior regions of the embryo supports the idea that several cellular mechanisms might function to control gastrulation movements along the anterior-posterior axis of the embryo (Kilian, Mansukoski et al. 2003).

A recent study by D'Amico and Cooper demonstrated that the nuclei of the YSL undergo movements associated with CE (D'Amico and Cooper 2001). It starts at shield stage, when a small portion of the nuclei converges towards the dorsal side. When internalization begins, the YSL nuclei move with the firstly internalized mesendodermal cells to the animal pole. CE movements of the nuclei in paraxial regions of the embryo couples this movement of internalization. These nuclei show increasingly faster CE movements the closer they are to the dorsal side, while the nuclei in axial regions move anteriorly towards the animal pole. Analogous to the situation in mesendodermal and neurectodermal germ layers, CE movements of the YSL nuclei seem to be mediated by mediolateral cell intercalation, signifying that the movements of the YSL nuclei and of cells in the overlying hypoblast and epiblast layers are synchronized (D'Amico and Cooper 2001).

It is still unknown which cells in the EVL exhibit CE movements during gastrulation. Theoretically, cells of the EVL can extend cellular protrusions and are motile within the level surface of the EVL, but whether they actively converge and extend has not yet been experimentally proved (Keller and Trinkaus 1987; Fink and Cooper 1996; Zalik, Lewandowski et al. 1999). In view of the fact that the EVL wraps the blastoderm to an equal proportion along its dorso-ventral axis throughout gastrulation, convergent movements of cells within the EVL might be of less importance (Kimmel, Ballard et al. 1995).

A great number of the studies analyzing the cellular mechanisms involved in gastrulation movements have focused on the cellular rearrangements within specific germ layers and tissues. Despite significant recent progress in understanding gastrulation movements in fish, there are major questions of the biomechanics of zebrafish convergence and extension are: what is the role of internally and externally generated forces? What are the external machines? Possible candidates are the extraembryonic epibolic machine and the autonomous extension of the underlying YSL (D'Amico and Cooper 2001). Finally, are the forces in zebrafish generated by mediolaterally polarized protrusive activity and mutual cell traction, similar to what is thought to occur in the *Xenopus* ?

PART II

Molecular Mechanisms

In this section I will introduce the possible molecular pathways that control the gastrulation movements, especially convergent and extension movements in zebrafish and emphasising the importance of to the non-canonical Wnt pathway.

II.1.1. Wnt pathway

The Wnt family of proteins is very diverse and it is implicated in many developmental processes during embryogenesis and is also involved in adult tissue homeostasis. Wnt family members have manifold effects including mitogenic stimulation, cell fate specification and differentiation (Logan and Nusse 2004). The Wnt family comprises a group of secreted glycoproteins existing in species throughout the animal kingdom, ranging from *Hydra* to humans. They are implicated in phenomena like axis formation and patterning, tissue and organ morphogenesis, asymmetric cell division and, as more recent studies confirm, also in axon guidance (Wodarz and Nusse 1998; Yoshikawa, McKinnon et al. 2003; Inoue, Oz et al. 2004).

One of the main functional differences among Wnt proteins is that different Wnts cause distinct phenotypes, dividing the superfamily in two classes. Accordingly some results from ectopic expression of Wnts in mammary epithelial cells and in *Xenopus* embryos there is a class of Wnt transforming, axis –inducing factors the so called “Wnt-1 class”, which includes Wnt1, Wnt3A, Wnt7A, Wnt8 and Wnt8b and then there is the non-transforming “Wnt5a class” which includes Wnt4, Wnt 5A and Wnt11 (Wong, Gavin et al. 1994; Torres, Yang-Snyder et al. 1996); Du et al., 1995). Consequently, it is possible to classify the Wnts in to “canonical” Wnts, which have transforming activity and usually lead to the stabilization of β -Catenin (described in more detail below) and is almost absolutely conserved through evolution. The other “non-canonical” Wnts do not have transforming

activity and have different functions, for example being involved in gastrulation movements and tissue separation.

The Wnt canonical pathway was found to specify segment polarity in *Drosophila* and mediate axis formation in *Xenopus*. The canonical pathway transduces the Wnt signal via attachment to its transmembrane receptor Frizzled (Fz). Sequentially there is activation of the cytoplasmic protein Dishevelled (Dsh). This leads to blocking of the breakdown of the complex containing APC, Axin and GSK-3, which in turn permit the stabilization of β -Catenin and its consequent translocation to the nucleus. Once stabilized, β -catenin binds proteins of the lymphoid enhancer factor/ T-cell factor family (LEF/TCF) family and is implicated in the transcriptional regulation of target genes (Cadigan and Nusse 1997; Huelsken and Birchmeier 2001).

II.1.2. Non-canonical Wnt Pathway

In this thesis I will focus on the non-canonical/Wnt pathway which has been shown to be mainly involved in cell movements, cell morphology and tissue separation, and in general morphogenetic movements.

II.1.2.1. Planar Cell Polarity in *Drosophila*

The planar cell polarity pathway (PCP) in *Drosophila* generates polarity signals that orientate cells in a given plane. The PCP signalling pathway bears considerable similarity to Wnt signalling in vertebrates: downstream of Wnt the serpentine receptor, *frizzled* (*fz*) is involved in the correct orientation of eye ommatidia, the polarized growth of sensory bristles in the thorax, and also in wing hair polarity in wing epithelium (Vinson, Conover et al. 1989; Adler and Lee 2001; Adler 2002). In the wing, hairs polarise in the proximo-distal axis of the wing epithelium. In the eye, ommatidial polarity is coordinated relative to the dorso-ventral and antero-posterior axes of the eye epithelium. In the eye, a single ommatidium bears 20 cells: these include eight photoreceptor cells, pigment cells, corneal cells, and bristles. The eight-photoreceptor cells (R1-R8) are arranged in a trapezoidal manner (Figure 1.6.A and B). Ommatidia on the dorsal and ventral sides of the eye have

mirror image symmetry. The imaginary line that separates dorsal from ventral is called the equator. The *fz* pathway controls ommatidial polarity by regulating the R3/R4 cell fate, which indicates both ommatidia chirality and the following rotation of the ommatidia as a unit (Zheng, Zhang et al. 1995; Strutt and Strutt 1999).

The key regulators of the PCP pathway are encoded by the *dishevelled* (*dsh*), *prickle* (*pk*), *Van Gogh/strabismus* (*Vang/stbm*), *flamingo/starry night* (*fmi/stan*) and *diego* (*dgo*) genes. They are frequently termed core components of the PCP pathway, but they most likely act as a multiprotein complex. A mutation in any of these genes gives rise to autonomous polarity defects in the wing and eye, and often in other tissues (Gubb and Garcia-Bellido 1982; Vinson and Adler 1987; Theisen, Purcell et al. 1994; Zheng, Zhang et al. 1995; Taylor, Abramova et al. 1998; Wolff and Rubin 1998; Chae, Kim et al. 1999; Gubb, Green et al. 1999; Usui, Shima et al. 1999; Feiguin, Hannus et al. 2001). Importantly, their protein products are asymmetrically localised in polarised cells of the wing and eye (Usui, Shima et al. 1999; Axelrod 2001; Feiguin, Hannus et al. 2001; Shimada, Usui et al. 2001; Strutt 2001; Strutt, Johnson et al. 2002; Tree DR 2002; Bastock, Strutt et al. 2003; Rawls and Wolff 2003).

In the wing epithelium, PCP is obvious by the outgrowth of a single actin- and tubulin-filled, distally pointing hair at the distal vertex of a wing cell (Adler 2002). Studying the phenotype of PCP gene mutants, it can be demonstrated that they subdivide into two main classes. Upstream members of the pathway, like *fz*, *dsh*, *pk*, *fmi* and *stbm*, lead to wing hairs pointing in a stereotypical incorrectly orientated pattern, signifying that they are necessary for the polarization of wing cells. On the contrary, abolishing or increasing the function of genes, which are more downstream in the pathway, like *rhoA* and the *Drosophila rho-associated kinase* (*Drok*), interferes with the number but not the polarity of the hairs, revealing that they are needed for the formation but not for polarization of wing hairs (Winter, Wang et al. 2001; Adler 2002).

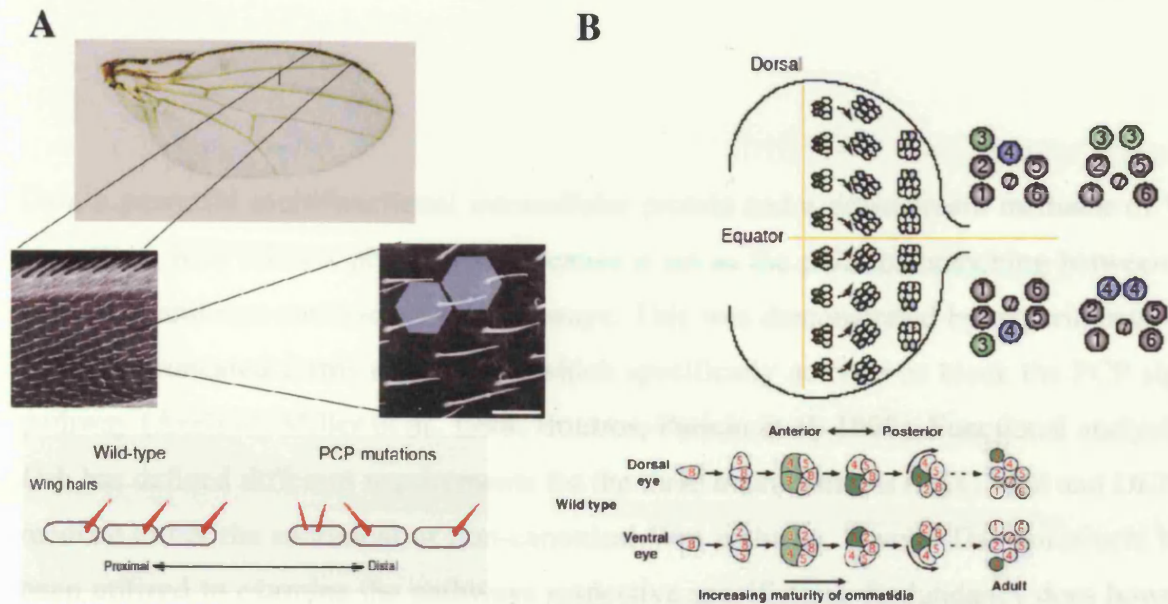


Figure 1.6. *Drosophila* wing and eye (A) *Drosophila* wing. External appearance of a wing: proximal to the left and distal to the right. Enlargement of wing surface covered with hairs. All wing hairs are pointing towards the distal end. Further enlargement: octagons represent each cell. Hairs distally located. Mutations of PCP genes cause disorder of wing hairs. PCP coordinates the organization of wing hairs. Loss of PCP genes in the wing can cause misorientation of hairs, or multiple hairs to form in a single cell. (B) Model for generation of polarity in eye development. Initially ommatidial preclusters are organized in the anterior–posterior axis and are symmetrical. Next they rotate 90° towards the equator (the D–V midline), and at the end chirality is created by the positions of the R3 and R4 cells. In the upper right side, representation of chiral arrangement of the respective ommatidia. Additionally, to the two chiral forms, symmetrical clusters with R3/R3 or R4/R4 cell pairs can be found in PCP mutants. R3 cells are highlighted in green and R4 cells in blue. In the down right side corner another representation of the eye, ommatidia are gradually formed by the aggregation of eight photoreceptor cells (R1–R8), and become polarised. In the R3/R4 cell pair (light green) for a correct chirality, the R3 cell (dark green) must rotate 90° clockwise in the dorsal half of the eye or anticlockwise in the ventral half. Adapted from Ueno and Greene (2003); Fanto and McNeill (2004); Moldzik (2002) and Strutt (2003)

Dsh, a powerful multifunctional intracellular protein and a downstream mediator of Wnt signalling, here takes a pivotal role because it act as the point of branching between the canonical and non-canonical Wnt pathways. This was demonstrated by experiments with different truncated forms of the Dsh, which specifically activate or block the PCP signal pathway (Axelrod, Miller et al. 1998; Boutros, Paricio et al. 1998). Functional analysis of Dsh has defined different requirements for the three main domains (DIX, PDZ and DEP) to mediate either the canonical or non-canonical Wnt pathway. Several Dsh constructs have been utilized to examine the pathways respective specificities. Redundancy does however exist between them: there is always some residual β -catenin signalling activity observed in the absence of one of the three conserved domains (Axelrod, Miller et al. 1998; Rothbacher, Laurent et al. 2000; Wallingford, Rowning et al. 2000). Thus activation of the PCP pathway requires regulation of Dsh and its accumulation at plasma membrane and it is the carboxy-terminus, the DEP domain, which is most important for the PCP pathway (Boutros and Mlodzik 1999) .

In *Drosophila*, the polarization and formation of hair cells involves the localized accumulation of PCP proteins, such as Fz and Dsh, at the distal edge of the corresponding wing cell (Strutt 2003). To explain in more detail, planar polarity in any part of the body in *Drosophila* could be controlled by a group of cells, maybe by the release of a putative morphogen that initiates the establishment of PCP. The gradient of a morphogen could provide a “polarity vector” to orient cells. Another possible mechanism is that a small group of cells could organize a bigger region if they release a signal that propagates across a tissue (Adler 2002). In the wing it is not really known which gene is involved in the production of a morphogen gradient. It could be Wingless, which is a probable ligand for the Fz receptor and that may possibly exist in a gradient across the wing (Adler, Krasnow et al. 1997; Axelrod 2001; Strutt 2001). Thus each cell would have a gradient of Fz signalling activity across its proximo-distal axis. Pk and Vang/Stbm are involved with Fz when this long range polarity cue is created. Considering the fly phenotypes and the genetic interactions between these loci, it has been postulated that they act all together to regulate a long range polarity signal (Adler, Taylor et al. 2000). Also *fmi/stan* could function by propagating polarity cues, as very weak non-autonomous phenotypes have been observed around *fmi/stan* clones (Chae, Kim et al. 1999; Usui, Shima et al. 1999). To be more

specific, in the wing of *Drosophila* the localised *fz* activity at the distal cell edge is due the Fz receptor being localised there (Strutt 2001). Dsh colocalises with Fz in this place (Axelrod 2001; Shimada, Usui et al. 2001). Therefore, Fz/Dsh signalling activity is confined to this part of the cell. Fmi/Stan, Vang/Stbm, Pk and Dgo proteins also become asymmetrically localised on the proximo-distal axis. Fmi/Stan and Dgo localize both proximally and distally (Usui, Shima et al. 1999; Feiguin, Hannus et al. 2001), while Vang/Stbm and Pk are found at proximal edge (Tree DR 2002; Bastock, Strutt et al. 2003) (Figure 1.7.A).

In the eye there is also asymmetric localization of these key regulators proteins especially in the R3/R4 photoreceptor pair. Fz preferentially localises on the R3 side of the R3/R4 border, while Vang/Stbm preferentially localises on the R4 border (Strutt, Johnson et al. 2002). Thus, the R3/R4 boundary appears to be similar to the distal/proximal cell boundary in the wing (Figure 1.7B) (Strutt, Johnson et al. 2002; Rawls and Wolff 2003).

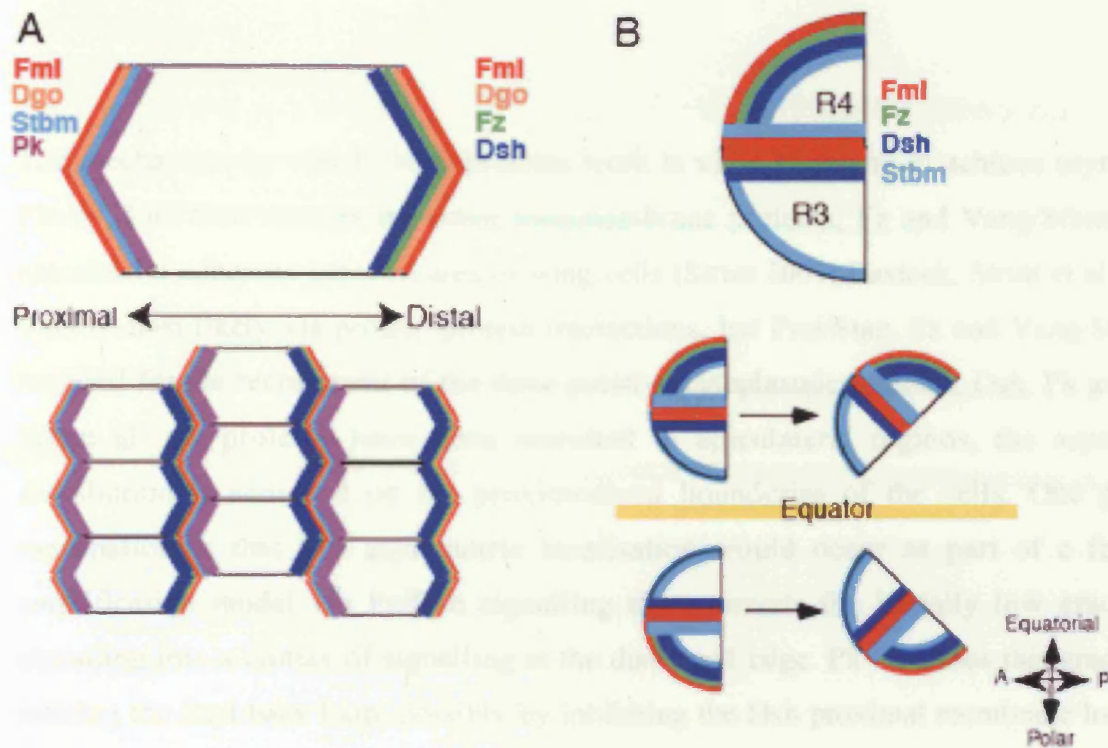


Figure 1.7. Polarized subcellular distribution of PCP genes in wing and eye cells. (A) Fz and Dsh accumulate on the distal membranes, Stbm and Pk accumulate on proximal side, and Fmi and Diego appear to be enriched on both sides. All are depleted from anterior and posterior membranes. Pk might act in an intercellular feedback loop to increase some initial bias by repeling Dsh from the proximal half of the cell while favouring Fz and Dsh to the distal side of the adjacent cell (Tree et al., 2002) (B) PCP proteins accumulate specifically at the R3/R4 interface. Fz and Dsh accumulate on the R3 cell at the R3/R4 interface, whereas Stbm is enriched in the R4 cell at the R3/R4 interface. It is not known where Pk is localized in the eye but may be a feedback loop similar to that proposed in the wing also functions in the eye. Adapted from Fanto and McNeill (2004).

The mechanism by which these proteins work is via a hierarchy to achieve asymmetry. Firstly, Fmi/Stan recruits the other transmembrane proteins, Fz and Vang/Stbm, to the apicolateral adherens junction area of wing cells (Strutt 2001; Bastock, Strutt et al. 2003). This is most likely via protein-protein interactions, but Fmi/Stan, Fz and Vang/Stbm are required for the recruitment of the three putative cytoplasmic proteins, Dsh, Pk and Dgo. When all six proteins have been recruited to apicolateral regions, the asymmetric distribution is achieved on the proximodistal boundaries of the cells. One possible explanation is that this asymmetric localisation would occur as part of a feedback amplification model via Fz/Dsh signalling that converts the initially low gradient of signalling into a climax of signalling at the distal cell edge. Pk increases this gradient by refining the feed back loop, possibly by inhibiting the Dsh proximal membrane localisation (Tree DR 2002). Alternatively, Fz/Dsh signalling may be triggered by ligand-independent activation of signalling, maybe by receptor clustering (Krasnow, Wong et al. 1995; Adler, Krasnow et al. 1997). Another possible mechanism could be that Fmi/Stan or Vang/Stbm could interact directly with the Fz receptor and act as ligands. Still the issue of the establishment of asymmetric distribution of the PCP proteins remains unsolved.

The atypical cadherins encoded by the genes *dachsous* (*ds*) and *fat* (*ft*) have non-autonomous action in planar polarity in the wing (Adler, Charlton et al. 1998). The type II transmembrane protein encoded by the *four-jointed* (*ff*) gene (Villano and Katz 1995; Brodsky and Steller 1996) also has non-autonomous activity in the regulation of planar polarity in the eye and wing (Zeidler, Perrimon et al. 1999; Zeidler, Perrimon et al. 2000). Work from different groups has revealed a molecular mechanism in which gradients of *ds*, *ft* and *ff* activities in the developing wing, eye and abdomen generate a long-range polarity signal (Zeidler, Perrimon et al. 1999; Zeidler, Perrimon et al. 2000; Casal, Struhl et al. 2002; Rawls, Guinto et al. 2002; Strutt and Strutt 2002; Fanto, Clayton et al. 2003). It is proposed that Ds (expressed in a graded way) inhibits Ft in a concentration-dependent manner, giving rise to a gradient of Ft activation with its high level at the equator in the eye. Ft supposedly activates Fz, generating a gradient of Fz activity that possibly specifies R3 and R4 cell fates and ommatidial polarity and chirality. In mosaic analyses, *ff* supports R3 development in a *ds*-dependent manner, signifying that *ff* functions upstream of *ds*. Many elements of this model mechanism are still missing, but epistatic analysis, suggest

that this pathway acts in parallel to *fz*, *Vang/stbm* and *pk*. There is evidence that *ff* may be controlling cell adhesion by modulating Ds/Ft heterophilic interactions (Strutt and Strutt 2002).

Subsequently, the second class of genes, the downstream components of the PCP, probably control the actin and microtubule cytoskeletons and become localized in the distal region, maybe initiating the outgrowth of a single hair (Eaton 1997). The downstream components frequently act in a subset of tissues where polarity is regulated by the core polarity genes. In addition, they often only control a subgroup of the downstream responses to core planar polarity protein activity. It has been proposed that upstream components of the PCP pathway give cell polarity by determining the place where the wing hair will come out, whereas downstream components control or associate with the actin and microtubule cytoskeleton, thereby regulating wing hair formation itself. Defects in these genes usually affect the hairs by mispolarisation or each cell produces more than one hair, affecting hair number (Adler 2002). Another suggestion for an interaction of these downstream components with the cytoskeleton comes from reports in which embryos were treated with drugs that antagonize the cytoskeleton, resulting in phenotypes looking very similar to mutant phenotypes of those regulators (Adler 2002). Possible downstream regulators are also *RhoA* (Strutt, Weber et al. 1997; Strutt, Johnson et al. 2002) and *Drok* (Winter, Wang et al. 2001). Furthermore, it has been proposed that a JNK cascade acts downstream of RhoA in the control of ommatidial polarity (Weber, Paricio et al. 2000).

II.1.2.2. Non-Canonical Wnt Signalling in Vertebrates

Recent studies suggest that the non-transforming Wnt ligands, especially Wnt5 and Wnt11, activate a Fz/Dsh-dependent pathway that is analogous to the *Drosophila* planar polarity pathway and regulates cell polarization during vertebrate gastrulation (Heisenberg, Tada et al. 2000; Tada and Smith 2000; Wallingford, Rowning et al. 2000; Wallingford and Harland 2001; Kilian, Mansukoski et al. 2003). This pathway shares significant similarities with the planar cell polarity pathway (PCP) in *Drosophila*. This vertebrate counterpart of the *Drosophila* PCP pathway is also involved in the regulation of other co-ordinated morphogenetic events such as neural tube closure and in the polarized orientation of sensory hair cells in vertebrate ears (Kibar, Vogan et al. 2001; Murdoch, Rachel et al. 2001; Wallingford and Harland 2001; Goto and Keller 2002; Hamblet, Lijam et al. 2002; Curtin, Quint et al. 2003; Montcouquiol, Rachel et al. 2003).

During vertebrate gastrulation, two main discoveries - the functional characterization of Dsh in *Xenopus* and the genetic analysis of the *silberblick* (slb)/wnt11 mutant in zebrafish provided initial data that a Wnt signalling pathway different from the canonical pathway is implicated in regulating gastrulation movements (Heisenberg, Tada et al. 2000; Tada and Smith 2000; Wallingford, Rowning et al. 2000).

The functional analysis of Dsh has defined different requirements for the three main domains (DIX, PDZ and DEP) to mediate either the canonical or non-canonical Wnt pathway. The single-domain deletion construct, Dsh- Δ DIX, blocks canonical β -catenin signalling. In contrast, the DEP domain is absolutely necessary for *Drosophila* PCP and vertebrate CE (Axelrod, Miller et al. 1998; Boutros, Paricio et al. 1998; Heisenberg, Tada et al. 2000). The Dsh Δ -DIX construct, which specifically activates the non-canonical Wnt pathway, can rescue the dominant-negative Wnt11 mediated inhibition of the elongation of activin-treated *Xenopus* animal caps, an *ex vivo* model used to study convergent extension in *Xenopus* (Tada and Smith 2000). Additionally, interference in non-canonical Wnt pathway disrupts mediolateral cell protrusions and cell polarity in cells under going convergent extension in *Xenopus* embryos (Wallingford, Rowning et al. 2000). Another

important piece of evidence is that wild-type Xdsh-GFP was translocated to cell membranes during CE (Wallingford, Rowning et al. 2000). This behaviour is characteristic of the activation of Dsh during planar cell polarity in *Drosophila* (Axelrod 2001; Shimada, Usui et al. 2001), even though in *Xenopus*, Xdsh-GFP seems to be uniformly spread with the membrane rather than a particular distribution. A recent study has proved that PKC δ (Protein kinase C δ) is also essential to control cell polarity and the change in cell shape by associating with Dsh during convergent extension (Kinoshita, Iioka et al. 2003).

II.1.2.2.1 Proposed non-canonical Wnt Pathway in Zebrafish

In zebrafish, several mutants exhibiting defective gastrulation movements have been identified (Hammerschmidt, Pelegri et al. 1996; Solnica-Krezel, Stemple et al. 1996). The two mutants, *trilobite* (*tri*) and *knypek* (*kny*), show the most dramatic extension defect of body axis, in which both convergence and extension are affected. The phenotype of *pipetail* (*ppt*) mutants embryos display defects only in morphogenetic processes underlying tail outgrowth and cartilage differentiation in the head (Rauch, Hammerschmidt et al. 1997). In *silberblick* (*slb*) mutants, convergent extension movements of the axial mesendoderm, and overlying ventral central nervous system (CNS) midline are disturbed, resulting in a transiently shortened and broadened body axis at the end of gastrulation and in a fusion of eyes (cyclopia) at later developmental stages. In *slb* mutants there is a gap between the anterior tip of the midline of the central nervous system (CNS) and the anterior edge of the neural plate (Heisenberg, Brand et al. 1996; Heisenberg and Nusslein-Volhard 1997).

On the contrary, *ppt*, *kny* and *tri* embryos have a shortened body axis from late gastrulation stages whereas the position of the eyes is only slightly changed (Hammerschmidt, Pelegri et al. 1996; Solnica-Krezel, Stemple et al. 1996; Marlow, Zwartkruis et al. 1998). Positional cloning of the *slb*, *ppt*, *kny* and *tri* loci has showed that they encode components involved in the Wnt signalling. It was shown that *slb* and *ppt* encode for Wnt ligands, Wnt11 and Wnt5, respectively (Rauch, Hammerschmidt et al. 1997; Heisenberg, Tada et al. 2000) while *kny* encodes a co-receptor glypican4/6 of the family of heparan sulphateproteoglycans, implicated in Wg/Wnt signalling (Topczewski, Sepich et al. 2001).

Positional cloning of the *tri* locus has revealed that it encodes Strabismus (Stbm), a core PCP protein (Jessen, Topczewski et al. 2002).

Additionally, extensive analysis has shown that the *slb* eye phenotype results from reduced elongation of the body axis during gastrulation. The *slb* locus encodes Wnt11, which expression pattern begins to be expressed in the dorsal region of the germ ring at dome stage, during gastrulation *wnt11* expression spreads out to the lateral and ventral germ ring, while at shield stage this expression in the germ ring becomes restricted to the epiblast layer (Ulrich, Concha et al. 2003). Later, the expression of *wnt11* is restricted to the anterior paraxial mesoderm and to the anterior lateral neuroectoderm by late gastrula stage. To understand the genetic and cellular mechanisms of Slb function, different approaches were used. Cell-labelling and tracking experiments demonstrated that the shortened body length of *slb* mutants is due to reduced cell intercalations along the medio-lateral axis during gastrulation. Also by cell and shield-transplantation experiments, it was elucidated that Slb/ Wnt11 acts cell-non-autonomously and that its required within paraxial tissues to drive normal convergent extension movements of axial and paraxial tissues (Heisenberg, Tada et al. 2000).

It was also shown that the *slb* phenotype is rescued by a truncated form of Dsh, which specifically transduces the PCP pathway in *Drosophila* and that does not signal through the canonical Wnt pathway. This suggests that, as in *Drosophila*, zebrafish Dsh is an intracellular mediator of both the canonical Wnt and PCP signalling pathways (Heisenberg, Tada et al. 2000). All these studies suggest that Slb/Wnt11 regulates convergent extension movements in zebrafish through a pathway similar to the PCP cascade in *Drosophila*.

Analyzes of the cellular function of *slb/wnt11* during zebrafish gastrulation have demonstrated that this gene is necessary in both epiblast and hypoblast cells for polarized growth of processes aligned to their individual movement directions and that failure of cell polarization in *slb* mutants is correlated with slower and less persistent movements of these cells at the beginning of gastrulation (Ulrich, Concha et al. 2003). This implies that *slb/wnt11* permits cells to correctly polarize in line with their individual movement directions and suggests that cell polarization is necessary to help stabilize cell movements.

Furthermore, other loci/genes genetically interact with *slb/wnt11* in controlling convergent extension movements. The *ppt/wnt5* mutants embryos have mild defects in convergent extension movements of the posterior body axis (Rauch, Hammerschmidt et al. 1997). However, double mutants for *slb/wnt11* and *ppt/wnt5* show a strong reduction in convergent extension, producing a more severe phenotype, possibly because Ppt/Wnt5 and Slb/Wnt11 have a functional redundancy or have partially overlapping functions (Kilian, Mansukoski et al. 2003). This is consistent with studies in *Xenopus* that demonstrated that Wnt5 can signal through a non-canonical Wnt-pathway to influence convergent extension movements during gastrulation (Wallingford, Vogeli et al. 2001, Du et al., 1995). Because of all this data, it is unexpected that zebrafish *wnt11* and *wnt5* are expressed in non-overlapping domains (anterior *versus* posterior) at tail bud stage, signifying that they have some broad cell-non-autonomous activity during late gastrulation. Alternatively, this could be due to the overlapped expression of the two genes in the germ ring at the early stage, especially at shield stage (Kilian, Mansukoski et al. 2003).

There is evidence that Fz7 could interact with Wnt11, in a receptor-ligand interaction to regulate convergent extension movements, in *Xenopus* animal cap explants (Djiane, Riou et al. 2000). In more detail, overexpression of Xfz7 affects the movements of CE. It changes the correct localization, but not the expression, of both mesodermal and neural markers. These effects can be rescued by extra-Xfz7, which is a secreted form of the receptor that weakly inhibits CE in overexpression. This suggests that the wild-type and truncated receptors have opposing effects when co-expressed and that over-expression of Xfz7 causes an increased signalling activity. Coherent with this, Xfz7 biochemically and functionally interacts with Xwnt11. Already some downstream regulators have already been proposed such as Cdc42 (Djiane, Riou et al. 2000).

The molecular analysis and functional studies of these mutants and the detection of more downstream components involved in the function of these genes during gastrulation have revealed a signalling pathway with high homology to the Fz/PCP pathway in *Drosophila*. Shared components include the Wnt receptors Fz2 and Fz7, the intracellular signalling mediator Dsh, as discussed above, the cytoplasmic protein Daam1, the small GTPases RhoA, Rac and Cdc42 and the Rho effector kinase Rok2 (Djiane, Riou et al. 2000; Heisenberg, Tada et al. 2000; Wallingford, Rowning et al. 2000; Habas, Kato et al. 2001;

Marlow, Topczewski et al. 2002; Habas, Dawid et al. 2003). Other regulators, which are involved some how with this signalling pathway, are the JNK module, the ankyrin repeat protein Diego, the transmembrane protein Strabismus/VanGogh, the protein phosphatase PP2A and the cytoplasmic protein Prickle (Pk) (Darken, Scola et al. 2002; Goto and Keller 2002; Hannus, Feiguin et al. 2002; Jessen, Topczewski et al. 2002; Park and Moon 2002; Schwarz-Romond, Asbrand et al. 2002; Yamanaka, Moriguchi et al. 2002; Carreira-Barbosa, Concha et al. 2003; Takeuchi, Nakabayashi et al. 2003; Veeman, Slusarski et al. 2003) (Figure 1.8).

Additional confirmation for a conserved pathway has come from data that vertebrate homologues of core PCP genes are also required for CE. A combination of overexpression, morpholino data and mutant studies have revealed a role for *Vang/stbm* in controlling gastrulation movements in fish and frogs (Darken, Scola et al. 2002; Goto and Keller 2002; Jessen, Topczewski et al. 2002; Park and Moon 2002). Epistasis analysis shows that *tri/stbm* probably acts in parallel pathway to Fz/Dsh rather than in a linear pathway in zebrafish (Jessen, Topczewski et al. 2002). These data go in support with epistasis data in flies (Taylor, Abramova et al. 1998).

Although there are no known mutations for vertebrate *pk* homologs, morpholino experiments have been used to demonstrate a similar function for zebrafish and *Xenopus pk* genes in being required for CE movements (Carreira-Barbosa, Concha et al. 2003; Takeuchi, Nakabayashi et al. 2003; Veeman, Slusarski et al. 2003). All the mutants and morphant embryos show defective CE movements without affecting cell fates, but also strong double-mutant, double-morpholino, or mutant/morpholino interactions have been detected between *slb* and *ppt* (Kilian, Mansukoski et al. 2003), *pk1* and *tri* ((Carreira-Barbosa, Concha et al. 2003; Veeman, Slusarski et al. 2003), *pk1* and *slb* (Carreira-Barbosa et al., 2003), and *pk1* and *ppt* (Carreira-Barbosa, Concha et al. 2003). In agreement with the genetic and physical interactions in *Drosophila* Pk and Vang/Stbm (Taylor, Abramova et al. 1998; Bastock, Strutt et al. 2003), zebrafish Pk and Vang/Stbm interact synergistically in regulating CE (Carreira-Barbosa, Concha et al. 2003; Veeman, Slusarski et al. 2003). (Figure 1.8.).

Finally, a zebrafish homologue of *diego*, a core PCP gene, has been identified as Diversin, which is ankyrin repeat protein, a molecule involved with canonical and non-canonical Wnt signalling, the loss of function produces defects in gastrulation movements (Schwarz-Romond, Asbrand et al. 2002).

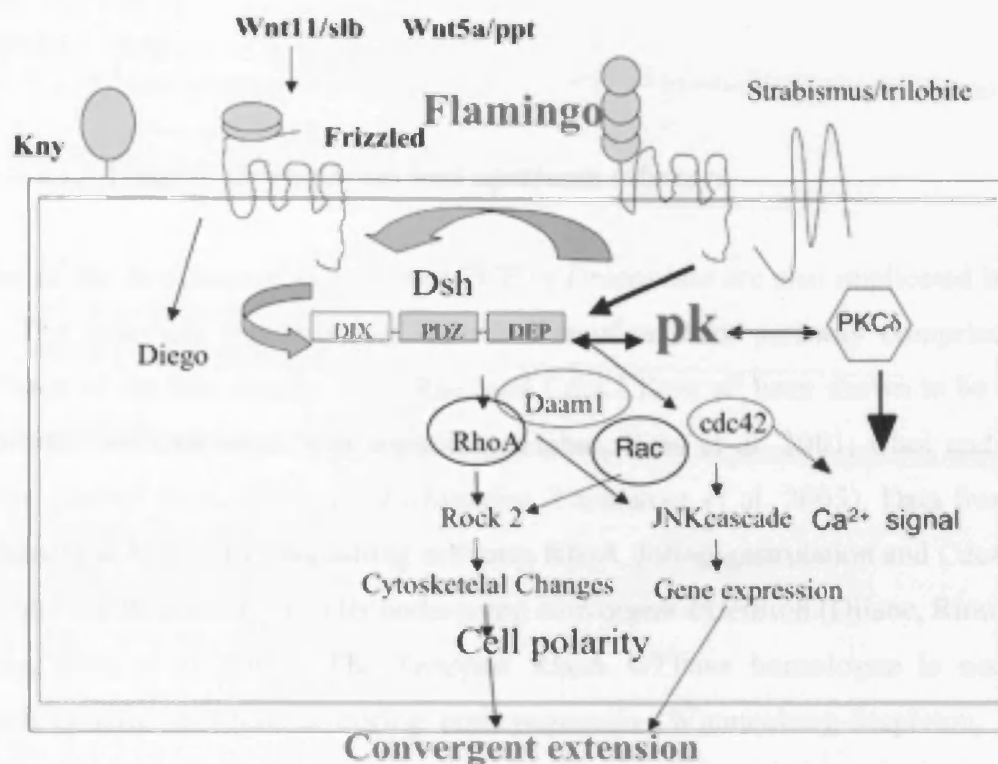


Figure 1.8. Updated model for the Wnt non Canonical pathway regulating CE during gastrulation in vertebrates (mainly zebrafish and *Xenopus*). The ligands, Wnt11/Slb and Wnt5a/Ppt, supposedly bind to the receptor Frizzled-7, an interaction facilitated by the proteoglycan co-receptor Kny. This leads to translocation of Dsh to the membrane. The PDZ and DEP domains of Dsh are responsible for the specificity of the CE/PCP pathway. Dsh also regulates the activity of members of the Rho family of small GTPases. RhoA, which binds to Daam1 with Dsh and activates the effector Rock, that directly controls the actin cytoskeleton. In addition, Dsh-mediated activation of Cdc42 signals to JNK that in turn regulates transcription of target genes. These two branches collaborate to regulate CE during zebrafish/*Xenopus* gastrulation (see also text). The Wnt/Ca²⁺ pathway may be a another branch of the non canonical Wnt pathway (see also text). As in the *Drosophila* PCP, Prickle, Flamingo and Strabismus seem to have the same role in this process, but not in a linear way. Adapted from Masa *et al* (2002) and Veeman *et al.* (2003).

II.1.2.2.1.1 Possible downstream and upstream effectors

Some of the downstream effectors of PCP in *Drosophila* are also implicated in vertebrate CE. The potential regulators of the non-canonical Wnt pathway comprise the small GTPases of the Rho family. Rho, Rac, and Cdc42 have all been shown to be involved in vertebrate non-canonical Wnt signalling (Habas, Kato et al. 2001; Choi and Han 2002; Habas, Dawid et al. 2003; Penzo-Mendez, Umbhauer et al. 2003). Data from *Xenopus* revealed that Wnt11/Fz7 signalling activates RhoA during gastrulation and Cdc42 may be a mediator for Wnt11/Fz7 in cells undergoing convergent extension (Djiane, Riou et al. 2000; Habas, Kato et al. 2001). The *Xenopus* RhoA GTPase homologue is necessary for morphogenetic movements during embryogenesis (Wunnenberg-Stapleton, Blitz et al. 1999), which probably is stimulated by binding to Dsh and through the novel Formin homology protein Daam1 (Habas, Kato et al. 2001). Additionally, the probable RhoA effector Rho kinase 2 acts downstream of the non-canonical Wnt pathway (Marlow, Topczewski et al. 2002). But there is some contradiction about whether activating Rho also activates both Cdc42 and Rac or Rac alone (Choi and Han 2002; Habas, Dawid et al. 2003; Penzo-Mendez, Umbhauer et al. 2003). Recently, a study demonstrated that blocking Has2 (synthesizing enzyme of polysaccharide hyaluronan (HA)) function in zebrafish embryo obstructs the ability of cells to form lamellipodia and to make dorsal convergence movements, suggesting a role of hyaluronan glycosaminoglycan in early morphogenesis (Bakkers, Kramer et al. 2004). These defects can be partially rescued by ectopic expression of the small GTPase Rac, signifying that, in zebrafish and cell culture, Rac is a key regulator of hyaluronan, an extracellular compound. In spite of these problems, the Rho family GTPases and their effectors is still the most evident link between non-canonical Wnt signalling and cytoskeletal rearrangement necessary for orchestrating CE.

Another possible downstream regulator of the non-canonical Wnt is the Jun amino-terminal kinase (JNK) signalling pathway. It was reported that mutant forms of Dsh, that have a PCP phenotype in *Drosophila* could activate the JNK in vertebrate cells (Boutros, Paricio et al. 1998; Li, Yuan et al. 1999; Moriguchi, Kawachi et al. 1999). In more detail, the C-terminal DEP domain is necessary for JNK induction and is essential for the rescue planar polarity

defects in flies, signifying a connection with the PCP pathway (Boutros, Paricio et al. 1998; Li, Yuan et al. 1999; Moriguchi, Kawachi et al. 1999). The DEP domain alone, generally is antimorphic with respect to the PCP pathway is sufficient to induce JNK activity (Boutros, Paricio et al. 1998; Li, Yuan et al. 1999; Moriguchi, Kawachi et al. 1999). It has been also shown that vertebrate homologues of Vang/Stbm, Pk and Diego can activate the JNK pathway in a zebrafish and *Xenopus* mainly in a biochemical and in cell culture context (Park and Moon 2002; Schwarz-Romond, Asbrand et al. 2002; Takeuchi, Nakabayashi et al. 2003; Veeman, Slusarski et al. 2003). JNK has also been reported to be activated via the non canonical Wnt pathway involving PKC (protein kinase C) in *Xenopus* (Pandur, Maurus et al. 2002), which is less obviously analogous to PCP in *Drosophila*. However, it is very difficult to have any solid conclusions about the involvement of the JNK pathway in the non canonical Wnt signalling since these experiments used different tests for JNK induction and the activations observed were fairly small. It needs to be clarified whether the JNK pathway is relevant to the activation of the non-canonical Wnt pathway in the gastrula embryo, as components of the JNK pathway have an insignificant function in PCP in flies (Boutros, Paricio et al. 1998; Weber, Paricio et al. 2000; Strutt, Johnson et al. 2002).

In addition to the activation of small GTPases by the non-canonical Wnts, there is evidence that heterotrimeric G proteins may be involved downstream of Fz. Stimulation of calcium flux in zebrafish embryos by noncanonical Wnts and Frizzleds is sensitive to pertussis toxin (Slusarski, Yang-Snyder et al. 1997), as is PKC (protein kinase C) and CamKII (calmodulin-dependent protein kinase) activation in *Xenopus* (Sheldahl, Park et al. 1999; Kuhl, Sheldahl et al. 2000) (detailed in the next section II.1.2.2.3.). Dsh Δ -DIX promotes calcium influx in a pertussis toxin-insensitive mode, suggesting that Dsh acts downstream of the heterotrimeric G proteins (Sheldahl, Slusarski et al. 2003). Moreover, a recent study suggests that G $\beta\gamma$ subunits may be the important module in this situation (Penzo-Mendez, Umbhauer et al. 2003). Involvement of specific heterotrimeric G protein subunits in non-canonical Wnt signalling still remains to be elucidated by loss-of-function techniques vertebrate embryos.

II.1.2.2.2. Mouse mutants with phenotypic defects due to defective CE

Closure of the neural tube is a very important event in the organization of the nervous system of vertebrates. The neural plate develops bilateral neural folds at its connection with non-neural ectoderm at the surface. The folds elevate, come into contact in the midline, and fuse to give rise to a tube that will be covered with epidermal ectoderm. Failure of any step of this morphogenetic sequence of events leaves the neural tube 'open', a condition that characterizes a group of severe human congenital malformations: the neural tube defects.

The vertebrate homologues of PCP genes can affect CE of neural tissues in *Xenopus* embryos, leading to defects in neural tube closure (Wallingford and Harland 2001; Goto and Keller 2002). Because of this, the necessity for CE during the beginning of neural tube closure has become clear. Furthermore, mutations in the *Vang/stbm*, *dsh* and *fmi/stan* homologues in mouse give defects in neural tube closure, that possibly result from abnormal CE of the neural plate in mutant mice (Kibar, Vogan et al. 2001; Murdoch, Rachel et al. 2001; Hamblet, Lijam et al. 2002; Curtin, Quint et al. 2003). In addition, the mouse mutants, *loop-tail*, *crash*, *circletail* and *dishevelled-1;dishevelled-2* double mutants, fail to undergo neural tube closure, resulting in craniorachischisis (when almost the entire neural tube from the midbrain to the lower spine remains open). Positional cloning demonstrates that the mutant genes encode proteins that have roles in non-canonical Wnt/frizzled signalling (Kibar, Vogan et al. 2001; Murdoch, Rachel et al. 2001; Curtin, Quint et al. 2003; Montcouquiol, Rachel et al. 2003; Murdoch, Chadwick et al. 2003). *loop-tail* is a mutation in the mouse orthologue of the *Drosophila* gene *strabismus/Van Gogh* (*Vang*), called *Vangl2*. *crash* mice have a mutation in *Celsr1*, which is a vertebrate orthologue of the *Drosophila* gene *flamingo/starry night* (*stan*). *Scrb1*, is tumour suppressor gene that is mutated in *circletail*, is also involved in PCP (Montcouquiol, Rachel et al. 2003), even though it regulates apical-basal polarity in *Drosophila*. The homozygotes for *loop-tail*, *circletail* and *crash* have severe neural tube defects, but also the double mutants *loop-tail; circletail* and *loop-tail; crash* have this phenotype (Murdoch, Rachel et al. 2001). This reveals that these regulators have a common developmental function.

A specific example of the function of planar polarity in vertebrates is the polarization of sensory hair cells in sense organs, as illustrated by the stereocilia in the cochlears of

mammalian ears (Lewis and Davies 2002). Similar to CE, this process is probably regulated by homologues of the PCP genes such as *Vang/stbm* and *fmi/stan* (Curtin, Quint et al. 2003; Montcouquiol, Rachel et al. 2003), and *Wnt7a* has also been implicated in this process (Dabdoub, Donohue et al. 2003). In relation to *Fmi*, the three mouse homologs of *fmi* are expressed in the organ of Corti (Shima, Copeland et al. 2002) and also the two mutant mice *spin cycle* and *crash*, which carry independent mutations in one of the homologs of mice, *Celsr1*. These mutant mice have an abnormal head-shaking behaviour that might be correlated with defective neural tube closure (Curtin, Quint et al. 2003).

As a consequence, there is a good indication that a pathway conserved from flies to mammals employs non-canonical Wnt/Fz signalling to organise cell polarisation. Homologues of all PCP genes act in vertebrates, however, it is still unknown if all PCP proteins operate together in the many contexts in which they act in vertebrates.

II.1.2.3. Calcium Pathway

The non canonical Wnt pathway appears to play a role in gastrulation not just via the Wnt/PCP pathway described above, but also through a pathway regulating intracellular calcium levels, the so called Wnt/ Ca^{2+} pathway. Several pieces of evidence support the idea that another possible bifurcation of the Wnt pathway controls intracellular Ca^{2+} levels and could be regulating convergent extension movements. Co-expression of *Xenopus wnt5a* with the rat *fz2* receptor in zebrafish embryos can increase the levels of intracellular Ca^{2+} through heteromeric G-proteins and inositoltriphosphate (IP_3) (Slusarski, Corces et al. 1997) and can therefore activate the two Ca^{2+} regulator enzymes Ca^{2+} /calmodulin-dependent protein kinase II (CamKII) and protein kinase C (PKC) (Kuhl, Sheldahl et al. 2000; Kuhl, Sheldahl et al. 2000; Sheldahl, Slusarski et al. 2003).

Recent experiments have shown that the Wnt/ Ca^{2+} pathway is regulating tissue separation during *Xenopus* gastrulation, suggesting that the Wnt/ Ca^{2+} pathway in vertebrates is necessary for the regulation of differential cell adhesiveness (Winklbauer, Medina et al. 2001). More specifically, interfering with *fz7* function gives rise to a failure of proper separation of the mesodermal and ectodermal layers, and this function could be mediated

via PKC in a G-protein-dependent manner. Thus Fz7 might regulate the adhesive characteristics of tissues during gastrulation by activation of the Ca^{2+} pathway but its inhibition does not directly affect CE (Winklbauer, Medina et al. 2001). Another study proposes that the Wnt/ Ca^{2+} pathway is Dsh-dependent and also Pk1 has the ability to stimulate calcium flux, suggesting that the Wnt/ Ca^{2+} and PCP pathways overlap to some extent (Sheldahl, Slusarski et al. 2003; Veeman, Slusarski et al. 2003). In more detail, full-length Dsh is able to activate both calcium signalling in the calcium flux, PKC, and CamKII assays. The Dsh- Δ DIX that is active in PCP signalling but not in canonical Wnt/ β -catenin signalling, was an activator in these assays suggesting the promiscuous role for Dsh (Sheldahl, Slusarski et al. 2003)(Figure 1.9).

Choi and Han have proposed a Dsh-independent Wnt/ Ca^{2+} pathway that activates PKC and directly affects CE by regulating the activity of the p21 GTPase, Cdc42 (Choi and Han 2002). Fascinatingly, PKC δ has been proposed to act as a complex with Dsh and is necessary for the translocation of Dsh to the cell membrane in response to Fz7, thereby regulating CE movements (Kinoshita, Iioka et al. 2003).

However, the exact role of these proteins in cell rearrangements during gastrulation is not fully understood (Figure 1.9); (Miller, Hocking et al. 1999; Kuhl, Sheldahl et al. 2000; Pandur, Maurus et al. 2002). In addition to the intracellular role of this pathway, Ca^{2+} -release into the extracellular space might play a role in the cell-cell-communication involving the co-ordination of cell movements during gastrulation (Slusarski, Corces et al. 1997; Tada and Concha 2001; Wallingford, Ewald et al. 2001). Calcium waves are generated dorsally in gastrula embryos with some frequency and transmitted to neighboring cells in long-range distances (Gilland, Miller et al. 1999). This event appears to be correlated with the initiation of CE dorsally. It is possible that Wnts regulates Ca^{2+} waves as their frequency is lowered when a dominant negative *xfz8* is over-expressed which inhibits both the canonical and non-canonical Wnt pathways. Together, these results suggest a permissive role for an intracellular Ca^{2+} signal in regulating CE (Wallingford, Ewald et al. 2001).

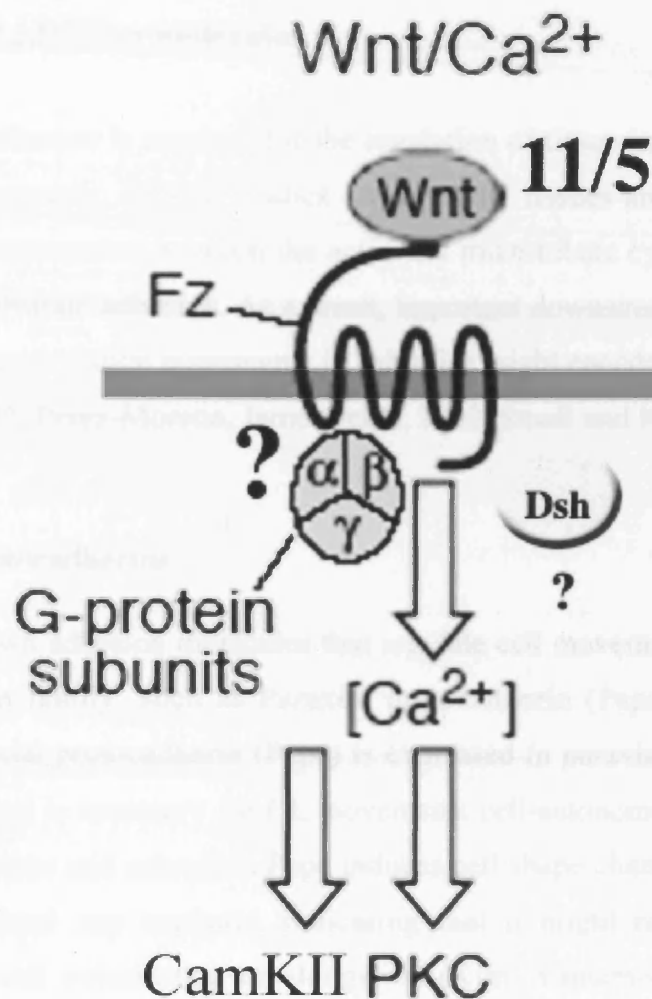


Figure 1.9. The Wnt/Ca²⁺ pathway probably signals via heterotrimeric G proteins and via Wnts, to mobilise intracellular Ca²⁺ and, to stimulate protein kinase C (PKC) and calcium/calmodulin-dependent kinase (CamKII). Whether this pathway needs Dsh remains controversial (see text for more details). In vertebrates, Wnt/Ca²⁺ signalling is activated by the same ligands as the PCP pathway, suggesting that these pathways may overlap. Adapted from Strutt (2003) and Veeman *et al.* (2003).

II.1.2.4. Cell adhesion molecules

Proper cell adhesion is required for the regulation of tissue integrity, cellular morphology and cell movements. Several studies on epithelial tissues and migrating cells showed a complicated connection between the actin and microtubule cytoskeleton and sites of cell-cell or cell-substrate adhesion. As a result, important downstream effectors of the pathways that controls gastrulation movements in zebrafish might encode the cell adhesion molecules (Wedlich 2002; Perez-Moreno, Jamora et al. 2003; Small and Kaverina 2003).

II.1.2.4.1. Protocadherins

The best-known adhesion molecules that regulate cell movements include members of the Protocadherin family, such as Paraxial protocadherin (Papc) and Axial protocadherin (Axp). Paraxial protocadherin (Papc) is expressed in paraxial mesendodermal tissues of the gastrula and is necessary for CE movements cell-autonomously in the mesendodermal tissue in *Xenopus* and zebrafish. Papc induces cell shape changes when over-expressed in *Xenopus* animal cap explants, indicating that it might regulate CE movements by determining cell polarization or elongation (Kim, Yamamoto et al. 1998; Yamamoto, Amacher et al. 1998). It was confirmed recently that XPAPC and Wnt/PCP signalling are not redundant, and the activity of both is necessary to regulate CE movements by activating RhoA (Medina, Reintsch et al. 2000; Unterseher, Hefele et al. 2004). Another protocadherin, Axpc, is involved in facilitating the homophilic sorting of notochordal precursor cells in the formation of the notochord in *Xenopus*, thus playing a role in tissue organization during gastrulation (Kuroda, Satoh et al. 2001). Although these results have shown a pivotal function of protocadherins in controlling gastrulation movements, little is known about the mechanism controlling gastrulation. In mouse and *Xenopus*, *papc* functions downstream of the transcriptional activator Lim1, which is expressed in the dorsal domain of the gastrulating embryo (Hukriede, Tsang et al. 2003). Work in zebrafish revealed that *papc* expression is controlled by *spadetail*, a T-box transcription factor necessary for morphogenetic movements during gastrulation (Ho and Kane 1990; Yamamoto, Amacher et al. 1998).

II.1.2.4.2. Non classical Cadherins

The best known non-classical cadherin is Fmi, which has a unique structure as a seven-pass transmembrane receptor with similarity to the secretin receptor, a member of family of the G protein coupled receptors (Usui, Shima et al. 1999; Uemura and Shimada 2003) (Figure 1.10.A.). But it remains unknown if Fmi is coupled to G proteins. Fmi also has a large extracellular domain composed of nine tandem arrays of cadherin repeats, which act as homophilic modules. Fmi also contains two laminin A globular domains and a cytoplasmic tail (Usui, Shima et al. 1999). Fmi is localised differentially at cell-cell boundary along the proximal-distal axis in the wing of *Drosophila* in a Frizzled (*fz*)-dependent manner (Usui, Shima et al. 1999). Fmi is possibly involved in the generation of different biological activities especially because of the amino acid sequences of the cytoplasmic domain that considerably diverge within the superfamily. Probably the initial signals are generated by the homophilic interactions of the cadherin repeats and then converted in different signals in cytoplasmic side (Takeichi, Nakagawa et al. 2000). Recent experiments performed in *Xenopus* suggested that Fmi could be blocking the non-canonical Wnt pathway by interacting with Fz, but this study just analyses effectors of the Wnt-canonical pathway and does not explore any possible function in gastrulation movements or CE movements (Morgan, El-Kadi et al. 2003).

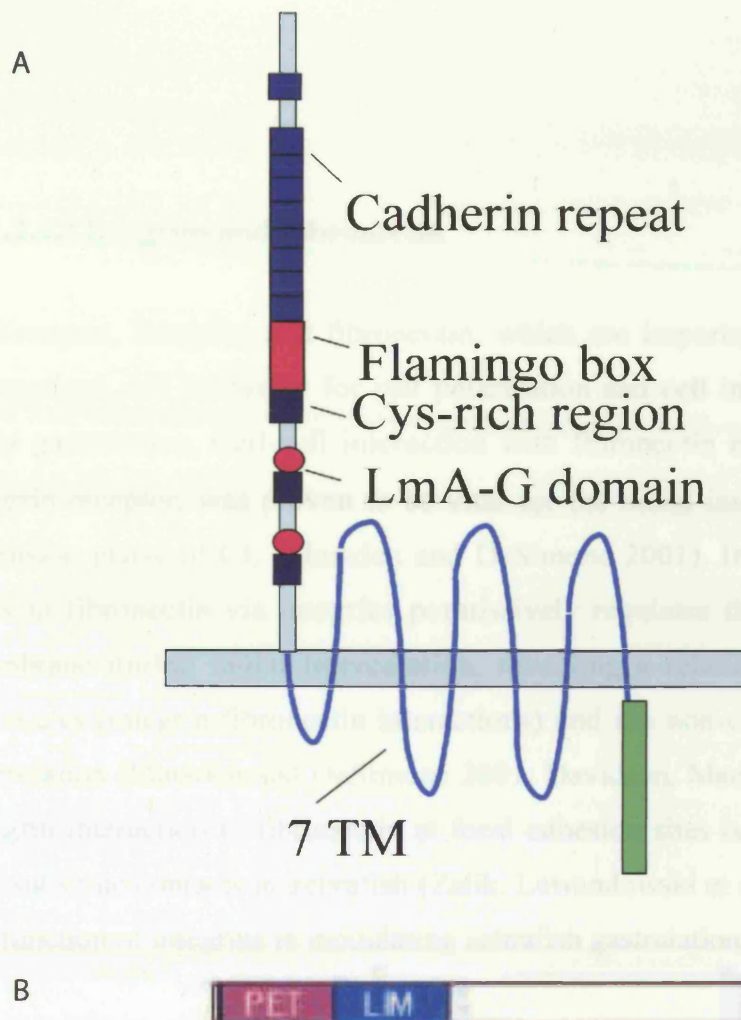


Figure 1.10. Structures of Flamingo and Prickle proteins. (A) Flamingo is a seven-pass transmembrane receptor (7 TM) with similarity to the secretin receptor, a member of family of the G protein coupled receptors (Uemura et al. 1998; Usui et al.1999). Fmi has a large extracellular domain composed of tandem arrays of cadherin repeats (9), which act as homophilic modules, and three cysteine-rich regions (Cys-rich), two laminin A globular domains (LmA-G) and a cytoplasmic tail. It also contains a sub domain called the Fmi box. (B) *pk* encodes an cytoplasmic protein containing a conserved "PET" domain (for Prickle, Espinas and Testin) and three LIM domains involved in protein-protein interaction. Adapted from Uemura et al. 1998; Usui et al.1999 ; Gubb et al. (1999) and Carreira-Barbosa et al. (2003)

II.1.2.4.3.Integrins and Fibronectin

In *Xenopus*, integrins and fibronectin, which are important mediators of cell-substrate interactions, are necessary for cell polarization and cell intercalation movements during early gastrulation. Cell-cell interaction with fibronectin matrix, mediated by the $\alpha 5\beta 1$ integrin receptor, was proven to be vital for the radial intercalation movements and the extension phase of CE (Marsden and DeSimone 2001). Interestingly, the attachment of cells to fibronectin via integrins permissively regulates the translocation of Dsh to the membrane during radial intercalation, revealing a relationship between cell adhesion molecules (integrin-fibronectin interactions) and the non-canonical Wnt pathway during gastrulation (Marsden and DeSimone 2001; Davidson, Mao et al. 2002). Even though the integrin interaction to fibronectin at focal adhesion sites is vital for the establishment of cell-substrate contacts in zebrafish (Zalik, Lewandowski et al. 1999), little is known about the function of integrins in modulating zebrafish gastrulation movements.

II.1.3.Other Pathways:

II.1.3.1.PDGF/PI3K Pathway

Phosphoinositide-3 kinase (PI3K) is necessary to polarise and move across a chemotactic gradient in cells from leukocytes to cells of *Dictyostelium* (Wang, Lim et al. 2002; Weiner, Neilsen et al. 2002). In vertebrate gastrulation, PI3K has been implicated in the regulation of mesodermal cell morphology and movement (Symes and Mercola 1996).

In response to an extracellular chemoattractant gradient, PI3K is stimulated and condensed to the leading edge of separate migrating cells. Upon stimulation, PI3K converts phosphoinositide-4,5-diphosphate ($PI(4,5)P_2$) to phosphoinositide-(3,4,5)-triphosphate (PIP_3), that associates with the PH-domain containing proteins like Akt/protein kinase B (Akt/PKB). These proteins consecutively can instruct the aggregation of actin filaments to the leading edge of the cells, which is then used for the creation of cellular protusions.

Therefore, a role of PI3K could be to prepare a cell to react to an extracellular gradient of a chemoattractant by polarising the development of cellular protusions along this gradient, making polarised movement possible (Comer and Parent 2002; Iijima, Huang et al. 2002; Weiner, Neilsen et al. 2002).

PI3K has been shown to be involved in cell polarisation and migration during vertebrate gastrulation by operating in a pathway downstream of *Platelet Derived Growth Factor* (PDGF). *XPDGF-A* is expressed in the ectoderm above the involuting mesodermal precursors, and it has been proposed that PDGF, produced by ectodermal cells, facilitates involution of underlying mesodermal cells (Ho, Symes et al. 1994). In support of this Ataliotis et al. demonstrated that PDGF can assist the adhesion of mesodermal cells to the overlying ectodermal tissue (Ataliotis, Symes et al. 1995). *In vitro* experiments where PDGF is ectopically expressed to *Xenopus* mesendodermal cells, support the observation that PDGF is involved in the development of lamellipodia and filopodia and the distribution of these cells over their substrate (Symes and Mercola 1996). The function of PDGF seems to be mediated by PI3K, indicating that PI3K might regulate the outgrowth and polarisation of mesodermal cell processes during vertebrate gastrulation. PDGF-A and its receptors in mice have a temporal and spatial expression profile during gastrulation that is very similar to that in *Xenopus*, implying that PDGF signalling might have conserved functions during vertebrate gastrulation (Orr-Urtreger, Bedford et al. 1992; Orr-Urtreger and Lonai 1992).

Recent work in zebrafish has demonstrated that, both PDGF and PI3K are involved in cell polarisation and protusion development of mesendodermal cells *in vivo* at the beginning of gastrulation (Montero, Kilian et al. 2003). PI3K seems to regulate mesendodermal cell polarisation and process formation by asymmetrically restricting Protein Kinase B (PKB) to the membrane at the leading edge of those cells. This is simultaneous with accumulation of actin at the front of the cells. Despite the fact that cell polarisation and process formation is blocked in mesendodermal cells with compromised PI3K activity, these cells are still able to move in a coordinated way. This implies that PI3K-dependent cell polarisation and process formation are dispensable for directed cell movements at the onset of gastrulation. As a graded distribution of PDGFs during the early stages of gastrulation has not been detected either in *Xenopus* or in zebrafish, it is still unknown if PDGFs might function endogenously as chemoattractants that direct the migration of mesodermal cells (Liu,

Chong et al. 2002; Liu, Korzh et al. 2002). Future studies will be needed to understand how the PDGF/PI3K and Wnt/PCP pathways could interact in the regulation of mesendodermal cell polarisation and movement.

II.1.3.2.JAK/STAT Pathway

The Janus kinase (JAK) and signal transducer and activator of transcription (STAT) pathway has been proposed to have a possible role in mesendodermal cell polarization/migration and germ-layer separation at the beginning of zebrafish gastrulation. This pathway seems to function as a modulator of cell movements during gastrulation. Various JAK and STAT homologs have been recognized and are expressed during gastrulation. Expression of a dominant-negative form of *jak1* blocks the normal radial cell intercalation movements during epiboly. Additionally, *stat3* is required cell-autonomously for the anterior movement of hypoblast cells and non-autonomously for the dorsal convergence of paraxial mesodermal cells (Conway, Margoliath et al. 1997; Oates, Wollberg et al. 1999; Yamashita, Miyagi et al. 2002).

Recent work demonstrated that STAT3 upregulates the expression of *LIV1*, encoding a Zn^{2+} transporter, and that LIV1 promotes hypoblast (mesendodermal) cell migration downstream of STAT3 by promoting an “epithelial to mesenchymal” transition in mesendodermal progenitors (Yamashita, Miyagi et al. 2004a). This suggests that STAT3 and LIV1 are required for certain features of mesendodermal progenitor cell motility, even though the mechanism during zebrafish gastrulation remains to be elucidated. Another recent study suggests that a downstream target of STAT3 in the organizer may be an unidentified secretory molecule that is capable of non-cell-autonomously activating Dsh-RhoA in the adjacent cells, thereby modulating the PCP pathway (Miyagi, Yamashita et al. 2004b).

Upstream regulators of JAK/STAT pathway during zebrafish gastrulation have not yet been identified, although the activation of Stat3 on the dorsal side of zebrafish embryos may depend on the activity of the maternal Wnt/ β -catenin pathway (Yamashita, Miyagi et al. 2002).

II.1.3.3.Slit/Robo Pathway

Zebrafish homologues of the *Drosophila slit* and *robo* genes have been implicated in the regulation of convergence and extension movements during gastrulation (Yeo, Little et al. 2001). In *Drosophila*, Slit, that is secreted by midline glia cells in the nervous system, inhibits the crossing of commissural axons expressing its receptor, Robo (Rajagopalan, Nicolas et al. 2000; Simpson, Kidd et al. 2000). During zebrafish gastrulation, *slit* genes are expressed in axial mesendodermal tissues including the notochord and prechordal plate (Yeo, Little et al. 2001), whereas *robo* genes are expressed throughout the whole gastrula (Challa, Beattie et al. 2001; Lee, Ray et al. 2001). Mis-expression of the zebrafish *slit-2* blocks convergence and extension movements during gastrulation (Yeo, Little et al. 2001), indicating that Slit, secreted by axial mesendodermal cells, might control the movement of axial and paraxial mesendodermal cells through Robo, in the gastrula stage prior to neurogenesis. Which cellular machinery specifically depends on *slit/robo* function and what molecular mechanisms mediate the Slit/Robo signal remain to be elucidated during gastrulation.

1.2. THE PROJECT

I have adopted a candidate approach to identify genes that regulate convergent extension movements in zebrafish. Two of the candidates I have studied are *flamingo* (*fmi*) and *prickle* (*pk*), members of the core group of PCP genes that controls planar polarity in the eye, leg and wing of *Drosophila* (Taylor, Abramova et al. 1998; Wolff and Rubin 1998; Chae, Kim et al. 1999; Gubb, Green et al. 1999; Usui, Shima et al. 1999; Feiguin, Hannus et al. 2001).

Flamingo is involved in establishing planar cell polarity in *Drosophila*. Flamingo is a seven-pass transmembrane receptor of the cadherin superfamily with extracellular tandem arrays repeats which act as homophilic modules. Flamingo is localised differentially at cell-cell boundary along the proximal-distal axis in the wing of *Drosophila* in a Frizzled (*fz*)-dependent manner (Usui, Shima et al. 1999). Therefore, it could be expected that Fmi might

be a downstream modulator of Slb/Wnt11 signalling in regulating convergent extension movements and that the localisation of Flamingo (Fmi) might act as a read-out of Wnt signalling in cells undergoing active convergent extension, informing us about cell polarity and directionality with respect to the axes of the gastrula embryo.

pk encodes an intracellular protein containing three LIM domains and a conserved “PET” domain (for Prickle, Espinas and Testin). Recently epistasis analyses have demonstrated that Pk is required for some aspects of Fz/Dsh-mediated PCP signalling, but is not placed in a linear cascade with Fz and Dsh (Carreira-Barbosa, Concha et al. 2003)(Figure 1.10.A and B).

To try to answer if functions of Fmi and Pk are conserved between the *Drosophila* PCP pathway and the vertebrate non-canonical Wnt pathway, I have analysed the function of zebrafish homologues of the *Drosophila* PCP genes *fmi* and *prickle* during gastrulation. I have used different approaches: gain of function and loss of function experiments, transplantation experiments, genetic interactions with different mutants and analyses for sub-cellular protein localisation, with the aim to understanding how Pk and Fmi modulate different types of cell behaviour especially during CE movements. Additionally, I also tried to address the specificity of putative receptors for non-canonical Wnt ligands in regulating CE movements.

CHAPTER 2

Material and Methods

2.1. Molecular Biology Techniques

2.1.1.Measurement of DNA/RNA concentration

DNA and RNA concentration were quantified by optical densitometry (OD) using a spectrophotometer. The OD was measured at 260nm for DNA (OD=1 equates to 50µg/ml) or RNA (40µg/ml) following calibration with distilled water. The concentration was then calculated based on dilution rates with water.

2.1.2.Polymerase Chain Reaction (PCR)

PCR reactions were carried out according to standard protocols using Applied Biosystems 9700 (Gene Amp) thermocycling machine. Taq- DNA polymerase, Promega was used for ordinary molecular characterisations. Pfu DNA polymerase, Stratagene was used for amplifying sequences to be cloned into expression vectors for RNA injection studies because it has a very low error rate. Annealing temperature specific to each primer was optimised with test reactions prior to use. Manufacturer's instructions were followed to vary the length of the various cycles within the PCR programme according to the enzymes used.

2.1.3.Bacterial Plasmid DNA extraction

Plasmid DNA preparation was done using Quiagen miniprep spin column kits according to manufacturers instructions or by alkaline lysis as described in Sambrook et al. 1989.

2.1.4. Basic DNA Manipulation

Basic molecular biology techniques were carried out as described in (Sambrook *et al.*, 1989). Restriction enzyme digestion was performed using enzymes from Promega in an appropriate buffer with 2-5 units of enzyme per 1 µg DNA at the temperature recommended.

Protein removal was carried out by phenol/chloroform extraction to purify DNA preparations.

Concentration or purification of nucleic acids was performed using 0.1 volume of 3M sodium acetate and 2.5 volumes of ethanol, incubated at -80°C for minimum for 30 minutes.

For plasmid transformation, circular DNA or ligated DNA was added into competent cells by incubation for 30 minutes on ice, a 30 second heat shock at 42°C and a further 2 minutes on ice. The cells were then incubated in LB media for 30 minutes at 37°C followed by plating on the appropriate antibiotic-containing LB agar plates.

2.1.5. Ligation reactions

Intermolecular ligations were performed in small volumes, usually 20 µl for approximately 20 ng of vector DNA with 50 ng of insert DNA. Ligation reaction was carried out overnight at 14°C with T4 DNA ligase (Invitrogen) and the ligation buffer provided. Sticky end ligation was performed where possible either using enzymes giving compatible ends or digesting primer-engineered restriction enzyme sites on the ends of PCR amplified DNA.

Transformation of the ligated plasmids was performed as described above and colonies containing the ligation product were detected by PCR selection. The direction of insertion was then tested by restriction digest mapping or by PCR.

2.1.6. Agarose Gel Electrophoresis and DNA Extraction from Agarose

Separation of DNA and RNA fragments was performed by agarose gel electrophoresis in TAE buffer (40mM Tris-acetate, 1mM EDTA). The agarose was dissolved in 1xTAE and ethidium bromide (10 mg/ml) was added for visualisation of DNA or RNA under ultraviolet light. The concentration of agarose ranged between 0.8 and 2% depending to the size of DNA fragment to be run. The DNA samples were loaded by mixing with loading buffer. A DNA ladder (1kb size standard) was run alongside the DNA. Extraction of DNA fragments from the agarose gel was performed using the QiaexII gel extraction kit (Qiagen) according to manufacturer's instructions.

2.1.7. DNA sequencing

Automated fluorescent sequencing was carried out by GenpaK Limited. Plasmid DNA as well as sequencing primers were supplied in concentrations according to their sequencing guidelines.

2.1.8. Extraction of Total RNA from tissues

Embryos of the required gastrulation stage were obtained and dechorionated. Lysis (RLT) buffer from RNeasy mini kit (Qiagen) was added, material homogenised and stored at -80°C. Tissue suspended in RLT buffer (Qiagen) with β -mercaptoethanol added was centrifuged through a QIAshredder according to manufacturer's instructions. RNeasy protocol (Qiagen) for extraction of RNA was then followed according to manufacturer's instructions.

2.1.9. Isolation of *fmi* genes

Total RNA was prepared from shield-stage embryos and cDNA was synthesised with SuperscriptII reverse transcriptase (Invitrogen) using oligo dT primers. PCR was done with degenerated primers corresponding to the conserved Cys-rich (CVFWNHS) and transmembrane domain (NPDFCWL). The primer sequences are as follows:

Sense primer:

5'-TGTGT(C/A)TT(C/T)TGGAA(C/T)CA(C/T) TC

Antisense primer:

5'-AGCCA(A/G)CA(A/G)AA(A/G)TC(A/G)GG(A/G)TT

The PCR fragments amplified were cloned into EcoRV site of pBluescriptIISK(-) and subject for sequence.

2.1.10. Screening of cDNA Libraries

2.1.10.1. Lambda Bacteriophage Library

Prior to screening, the library was titrated by serial dilution so that 250.000 plaque forming units (PFU) would be plated on a 22x22 plate. The necessary number of plates was used so that more than 10^6 plaques would be screened in the first round. The library (zebrafish cDNA from shield stage in Lambda ZAPII (EcoRI)) was kindly obtained from Mike Rebagliati and grown in XL-1B MRF bacterial cells.

Filters were made in duplicate from each plate and the library filters were screened by hybridisation with ^{32}P -labelled DNA probes according to modified protocols of (Sambrook 1989).

Hybridisation was performed at 65°C in 50mM NaPO_4 (PH 7.2), 6xSSC, 1%SDS, 5xDenhardtts, 5mM EDTA with 100 $\mu\text{g/ml}$ torula RNA and probe added just prior to incubation. Washing was carried out at $42\text{-}55^{\circ}\text{C}$ in 0.2-2xSSC, 0.1%SDS depending on the stringency required.

Hybond-XL filters were used for hybridisation (Amersham); Fujifilm RX was used to detect positive colonies. Subsequent rounds of screening were performed until the plates were "plaque pure" i.e. containing only positive hybridising clones.

2.1.10.2. Rescue of Phagemids from Bacteriophage.

Phagemid (pBluescript SK II-Stratagene) from positive plaques was rescued using R408 helper phage (Stratagene) according to retailer's instructions.

2.1.10.3. Micro-Arrayed cDNA Library

Filters were obtained from the RZPD (German Resource Centre for Genome Research) containing three libraries: adult brain cDNA, 16-17 somite total embryo cDNA and shield stage cDNA (total 6 filters).

Filters were pre-hybridised in Church medium (7%SDS, 0.5M sodium phosphate pH7.2, 1mMEDTA) and 0.1mg/ml yeast torula RNA. These were screened with denatured ³²P-labelled zebrafish *fmi* in Church medium overnight at 65°C. Filters were washed in 40mM sodium phosphate pH7.2, 0.1% SDS at 42°C, 50°C, 55°C and 65°C according to the signal remaining.

Positive clone co-ordinates were calculated according to filter instructions and the clones ordered from the database.

2.2. Embryological Techniques

2.2.1. Maintenance of zebrafish lines

Breeding zebrafish (*Danio rerio*) lines were maintain at 32°C on 14 light/10h dark cycle (Westerfield 1993). Fertilised eggs were obtained from natural spawning and grown in incubators at 28.5°C, 22°C (to slow development) or 31°C (to accelerate development) according to the stages required. Embryos were staged according to standard references (Kimmel, Ballard et al. 1995).

Embryos were generated from wild-type *AB, Tübingen and Tup Longfin. The mutant lines used were *ppt*^{ta98}, *tri*^{m209}, *slb*^{tx226} and *off-road (ord)/fmi2*^{rw71}, kindly provided by

Hitoshi Okamoto. For injection studies, mutant embryos were obtained by crossing homozygous *slb*, homozygous *ord*, heterozygous *ppt* and heterozygous *tri* carriers.

2.2.2. Observation of live embryos

2.2.2.1. DIC microscopy

Embryos at stage of somitogenesis and late stages (pharyngula) of development were visualised in fish tank water and manually dechorionated with # 5 watchmaker's forceps. When necessary, for photographing live, embryos were anaesthetised with 0.02% tricaine (3-amino benzoic acid ethyl ester) and mounted for viewing in 3% methylcellulose in fish tank water. Embryos at different stages of epiboly were dechorionated on agarose-coated Petri dishes in fish tank water.

2.2.2.2 Confocal microscopy

Embryos at different stages of epiboly were dechorionated and embedded in 1% low melting agarose (Sigma) in fish water (60ug/ml "Instant Ocean" sea salts) and placed in a glass ring (Fisher) on the slide. Image analysis of living embryos was carried out using a Leica DMLFS confocal fluorescence microscope, which had a TCS SP Confocal head and TCSNT software, with a 63X water-immersion lens.

2.2.3. RNA *in situ* hybridisation

2.2.3.1. Synthesis of antisense RNA probes for *in situ* hybridisation

Templates for synthesis of antisense RNA probes were produced by linearising the DNA clone at the 5' end with a suitable restriction enzyme. Followed by purification of the DNA by 1 x phenol: chloroform: isopropanol extraction and precipitation with 0.1 volumes of NaAc 3M pH 5.1 and 2 volumes of 100% of ethanol at -80°C for 30 min, and washed one time with 1,5 volumes of 70% ethanol, the DNA was then resuspended in 5 μl ddH₂O.

One µg of the linear DNA was used for the *in vitro* transcription reaction in which the RNA probe was labelled with either digoxigenin-11-UTP or fluorescein –11-UTP. A 50 µl reaction was set up in 1X transcription buffer, 10 mM DTT, NTP- digoxigenin/fluorescein labelling mix, 40 units of and RNase inhibitor and 10 unit Sp6/T7/T3 RNA polymerase (all Promega). This mix was incubated for 2hours at 37°C before 1 unit of DNase was added to breakdown any trace of the template. The DNase reaction was stopped after 20 min at 37°C by heat shock of 70 °C for 5 min. The RNA was purified in Probe Quant G50 microcolumn (Amersham Pharmacia biotech), to remove the unincorporated nucleotide and digested template DNA, and precipitated as described above. The RNA probe was finally resuspended in 50 µl of ddH₂O and 50 µl of formamide. If needed the probe was further hydrolysed in 40mM NaHCO₃, 60mM Na₂CO₃ and 5mMDTT at 60°C for 30min.

2.2.3.2. Single whole -mount *in situ* hybridisation

The single whole-mount *in situ* hybridisation was performed essentially as previously described (Barth and Wilson 1995). Embryos were dechorionated and fixed in 4% paraformaldehyde in PBS, pH 7.4 (4% PFA) overnight at 4°C. Embryos were rinsed in PBS or in PBST (PBS, 0,1% Tween-20) and stored in 100% methanol at –20°C.

Embryos were rehydrated with 3 x 10 min washes of progressively decreasing concentrations of methanol:PBST (PBS 0,1% Tween 20) followed by 3 x 15 min washes in PBST at room temperature in a shaker. Embryos were pre-hybridised at 70°C for a minimum of 2 hour in pre-hybridisation solution (50% formamide, 5xSSC (pH6), 50ug/ml heparin, 200ug/ml yeast RNA, 5mM EDTA, 1xDenharts and 0.1% Tween-20). This solution was replaced by hybridisation solution containing the anti-sense riboprobe in the best working concentration and the embryos incubated at 70°C overnight.

Post-hybridisation washes were carried out at 70°C. Embryos were washed first in hybridisation solution, and then 10 min washes with decreasing concentrations of hybridisation solution: 2x SSC (75%, 50%, 25%) followed by 2 x30 min washes in 2x SSC and by 2 x30 min washes in 0.2x SSC.

After that embryos were rinsed in antibody block at room temperature in MABT (0.1M maleic acid, 0.15M NaCl, pH7.5 and 0.1% Triton) and then blocked in 2% Boehringer blocking reagent (Roche) in MABT plus 10% of lamb serum for at least 2 h. The embryos were incubated in the appropriate antibody, either anti-digoxigenin-alkaline phosphatase conjugated F_{ab} fragments (Roche) (1 in 5000) or anti-fluorescein-alkaline phosphatase conjugated F_{ab} fragments (Roche) (1 in 2000) overnight 4°C.

The antibody was washed six times for 30 min in MABT at room temperature. The embryos were equilibrated with staining buffer (100 mM Tris-HCl, pH 9.5, 100mM NaCl, 5mM MgCl₂, 0.1 % Tween-20) for 10 min. Then they were developed in BM purple (Boehringer Mannheim) in the dark. The reaction was stopped by rising with PBS and refixing with 4%PFA. Embryos were then gradually washed into glycerol 85% for storage and photographed.

2.2.3.3. cDNAs used for *in situ* hybridisation

The zebrafish cDNAs that were used as templates for the synthesise of RNA probes come from plasmids containing cDNA for *pk1* (Carreira-Barbosa et al., 2003 and this study), *fmi1* and *fmi2* (this study), *wnt11* (Heisenberg et al., 2000), *wnt5* (Kilian et al., 2003 and this study), *fz7* (El-Messaoudi and Renucci, 2001), *fz2* (this study), *ntl* (Schulte-Merker et al., 1994), *hgg1* (Thisse et al., 1994), *dlx3* (Akimenko et al., 1994), *papc* (Yamamoto et al., 1998), *myoD* (Weinberg et al., 1996), *emx1* (Morita et al., 1995), *rx3* (Chuang et al., 1999), *pax2.1* (Krauss et al., 1991), *chordino* (*chd*) (Schulte-Merker et al., 1997), *bmp2b* (Nikaido et al., 1997) and *sna2* (Thisse et al., 1995), *gsc* (Stachel et al., 1993)

2.2.4. RNA and morpholino antisense oligonucleotide (Mo) injection

2.2.4.1. *In vitro* transcription of mRNA synthesis

The constructs to be injected were first cloned into an expression vector, generally pCS2+ containing the SV40 poly A region to promote RNA stability. Capped mRNA was

synthesised from cut, purified DNA. Five µg of the linear DNA pure and linear was used for the *in vitro* transcription reaction. A 50 µl reaction was set up in 1X transcription buffer, 10 mM DTT, NTP- Cap labelling mix (1mM ATP, CTP, UTP, 0.1mM GTP, 0.5mM m⁷G(5')ppp(5')G, a cap structure analog, 40 units of and RNase inhibitor and 20 unit Sp6 RNA polymerase (all Promega). This mix was incubated for 30 minutes at 37°C before 0.5mM of GTP was added to terminate the incorporation of cap nucleotides. This mix was incubated for 1hour at 37°C before 5 unit of DNase was added. The DNA template was then removed by a 30 min incubation with Rnase-free DNase. The RNA was extracted by 1 x phenol: chloroform: isopropanol extraction. Following purification of the RNA in DCPC-H₂O BD Chroma spin-100 columns (Clontech), to remove the unincorporated nucleotides and digested template DNA. The eluate (RNA) was then precipitated with with 1 volumes of 3M NaOAc and 2 volumes of 100% of ethanol at – 80°C for 30 min. The RNA was centrifuged for 15 min at 4°C, washed one time with 1,5 volumes of 70% ethanol, the RNA was then resuspended in 30 µl ddH₂O.

The RNA was run on an agarose gel to check integrity and optical density was measured (1 OD=40ug/ml) to check concentration and for contamination.

2.2.4.2. Morpholino Preparation

Morpholino antisense oligonucleotides were provided by Genetools. The supplied 300nmol (approx. 2.5mg) of lyophilised powder was diluted as a stock of 4mM in Hepes buffer (5mM HEPES pH7.5 and 200mM KCl). This was then diluted further for injection to test different concentrations.

List of Morpholinos:

- Splice morpholinos:

fmi1a Mo -CAGTTGTTGTACCGGGATCACAGGT

fmi2 Mo- CGAGAGTCTGACCTTCACATCCACT

- 5'-prime morpholinos:

fmi1a Mo-CATGGTGTAACAACTCCGCAAACAGG

fmi1b Mo-CATCCATATCACTGGTAATTCCATG
fmi2 Mo-CAAAGAGCAACAAATCCCCCTTCAT
pk1 Mo-GCCCACCGTGATTCTCCAGCTCCAT
*pk1*Mo (Mis)- GCCCGCCATGATTCTCCAACCTTCAT-

2.2.4.3. Injection of mRNA into early stage embryos

Embryos at the 1 cell stage were aligned in a plastic through, still with their corions, and microinjection targeted to the cytoplasm or to yolk syncytial layer or to the interface between them. Needles were pulled from glass capillary tubes by Clark Electromedical Instruments needle puller and injections were performed using a Picospritzer micro-injector. The injected embryos were left to develop at 32°C.

2.2.5. Analyses for sub-cellular protein localization

To monitor Dsh localisation, embryos at the one-cell stage were injected with 200 pg RNA encoding Dsh-GFP either with or without 50 pg *fz7* RNA and either with or without 5 pg *pk1* RNA. Additionally, for the flamingo functional analyses the embryos were injected with 200 pg RNA encoding Dsh-GFP either with or without 50 pg *fz7* RNA and either with or without 100 pg Lyn-Fmi RNA. To examine Lyn-Fmi localization, embryos were injected with 100pg Lyn-Fmi-Venus. To analyse Pk1 localisation embryos were injected with 25 pg RNA encoding Venus-Pk1 (Venus is an YFP-derivative that was kindly provided by Atsushi Miyawaki) and fixed at 40% epiboly for anti-GFP antibody staining. For co-localization studies the wild type embryos were injected with a triple mixture of RNAs encoding Dsh-GFP (200 pg), *fz7* (50 pg) and Lyn-Fmi-RFP (100pg). All embryos were mounted in 1% agarose at 40% epiboly, followed by confocal microscopy analysis (Leica DMLFS confocal fluorescence microscope, which had a TCS SP Confocal head and TCSNT software, with a 63X water-immersion lens).

2.2.6. Cell transplantation

For transplantations, in the *pk* study, the donor embryos were injected with either rhodamine-dextran (MW 10,000, Molecular probe) plus 5 pg *pk1* RNA or fluorescein-dextran (MW 10,000, Molecular probe) at the one-cell stage. Cells were taken from late-blastula host embryos and transplanted into deep regions of the germ ring of host wild-type embryos as described previously (Heisenberg, Tada et al. 2000).

In the Flamingo study, double transplantations experiments were performed. The donor embryos were injected with either 100pg Lyn-CFP and rhodamin-dextran (RDx) (MW 10,000, Molecular probe) or 100pg Lyn-Fmi and fluorescein-dextran (FDx) (MW 10,000, Molecular probe) at the one-cell stage. Cells from these donors at late-blastula were transplanted simultaneously into the germ rings of wild-type, shield-stage hosts, in the shield or lateral to the shield. After transplantation tailbud staged embryos were visualized using Openlab software.

2.2.7. Production and Purification of Fmi2 antibody

A polyclonal antibody has been produced against the cytoplasmic region of the zebrafish Flamingo 2 in rabbits from Eurogentec. The DNA containing the cytoplasmic region of Fmi2 was cloned into the pGEX-6P-3, a GST gene fusion vector (Amersham). The antigen was prepared initially by the production of Fmi-GST fusion protein BL21 *Escherichia coli* cells, followed by purification of a Fmi protein by cleavage of Fmi-GST protein and then the purified protein was injected in rabbits to create an antibody.

For large-scale purification, *E.coli* cells were collected from 1L culture 5hours after IPTG induction (1mM) and the extract was prepared in PBS containing complete protease inhibitor cocktail and 1mM PMSF by sonication. The extract was applied onto a GST column (Amersham) that had been equilibrated in PBS containing 1% Triton and 1mM DTT. After washing with the same buffer extensively, 500 units of ProScission enzyme in 50mM Tris-Hcl, pH 7.0; 150mM NaCl, 1mM EDTA, 1mM DTT was added onto the column to release the Fmi2 protein from GST. The eluate was further purified onto a Q

sepharose ion exchange column (Amersham) that had been equilibrated in Q buffer (20mM Tris-HCl (pH 7.5), 50mM NaCl, 1mM DTT and 1mM EDTA). After washing with the same buffer, the protein was eluted in Q buffer containing 300mM NaCl. The purified protein was dialysed against PBS and used as an antigen.

For purification of Fmi2 antibody, the GST-Fmi2 fusion protein was eluted in 50mM Tris-HCl (pH 8) and 20mM reduced glutathione from GST column, instead of using the ProScission enzyme. Subsequently by choosing the sample from the eluate with highest concentration of protein from the last column and passing it through a GST-FMI affinity column previously made (Hi-Trap affinity columns, NHS-activated HP, Amersham Pharmacia Biotech) according to manufacturer's instructions. The anti-Fmi serum (antigen raised in rabbits from Eurogentec) was applied to the affinity column and eluted in the presence of 0.3mM glycine (pH2). The eluate was subsequently neutralised in 1/10 volume of 2M Tris-HCl (pH 8.5), followed by dialysed against PBS. Between each step the O.D (optical density) of the different samples was measured and all the proteins sizes were checked in SDS page gels. The purified antibody was stored at -80°C in the presence of 50% glycerol.

2.2.8. Immunohistochemistry

2.2.8.1 Antibodies used

Primary antibodies that were used for immunohistochemistry were rabbit anti Flamingo 2 Eurogentec and anti-GFP polyclonal antibody (AMS Biotechnology). The secondary antibody used was Alexa fluor 488 anti-rabbit IgG (Molecular probes) for confocal analysis.

2.2.8.2. Whole-mount antibody staining

Detection of expression of GFP was essentially done as described previously (Shanmugalingam, Houart et al. 2000).

For Fmi 2 antibody staining the embryos were fixed with 4% PFA for 1-2 hours at room temperature and then washed three times in PBS for 5 min each time. After this a permeabilization treatment was performed for one hour with a 0.1% Saponin and 0.1% BSA (bovine serum albumin from Sigma) solution in PBS. After permeabilization the embryos were washed 3 times for 15 min in PBST (a solution of 0.1% Tween 20 and 0.1% BSA in PBS) and blocked at least one hour in 10% goat serum, 1% DMSO (Dimethylsulfoxide), 0.5% Triton X-100, 0.1% BSA in PBS (IB). The embryos were incubated in the primary antibody in IB overnight at 4°C in a concentration of 1/100.

The embryos were washed out of the antibody by rising several times with PBST and washed five times for 30 min in PBST on a shaker and block again at least one hour in IB. Then the embryos were incubated overnight at 4°C with Alexa 488 anti-rabbit diluted 1 in 200 of solution of IB. Rinsing several times for 24 hours in PBST, washed out this secondary antibody. Following the washes the stained embryos were detected by fluorescence with a confocal microscope.

2.2.9. Polyacrylamide gel electrophoresis (Page) Western-blotting and Chemilluminuscent detection of proteins

In the *pk* study, to monitor the levels of Dsh protein, embryos were injected with 200pg RNA encoding myc-Dsh either with or without 50 pg *fz7* RNA and either with or without 5 pg *pk1* RNA at the one-cell stage. Blastoderms from 20 embryos at 40% epiboly were collected for western-blot analysis after removal of the yolk according to a protocol kindly provided by Carl-Philipp Heisenberg (personal communication). Protein from the equivalent of five blastoderms was subject to SDS-PAGE (8% acrylamide gel) and then blotted to a PVDF membrane (Amersham). The membrane was reacted with 9E10 anti-myc monoclonal antibody (Santa Cruz Biotechnology) and subsequently with anti-mouse IgG conjugated with HRP followed by detection with ECL (Amersham). For loading control, the membrane was counter-stained with anti- β -tubulin monoclonal antibody (Sigma) and visualised with NBT and BCIP.

All the rest of the western blot analyses performed in this thesis to monitor the levels and the specificity of Flamingo protein, were as described above. Around 50 zebrafish embryos at 90% epiboly or 10 caps from *Xenopus* embryos injected with the constructs expressing the proteins of interest were collected and frozen at -80°C . Subsequently the embryos were mixed with appropriate volume of 2xSDS (sodium dodecyl sulphate or lauryl sulphate) sample buffer before heating to 95°C for 5 min, followed by a short spin of 5 min at 15 000 rpm and loading onto pre-made SDS-PAGE (Invitrogen-NUPAGE Novex gels) gels. Gels were run firstly at 50V and then the voltage increased for 150V for around 90 min. In the case of GST fusion protein detection (section 2.6.Fmi protein purification), gels were soaked for 30 min Coomassie brilliant before being washed in destain solution until bands could clearly be viewed over background staining according to Sambrook (1989). The gel was then dried for records.

Next step, the proteins were electrotransfer to nitrocellulose, gels were overlaid with nitrocellulose (PVDF membrane (Amersham)) and sandwiched between a two layers of Whatman chromatography paper in Biorad transfer cassettes. Transfer was at 15V at RT for 30 min. After blocking in block solution (5% skim milk in PBST (0.1% Tween-20/PBS) for 1 hour, membranes were incubated with primary antibody overnight at 4°C (Fmi antibody 1/500 and GFP antibody 1/1000).

Usually the secondary antibody was anti-rabbit conjugated to horseradish peroxidase (HRP) (1:4000 or 1:5000). This antibody was diluted in appropriate volume of blocking solution and incubated with membranes at room temperature. All washes between antibody layers were 1h changing the PBST (0.1% Tween-20/PBS) four times. Proteins were visualized using the ELC chemilluminescence detection kit and exposure on Hyperfilm as recommended by the manufacturer (Amersham, UK). For detection of myc-tagged constructs the membrane was reacted with 9E10 anti-myc monoclonal antibody (Santa Cruz Biotechnology). For detection of GFP-tagged constructs the membrane was reacted anti-GFP polyclonal antibody (AMS Biotechnology).

CHAPTER 3

Possible role of Wnts and Fz receptors in regulating convergent extension (CE) movements

3.1.Introduction

Several lines of evidence indicate that Wnts are involved in regulating gastrulation movements: studies in *Xenopus* show that overexpression of *wnt4*, *wnt5a* or *wnt11* interferes with CE (Tada and Smith 2000; Wallingford and Harland 2001; Du et al., 1995), whereas in zebrafish *silberblick (slb)/wnt11* and *pipetail/(ppt) wnt5* mutant embryos exhibit an impaired CE (Heisenberg, Brand et al. 1996; Heisenberg and Nusslein-Volhard 1997; Heisenberg, Tada et al. 2000). These Wnts exert their function via a pathway related to planar cell polarity (PCP) pathway in *Drosophila* rather than the canonical Wnt pathway (Tada and Smith 2000; Wallingford, Rowling et al. 2000). Wnt genes have also been reported to regulate gastrulation movements via the so-called “calcium pathway” (Sheldahl, Park et al. 1999; Kuhl, Sheldahl et al. 2000). *frizzled* genes, encoding receptors for Wnts, have been also implicated in regulating CE in *Xenopus* studies. Overexpression of different forms of *fz7* in wild type embryos disrupts normal CE movements (Djiane, Riou et al. 2000; Medina, Reintsch et al. 2000; Sumanas, Strege et al. 2000) while injection of a morpholino against *fz7* leads to impaired CE and failure of tissue separation (Sumanas and Ekker 2001; Winklbauer, Medina et al. 2001). Moreover, from epistatic studies in *Xenopus* and direct binding *in vitro* analyses, Fz7 has been proposed as a potential receptor for Wnt11 (Djiane, Riou et al. 2000). Additionally, *fz7* is expressed in largely overlapping domains with *wnt11* in zebrafish and *Xenopus* during early stages of gastrulation (Djiane, Riou et al. 2000; Medina, Reintsch et al. 2000; Sumanas, Strege et al. 2000; El-Messaoudi and Renucci 2001 and this work), raising the possibility that Fz7 might be a Wnt11 receptor. In addition, Fz2 may act as a receptor for Wnt5 as injection of *fz2* morpholinos into zebrafish embryos leads a phenotype similar to *ppt/wnt5* (Sumanas, Kim et al. 2001).

In this chapter, I analyze the expression pattern of *wnt5* and the function of Wnt5 during zebrafish gastrulation. I show that Ppt/Wnt5 is required for regulating CE movements in the posterior mesendoderm and ectoderm while its function in the anterior mesendoderm is largely redundant to that of Slb/Wnt11. Finally, I tested if Fz2 and Fz7 might function as a receptor for Wnt11 using epistatic analyses in zebrafish.

3.2.Results

3.2.1.Possible interaction between *wnt11* and *wnt5*

It has been demonstrated that Wnt11 is a key regulator of CE during gastrulation (Heisenberg, Tada et al. 2000; Tada and Smith 2000). However, the expression domains of *wnt11* are restricted to the anterior half of the embryo at the end of gastrulation in zebrafish (Heisenberg, Tada et al. 2000)(Figure 3.1. G, H). This raised the question of which molecule regulates CE in the posterior domain of the gastrula embryo. The gene *wnt5* is a good candidate because it belongs to the same functional group of Wnts as *wnt11*, based on their ability to alter cell movements and to reduce cell adhesion when overexpressed in *Xenopus* embryos (Du et al.1995).

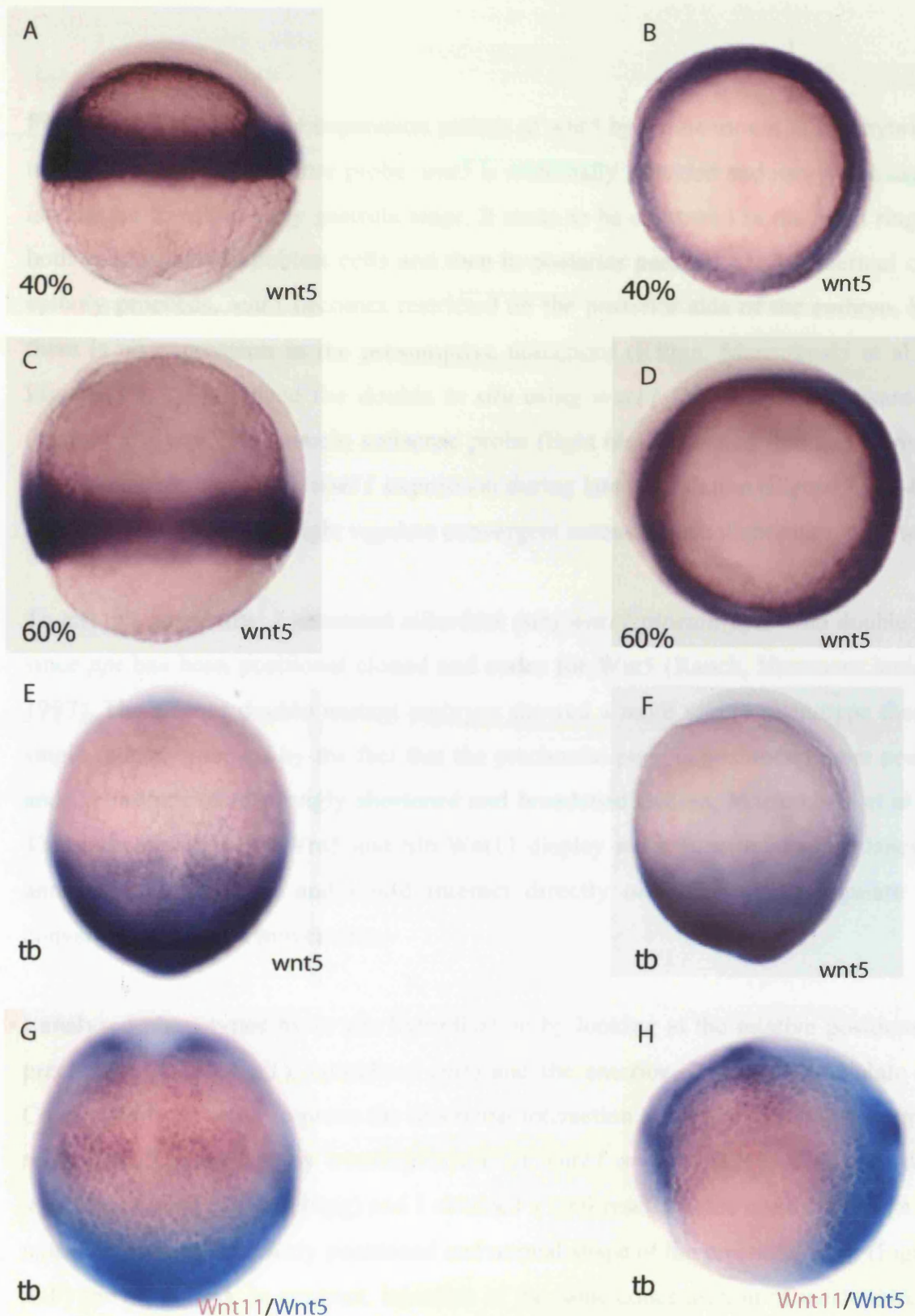


Figure 3.1. Expression pattern of *wnt5* during zebrafish gastrulation visualised by in whole mount *in situ* hybridisation. (A -lateral view with dorsal to the right, B-animal view, C-lateral view with dorsal to the right, D- animal view, E-dorsal view anterior is up, F-lateral view anterior is up with dorsal to the right). Expression pattern of *wnt5* is complementary to *wnt11* expression pattern revealed by a double *in situ* (G- dorsal view anterior is up, H-lateral view anterior is left) using *wnt11* DIG labelled antisense probe (purple) and *wnt5* fluorescein antisense probe (light blue)

First of all, I analysed the expression pattern of *wnt5* by whole mount *in situ* hybridisation using DIG labelled antisense probe. *wnt5* is maternally provided and its zygotic expression is detected from the early gastrula stage. It starts to be expressed in the germ ring, within both epiblast and hypoblast cells and then in posterior paraxial mesendodermal cells. As epiboly proceeds, *wnt5* becomes restricted on the posterior side of the embryo, however there is no expression in the presumptive notochord (Kilian, Mansukoski et al. 2003)(Figure 3.1.A-F). Indeed the double *in situ* using *wnt11* DIG labelled antisense probe (purple) and *wnt5* fluorescein antisense probe (light blue) revealed that the expression of *wnt5* is complementary to *wnt11* expression during late gastrulation (Figure 3.1.G-H). This result implies that *wnt5* might regulate convergent extension in collaboration with *wnt11*.

To test this possibility, I generated *silberblick (slb)/wnt11;pipetail(ppt)/wnt5* double mutants since *ppt* has been positional cloned and codes for Wnt5 (Rauch, Hammerschmidt et al. 1997). The *slb;ppt* double mutant embryos showed a more severe phenotype than either single mutant embryos by the fact that the prechordal plate is positioned more posteriorly and the notochord is strongly shortened and broadened (Kilian, Mansukoski et al. 2003). This indicates that Ppt/Wnt5 and Slb/Wnt11 display some functional redundancy in the anterior mesendoderm and could interact directly or indirectly to regulate correct convergent extension movements.

I analysed phenotypes by *in situ* hybridisation by looking at the relative positions of the prechordal plate (*hgg1*), notochord (*ntl*) and the anterior edge of neural plate (*dlx3*). Consequently, in order to prove the functional interaction of these two genes, I attempted to rescue *slb*^{-/-} embryos, by overexpression of *wnt11* or *wnt5* RNA. This was done by injection of *wnt11* RNA (10pg) and I obtained a total rescue of the embryos with a thinner notochord and an anteriorly positioned and normal shape of the prechordal plate (Figure 3.2. A-F) (n=10, 100%). In contrast, injection of the same concentration of *wnt5* RNA totally rescued (n=12, 50%) or partially rescued (n=12, 50%) (Figure 3.2.G-I), in the sense that the prechordal plate reaches the anterior edge neural plate but the notochord becomes shorter and thicker than in *slb* mutants (Figure 3.2 J-M). Even at higher doses of injected *wnt5* RNA there was no rescue but rather an enhanced *slb* phenotype. These results suggest that *wnt5* may have a function in regulating convergent extension movements in a similar, but

distinct, manner to *wnt11*. While *ppt/wnt5* can functionally replace *slb/wnt11* in the anterior mesendoderm, it is less efficient in doing so.

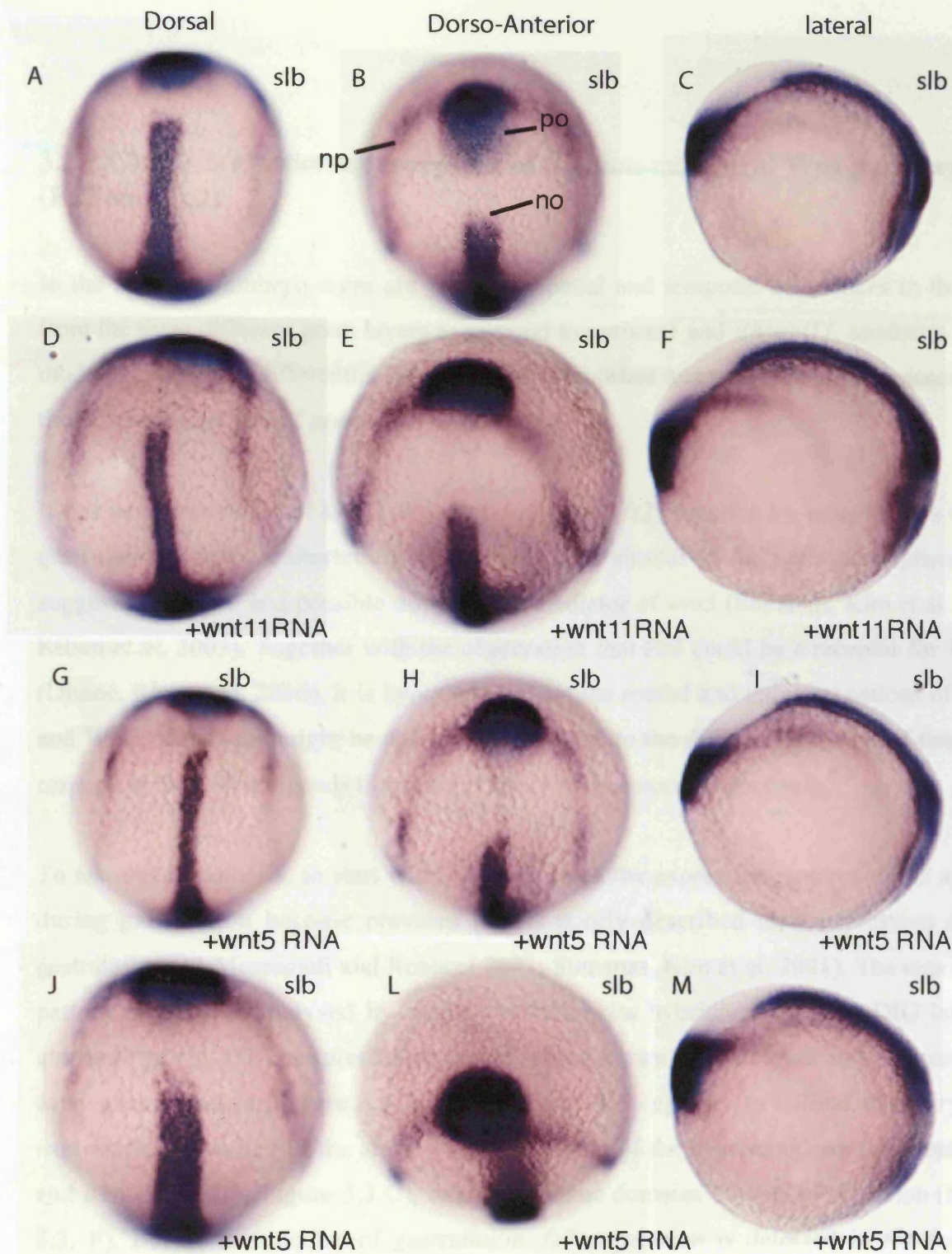


Figure 3.2. Injection of *wnt11* and *wnt5* RNA rescues the *slb*^{-/-} mutant phenotype. The embryos were examined at tailbud stage for extension of the axial tissues in relation to the overlying anterior edge of the neural plate and shape of notochord. Expression of *dlx3* stains for the anterior edge of neural plate (np) and *hgg1* for the polster (po) and *ntl* for the notochord (no). A, D, G, J dorsal view; B, E, H, L dorso -anterior views; C, F, I and M lateral views anterior is left. G-I *wnt5* totally rescues the *slb* phenotype. J-M *wnt5* partially rescues the *slb* phenotype.

3.2.2.Characterisation of receptors of the non-canonical Wnt pathway (Fz7 and Fz2)

In the zebrafish embryo there are probably spatial and temporal differences in the cells from the three different germ layers to respond to *ppt/wnt5* and *slb/wnt11*, another possible model could be that differential expression of appropriate receptor(s) might also account for the different activities of *ppt/wnt5* and *slb/wnt11*.

It has been reported that knock-down of *frizzled-2* (*fz2*) function by morpholinos during gastrulation causes a shortening of the body axis similar to the *ppt* mutant phenotype, suggesting that *fz2* is a possible downstream mediator of *wnt5* (Sumanas, Kim et al. 2001; Kilian *et al*, 2003). Together with the observation that Fz7 could be a receptor for Wnt11 (Djiane, Riou et al. 2000), it is hypothesized that the spatial and temporal actions of Wnt5 and Wnt11 functions might be at least partially due to the differential ability of tissues to respond to these Wnt ligands through Fz2 and Fz7 receptors, respectively.

To test this hypothesis, to start with, I re-examined the expression patterns of *fz2* and *fz7* during gastrulation because previous papers poorly described their expression during gastrulation (El-Messaoudi and Renucci 2001; Sumanas, Kim et al. 2001). The expression pattern of *fz7* was analysed by whole mount *in situ* hybridisation using DIG labelled antisense probe. *fz7* is expressed maternally (not shown) and ubiquitously expressed at early gastrula stage (Figure 3.3.A and B). From 90% epiboly to tailbud stages zygotic expression is detected in the anterior lateral domain of the neuroectoderm (El-Messaoudi and Renucci 2001)(Figure 3.3 C), one of the same domains of *wnt11* expression (Figure 3.3. F). Before completion of gastrulation, *fz7* expression is detected in the forming presomitic mesoderm but is clear from the presumptive notochord (Figure.3.3.D, E). At late stages of development (24h post-fertilization) there is ubiquitous expression in the brain (data not shown). In contrast, *fz2* starts to be expressed around shield stage. From 75% epiboly to tailbud stages expression is detected strongly in the midline and weakly on the dorsal side (Figure 3.3. G). By 1-2 somite stage this dorsal expression becomes restricted to the forming somites where it appears to be around the border of *wnt11* and *wnt5* expression

domains (Figure 3.3. H, I). This expression pattern reinforces the hypothesis that Fz2 is a receptor for Wnt5 or Wnt11.

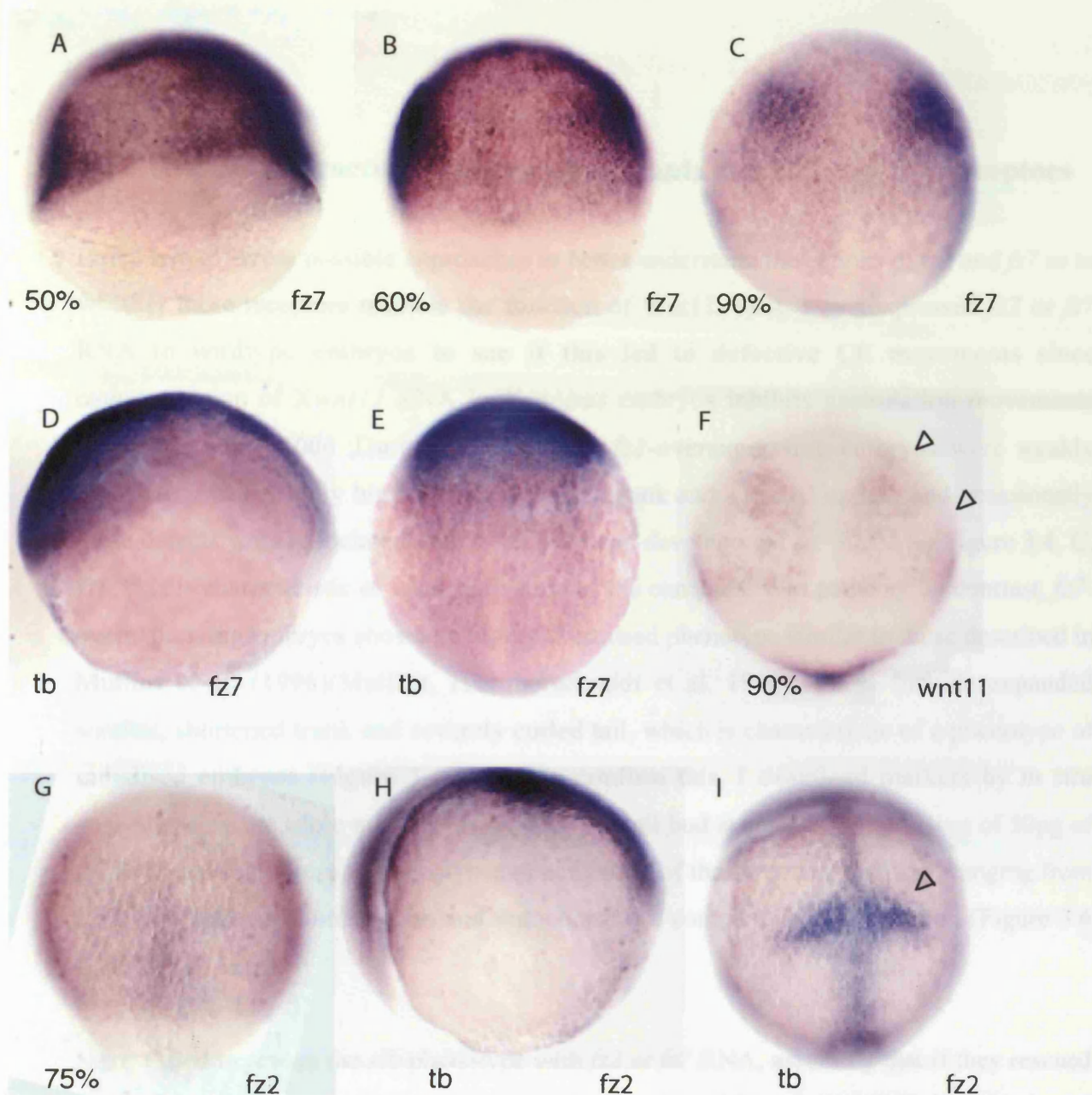


Figure 3.3. Expression patterns of *fz7* and *fz2* during gastrulation in wild type embryos. Expression of *fz7* was visualised by in whole mount *in situ* hybridisation [A (lateral view), B (dorsal view anterior is up) , C (dorsal view anterior is up), D (tailbud lateral view anterior is left) E (dorsal view, anterior is up) F (expression of *wnt11* at 90% epiboly dorsal view anterior is up). *fz7* expression overlaps with that of *wnt11* in the anterior lateral neuroectoderm and anterior paraxial mesoderm (arrow heads). Expression of *fz2* during gastrulation at (G) 75% epiboly dorsal view anterior is up. (H,I) tailbud stage, lateral view anterior is left (H) and dorsal view anterior is up (I). The arrow head shows expression around the border between the anterior and posterior regions of the embryo (I).

3.2.3. Genetic interaction between *slb* mutants and Fz2 and Fz7 receptors

I tried two different possible approaches to better understand the actions of *fz2* and *fz7* as to whether these receptors mediate the function of Wnt11. First, I overexpressed *fz2* or *fz7* RNA in wildtype embryos to see if this led to defective CE movements since overexpression of *Xwnt11* RNA in *Xenopus* embryos inhibits gastrulation movements (Tada and Smith 2000 ;Du et al., 1995). The *fz2*-overexpressing embryos were weakly dorsalized with slightly bigger eyes, a shorter trunk and a curled up tail, and occasionally these defects were associated with defective head development (n=30, 36%)(Figure 3.4. C, D). This is characteristic of weak activation of the canonical Wnt pathway. In contrast, *fz7*-overexpressing embryos showed a highly dorsalised phenotype similar to those described in Mullins et al. (1996)(Mullins, Hammerschmidt et al. 1996). These include expanded somites, shortened trunk and severely curled tail, which is characteristic of a phenotype of radialised embryos (Figure 3.4.E, F). To confirm this, I examined markers by *in situ* analysis using the triple mix (*hgg1*, *ntl*, *dlx3*) at tail bud stage. Over-expression of 50pg of *fz7* RNA led to pleiotropy phenotypes of activation of the canonical pathway, ranging from a slightly split prechordal plate and notochord to a complete axis duplication (Figure 3.6 C,D) (n=45, 32%).

Next, I tried to rescue the *slb* phenotype with *fz2* or *fz7* RNA, assuming that if they rescued it, these receptors are capable of mediating the function of Wnt11. Surprisingly, injection of 10pg *fz2* RNA in *slb* embryos led to two different phenotypes at tail bud stage; an enhancement of the *slb* phenotype with a thicker and shorter notochord and a slightly enlarged prechordal plate (n=27; 70%) or a complete axis duplication (n=27, 20%)(Figure 3.5.C, D, E and F). Similarly, over-expression of *fz7* RNA (10pg) in *slb* embryos led to a severely dorsalised phenotype in that the prechordal plate is enlarged and the notochord is much thicker (n=53, 44%) and occasionally these defects are associated with a complete axis duplication (n=53, 12%) (Figure 3.6 G, H, I, J). The dorsalising activity of *fz7* is more pronounced in *slb* embryos because even higher dose (50pg) of *fz7* RNA caused a weaker effect in wild type embryos. (Figure 3.6.C, D). These results suggest that *fz7* and, to a lesser extent, *fz2* can activate the Wnt canonical pathway, in particular in *slb* background.

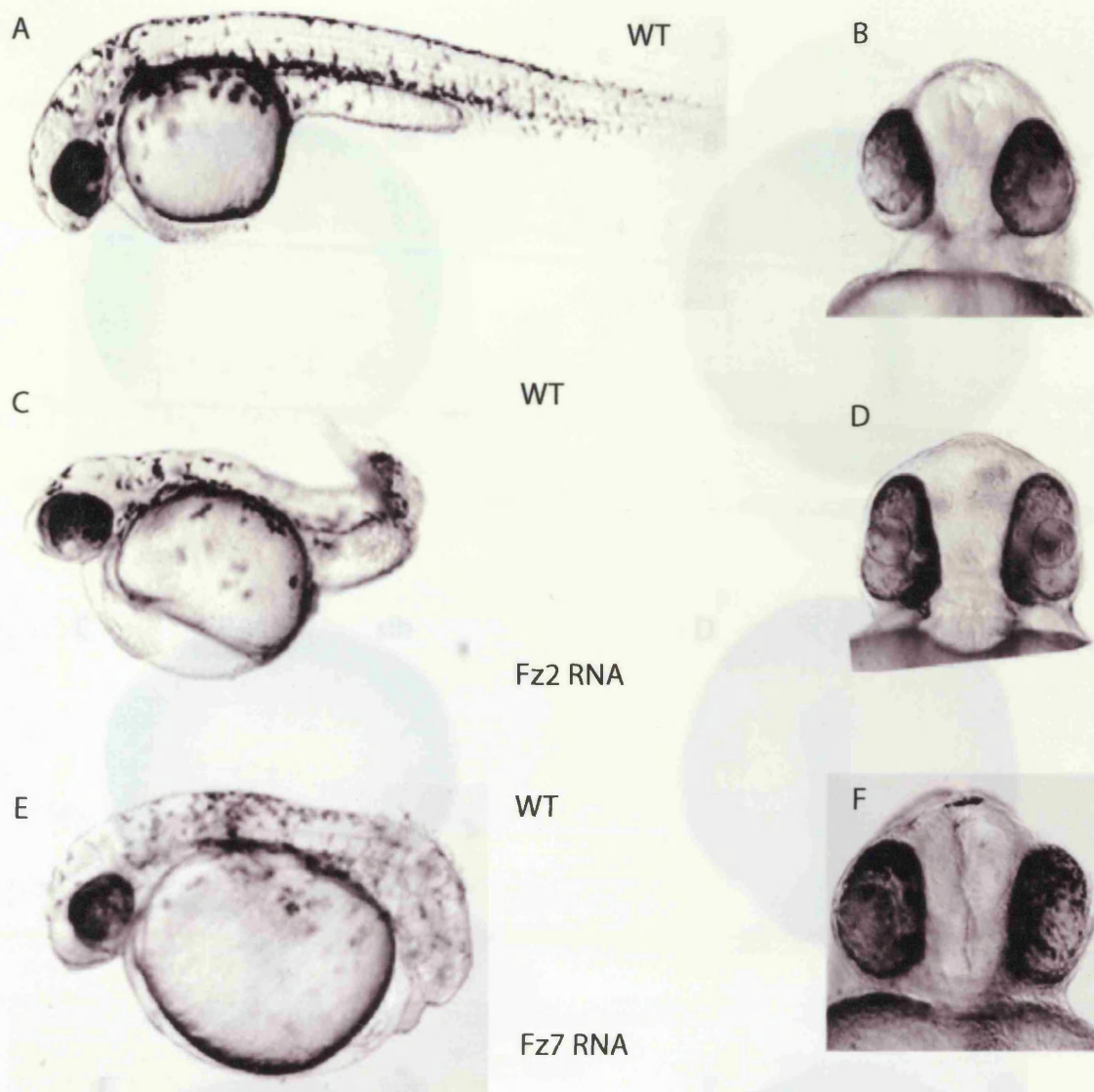


Figure 3.4. Injection *fz2* or *fz7* RNA in wild type embryos at pharyngula stage. Lateral and frontal views of wildtype embryos (A, B) and injected embryos (C, E and D, F). Wildtype embryos injected with 100pg *fz2* RNA (C, D), or wildtype embryos injected with 100pg *fz7* RNA (E, F).

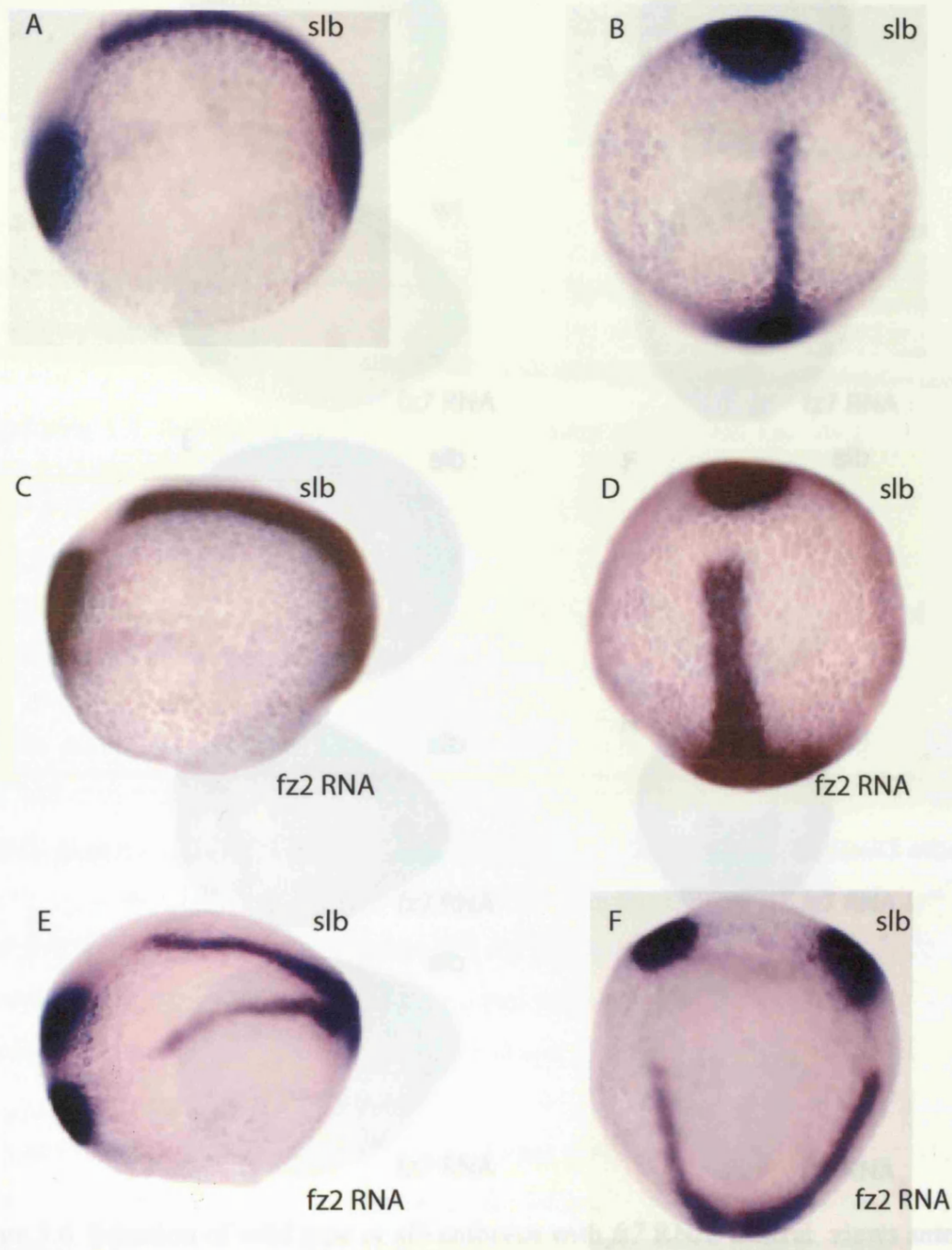


Figure 3.5. *slb* embryos injected with 10pg *fz2* RNA at tail bud stage (C, D, E, F). Lateral views, anterior is left (A, C, E) and dorsal views, anterior is up (B, D, F). *slb* embryos (A, B). Injection of 10pg in *slb* embryos leads to an enhancement of the *slb* phenotype with an enlarged notochord (C,D) or to an axis duplication(E, F) .

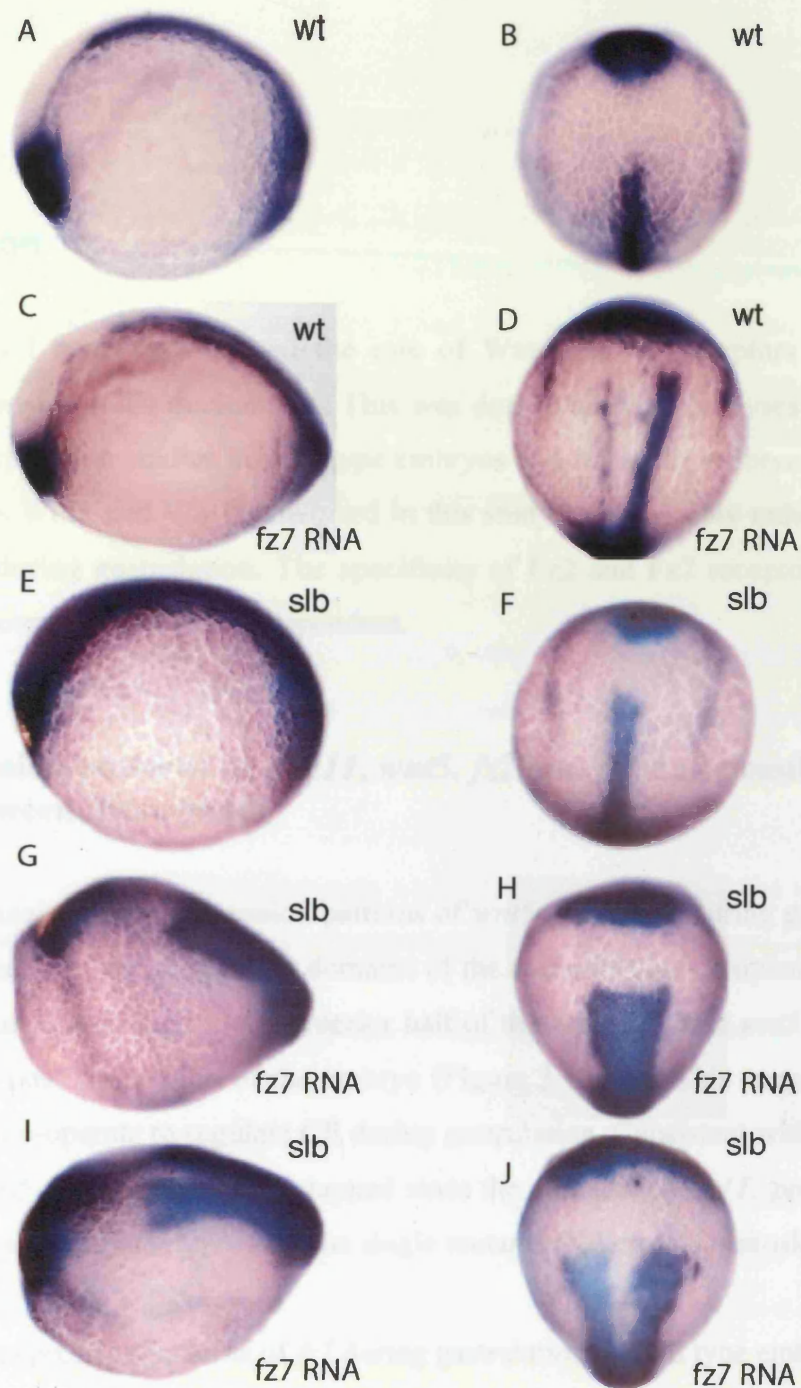


Figure.3.6. Injection of wild type or *slb* embryos with *fz7* RNA. Lateral views anterior is left (A, C, E, G, I) and dorsal views anterior is up (B, D, F, H, J). Wild type embryos (A, B) and wt embryos injected with 50pg *fz7* RNA (C,D). *slb* embryos (E,F) and *slb* embryos injected with 10 pg *fz7* RNA (G, H, I, J). Injection of wt embryos with 50 pg *fz7* RNA causes a partial axis duplication (C, D). Injection of *slb* embryos with 10pg *fz7* RNA leads to a highly dorsalized phenotype (G, H) or a complete axis duplication (I, J).

3.3. Discussion

In this analysis I have investigated the role of Wnts and Fz receptors in regulating convergent extension (CE) movements. This was done mainly by analyses of expression patterns, overexpression studies in wild type embryos and *slb/wnt11* embryos experiments. The two ligands Wnt5 and Wnt11 analyzed in this study have possibly redundant roles in regulating CE during gastrulation. The specificity of Fz2 and Fz7 receptors to Wnt5 or Wnt11 is time- concentration-place dependent.

3.3.1. Expression patterns of *wnt11*, *wnt5*, *fz2* and *fz7* and possible relations between these genes

In this study I analyzed the expression patterns of *wnt5* and *wnt11* during gastrulation. At the end of gastrulation, the expression domains of the two genes are complementary in that *wnt11* expression is restricted to the anterior half of the embryo while *wnt5* expression is localised to the posterior region of the embryo (Figure 3.1.G-H). This suggests that *wnt5* and *wnt11* may co-operate to regulate CE during gastrulation. Consistent with this idea, the functions of Wnt5 and Wnt11 are overlapped since the double *slb/wnt11*; *ppt/wnt5* mutant exhibits a more severe phenotype, than the single mutants (Kilian, Mansukoski et al. 2003).

In addition, the expression patterns of *fz7* during gastrulation in wild type embryos revealed that *fz7* expression largely overlaps with that of *wnt11* in the anterior lateral domain of the neuroectoderm and there is no expression in the presumptive notocord at tail bud stage (Figure 3.3. C, F). This pattern of expression leads to the hypothesis that *wnt11* and *fz7* may interact to regulate the convergent extension movements. In contrast, expression patterns of *fz2* slightly overlap with *wnt5* at the border between the anterior and posterior mesendoderm at tail bud stage (Figure 3.1. E and Figure 3.3. I). These results suggest that Fz7 may be a receptor for Wnt11 and Fz2 could be a receptor for both Wnt11 and Wnt5.

Recently based on imaging analysis, the distinct cell behaviors were examined and there is no specific relation between ligand-receptor. It is likely that the different local requirements

of *ppt/wnt5* and *slb/wnt11* along the anterior–posterior axis of the gastrula reflect some functional and/or structural subdivision of the developing mesendoderm. Actually, *in vivo* analyses of cell behaviour in zebrafish show that anterior mesendodermal cells seem not to undergo the classical CE movements described for more posterior tissues but instead exhibit a highly co-ordinated type of migration over a substrate cell movement (Ulrich, Concha et al. 2003). Thus, it is possible that Slb/Wnt11 regulates the migration of anterior mesendodermal cells while both Ppt/Wnt5 and Slb/Wnt11 are required for CE movements in more posterior mesendodermal tissues. These two genes are redundant in some functions but “when and where” they act is a context-dependent situation. The two different patterns of expression in zebrafish and the double mutant *slb:ppt* phenotype showed that there is some level of redundancy between them (Kilian, Mansukoski et al. 2003), but to quantify this is a really overwhelming task.

3.3.2. Overexpression of Wnt ligands and Fz receptors on wild type and mutant background

In order to prove the functional interaction, I attempted to rescue the *slb* embryos by overexpression of *wnt11* RNA. This was done by injection of *wnt11* RNA (10pg) and I obtained a total rescue in 100% of the embryos with a longer notochord and anteriorly positioned precordal plate as in wild-type embryos (Figure 3.2. D-F). In contrast, injection of 10pg of *wnt5* RNA did a partial rescue of the *slb* phenotype, in the sense that the prechordal plate reaches the anterior edge of neural plate while the notocord remains shorter or even wider (Figure 3.2. G-M). These results implied that Wnt5 might have a function in regulating CE movements in a similar but distinct way to Wnt11. Nevertheless, higher amounts of *wnt5* RNA were necessary to fully rescue the *slb* prechordal plate phenotype compared to the amount of *wnt11* RNA injected. This indicates that, while *wnt5* can functionally replace *wnt11* in the anterior mesendoderm, it is less efficient in doing so (Kilian, Mansukoski et al. 2003).

Conversely, in collaboration with Carl-Phillip Heisenberg’s group I tried to rescue the *ppt* embryos with *wnt5* or *wnt11* RNA (data not shown). It was impossible to rescue the *ppt* mutant phenotype by over-expressing either *wnt5* or *wnt11* RNA. However, *ppt* embryos injected with various concentrations of *wnt11* or *wnt5* RNA had different malformations.

Injection of *wnt5* RNA in *ppt* embryos led to a severely dorsalised phenotype; while injection of *wnt11* RNA caused a milder phenotype. The reason why the *ppt* phenotype is not rescued even with *wnt5* RNA is unclear, but it might be possible that the posterior mesendoderm is more sensitive to the dosage of Wnt5 rather than Wnt11 to activate the canonical Wnt pathway.

A dorsalisation phenotype was also detected when I overexpressed *fz2* or *fz7* RNA in wild-type embryos (Figure 3.4. C, E and Figure 3.6. C, D). When *fz2* or *fz7* RNA was overexpressed in *slb* embryos for a possible rescue of the mutant phenotype, the injected embryos exhibited an even more severely dorsalized phenotype instead of being rescued, such as a shortened/truncated notochord, a misshaped and displaced prechordal plate and a split body axis (Figure 3.5.C-F and Figure 3.6.). This phenotype was observed especially when *fz7* RNA was overexpressed in *slb* (Figure 3.6.G-J). The reason for this might be that the *slb* mutant could be over-sensitive to the dosage of Fz2 or Fz7 receptors and that ubiquitous expression may block the normal CE movements in the mutant. Therefore, overexpression experiments in *slb* or *ppt* mutants might not be a good way to interpret the specificity of the receptors to the ligands.

3.3.3. Loss of function experiments to assess the specificity of the non-canonical pathway

Although I did not show any results to describe a genetic interaction between *slb/wnt11* and *ppt/wnt5* in this thesis, I will discuss the specificity between ligands, Wnt11 and Wnt5, and receptors, Fz7 and Fz2 based on loss-of function experiments in a collaborative work with Carl-Phillip Heisenberg's group (Kilian, Mansukoski et al. 2003).

As discussed in section 3.3.1 of this chapter, Fz2 could be a receptor for Wnt11 and Wnt5 based on their expression domains at late gastrula stage. However, several lines of evidence support the possibility that Fz2 is a receptor for Wnt5. It was reported that abrogation of Fz2 function with morpholinos during gastrulation causes a shortening of the body axis analogous to the *ppt* mutant phenotype (Sumanas, Kim et al. 2001). During my collaboration project, morpholinos (Mos) against *fz2* were injected into *ppt* mutant to evaluate if *fz2* functions downstream of *ppt/wnt5*. The main assumption was if Fz2 was a

receptor primarily for Wnt5 in a linear pathway, abrogation of its function in *ppt* mutants would not enhance the *ppt* phenotype. Indeed, the length of the notochord was not affected or only slightly shortened in mutants injected with *fz2*Mo as compared to uninjected *ppt* mutants, suggesting that Fz2 possibly acts as a downstream receptor of Wnt5 during gastrulation (Kilian, Mansukoski et al. 2003). To reinforce this idea, a combination of morpholinos was made for *fz2* and *wnt5* and injected in wild type embryos. *wnt5* morpholino injected embryos showed a slightly shorter notochord than in *ppt* mutant embryos (Lele, Bakkers et al. 2001; Kilian, Mansukoski et al. 2003). However, there was no enhancement of the *wnt5* morphant notochord phenotype together with *fz2* morpholino injection, confirming that *fz2* functions downstream of *ppt/wnt5* (Kilian, Mansukoski et al. 2003). On the other hand, *slb* embryos injected with *fz2* morpholino showed an enhanced CE phenotype similar to the *slb;ppt* double mutant phenotype, indicating that Fz2 may act in a parallel pathway to Wnt11 (Kilian, Mansukoski et al. 2003).

Taken together with the discussion in section 3.3.2 of this chapter, it might be more reliable to test the specificity between the non-canonical ligands and their putative receptors based on loss of function experiments rather than gain of function experiments.

In a recent study the loss of function analyses by morpholino approach and by mutant analyses combined showed that loss of function of Wnt5 leads to hyperdorzaliation and duplication of the axis possibly by activation of the canonical Wnt pathway may be by leading to accumulation of β -catenin protein (Westfall, Brimeyer et al. 2003). Through loss-of-function analyses, these results have revealed a raise in β -catenin accumulation and activation of downstream genes sustaining a hypothesis for a function of the Wnt/ Ca^{+2} by possibly antagonizing the Wnt/ β -catenin activity in vertebrate development (Westfall, Brimeyer et al. 2003). However these results are contradictory to our collaborative results (Kilian, Mansukoski et al. 2003). Maternal zygotic (MZ) *ppt/wnt5* mutants resemble zygotic *ppt/wnt5* mutants. In addition, MZ *ppt/wnt5; slb/wnt11* double mutants exhibit a phenotype identical to the zygotic *ppt;slb* mutants. Therefore, there is no necessity for maternal *ppt/wnt5* either to regulate CE during gastrulation or to activate the canonical Wnt pathway at a significant level.

3.4. Summary

In this chapter I have shown the possible functions of Wnt5, Wnt11 ligands and Fz2, Fz7 receptors in regulating convergent extension (CE) movements. The analyses of expression patterns of these genes did not correlate with their actual *in vivo* function. However, the over-expression revealed the specificity between ligands-receptors to transduce the non-canonical Wnt pathway remains unclear. Based on the loss of function experiments, the two ligands Wnt5 and Wnt11 have possibly redundant roles and the specificity of Fz2 and Fz7 receptors to any of these Wnt ligands is time-concentration-place dependent. In conclusion, the analyses of expression patterns of these genes to some extent, but not totally, correlate with their actual *in vivo* function.

CHAPTER 4

Prickle1 regulates cell movements during gastrulation in zebrafish

4.1.Introduction

Recent functional studies in *Xenopus* and genetic analyses of gastrulation mutants in zebrafish have revealed that a non-canonical Wnt pathway is involved in the regulation of CE. This pathway is associated with the planar cell polarity (PCP) pathway that mediates the establishment of cell polarity in the plane of epithelia in *Drosophila* (reviewed in (Adler 2002; Mlodzik 2002; Tada, Concha et al. 2002; Wallingford, Fraser et al. 2002)). In vertebrates, the glycoproteins Wnt11/Silberblick (Slb) and Wnt5/Pipetail (Ppt) act as ligands (Heisenberg, Tada et al. 2000; Tada and Smith 2000), although a Wnt ligand mediating PCP has yet to be found in *Drosophila*. Shared components of the non-canonical Wnt pathway and the PCP pathway include Frizzled (Fz) receptors, an intracellular signal proteins such as Dishevelled (Dsh), a 4-pass transmembrane protein Vangogh/Strabismus/Trilobite (Vang/Stbm/Tri), small GTPases RhoA and Cdc42 and a RhoA effector Rho kinase 2 (Rok2).

prickle (pk) is one of the core PCP genes that controls planar polarity in the eye, leg and wing of *Drosophila* and encodes an intracellular protein containing three LIM domains and a conserved “PET” domain (for Prickle, Espinas and Testin)(Gubb, Green et al. 1999). Epistasis analyses have showed that Pk is required for some aspects of Fz/Dsh-mediated PCP signalling, but is not placed in a linear cascade with Fz and Dsh. Recent studies in *Drosophila* suggested that Pk regulates the subcellular distribution of Fz through binding to Dsh, thereby localising the Fz/Dsh complex to one side of the epithelial cells (Tree DR 2002).

In this chapter, I analysed the expression pattern of a zebrafish homologue of the *Drosophila* PCP gene *prickle (pk1)* and its function, during gastrulation. I have perceived

that zebrafish *pk1* functions together with Slb/Wnt11 and Ppt/Wnt5 to regulate CE movements. Consistent with the results in flies, I have found that Pk1 can destabilise Dsh and thereby block the ability of Fz to target Dsh to the cell membrane. These results show that Pk1 modulates different types of cell behaviour during CE.

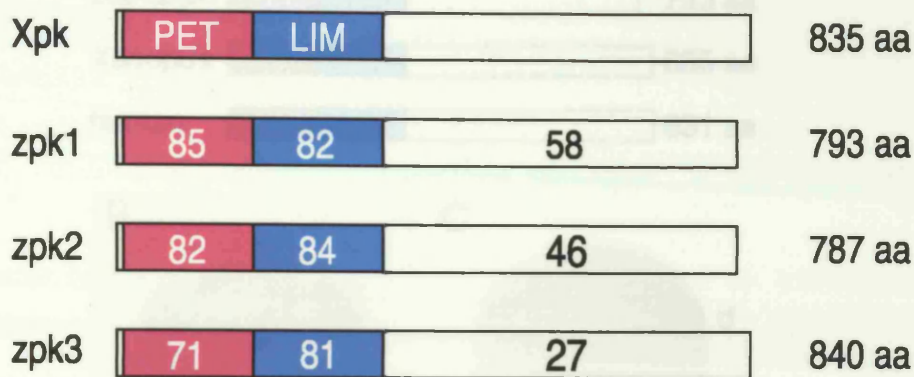
4.2.Results

4.2.1. The expression patterns of zebrafish *prickle* genes

To investigate whether homologues of the *Drosophila* PCP gene *prickle* (*pk*) function during vertebrate gastrulation, three full-length clones of zebrafish *pk* genes were isolated from shield gastrula library. The predicted proteins encoded by zebrafish *pk1*, *pk2* and *pk3* shared 85% and 82%, 82% and 84 % and 71% and 81%, respectively, of amino acid identity to *Xenopus* XPk-A. Within a highly conserved PET domain of unknown function and three LIM domains, respectively (Figure. 4.1A, B, 4.2.A).

pk1 is expressed maternally (Figure. 4.2.B) and zygotic expression is initiated on the dorsal side of the embryo at pre-gastrula stages (Figure. 4.2.C) and spreads throughout the germ ring by the shield stage (Figure. 4.2.D). As gastrulation continues, expression becomes restricted to dorsal involuted cells and to overlying axial ectodermal cells (data not shown). By tail-bud stage, expression is down-regulated in the ectoderm and becomes restricted to adaxial cells, presomitic mesoderm and the lateral edge of the neural plate (Figure. 4.2.E). *pk2* starts to be expressed after shield stage and becomes restricted to the presomitic mesoderm and notochord (Figure 4.2.F, H). *pk3* is expressed zygotically and in the presumptive eye field and in the midline, which is not correlated with the notochord, at tail bud stage (figure 4.2 G, I).

A



B

	PET
Xpk	QRSSTSDDDSGCA E EYTWPPGLR EOVLYFACLPEEK PYVNS GEKYRIKOLLYQL
zpk1	QRSSTSDDDSGCALEEY WVPPGLRPEQV LYFSCLPEDKVPYVNSPGEK RIKOLLYQL
zpk2	QRSSTSDDDSGCALEEYTWPPGLR EOVQ YFSCLPPEEKVPYVNSPGEK RI OLLYQL
zpk3	QR STSDDDSGCALEEY WVPPGLR EOVQ Y S LPEI KVPYVNSPGEKYRIKQLL QL
	LIM1
Xpk	PPHDNEVRYCQSLSEEEKKEL MFS ORKKEALGRGN K L RAV HA CE CGE INGG
zpk1	PPHDNEVRYCQSLSEEEKKELMFS ORKKEALGRG TLK LPRTV HA CEHGERLS GG
zpk2	PPHDNE RYCQSLSDEERRELHMFS ORKKEALGRG K L PRA QHN CEHCKE INGG
zpk3	PPHDNE RYC SL DEEKREL KL FS ORK E LGRGN VRPF PVTMTGA CE CGG INGG
	LIM2
Xpk	EVA FVSRAAGP VCWHP CFVCSTC ELLVDLIYFYQDGKIHCGRHHAELLKPRCSACD
zpk1	EMAV VSRAAAGP CWHAPCF CSTC ELLVDLIYFY DGK HCGRHHAEELLKPRCS CD
zpk2	EMAVF SRAGPG CWHAPCF CY TC ELLVDLIYFY NGN HCGRHHAEELLKPRCSACD
zpk3	DI AVF SRAGHG VCWHP CFVCS C ELLVDLIYFYQDGKI CGRHHAE LKPRCSACD
	LIM3
Xpk	EIIFADECTEAEGRHWHM HFCC ECETVLGGORYIMKDGRPFCCGCFES YAEYCSCG
zpk1	EIIFADECTEAEGRHWHMKHF C ECEV LGGORYIMKDGRPFCCGCF SLYAEYCACA
zpk2	EIIFADECTEAEGRHWHMKHF CFECET LGGORYIMKDGRPFCCGCFESLYAEYCE CG
zpk3	EII ADECTEAEGRHWHMKHFCCFECETVLGGORYIMK GRPYCC CFESLYAEYC SCG
	LIM3
Xpk	EHIGVDHAQMTYDGOHWHATE CFSCAOCK SLLGCPFLPK GRIYC KACSLGE
zpk1	EHIGVDHAQMTYDG HWHAT ACFSCAOCK SLLGCPFLP OGRIYCSKACSLGE
zpk2	ENIGVDHAQMTY G HWHAT CF CAOCK SLLGCPFLPK GRIYCSK CSLGE
zpk3	EHIG D QMTYDGOHWHATEACFSCARCK SLLG PFLPKQGTI CS ACSVG

Figure 4.1. Homology of Prickle proteins between zebrafish (*Pk1*, *Pk2*, *Pk3*) and *Xenopus* (XPK-A (Wallingford et al., 2002b)). A- schematic representation of the homology .The numbers refer to the percentage amino acid identities between the different orthologues. B- Alignment of amino acid residues of Prickle proteins in the conserved PET-LIM domain. Identical amino acid residues are highlighted in bold.

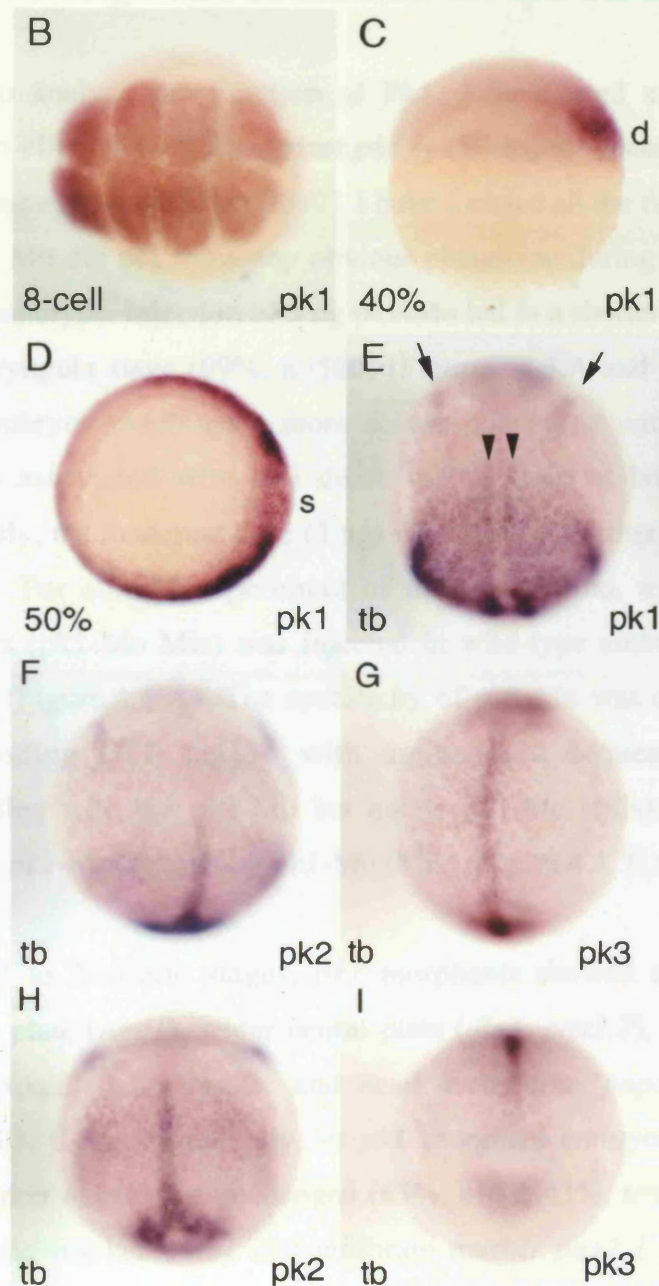
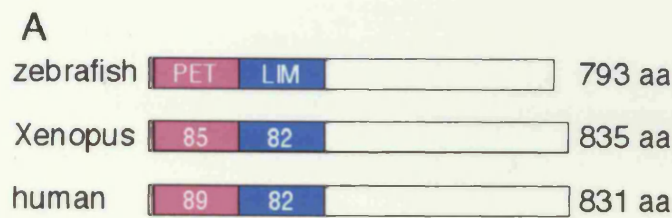


Figure 4.2. *pk1* is expressed maternally and in migrating mesodermal precursors in zebrafish. (A) Homology of Prickle proteins between zebrafish (Pk1), Xenopus (XPk-A (Wallingford et al., 2002b)) and human (BAB71198). The numbers refer to the percentage amino acid identities between the different orthologues. (B-E) Expression of *pk1* at early stages. *pk1* is expressed maternally at 8 cell stage (B, animal view), on the dorsal side at around 40% epiboly (C, lateral view with dorsal to the right), and around the germ ring at 50% epiboly (D, animal view with dorsal to the right). At tailbud stage (E, dorsal view and anterior is up), expression is restricted to the presomitic mesoderm, adaxial cells (arrowheads) and the lateral edge of neural plate (arrows). F-G. Expression of *pk2* (F,H) and *pk3* (G,I) at tail bud stage. Dorsal view (F, G), dorso-vegetal view (H) and animal view with dorsal to the top (I). F-H anterior is up. Abbreviations: d, dorsal; s, shield. 102

4.2.2. Interfering with Pk1 function disrupts CE during gastrulation

In order to analyse the function of Pk1, I have used an anti-sense approach using morpholino oligonucleotides against *pk1* (pk1-Mo) to reduce the level of endogenous Pk1 protein (Nasevicius and Ekker 2000). I have focused all the functional analyses of *pk1* since *pk2* or *pk3* Mo did not show any obvious phenotype during gastrulation nor enhances the pk1-Mo phenotype. Injection of 3 ng pk1-Mo led to a shorter body axis with a curled down tail at pharyngula stage (99%, n>500) (Figures. 4.3.A and B). At higher concentrations, injected embryos exhibited a more severe phenotype with shorter trunk and tail, but sometimes associated with cell death in the brain at later stages (data not shown). Subsequently, the moderate dose (3 ng) was used for further analyses of the pk1 morphant phenotype. For control experiment of the morpholino, a Mo including 4 nucleotides mismatches (pk1-Mo Mis) was injected in wild-type embryos and causes no defective phenotype (Figure.4.4 A). The specificity of pk1-Mo was determined by co-injection of RNA encoding GFP tagged with amino acid sequences that include sequence corresponding with the pk1-Mo but not to pk1-Mo (Mis). The level of GFP is totally reduced by pk1-Mo, but not by pk1-Mo (Mis) (Figure 4.4. B and C).

At tail-bud to 2-somite stages, *pk1* morphants showed a slightly posteriorly located prechordal plate (*hgg1*), wider neural plate (*dlx3*, *pax2.1*), a shorter notochord (*ntl*) and laterally expanded presomitic and head mesoderm (*papc* and *snail2*) (72%, n=102) (Figures. 4.3. C-J). Additionally, in *pk1* morphant embryos, the dorsal marker *chd* and ventral marker *bmp2b* are unchanged (63%, n=57, 43%, n=64) (Figure. 4.3.K-N) and the telencephalic marker *emx1* and midbrain marker *pax2.1* are expressed in the correct positions, although their expression domains are laterally expanded (45%, n=37, 56%, n=47) (Figure. 4.3.O-R), reflecting reduced convergence of the neural plate (Fig. 4.3.G,H).

Additionally, the canonical Wnt signalling is not affected at very early stages of development in *pk1* morphants, because there is no phenotype with disruption of early organiser formation or fates, the expression of anterior mesendodermal markers *gsc*, *dkk1* (74%, n=27, 83%, n=34) (Figure 4.5.A-D) and *hgg1* (Figure. 4.3. G, H) is unchanged. The

only changes in expression of these genes reflect the fact that the expression domains are less converged and less extended.

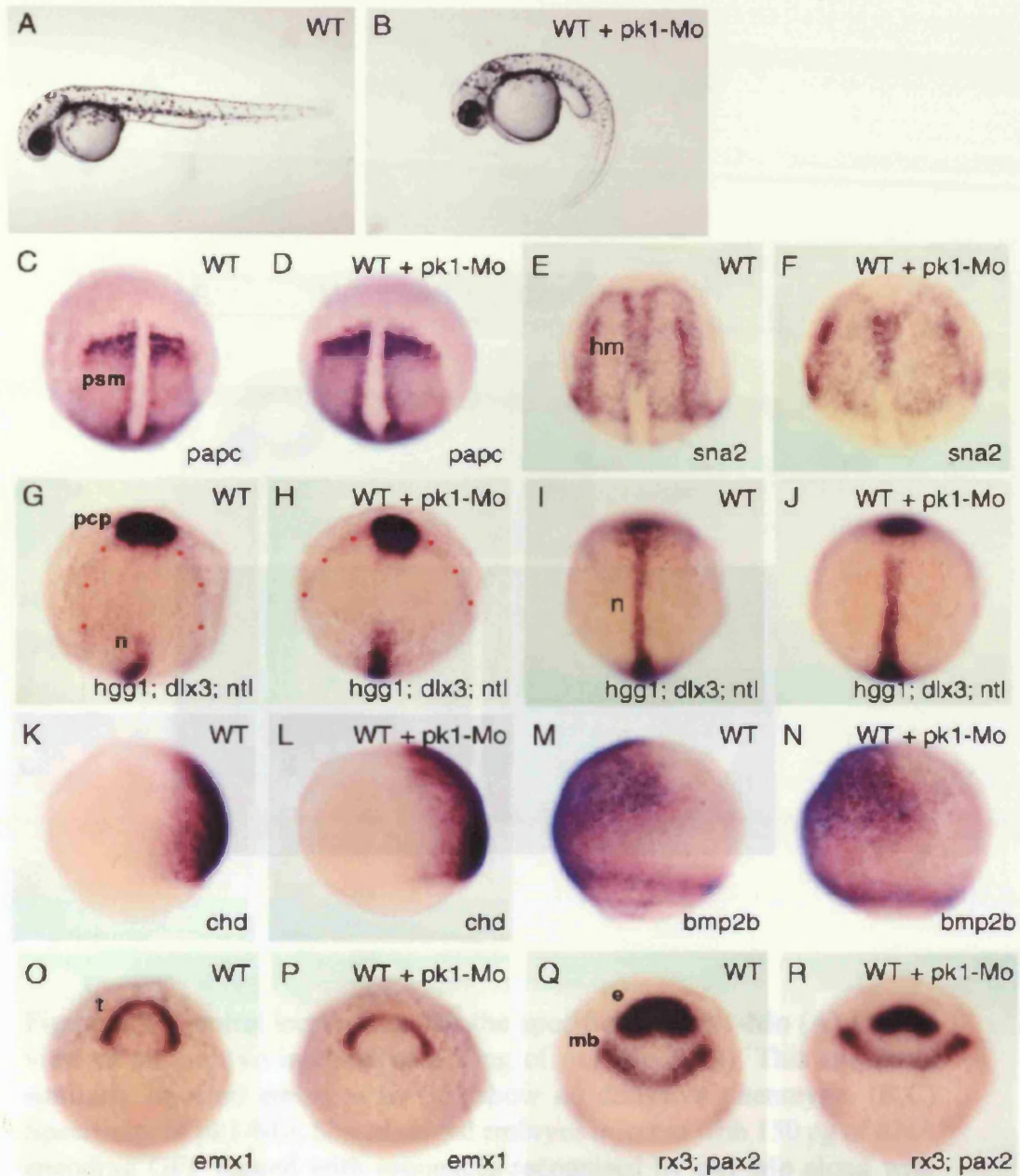


Figure 4.3. *pk1* morphants exhibit defects in convergent extension movements. (A,B) Lateral views of pharyngula stage living wild-type (A) and *pk1*-morphant (B) embryos. The *pk1*-morphant embryo (B) shows a slightly compressed trunk with a curled down tail. (C-J,O-R) Dorsal views of tailbud-stage wildtype (WT) and *pk1*-morphant (WT + *pk1*-Mo) embryos. (K-N) Lateral views of 80% epiboly wild-type (WT) and *pk1*-morphant (WT + *pk1*-Mo) embryos. Anterior is up and genes analysed are indicated bottom right. Dots outline the prospective neural plate. e, eye field; mb, prospective midbrain; t, prospective telencephalon; psm, presomitic mesoderm; hm, head mesoderm; n, prospective notochord, pcg, prechordal plate.

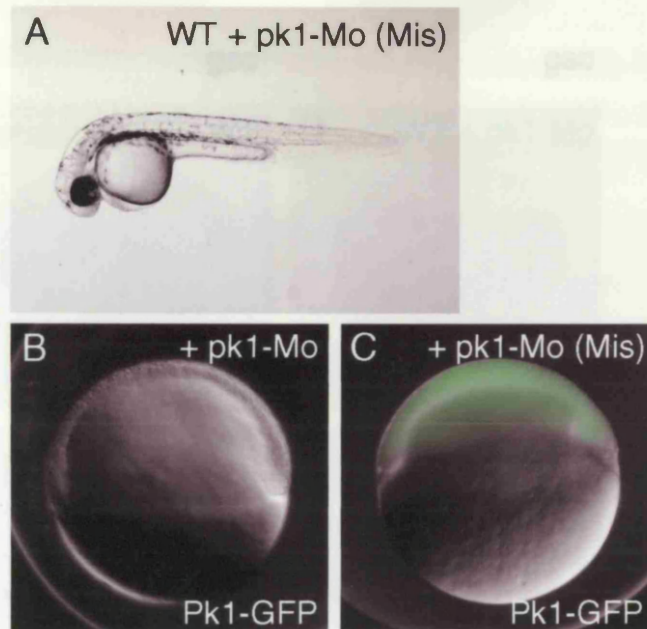


Figure 4.4. Control experiment for the specificity of pk1-Mo (A) Lateral view of an embryo injected with 3 ng of pk1-Mo (Mis). This and other similarly injected embryos (n=30) show no defective phenotype. (B,C) Specificity of pk1-Mo. Shield staged embryos injected with 150 pg of RNA encoding GFP tagged with sequences recognised by pk1-Mo along with either 3 ng of pk1-Mo (B) or 3 ng of pk1-Mo (Mis) (C). The level of GFP is totally reduced by pk1-Mo (n=62), but not by pk1-Mo (Mis)(n=40).

Figure 4.4 (A) Lateral view of an embryo injected with 3 ng of pk1-Mo (Mis). This and other similarly injected embryos (n=30) show no defective phenotype. (B,C) Specificity of pk1-Mo. Shield staged embryos injected with 150 pg of RNA encoding GFP tagged with sequences recognised by pk1-Mo along with either 3 ng of pk1-Mo (B) or 3 ng of pk1-Mo (Mis) (C). The level of GFP is totally reduced by pk1-Mo (n=62), but not by pk1-Mo (Mis)(n=40).

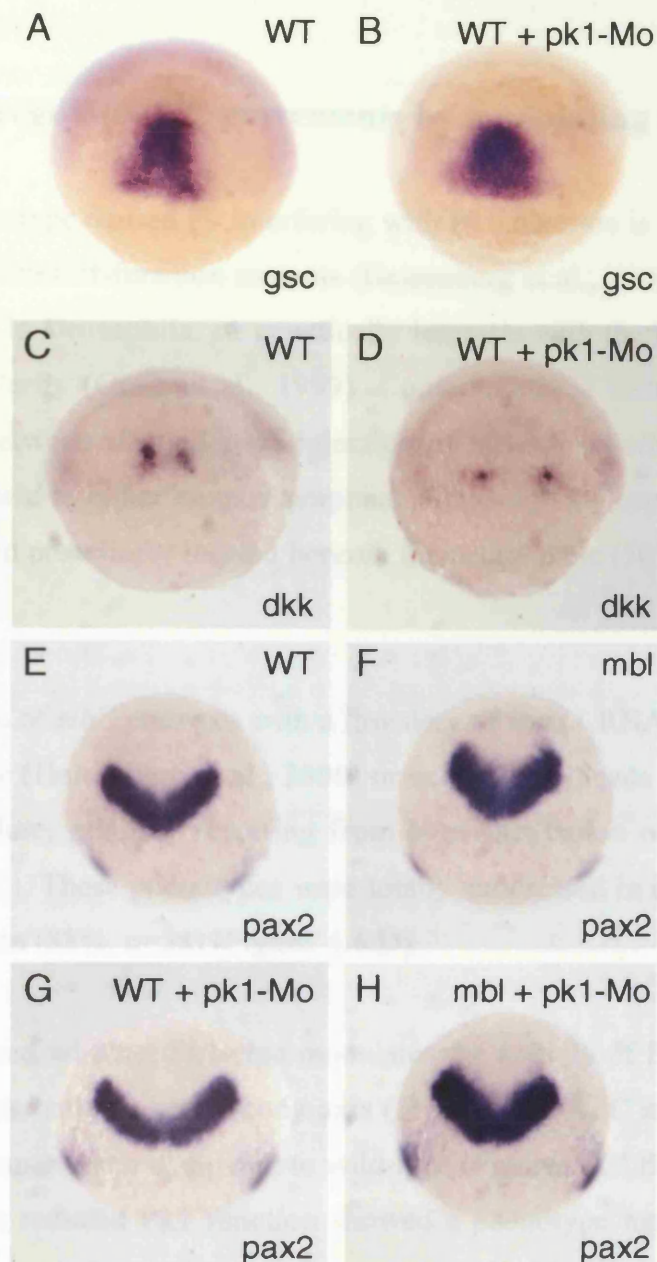


Figure 4.5. Pk1 function does not alter AP patterning of the neural plate (A-D) Dorsal views of 55% epiboly wild-type (WT) and *pk1* morphant (WT+ pk1-Mo) embryos. Anterior is up and genes analysed are indicated bottom right. Note that involuted dorsal mesendodermal cells expressing *gsc* or *dkk1* are less converged in *pk1* morphant embryos, but their expression levels are not significantly changed. (E-H) Dorsal views of tail-bud stage wild-type (E,G) and *masterblind* (*mbi*) embryos injected with pk1-Mo (G,H). The *pax2.1* expression domain in *mbi* embryos, in which the level of canonical Wnt activity is increased, remains unchanged by abrogation of Pk1 function. This, together with the observation that the telencephalic marker *emx1* is expressed in the correct position in *pk1* morphants (Fig. 4.3 P), argues that abrogation of Pk1 function does not alter AP patterning of the neural plate and therefore is unlikely to influence the activity of the canonical Wnt pathway.

4.2.3. Pk1 regulates CE movements by modulating the Wnt/PCP pathway

The CE phenotype caused by interfering with Pk1 function is similar to those in *slb/wnt11* and *ppt/wnt5* loss-of-function mutants (Heisenberg et al., 2000; Kilian et al., 2003; Rauch et al., 1997). In *Drosophila*, *pk* genetically interacts with the Fz/PCP pathway to establish epithelial polarity (Gubb et al., 1999). Consequently, I tested if there was any genetic interaction between *slb* and *pk1*. Injection of pk1-MO in *slb* embryos enhanced the CE defect compared to either mutant/morphant alone, with the consequence that the prechordal plate remained posteriorly located beneath the neural plate (50%, n=92) (Figure. 4.6. A and B).

Also injection of *slb*^{-/-} embryos with a low dose of *wnt11* RNA (10 pg) either fully rescues the phenotype (Heisenberg et al., 2000) or occasionally leads to lateral mis-positioning of prechordal plate, possibly resulting from hyper-activation of the pathway (13%, n=53) (Figure. 4.6.C). These phenotypes were totally suppressed in embryos with reduced levels of Pk1 function (88%, n=58) (Figure. 4.6.D).

I also examined whether Pk1 also modulates the activity of Ppt. Both *ppt*^{-/-} embryos and *pk1* morphants have a shorter body axis (Figures. 4.7 A, C and E), in which somites are wider and thinner when compared to wild-type (Figures. 4.7.B, D and F). *ppt/wnt5* mutant embryos with reduced Pk1 function showed a phenotype much more severe than either single mutant/morphant with greatly compressed wider somites (42%, n=118) (Figures. 4.7.G and H).

To more directly assay if Pk1 is likely to modulate canonical Wnt signalling, we injected the pk1 MO into *mb1* embryos to assess if abrogation of Pk1 activity affects the phenotypic severity of *mb1* mutants. *mb1* embryos show expansion of diencephalic fates and concomitant loss of eye and telencephalic fates (Heisenberg, Houart et al. 2001). Although midbrain is specified normally in *mb1* embryos, midbrain fates expand to the front of the neural plate in *headless* mutants (which show a greater increase in Wnt activity than *mb1* embryos; (Kim, Oda et al. 2000). Thus, any further increase of canonical Wnt activity in the

mb1 neural plate would lead to expansion of expression of midbrain markers (Houart, Caneparo et al. 2002). Injection of pk1-Mo into *mb1* embryos had no effect upon pax2.1 expression (23%, n=32) (Figure 4.5.E-H), strongly arguing that loss of Pk1 activity does not enhance the canonical Wnt signalling.

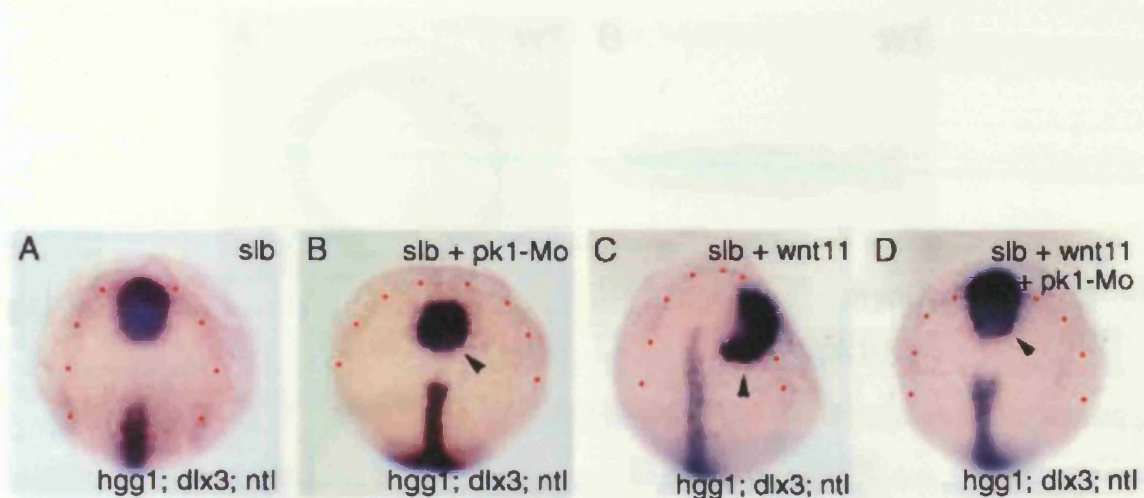


Figure 4.6. Abrogation of Pk1 function enhances the *slb* phenotype and suppresses elevated Wnt11 activity. (A-D) Dorsal views showing prechordal plate position (arrowheads) in a *slb* embryo (A), a *slb* embryo injected with 3 ng of pk1-Mo (B), a *slb* embryo injected with 10 pg *wnt11* RNA (C) and a *slb* embryo injected with 10 pg *wnt11* RNA plus 3 ng of pk1-Mo (D). Dots outline the prospective neural plate. The positions of the prechordal plate are indicated by arrowheads.

Figure 4.7. Abrogation of PK1 function enhances the pipetail (*ppt*) phenotype. Lateral (A, C, E, G) and dorsal (B, D, F, H) views of 18 somite embryos with anterior to the left. *myoD* expression shows the shape of the myotome (A, B, D, F, H). Arrowheads indicate the ventral surface and posterior extent of the myotome (A, B) and of the *ppt* embryos (C, E). *ppt* embryos injected with 3 ng of pk1-Mo (D, F) *ppt* phenotype (D, F). *ppt* embryos injected with 3 ng of pk1-Mo (G, H).

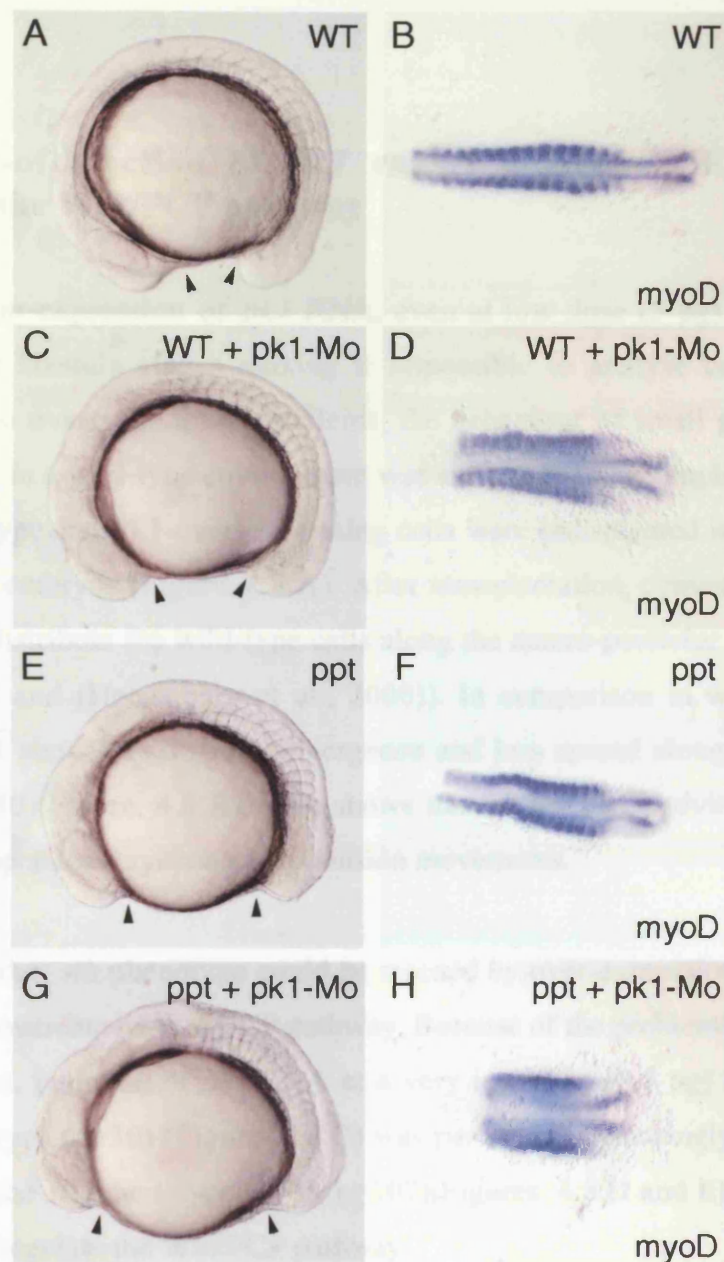


Figure 4.7. Abrogation of Pk1 function enhances the pipetail (ppt) phenotype. Lateral (A, C, E, G) and dorsal (B, D, F, H) views of 14 somite embryos with anterior to the left. *myoD* expression shows the shape of the somites in (B, D, F, H). Arrowheads indicate the most anterior and posterior extent of the axis. (A, B) wild-type embryos. (C, D) wild-type embryos injected with 3 ng of pk1-Mo. (E, F) ppt embryos. (G, H) ppt embryos injected with 3 ng of pk1-Mo.

4.2.4. Gain-of-function of *pk1* causes defective CE movements by modulating the Wnt/PCP pathway

Ubiquitous over-expression of *pk1* RNA, even at low dose (5 pg), caused strange cell aggregation at blastula stages making it impossible to analyse cell migration during gastrulation. To overcome these problems, the behaviour of small groups of cells over-expressing Pk1 in a wild-type environment was analyzed. To accomplish this, differentially labelled wild-type and Pk1-over-expressing cells were transplanted into the germ rings of wild-type host embryos (Figure. 4.8.A). After transplantation, convergence and extension movements redistribute the wild-type cells along the antero-posterior axis by tailbud stage (Figure. 4.8 B and (Heisenberg et al., 2000)). In comparison to wild-type, cells over-expressing Pk1 show less dorsal convergence and less spread along the antero-posterior axis (70%, n=40)(Figure. 4.8 B). This shows that higher Pk1 activity inhibits cells from undergoing proper convergence and extension movements.

I examined whether *slb* phenotype could be rescued by over-expression of *pk1* RNA if Pk1 was acting downstream of Wnt/PCP pathway. Because of the problems associated with *pk1* over-expression, injection of *pk1* RNA at a very low dose (0.5 pg) that has no effect in wild-type embryos (n=30) (Figure. 4.8.C) was performed. Amazingly, rather than rescue, this enhanced the *slb* phenotype (27%, n=107)(Figures. 4.8.D and E), indicating that Pk1 can negatively regulate the Wnt/PCP pathway.

Subsequently, I attempted to assay if Pk1 modulates the Wnt/PCP pathway by regulating the sub-cellular localisation of components of this pathway. Therefore, I examined whether Pk1 affects the localisation of Fz/Dsh complex in zebrafish embryos. When Dsh-GFP is expressed in the animal pole blastomeres, it predominantly localises to the cytoplasm, sometimes associated with vesicles-like structures (100%, n=10)(Figure.4.8.F). This most probably reflects the requirement of Dsh to localise to vesicles for canonical Wnt signalling (Capelluto, Kutateladze et al. 2002). In response to Fz7, Dsh is targeted to the membrane (90%, n=30) (Figure. 4.8.G), but this is inhibited by increasing Pk1 activity (100%, n=21)(Figure. 4.8.H). The predominantly cytoplasmic localisation of Pk1 remains

unchanged in the presence of Fz7 (Figure. 4.8.I). These observations, together with the fact that cytoplasmic Dsh-GFP becomes faint and hazy when Pk activity is increased (Figure. 4.8.H), raised the hypothesis that Pk1 activity may destabilise Dsh, thereby blocking Fz7-mediated membrane localisation of Dsh. To test this, I quantified myc-tagged Dsh in the presence of Fz7 with or without Pk1. Western blot analysis revealed that the levels of Dsh are significantly decreased in the presence of Pk1 (Figure. 4.8.J).

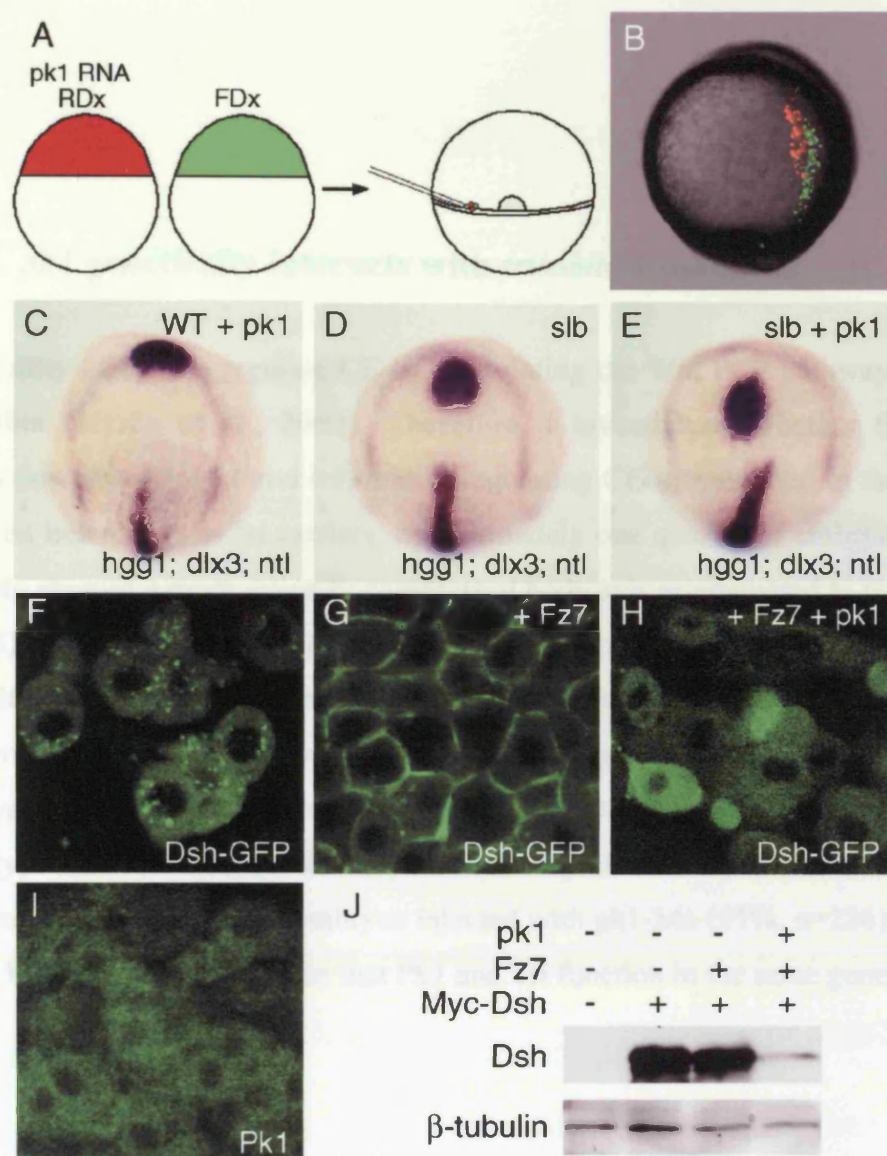


Figure 4.8. Over-expression of *pk1* causes defective morphogenetic movements and enhances the *silberblick* (*slb*) phenotype. (A) Schematic of the experiment. Cells from embryos that received 5pg *pk1* RNA and rhodamin-dextran (RDx) and cells from embryos that received fluorescein-dextran (FDx) were simultaneously transplanted into the germ rings of wild-type shield-staged hosts. (B) Lateral view of a living tailbud stage host embryo with dorsal to the right. Pk1-expressing cells (red) are more laterally positioned as compared to wild-type cells (green). (C-E) Gain-of-function of *pk1* enhances the *slb* phenotype. Dorsal views of a tailbud stage embryo injected with 0.5 pg of *pk1* RNA (C), a *slb* embryo (D) and a *slb* embryo injected with 0.5 pg *pk1* RNA. The position and shape of prechordal plate (*hgg1*) in relation to the anterior edge of neural plate (*dlx3*) in the *pk1* morphant (C) are similar to wild-type (see Figure 2.I). The prechordal plate is displaced caudally in the *slb* embryo (D) and even further caudally in the *slb* embryo injected with the *pk1*-Mo (E). (F-H) Confocal images of animal pole cells of 40% epiboly embryos injected with 200 pgRNA encoding Dsh-GFP (F), 200 pgRNA encoding Dsh-GFP + 50 pg *fz7* RNA (G) and 200 pgRNA encoding Dsh-GFP + 50pg *fz7* RNA + 5 pg *pk1* RNA (H). Dsh preferentially localises to vesicles (F), but relocates to the membrane in the presence of Fz7 (G). The Fz7-induced membrane localisation of Dsh is inhibited by Pk1 (H). (I) Sub-cellular localisation of Pk1 in animal pole cells of 40% epiboly embryos injected with 25 pg RNA encoding Venus-Pk1 (Pk1 tagged with a modified version of EGFP). Pk1 localises in the cytoplasm. (J) Western blot analysis of the levels of tagged-Dsh in embryos injected with 200 pg RNA encoding myc-Dsh along with 50 pg *fz7* RNA in the presence or absence of 5 pg *pk1* RNA. The blot was detected with either an anti-myc antibody for Dsh or an anti-β-tubulin antibody for loading control. The level of Dsh is reduced by *pk1*.

4.2.5. *pk1* genetically interacts with *trilobite/strabismus*

The ability of Pk1 to regulate CE by modulating the Wnt/PCP pathway is similar to that of Tri/Stbm (Jessen et al., 2002). Therefore, I investigated whether there is any genetic interaction between *pk1* and *tri stbm* in regulating CE movements. In the progeny of crosses between heterozygous *tri* carriers, approximately one quarter of embryos injected with 3 ng pk1-Mo showed a more severely compressed body axis as compared to *tri* homozygotes (25%, n=263) (Figures. 4.9. A, B, G, H, I and J). In addition, a further half of the injected population exhibited a phenotype indistinguishable from homozygous *tri* embryos (51%, n=263). To confirm that the tri-like phenotype arose from abrogation of Pk1 activity in heterozygous *tri*^{+/-} embryos, we injected pk1-Mo in embryos from crosses between heterozygous *tri* female and wild-type male fish. About 49 % (n=226) of injected embryos showed a *tri*-like phenotype, more severe than wild-type embryos injected with pk1-Mo (51%, n=226) (Figures. 4. 9. C, D, E and F). These results suggest that Pk1 and Tri function in the same genetic pathway.

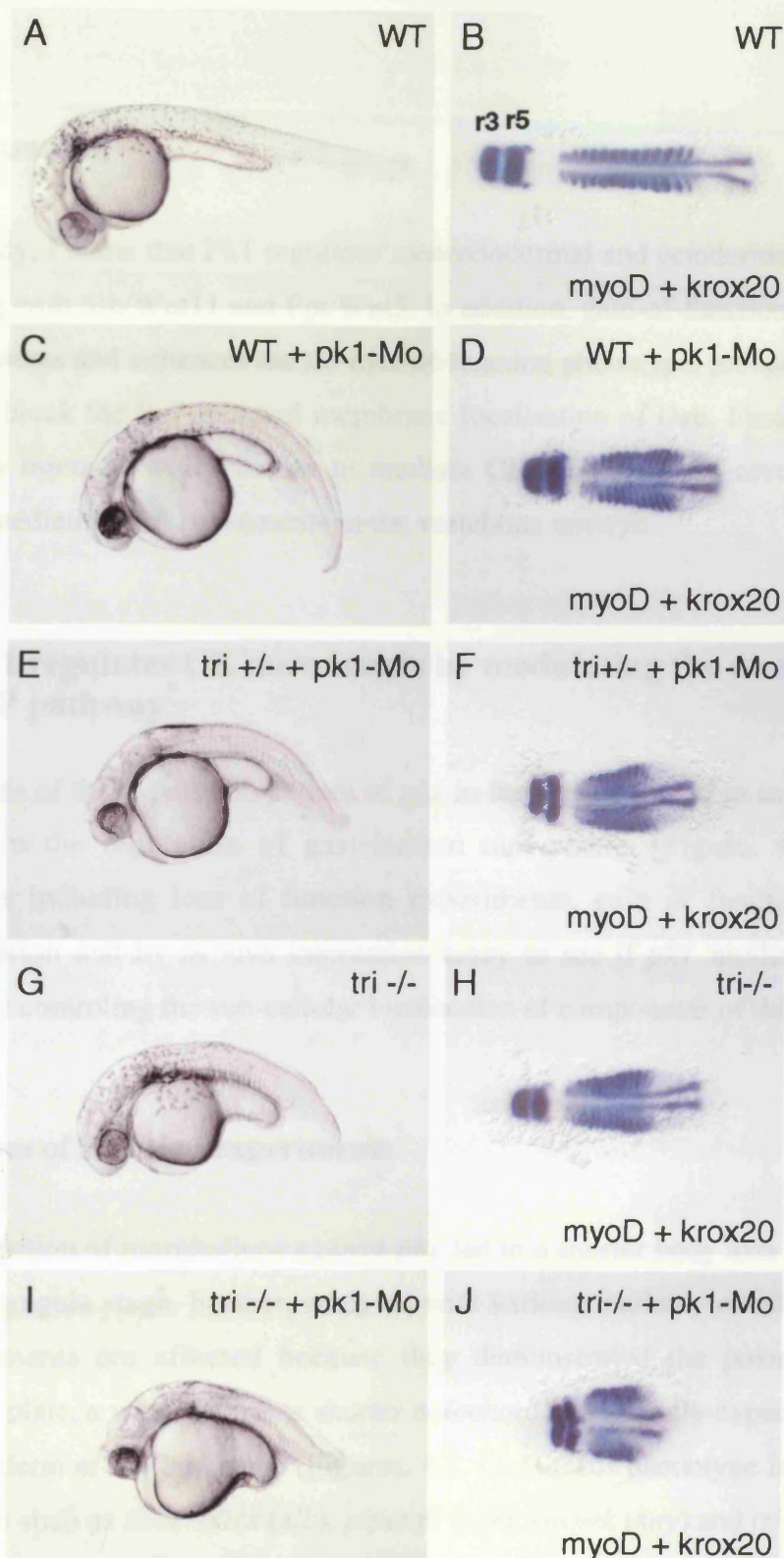


Figure 4.9. *pk1* and *tri* show a strong genetic interaction in regulating convergent extension. Lateral views of pharyngula-stage embryos (A,C,E,G,I) and dorsal views of 14-somite embryos (B,D,F,H,J) with anterior to the left. *myoD* expression shows the shape of the somites and *kroxD20* the position of rhombomeres (r3 and r5) in (B,D,F,H,J). (A,B) Wild-type embryos. (C,D) Wild-type embryos injected with 3ng of *pk1*-Mo. (E,F) *tri* heterozygous embryos injected with 3 ng of *pk1*-Mo. (G,H) *tri* homozygous embryos. (I,J) *tri* homozygous embryos injected with 3 ng of *pk1*-Mo.

4.3.Discussion

In this study, I show that Pk1 regulates mesendodermal and ectodermal CE movements by interacting with Slb/Wnt11 and Ppt/Wnt5. In addition, gain-of-function of Pk1 also impairs CE movements and enhances the *slb* loss-of-function phenotype, probably due to the ability of Pk1 to block the Fz7-induced membrane localisation of Dsh. Finally, I show that *pk1* genetically interacts with *tri/stbm* to mediate CE. These results reveal Pk1 to be a key player in mediating cell movements in the vertebrate embryo.

4.3.1. *pk1* regulates CE movements by modulating the non-canonical Wnt/PCP pathway

The analysis of the expression pattern of *pk1* in the mesoderm led us to investigate if it was involved in the regulation of gastrulation movements (Figure. 4.2.E) by different approaches including loss of function experiments, gain of function experiments by transplantation and by *in vivo* interaction assay to see if *pk1* modulates the Wnt/PCP pathway by controlling the sub-cellular localisation of components of this pathway.

4.3.1.1.Loss of function experiments

Firstly, injection of morpholinos against *pk1* led to a shorter body axis with a curled down tail at pharyngula stage. Further, analyses with various markers revealed that gastrulation cell movements are affected because they demonstrated the posteriorisazion of the prechordal plate, a wider neural, a shorter notochord and laterally expanded presomitic and head mesoderm at tail bud stage (Figures. 4.3. C- J). This phenotype is reminiscent of the CE mutants such as *silberblick (slb)*, *pipetail (ppt)*, *knypek (kny)* and *trilobite (tri)* in which gastrulation cell movements are disrupted but dorso-ventral and antero-posterior patterning remains unaffected (Hammerschmidt et al., 1996; Heisenberg and Nusslein-Volhard, 1997; Heisenberg et al., 2000; Jessen et al., 2002; Kilian et al., 2003; Rauch et al., 1997; Solnica-Krezel et al., 1996; Topczewski et al., 2001). Also the cell fate markers, in *pk1* morphant embryos, are expressed in the correct places, although their expression domains are

laterally expanded (Figures. 4.3 O-R), reflecting reduced convergence (Figures. 4.3.G, H). These results suggest that *pk1* is required for correct gastrulation CE movements of both mesendoderm and ectoderm but has no obvious role in the specifying cell fates.

To test the possibility that vertebrate Pk regulates CE through interaction with the Wnt/PCP pathway I examined if there was any genetic interaction between *slb* and *pk1*. Injection of *pk1*-Mo in *slb* embryos enhanced the CE defect compared to either mutant/morphant alone (Figure. 4.6.A and B). This indicates that Pk1 may function in the Wnt/PCP pathway or in parallel to this pathway. To solve the enigma as to whether *pk1* acts downstream of Wnt signals, I assessed if elevated Wnt11 activity can be suppressed by interfering with Pk1 function. I reproduce the rescuing of *slb*^{-/-} embryos by injection of *wnt11* RNA or the laterally mis-positioning of the prechordal plate also by injection of *wnt11* RNA, possibly resulting from hyper-activation of the pathway (Heisenberg et al., 2000) and Figure. 4.6.C). These phenotypes were totally suppressed in embryos with reduced levels of Pk1 function (Figure. 4.6.D), suggesting that Pk1 function promotes Slb activity.

Because *ppt/wnt5* genetically interacts with *slb/wnt11* and is required for CE movements in the posterior region of the gastrula (Kilian et al., 2003) and also is expressed in very similar domains to *pk1*, I examined whether Pk1 also modulates the activity of Ppt. *ppt/wnt5* mutant embryos with reduced Pk1 function showed a phenotype much more severe than either single mutant/morphant with greatly compressed wider somites (Figures. 4.7.G and H) indicating that Ppt and Pk1 function redundantly in regulating CE in the posterior region. Altogether, the loss of function results support the idea that Pk1 modulates the activity of the Wnt/PCP pathway, thereby influencing regulation of CE movements during gastrulation.

4.3.1.2. Overexpression experiments

To complete the analysis of cell movements in embryos with reduced Pk1 activity, I studied the consequences of overexpression of Pk1 and making use of transplantation assays I have detected that higher Pk1 activity inhibits cells from undergoing proper convergence and extension movements (Figure. 4.8. B).

The feature that Pk1 may act downstream of the Wnt/PCP pathway to regulate CE movements during gastrulation led us to test whether the *slb* phenotype could be rescued by over-expression of *pk1* RNA. But this injection enhanced the *slb* phenotype (Figures. 4.8.D and E), implying that excess Pk1 compromises Wnt/PCP-pathway dependent cell movements.

Taken together, the loss and gain of Pk1 function studies suggest that Pk1 regulates CE movements by modulating the Wnt/PCP pathway, but is not simply a positive or negative linear component of this pathway.

The analysis of Pk1 function provided an evidence of a molecular pathway, involving non-canonical Wnts and homologues of fly PCP genes (Adler, 2002; Mlodzik, 2002), in regulating cell movements underlying CE in vertebrates. Although Pk1 acts together with Wnt11 and Wnt5, it is not simply a linear component of the Wnt/PCP pathway since both loss- and gain-of-functions of Pk1 enhance the *slb* mutant phenotype. Consistent with this conclusion, in *Drosophila* PCP, Pk is a context-dependent positive or negative modulator of Fz/PCP signalling and not simply a downstream component of the pathway (Adler et al., 2000; Gubb et al., 1999; Tree et al., 2002).

4. 3.1.3.Sub-cellular localisation of components of this pathway

In the *Drosophila* wing, asymmetric localisation of the Fz-Dsh complex at the distal region of each cell establishes cell polarity within the plane of the epithelia (Axelrod, 2001; Strutt, 2001). During this process, Pk regulates localisation of Fz/Dsh by inhibiting the complex from forming at the proximal edge (Tree et al., 2002). Proximally localised Pk inhibits the Fz/Dsh complex from forming on the proximal edges of the epithelial cells, thereby functioning in a feedback loop that amplifies differences between Fz/Dsh levels on adjacent cells (Tree et al., 2002) In vertebrates, membrane localisation of Dsh in cells undergoing CE (Wallingford et al., 2000) is dependent upon Fz (Axelrod et al., 1998; Rothbacher et al., 2000; Umbhauer, Djiane et al. 2000)). Similarly, I have shown that vertebrate Pk1 can disrupt the Fz7-dependent membrane localisation of Dsh, despite the fact that Pk1 is neither

localised to the membrane nor recruited to the membrane by Fz7. Also, the cytoplasmic Dsh-GFP becomes faint and hazy when Pk activity is increased (Figure. 4.8.H).

A draw back in this analysis is that colocalisation or differential localisation of Dsh and other planar cell polarity components has not been yet described in cells undergoing cell intercalations, though Dsh and Pk colocalize to the membrane in the presence of Fz7 in static *Xenopus* animal pole cells (Veeman, et al., 2003; Takeuchi, et al., 2003), while Pk1 inhibits Fz7-mediated membrane localisation of Dsh in zebrafish animal pole cells in my assay.

These data lead to the model that Pk1 activity may destabilise Dsh, thereby blocking Fz7-mediated membrane localisation of Dsh. The Western blot analysis revealed that the levels of Dsh are decreased in the presence of Pk1 (Figure. 4.8.J) suggesting the disruption/degradation of the Fz/Dsh complex by Pk1 may contribute to the ability of exogenous Pk1 to negatively regulate the Wnt/PCP pathway. In addition, increasing Pk1 activity alters the stability of exogenous Dsh. Considering that Pk can directly bind to Dsh *in vitro* (Tree et al., 2002), Pk might dissociate Dsh from the membrane to the cytoplasm by direct binding and subsequently mediate the degradation of Dsh by unknown mechanisms. Alternatively, Pk1 might destabilise Dsh at the membrane through an indirect mechanism. In this scenario, Pk1 might co-operate with a factor at the membrane that in turn binds to Dsh and leads to dissociation from Fz.

One such candidate is the 4-pass transmembrane protein Tri/Stbm/ Van Gogh (Jessen et al., 2002; Taylor et al., 1998; Wolff and Rubin, 1998). In *Drosophila stbm* mutants, as in *pk* mutants, Fz is symmetrically localised in the membrane (Strutt, 2001) and indeed, *stbm* genetically interacts with *pk* (Taylor et al., 1998). Recently it was discovered that Stbm also physically binds to PK (Bastock et al, 2003). These observations suggest that in flies, Stbm functions together with Pk to establish PCP. Supporting a similar interaction in vertebrates, we show that heterozygous *tri*^{+/-} embryos injected with *pk1*-Mo exhibit a *tri*-like phenotype, revealing a strong genetic interaction between *pk1* and *tri* in the regulation of CE. Taken together with evidence that both Stbm and Pk1 can bind to Dsh and activate JNK in cultured cells (Park and Moon, 2002; Tree et al., 2002), it seems likely that Pk and Stbm

function by similar mechanisms in the regulation of vertebrate CE and in the establishment of PCP in *Drosophila*.

4.4. Summary

In this chapter I describe the isolation and functional characterisation of the zebrafish homologue of *Drosophila prickles*. Zebrafish *pk1* is expressed maternally and in moving mesodermal precursors. Abrogation of Pk1 function by morpholino leads to defective convergent extension movements, enhances the *silberblick (slb)/wnt11* and *pipetail/wnt5* phenotypes and suppresses the ability of Wnt11 to rescue the *slb* phenotype. Gain-of-function of Pk1 also inhibits convergent extension movements and enhances the *slb* phenotype, probably due to the ability of Pk1 to block the Fz7-dependent membrane localisation of Dsh by down-regulating levels of Dsh protein. Furthermore, *pk1* genetically interacts with *trilobite (tri)/strabismus* to mediate convergent extension. These results suggest that during zebrafish gastrulation, Pk1 acts downstream of the non-canonical Wnt11/Wnt5 pathway to regulate convergent extension cell movements, but is unlikely to simply be a linear component of this pathway.

CHAPTER 5

Cloning and Characterisation of the expression pattern of the *fmi* genes during zebrafish gastrulation

5.1.Introduction

From work done in *Xenopus* and zebrafish, it has been proposed that the non-canonical Wnt pathway is related to the planar cell polarity (PCP) pathway in *Drosophila* (Axelrod et al., 1998; Boutros et al., 1998; Rothbacher et al., 2000; Heisenberg et al., 2000; Tada and Smith, 2000; Wallingford et al., 2000). The genes *frizzled* (*fz*), *dishevelled* (*dsh*), *prickle* (*pk*), *strabismus* (*stbm*), *flamingo* (*fmi*) and *diego* (*dgo*) cause aberrant cellular orientation in several different tissues in *Drosophila*, they are called primary polarity genes or core PCP genes and are possible common key regulators of these pathways (Gubb and García-Bellido, 1982; Vinson and Adler, 1987; Theisen et al., 1994; Zheng et al., 1995; Taylor et al., 1998; Wolff and Rubin, 1998; Gubb et al., 1999; Chae et al., 1999; Usui et al., 1999; Feiguin et al., 2001). Furthermore, their protein products all adopt similar asymmetric subcellular localisations in polarising cells of the wing and eye in *Drosophila* (Usui et al., 1999; Axelrod, 2001; Feiguin et al., 2001; Shimada et al., 2001; Strutt, 2001; Strutt et al., 2002; Tree et al., 2002; Rawls and Wolff, 2003; Bastock et al., 2003).

Mainly, I have focused my project on a gene called *flamingo* (*fmi*), assuming that key regulators between the Wnt non-canonical pathway in vertebrates and PCP pathway in *Drosophila* are conserved. Flamingo is a seven-pass transmembrane receptor of the cadherin superfamily with extracellular tandem arrays repeats which act as homophilic modules (Usui et al., 1999). While it shows high similarity to G proteins-coupled receptors and a yet unknown cytoplasmic tail, which does not have a catenin-binding site. Therefore being categorised as protocadherin.

Flamingo is localised differentially at cell-cell boundaries along the proximal-distal axis in the wing of *Drosophila* in a Frizzled (*fz*)-dependent manner (Usui et al., 1999). Therefore,

the prediction was that Fmi could be a downstream modulator of Slb/Wnt11 signalling to regulate convergent extension movements, implying that flamingo (*fmi*) might be a read-out of active convergent extension or Slb/Wnt11 signal by informing us about cell polarity.

Recently, in mice several genes have been identified that have neural tube defects, especially two chemically induced mutants, *spin cycle* and *crash*, carrying independent mutations in a single gene product Celsr1, the mouse ortholog of Flamingo (Curtin et al, 2003). The *fmi* heterozygous mice have defects in the orientation of sensory hair cells in the organ of Corti, typical PCP phenotype while its homozygous mutant exhibits a severe neural tube defect (NTD) (Curtin et al, 2003). There are at least three *flamingo* genes orthologs in human and rodents are named, respectively, CELSR1–3 and Celsr1–3. All the *celsr* genes are expressed, in the brain and epithelia during early development, both in rodent and chicken embryos. This provides evidence for the function of the Flamingo family in regulating co-ordinated morphogenesis in mammals and higher vertebrates (Shima, Copeland et al. 2002; Tissir, De-Backer et al. 2002; Formstone and Mason 2005) reinforcing the study of this gene in zebrafish in terms of expression patterns and functional analysis.

In this chapter, I have cloned zebrafish flamingo (*fmi*) genes and examine the expression pattern of the *fmi* genes during zebrafish embryogenesis, especially during gastrulation. In the second part of this chapter I analyse possible functions of *fmi* genes during gastrulation. I have done three comprehensive approaches: a morpholino approach, a dominant negative approach with an *in vivo* imaging assay (as already explain in chapter 3 in the section 3.2.4) and studies of protein localization.

5.2.Results:

5.2.1.Cloning of the *fmi* genes

In order to isolate zebrafish flamingo genes, to start with, partial fragments were cloned from gastrula zebrafish embryos by RT (Reverse Tanscription) –PCR (Polymerase chain reaction) using degenerate primers corresponding to conserved regions of the mouse Fmi1 protein across the species (Figure 5.1.). A zebrafish gastrula library (λ ZAPII, random-primed) was screened with a P³²-labelled PCR fragment as a probe. As a result we cloned two species of clones *fmi1* and *fmi2*, which are 62% and 47% identical to mouse *celsr1* and *celsr2* genes, at amino acid levels in the transmembrane and cytoplasmic domain, respectively (Figure 5.1.). In order to clone the full-length cDNA of *flamingo* genes, screening of a zebrafish BAC (Bacterial artificial chromossome) library (library RPCI-71 zebrafish BAC RPZD- The Resource Center of the German Human Genome Project) was done using the cDNA fragments of (*fmi1*) and (*fmi2*) as radioactive P³²-labelled probes. The positive clones were further confirmed by Southern blot analysis. The sequences did not contain the most 5' prime region of the gene and therefore I decided to continue to screen a zebrafish gastrula library (a kind gift from Mike Rebagliati). Based on the sequence data from the Sanger Centre zebrafish databases (www.ensembl.org/Danio-erio), I cloned the rest of cDNAs by different RT-PCR reaction. Based on the information available in the genome databases for zebrafish *fmi* sequences and in sequence data from mouse *Celsr3* (Tissir, De-Backer et al. 2002), human *fmi1* and *fmi2* and using DNASTAR software and other blast software to analyse the sequences. I summarise the nomenclature of *fmi* genes in vertebrates (Table 5.1).

Table 5.1. Nomenclature of *flamingo* genes adapted from Tissir et al., 2002 and Curtin et al. 2003:

Name	Others, man	Human map	Mouse	Mouse map	Rat	Zebrafish
CELSR1	FMI2	Chr22	Celsr1, <i>spin cycle</i> and <i>crash</i>	Chr15		<i>fmi1a</i> <i>fmi1b</i> *
CELSR2	EGFL2	Chr1	Celsr2, Fmi1	Chr3	MEGF3	<i>fmi2</i>
CELSR3	MEGF2, EGFL1, FMI1	Ch3	Celsr3	Chr9	MEGF2	

* see page 124 and 125

Another round of screening of the zebrafish gastrula library was done with one of the positive clones, the clone FM8 (around 3kb), which is more 5' prime of the initial clones. For *fmi2* another clone move 5' within the gene, FM9, was use to screen again the libraries. Two more rounds screen of were done by screening again the zebrafish gastrula library (λ ZAPII, random-primed) and a cosmid library (genomic library) with most 5' prime region of these clones. For *fmi1* it was possibly to detect that FM8 was corresponding to one of the contigs available in the database, I confirm it by PCR and restriction digestion. For *fmi2* another partial clone that did not reach the 5' prime region was detected. But this last clone was corresponding to another contig available in the database, and I confirmed it by PCR and restriction digestion as well. By recent analyses of *fmi* sequences in the Ensemble database I have found that in fact there are at least 3 *fmi* genes in 3 different chromosomes, which comprise 3 different contigs, *fmi1a*, *fmi1b*, and *fmi2*.

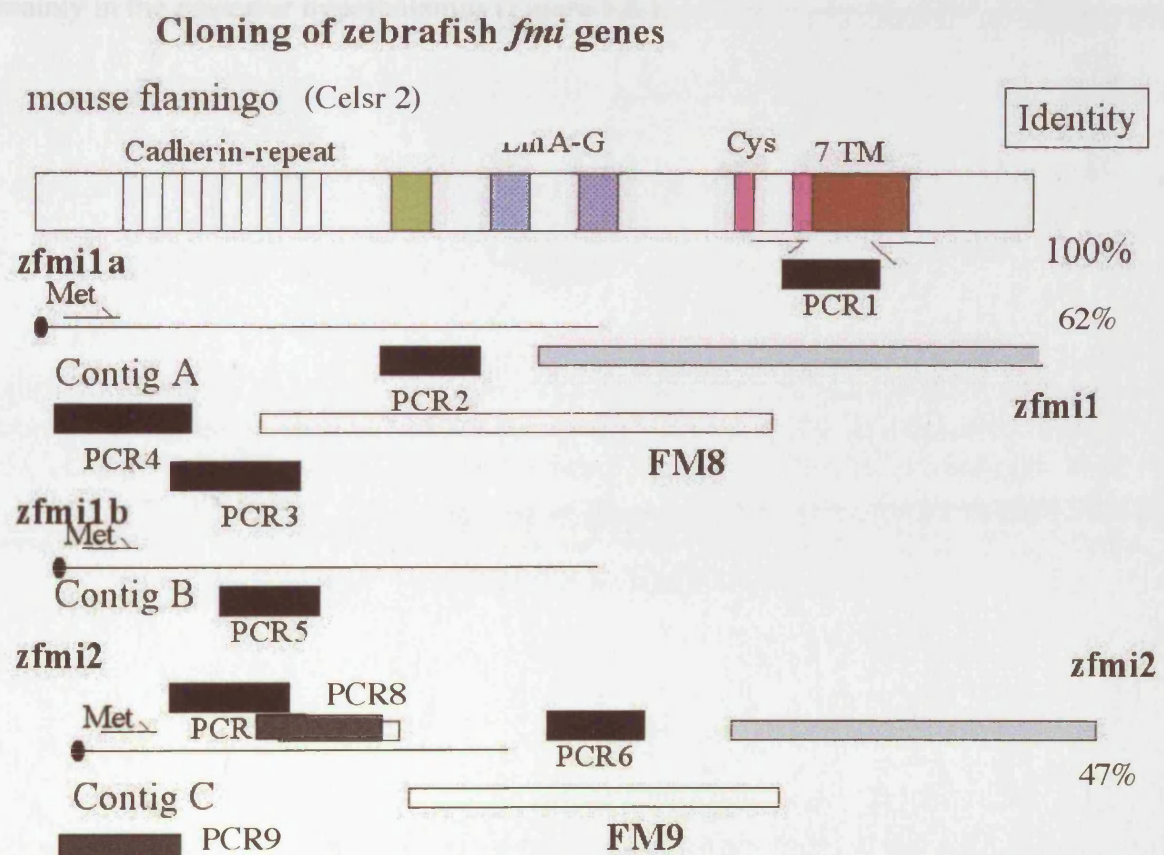


Figure 5.1. Schematic representation of the cloning strategy of *flamingo* genes

5.2.2.Expression pattern of the *fmi* genes

The expression pattern of *fmi1a* and *fmi2* was analysed by whole mount *in situ* hybridisation using DIG labelled antisense probes. Both genes are expressed maternally (Figure 5.2 and Figure 5.3). At the early gastrula stage, *fmi1a* starts to be expressed more strongly in the shield. As epiboly proceeds, *fmi1a* becomes restricted on the dorsal side, particularly in the presumptive notochord by 90% epiboly and tail-bud stage (Figure 5.2). *fmi2* RNA is distributed in a similar pattern to *fmi1a* during gastrulation (Figure 5.3.). The expression of *fmi2* on the dorsal side was confirmed in the mesoendodermal layer and mainly in the presumptive notochord by plastic section (Figure 5.4. A, B). *fmi1a* is expressed broadly in the somites, with no correlation to segmentation of each somite (Figure 5.4. (C, D, E, F)). In the brain at 24 hpf *fmi1a* is expressed in the floorplate, in the primordium of cerebellum, in the mid-hind brain boundary and also in the hindbrain. It was also detected at a very high level in the telencephalon at this stage, in the diencephalon mainly in the posterior hypothalamus (Figure 5.5.).

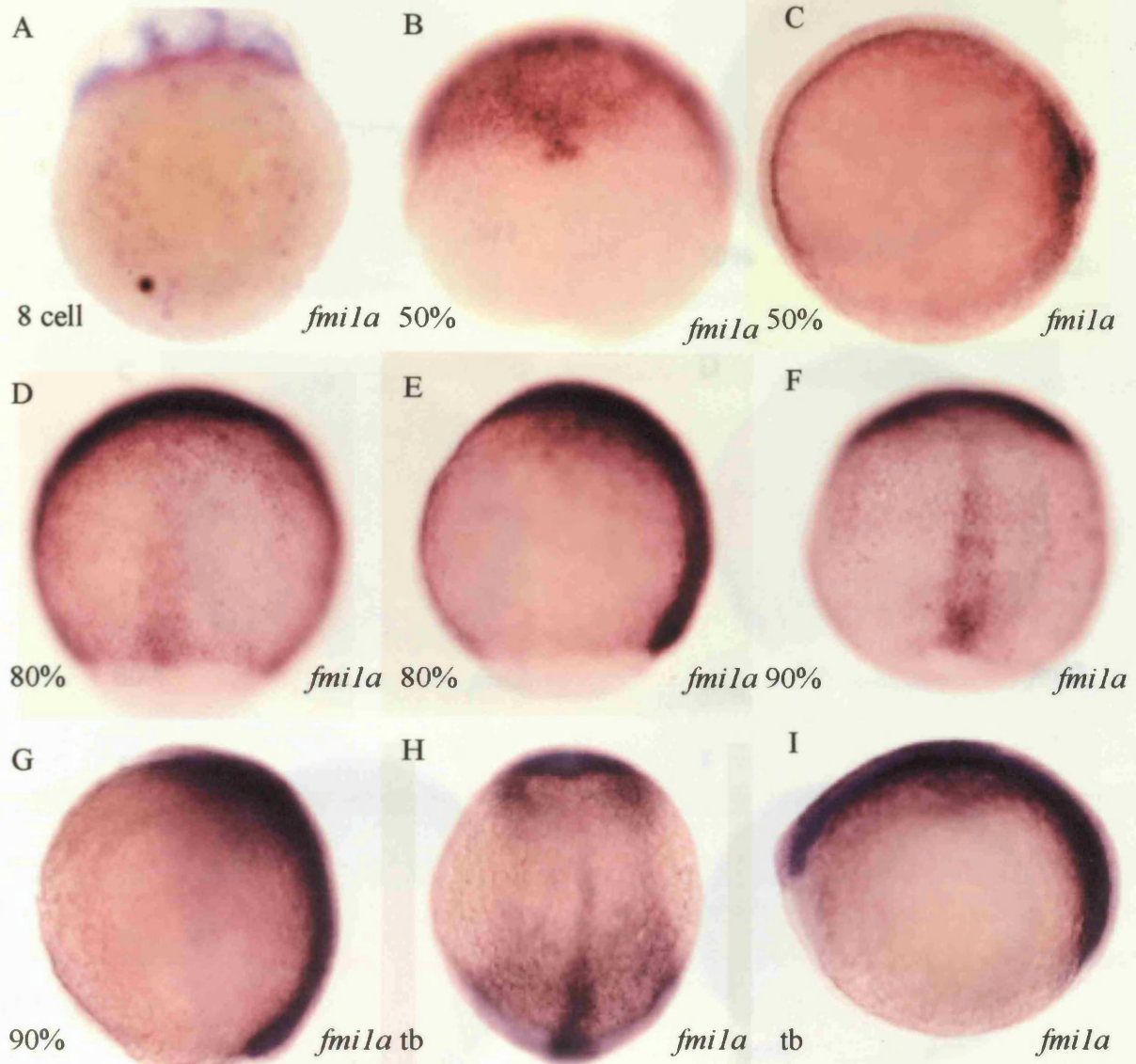


Figure 5.2. Expression pattern of *fmila* during zebrafish development in wild type embryos during gastrulation visualised by in whole mount *in situ* hybridisation. Lateral view at early stage (8 cells) (A), dorsal view: anterior is up (B), animal pole view: dorsal is right (C), dorsal view: anterior is up (D), lateral view: dorsal is right (E.), dorsal view: anterior is up (F), lateral view: anterior is up and dorsal is right (G), dorsal view: anterior is up (H), lateral view: anterior is right and dorsal is up (I).

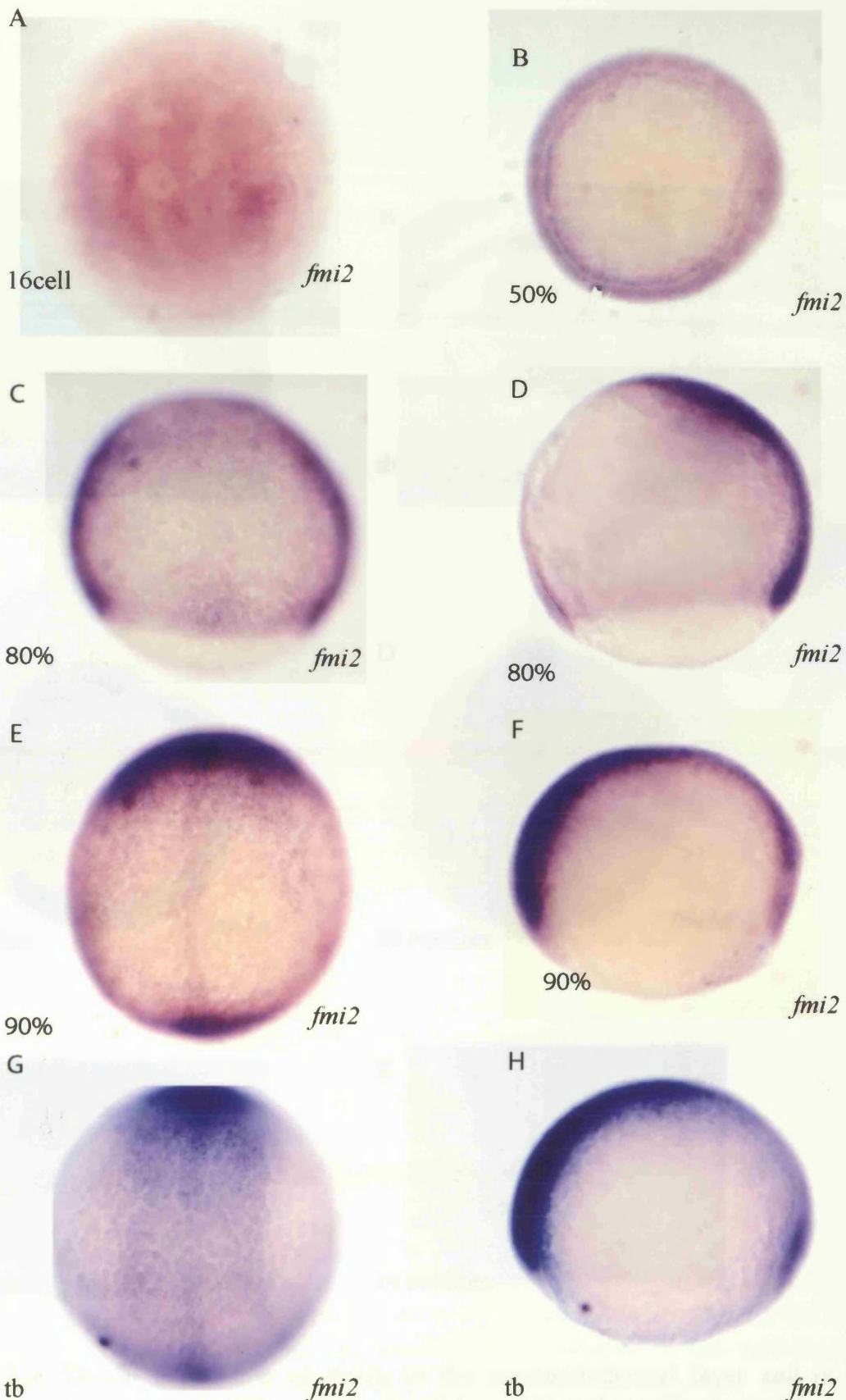


Figure 5.3. Expression pattern of *fmi2* during zebrafish development in wild type embryos during gastrulation visualised by in whole mount *in situ* hybridisation. Animal pole view at 16- cell stage (A), animal pole view, dorsal is right (B), dorsal view: anterior is up (C), lateral view: dorsal is right and anterior is up (D), dorsal view: anterior is up (E), lateral view: anterior is left and dorsal is up (F), dorsal view : anterior is up (G), lateral view: anterior is left and dorsal is up (H).

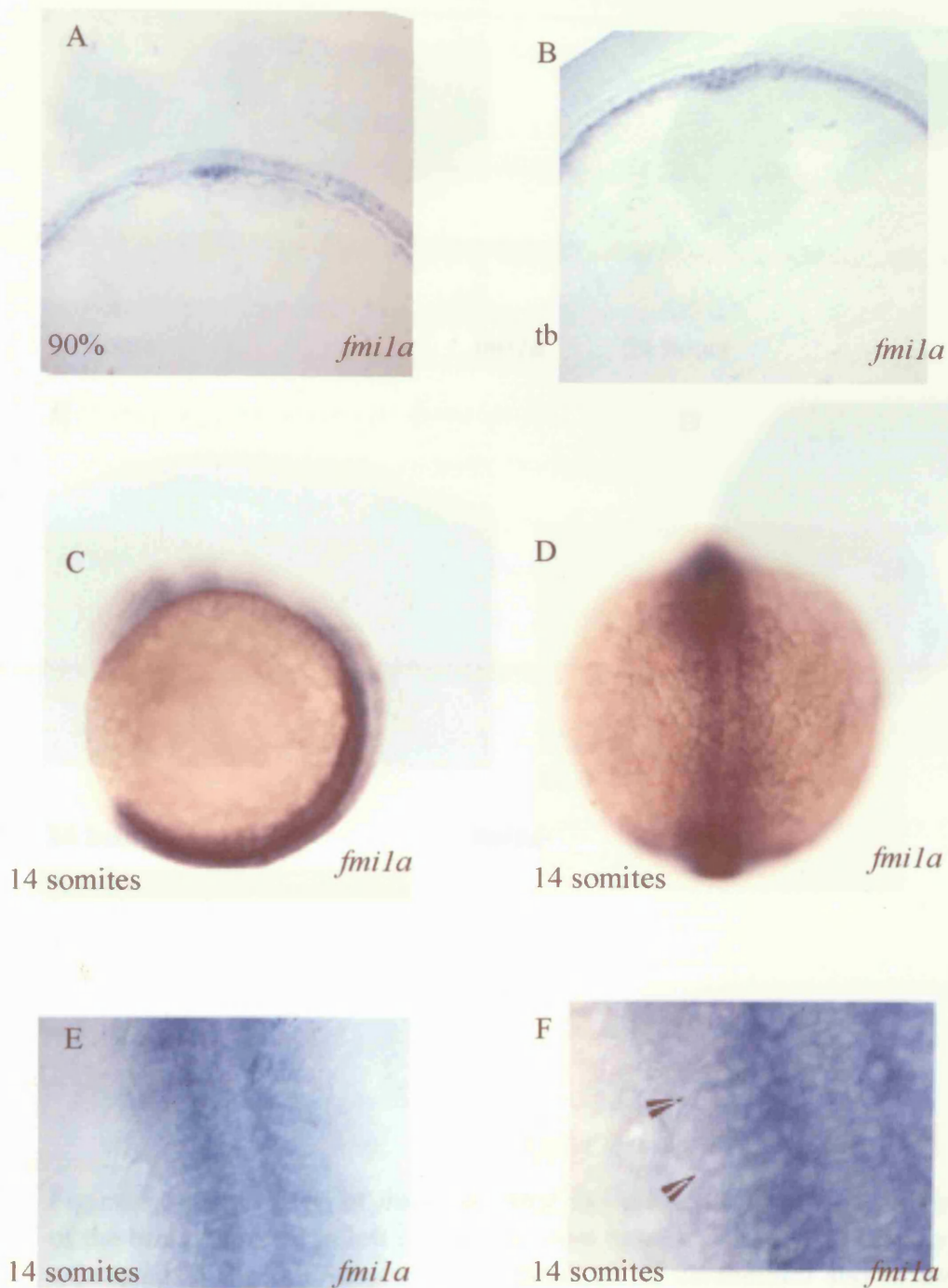


Figure 5.4. Dorsal expression of *fmila* in the mesoendodermal layer and in the presumptive notochord. At 90% epiboly dorsal is up (A) and at tailbud stage dorsal is also up (B) of wildtype embryos in plastic sections. Expression of *fmila* at 14 somites in wildtype embryos. Lateral view: anterior is up and dorsal is right (C) and dorsal view anterior is up (D). Expression in the somites of wild type embryos (E,F). Arrowheads point to the somite boundary.

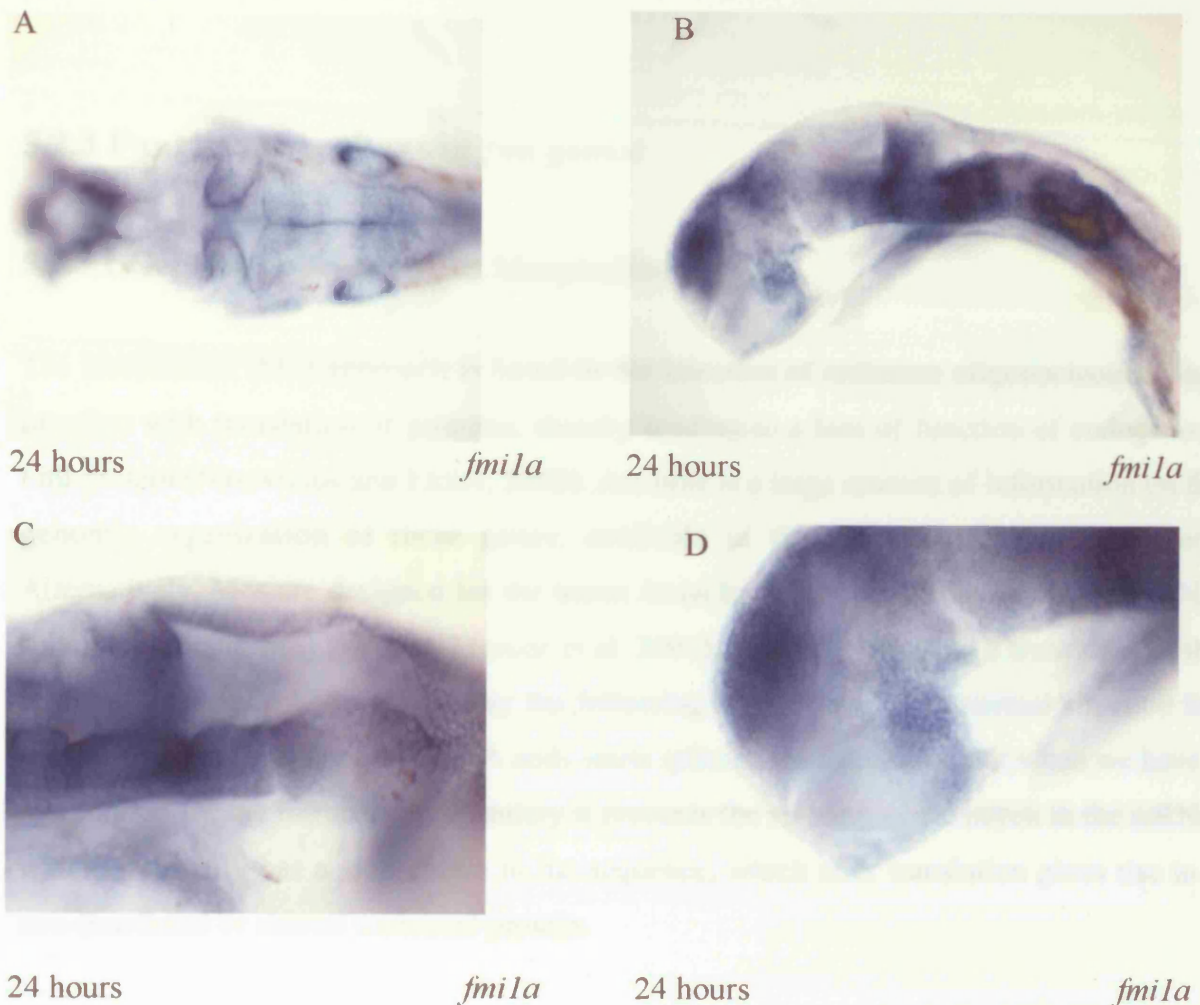


Figure 5.5. Expression of *fmila* at 24hpf in the brain of wildtype embryos. Dorsal view of the brain: anterior is left (A) lateral view anterior is left and dorsal is up (B). *fmila* is expressed in the midline, in the primordium of cerebellum and in the mid-hindbrain boundary and also in the hindbrain (A, B). Lateral view of ventriculum of the tectum with low expression of *fmila*. The expression is posterior to the mid-hindbrain boundary anterior is up (C). Lateral view of the forebrain focused on the telecephalon and diecephalon (in the left side) with a very high level of expression, in the diencephalon there is expression mainly in the posterior hypothalamus (D).

5.2.3 Functional analyses of *fmi* genes:

5.2.3.1. General approach with Morpholino (Mo):

The morpholino (Mo) approach is based in the injection of antisense oligonucleotides that interfere with translation of proteins, thereby leading to a loss of function of endogenous Fmi protein (Nasevicius and Ekker, 2000). As there is a large amount of information on the genomic organization of these genes, available in the zebrafish database (Sanger). Alternatively, Mos are designed for the intron /exon boundary which blocks the pre-mRNA splicing (splicing Mo) (Draper, Morcos et al. 2001), thereby generating a truncation of the protein. These morpholinos work by the following mechanism: in an normal situation the spliceosome binds to the pre-mRNA and starts splicing the introns out but when we have a morpholino for the intron/exon boundary it prevents the splicing of the intron in the mRNA which eventually has a stop codon in the sequence, which after translation gives rise to a non-functional or altered truncated protein.

5.2.3.1.1 Splice morpholinos

I have designed a morpholino sequences against exon/intron boundaries for the boundary between the exon13 and the following intron of *fmi1a* and for the boundary between the exon 14 and the following intron of *fmi2*, with the intention that *fmi1a*Mo would create a truncation in the EGF-like 5 domain and *fmi2* Mo would create a truncation after the EGF-like 8 domain. Injection of 6.4 ng of either *fmi1a* or *fmi2* Mo alone does not show any defective phenotype (Figure 5.6 C, D, G, H,). Injection of both Mos causes a weak convergent extension phenotype; leading to delayed development, a curly down tail, small eyes and heads at pharyngula stage (75%, n=88). (Figure 5.6. I, J). At higher doses, injected embryos had a more severe phenotype with shorter trunk and tail, but frequently this was coupled with cell death in the brain at late stages (data not shown).

Although the curly down tail phenotype of *fmi1a*;*fmi2* morphants is not clearly indicative of CE defects, analyses with different markers showed that gastrulation movements are

weakly affected. At tail-bud stage, *fmi1a* + *fmi2* morphants showed a slightly posteriorly located prechordal plate (*hgg1*), a wider neural plate (*dlx3*), a wider notochord (*ntl*) (74%, n=72), laterally expanded presomitic mesoderm (*papc*) (68%, n=33) and occasionally these defects were associated with epiboly defects in the posterior region (33%, n=37) (Figure 5.7. C, D, E, F and data not shown). These results suggest that two *fmi* genes are functionally redundant in regulating CE. However, to obtain more conclusive results I had to design morpholinos against the 5' prime region after reaching the full-length of the sequence for *fmi1a* and *fmi2*.

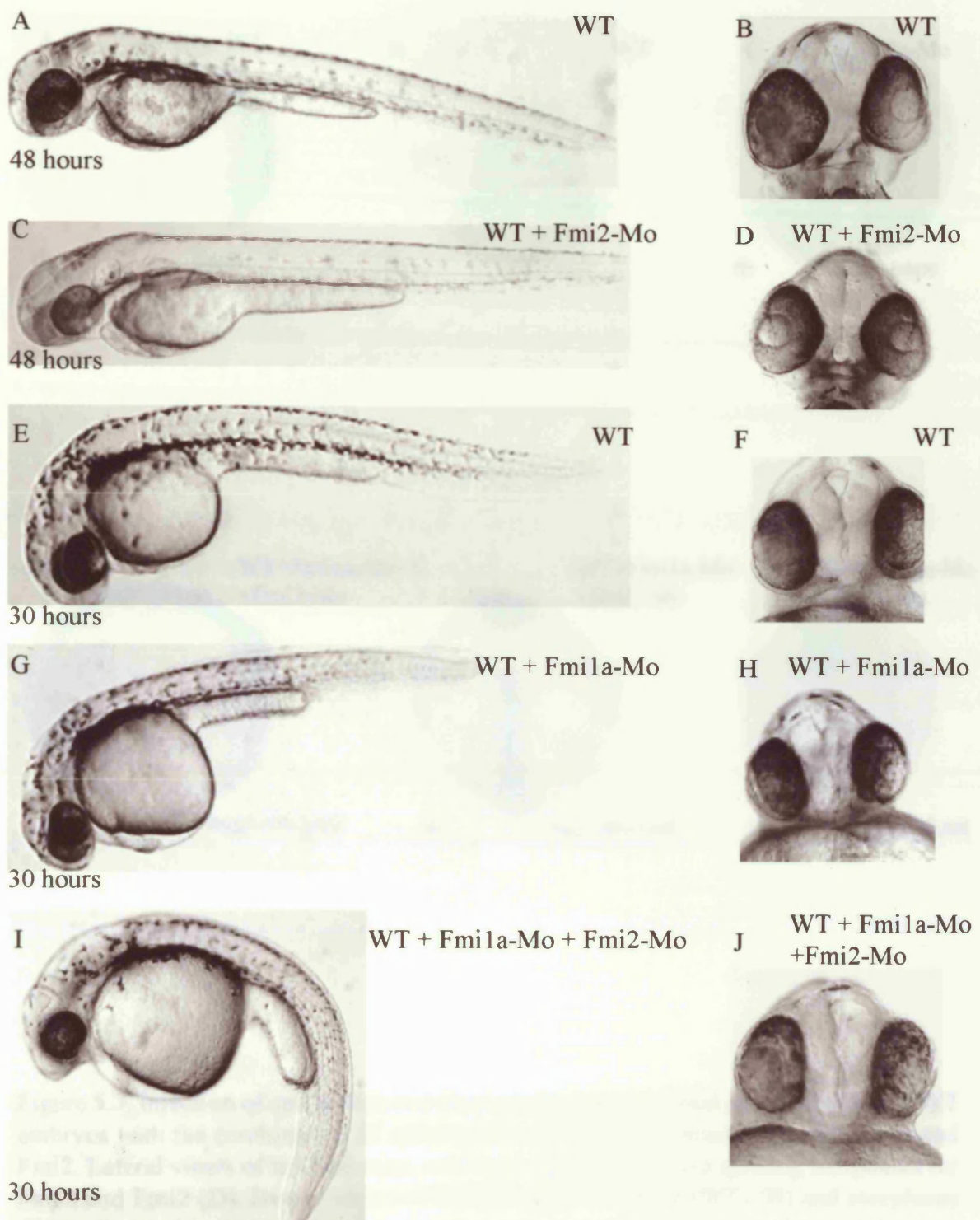


Figure 5.6. Injection of splice Morpholinos (Mos) in wild type embryos. Wild type embryos at pharyngula stage (A, B, E, F), WT embryos injected with 6.4 ng Fmi-2 splicing Mo alone (C, D), WT embryos injected with 6.4 ng Fmi-1a splicing Mo alone (G, H) and WT embryos injected with the combination of Mos (6.4 ng total amount) against Fmi1a and Fmi2 (I, J). Lateral views where anterior is left (A, C, E, G, I) and frontal views of the head region (B, D, F, H, J).

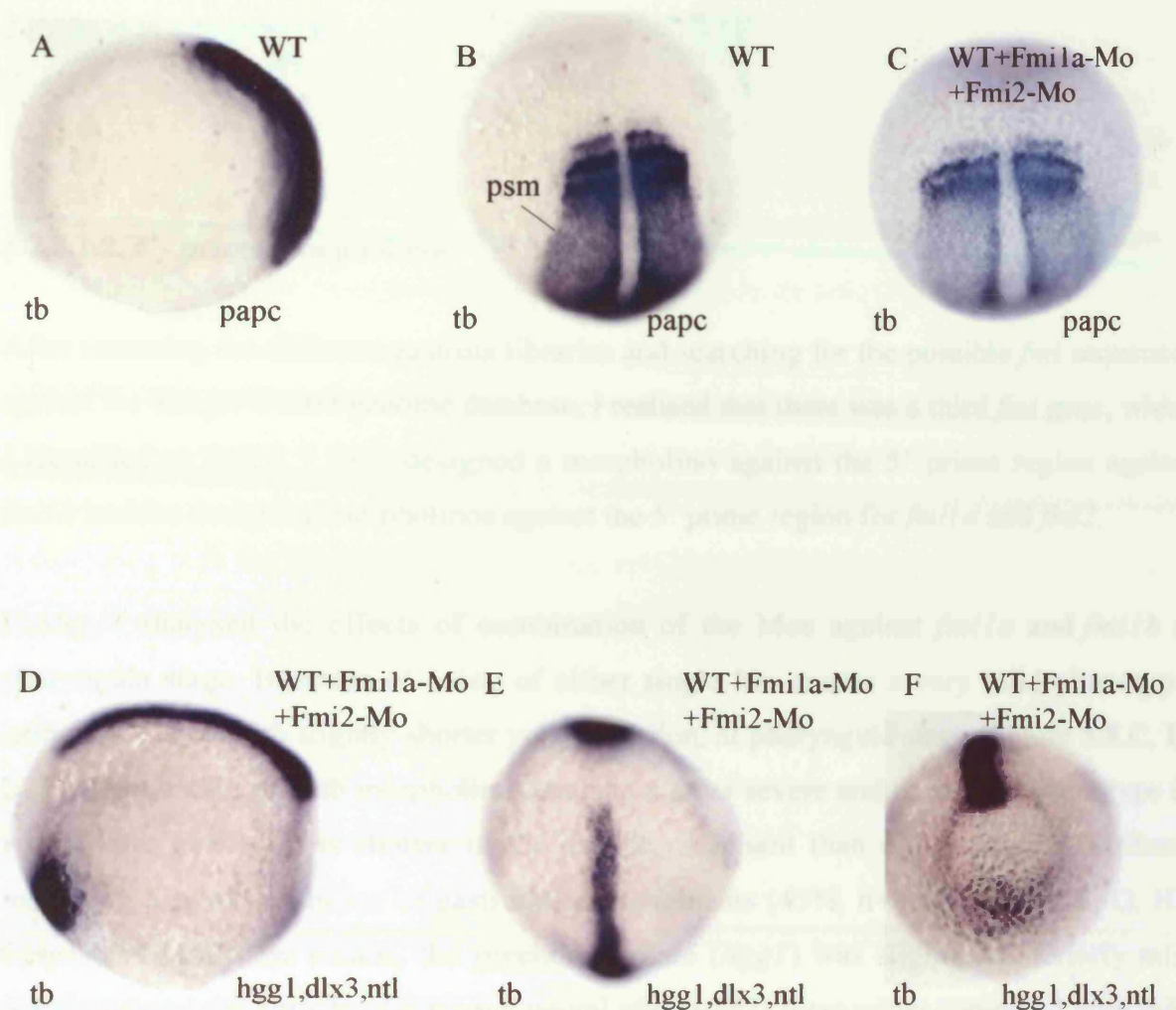


Figure 5.7. Injection of splice Mos and characterization at tail bud stage. Injection of WT embryos with the combination of splicing Mos (6.4ng total amount) against Fmi1a and Fmi2. Lateral views of tail bud stage wild type embryos (A) and splicing morphants for Fmi1a and Fmi2 (D). Dorsal views of tailbud stage wild-type (WT) (B) and morphants (WT + Fmi1a-Mo+Fmi2-Mo) embryos(C dorsal view; E, dorsal view; F, vegetal view). Anterior is up except in A, D, F and genes analysed are indicated bottom right. Abbreviations: psm, presomitic mesoderm

5.2.3.1.2. 5'- prime morpholinos

After screening the different gastrula libraries and searching for the possible *fmi* sequences against the Sanger Centre genome database, I realised that there was a third *fmi* gene, which I identified as *fmi1b*. I have designed a morpholino against the 5' prime region against *fmi1b* besides designing morpholinos against the 5' prime region for *fmi1a* and *fmi2*.

Firstly, I analysed the effects of combination of the Mos against *fmi1a* and *fmi1b* at pharyngula stage. Injection of 6.4ng of either single Mo causes a very mild phenotype, being associated with slightly shorter yolk extension, at pharyngula stage (Figure 5.8.C, D, E, F). Application of both morpholinos leads to a more severe and consistent phenotype in which yolk extension is shorter in the double morphant than either single morphant, indicating a weak inhibition of gastrulation movements (45%, n=86) (Figure 5.8. G, H). Consistent with these results, the prechordal plate (*hgg1*) was slightly posteriorly mispositioned and the notochord (*ntl*) and neural plate (*dlx3*) were wider compared with wild type embryos (50%, n=52) (Figure 5.9. D, E, F.). Correlated with this, the morphant embryos had a shorter body axis (Figure 5.9.F). Additionally, *fmi1a+fmi1b* double morphants at tail bud stage had epiboly defects in the posterior region and the presomitic mesoderm was affected (*papc*) (40%, n=23) (Figure 5.9. G, H).

Secondly, I investigated the effects of combination of the Mos against *fmi1a* and *fmi2* at pharyngula stage in wild type embryos. Injection of 8ng of either single Mo causes a very weak phenotype at pharyngula stage. The single morphants exhibited a slightly curly down tail phenotype and a yolk extension (Figure 5.10.C, D, E, F). Injection of 8ng (total amount) of both morpholinos leads to a more severe and consistent phenotype. Injection of low concentrations (4ng) leads to a more reduced yolk extension in the double morphant than either single morphant indicative of weak inhibition of gastrulation movements (Figure 5.10. G, H). But application of both morpholinos at higher concentrations (8 ng) leads to a severe curly down tailed phenotype with severe problems in the yolk extension (Figure 5.10. I, J). Consistent with these results, analyses with different markers for gastrulation, the usual triple mix of RNA probes (*hgg1*, *dlx3*, *ntl*) showed that gastrulation movements are affected. As a result, *fmi1a + fmi2* double morphants at tail-bud stage

showed a slightly posteriorly mis- positioned prechordal plate (*hgg1*), wider neural plate (*dlx3*), a shorter and thicker notochord (*ntl*) (60%, n=95) (Figure 5.11. C, D, E, F). Related with these data, all the morphant embryos had a shorter body axis (Figure 5.10).

All these data suggest that there is a functional redundancy between of *fmi1a* and *fmi2* genes in regulating CE during gastrulation. In the end, the reason why the CE phenotype caused by any combinations of two *fmi* Mos was very mild could be due to functional redundancy with the third *fmi* gene. Alternatively, it could be due to maternal contribution of Fmi proteins, which cannot be cancelled by a Mo approach.

Consequently, in order to abrogate Fmi functions during gastrulation, I injected maternal-zygotic (MZ) *off-road (ord)/fmi2* mutants with *fmi1a+fmi1b* 5'-prime morpholinos with the purpose to generate a possible triple knock down of the three *fmi* genes that are expressed maternally and zygotically during gastrulation. This was done in *off-road* mutants which were found by Hitoshi Okamoto laboratory in a screen for neuronal migration defects in facial motor neurons. The phenotype of these mutants was confirmed by defects in migration of facial motor neurons at 36 hpf (data not shown). At tail bud stage Mz *ord* embryos did not show any defects in convergent extension movements, although they exhibited a slightly wider but not shorter notochord (90%, n=40) (Figure 5.12. A, B) and a delay in epiboly in the posterior region (70%, n=32) (Figure 5.12. D, E). The dorso-ventral patterning remained unaffected in the Mz *ord* mutants by staining with *bmp2b* and *chordin* (71%, n=32; 50%, n=25) (Figure 5.12. G, H, J, K).

Injection of the two morpholino against *fmi1a* and *fmi1b* in Mz *ord* mutants showed a thicker notochord and wider presomitic mesoderm, indicating a defective convergent movement (66%, n=52) (Figure 5.12. C, F). This could be more associated with defective epiboly, which is reminiscent of epiboly mutants such as *half baked*, *avalanche*, *lawine*, and *weg* where the epibolic movements of the DEL, YSL and EVL cells can be uncoupled from each other (Kane et al.1996; Solnica-Krezel et al., 1996, Kane and Adams, 2002). Therefore, these defects are due primarily to epiboly deficiencies but secondarily they could weakly affect the CE movements. The dorso-ventral patterning remained unaffected in the injected mutants since the staining with *bmp2b* and *chordin* in mutant embryos is similar to wild type embryos (40%, n=12; 30%, n=15) (Figure 5.12. G, H, J, K, I, L).

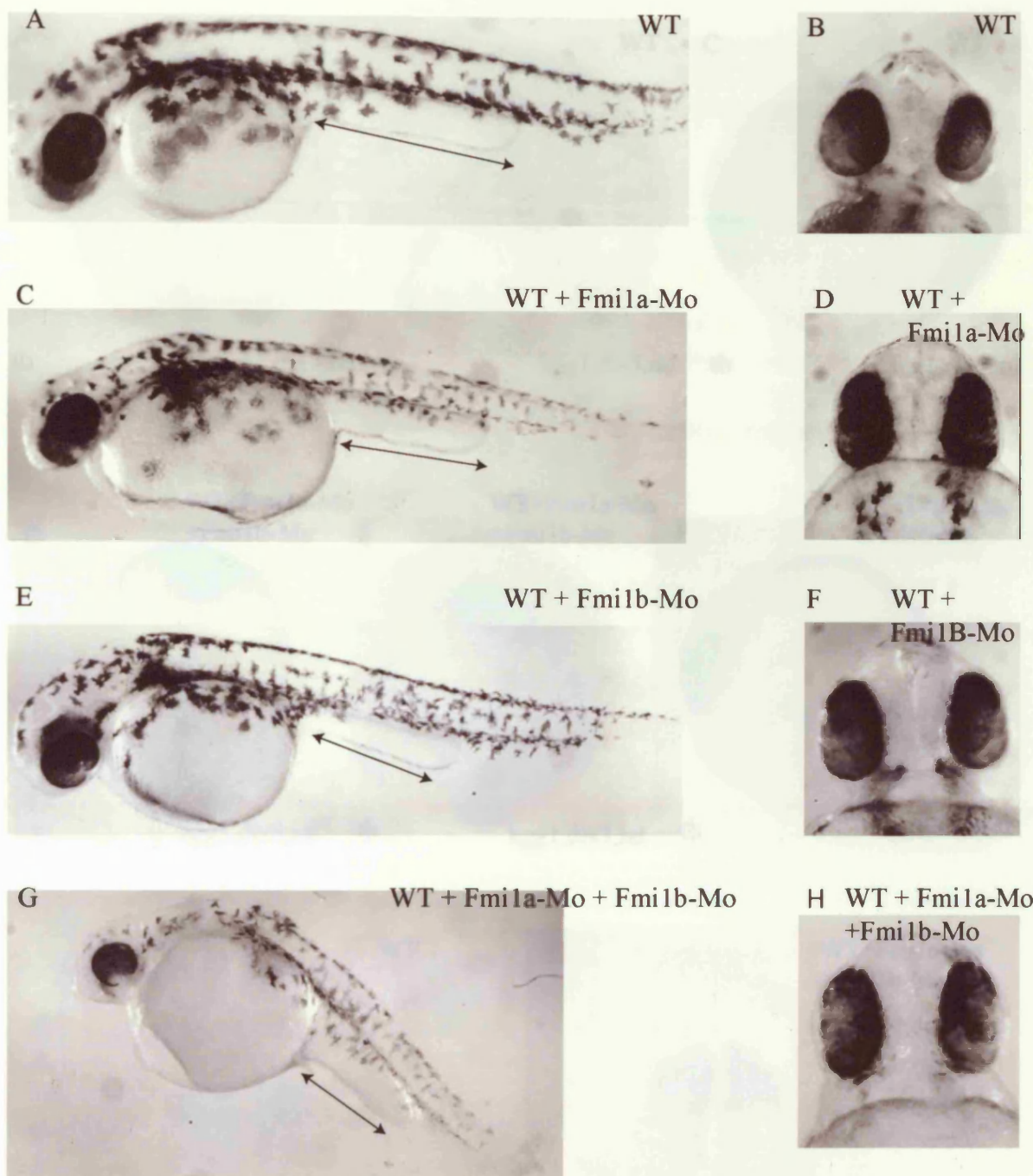


Figure 5.8. Injection of 5'- prime Mos (Fmi1a + Fmi1b) in wild type embryos. Wild type embryos (A, B), WT embryos injected with 6.4 ng Fmi-1a Mo alone (C, D), WT embryos injected with 6.4ng Fmi-1b Mo alone (E, F) and WT embryos injected with the combination of Mos (6.4ng total amount) against Fmi1a and Fmi1b (G, H). Lateral views where anterior is left (A, C, E, G) and frontal views of the head region (B, D, F, H). Arrows indicate the length of yolk extension.

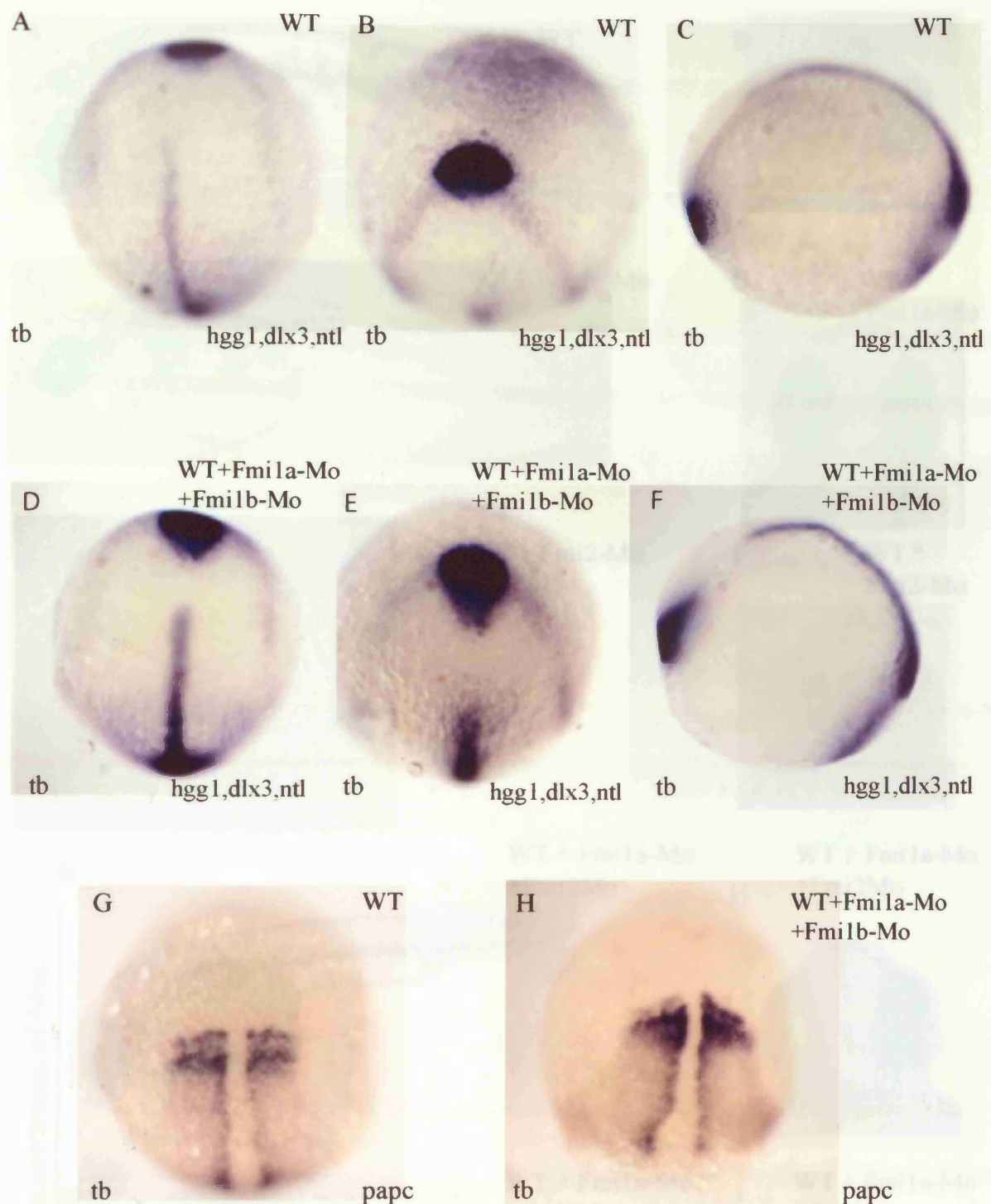


Figure 5.9. Injection of WT embryos with the combination of Mos against Fm1a and Fm1b and characterization at tail bud stage (6.4ng total amount) Dorsal views of tailbud stage wild-type (WT) (A) and morphants (WT + Fm1a-Mo+Fm1b-Mo) embryos (D) stained for *hgg1*, *dlx3*, *ntl*. Animal views and lateral views of tail bud stage WT embryos (B, C) and double morphants (WT + Fm1a-Mo+Fm1b-Mo) (E, F). Dorsal views of tail bud stage wild type embryos (G) and morphants for Fm1a and Fm1b stained for *papc* (H). In dorsal views anterior is up and in lateral views anterior is left. Genes analysed are indicated bottom right.

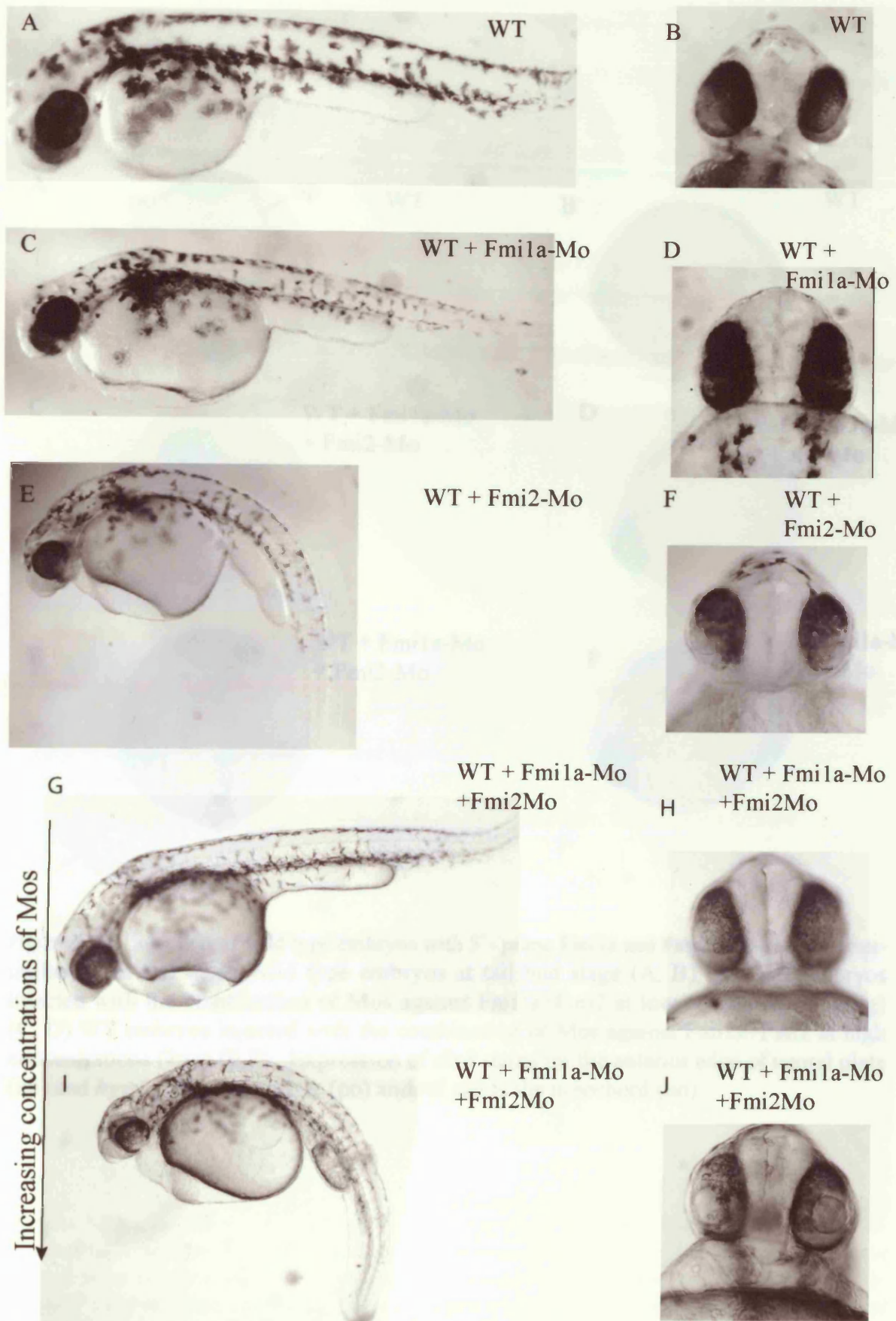


Figure 5.10. Injection of wild type embryos with 5'-prime Fmi1a and Fmi2 Mos . Wild type embryos (A, B), WT embryos injected with 8ng Fmi-1a Mo alone (C, D), WT embryos injected with 8ng Fmi2 Mo alone (E, F) and WT embryos injected with the combination of Mos against Fmi1a and Fmi2 at low concentrations(4ng) (G,H) WT embryos injected with the combination of Mos against Fmi1a and Fmi2 at high concentrations (8ng) (I, J) . Lateral views where anterior is left (A, C, E,G, I) and frontal views of the head region (B, D, F, H, J).

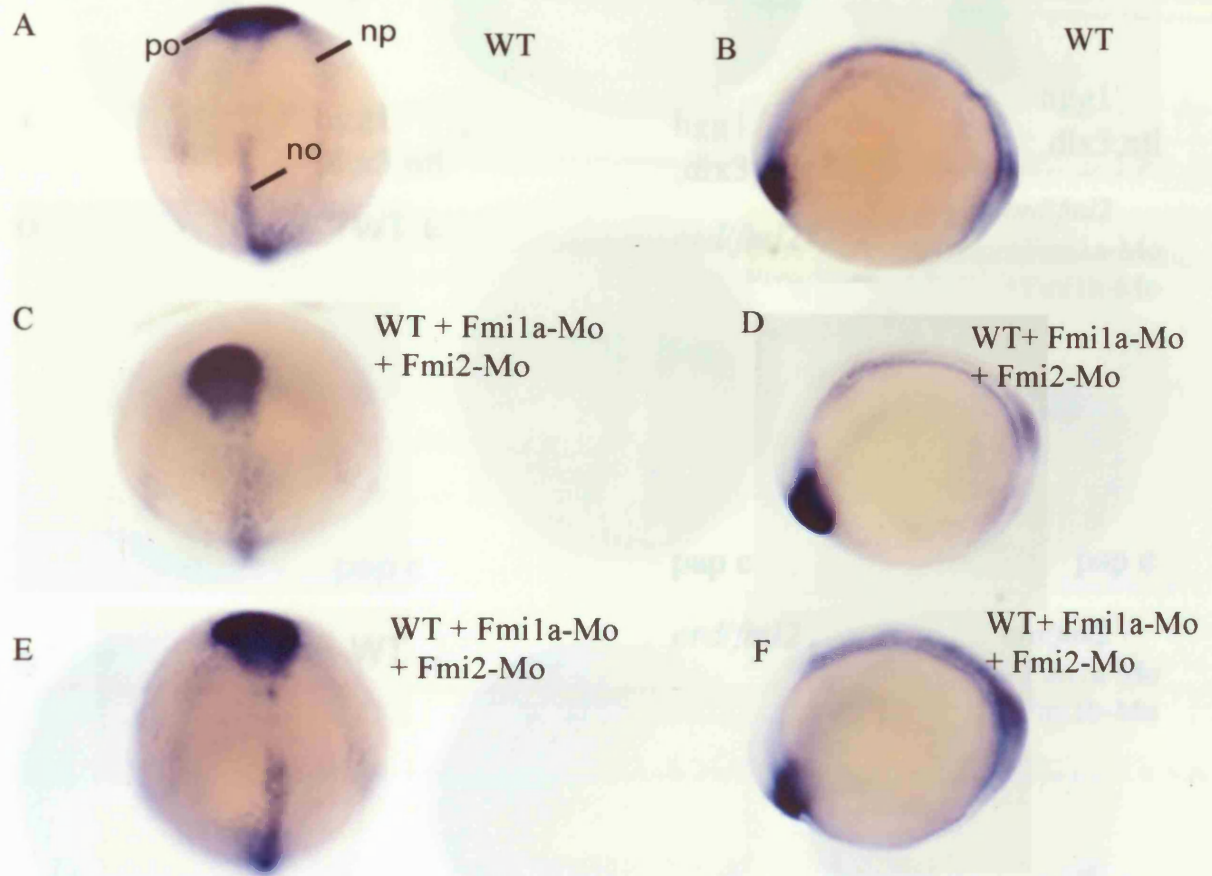


Figure 5.11. Injection of wild type embryos with 5'- prime Fmi1a and Fmi2 Mos and characterization at tail bud stage .Wild type embryos at tail bud stage (A, B), and WT embryos injected with the combination of Mos against Fmi1a+Fmi2 at low concentrations (4ng) (C, D) WT embryos injected with the combination of Mos against Fmi1a+Fmi2 at high concentrations (8ng) (E,F). Expression of *dlx3* stains for the anterior edge of neural plate (np) and *hgg1* stains the polster (po) and *ntl* stains the notochord (no).

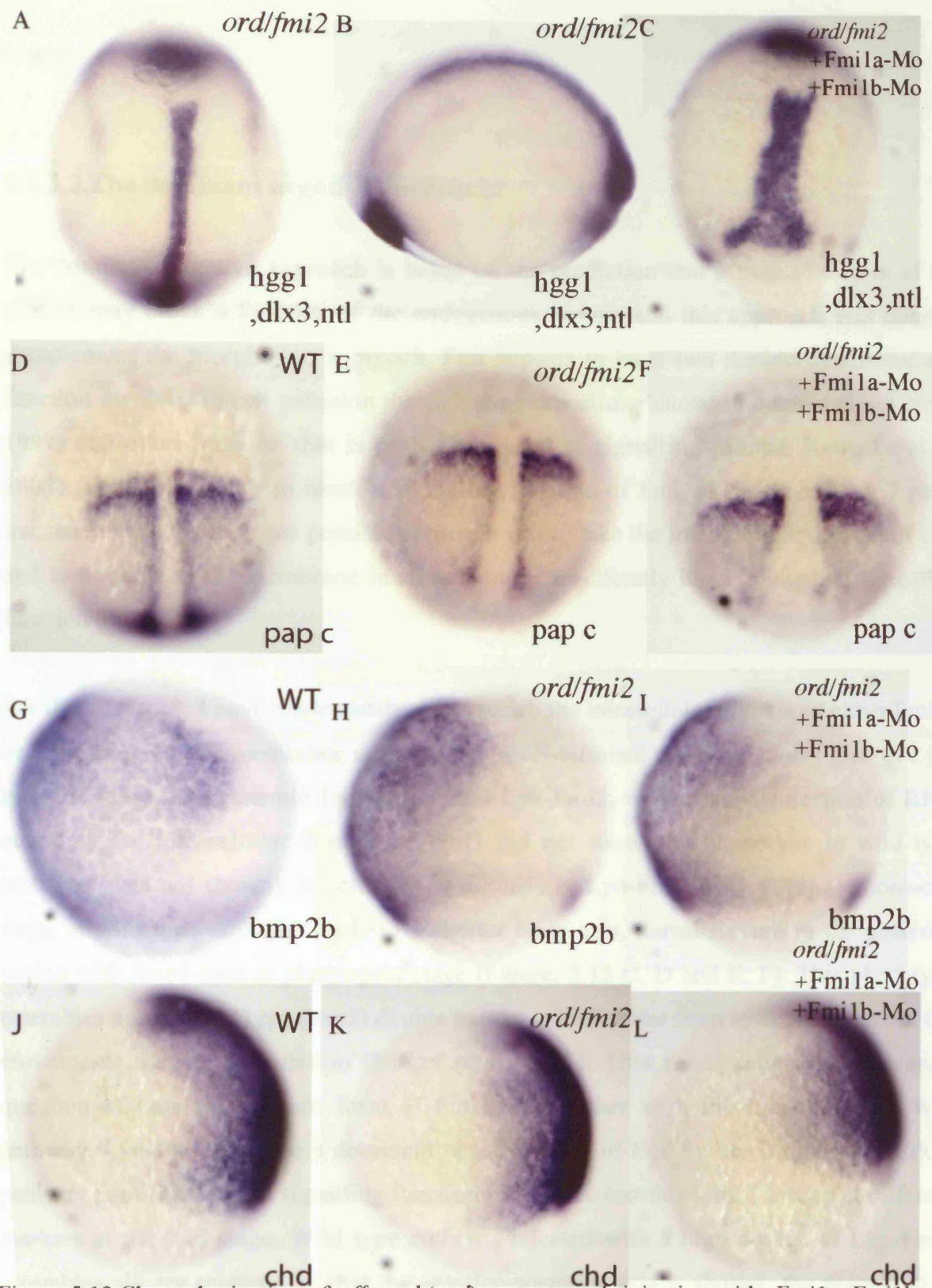


Figure 5.12. Characterization of *off road* (*ord*) mutants and injection with *Fmila*+*Fmilb* Mos at 80% epiboly and tail bud stage. Dorsal and lateral views of *ord* mutants (A,B) and dorsal view injected with (8ng total amount) *Mos1a*+*1b* (C) expression of *dlx3* stains the anterior edge of neural plate (np) and *hgg1* stains the polster (po) and *ntl* stains the notochord (no). Dorsal views of tailbud-stage wildtype (WT) and *ord* embryos (D,E) and *ord* injected with 8ng *Mos1a*+*1b* (F) stained with *papc*. Lateral views of 80% epiboly wild-type (WT) and *ord* embryos (G, H, J, K) and *ord* mutants injected with 8ng *Mos1a*+*1b* (I, L). Anterior is up, dorsal to the right and genes analysed are indicated bottom right.

5.2.3.2. The dominant negative approach:

The dominant negative approach is based on the prediction that a truncated form of the protein may block a function of the endogenous protein and this approach was done to complement the morpholino approach. Fmi appears to have two distinct functions; one function involved in cell adhesion through the extracellular cadherin domain (Usui et al., 1999) and other function that is probably related to signalling (Shima, Kengaku et al. 2004). Therefore, to try to block a signalling function of Fmi, as *fmi* encodes a 7 pass-transmembrane protein, one possible approach was to take the intra-cellular domain of Fmi and to target it to the membrane in an attempt to specifically block a putative signalling function of Fmi.

For these reasons, I have made constructs in which the intracellular domain of either Fmi1a or Fmi2 is fused to a membrane target signal (an N-terminal myristoylation signal of Lyn-tyrosine kinase) to generate Lyn-Fmi1a and Lyn-Fmi2, respectively. Injection of RNA encoding the intracellular domain of Fmi2 did not show any phenotype in wild type embryos (data not shown). Injection of Lyn-Fmi1a or Lyn-Fmi2 RNA (100pg) at one-cell stage in wild type embryos leads to a shorter body axis, dorsal flexure in the posterior region with fused eyes at pharyngula stage (Figure. 5.13 C, D and E, F). This phenotype resembles a *slb (wnt11);ppt (wnt5)* double mutant, which arises from severely disturbed CE movements during gastrulation (Kilian et al, 2003). This result raises an interesting question of how this mutant form of Fmi acts together with the non-canonical Wnt pathway. Lyn-Fmi could be a dominant negative form of Fmi by blocking the Wnt/PCP pathway possibly through signalling function of Fmi. To test this idea, I looked at different markers at tail bud stage. Wild type embryos injected with a high dosage of Lyn-Fmi2 resembles *slb;ppt* mutants, in that the anterior-posterior axis is shorter, the notochord is shorter and wider, the neural plate is wider, and the precordial plate is posteriorly mispositioned (61%, n=102) (Figure 5.13 G, H, I, J).

Overexpression of Lyn-Fmi at high concentrations (100pg) in wild type embryos causes a lateral expansion of the presomitic and head mesoderm (*papc* and *snail2*) at tail bud stage (62%, n=42; 73%, n=34) (Figure 5.14. A, B, C, D). However, dorso-ventral and antero-

posterior patterning remains unaffected as the dorsal marker *chd* and ventral marker *bmp2b* are unchanged (58%, n=21; 63%, n=14) (Figure 5.14. E, F, G, H). Additionally, these embryos show the telencephalic marker *emx1* is unchanged while expressed in the correct position, although its expression domain is laterally expanded, reflecting reduced convergence of the neural plate (76%, n=32) (Fig. 5.15. E, F). The midbrain marker *pax2.1* is unchanged while the eye field marker *rx3* suffers a complete reorganization; size of the *rx3* domain is decreased (85%, n=79) (Figure 5.15.A, B, C, D). There is a lateral expansion of presomitic mesoderm similarly to the *slb;ppt* double mutant in the posterior region of the embryo and the A-P axis is also much shorter (80%, n=111) (Figure 5.15. C, D) (Kilian et al, 2003).

All together, these results suggest that over-expression of Lyn-Fmi leads to severely defective CE movements but no epiboly movement defects.

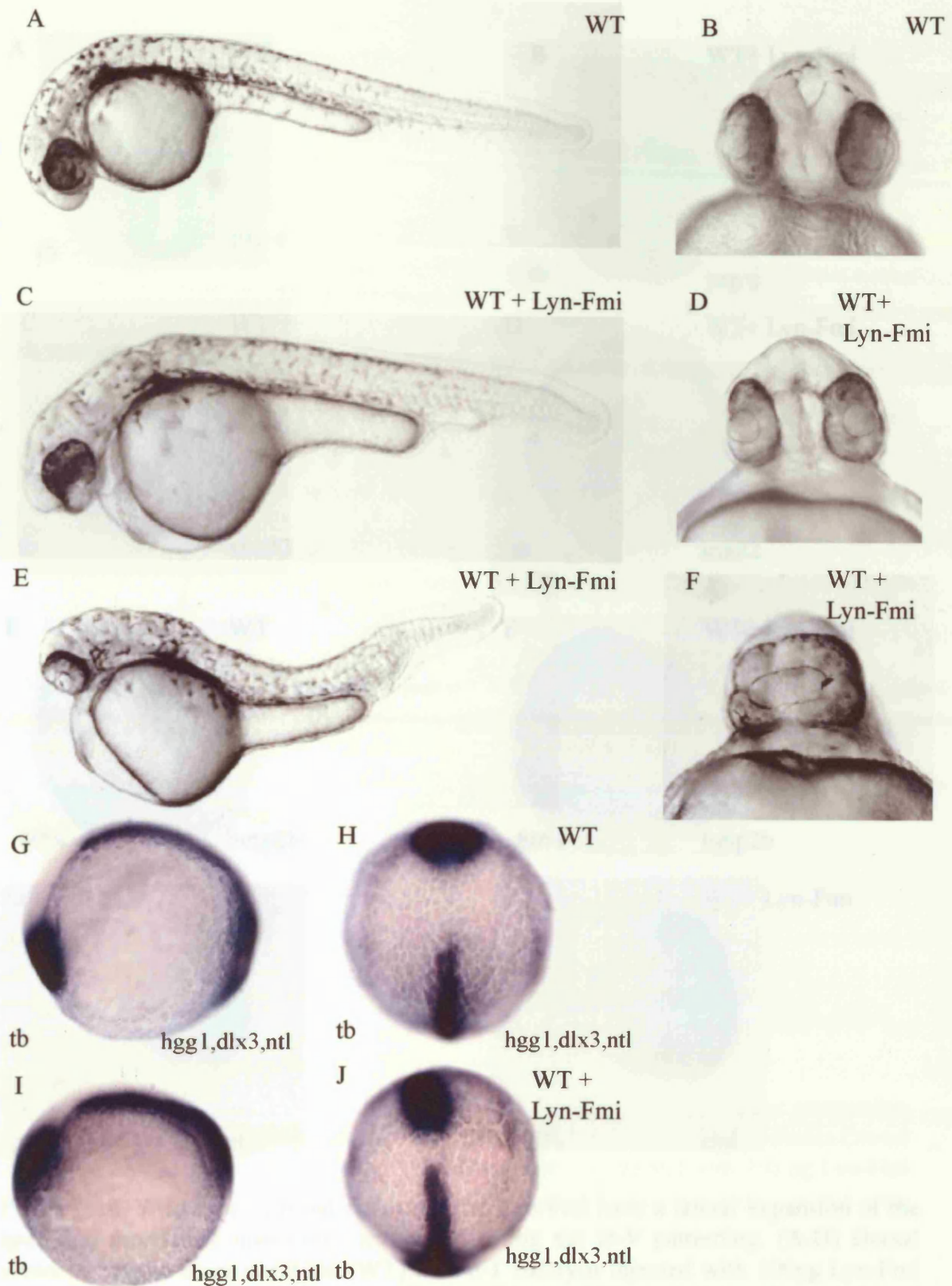


Figure 5.13. Overexpression of Lyn-Fmi causes defective CE movements and is similar to *slb*. Wild type embryos (A, B), WT embryos injected with 50pg of Lyn-Fmi RNA (C, D), WT embryos injected with 100pg of Lyn-Fmi RNA (E, F) at pharyngula stage. Lateral views where anterior is left (A, C, E,) and frontal views of the head region (B, D, F). At tail bud stage wild type embryos lateral and dorsal views (G,H) and wt embryos injected with Lyn-Fmi RNA (100pg) lateral and dorsal views (I,J). In dorsal views anterior is up and in lateral views anterior is left. Genes analysed are indicated bottom right. 144

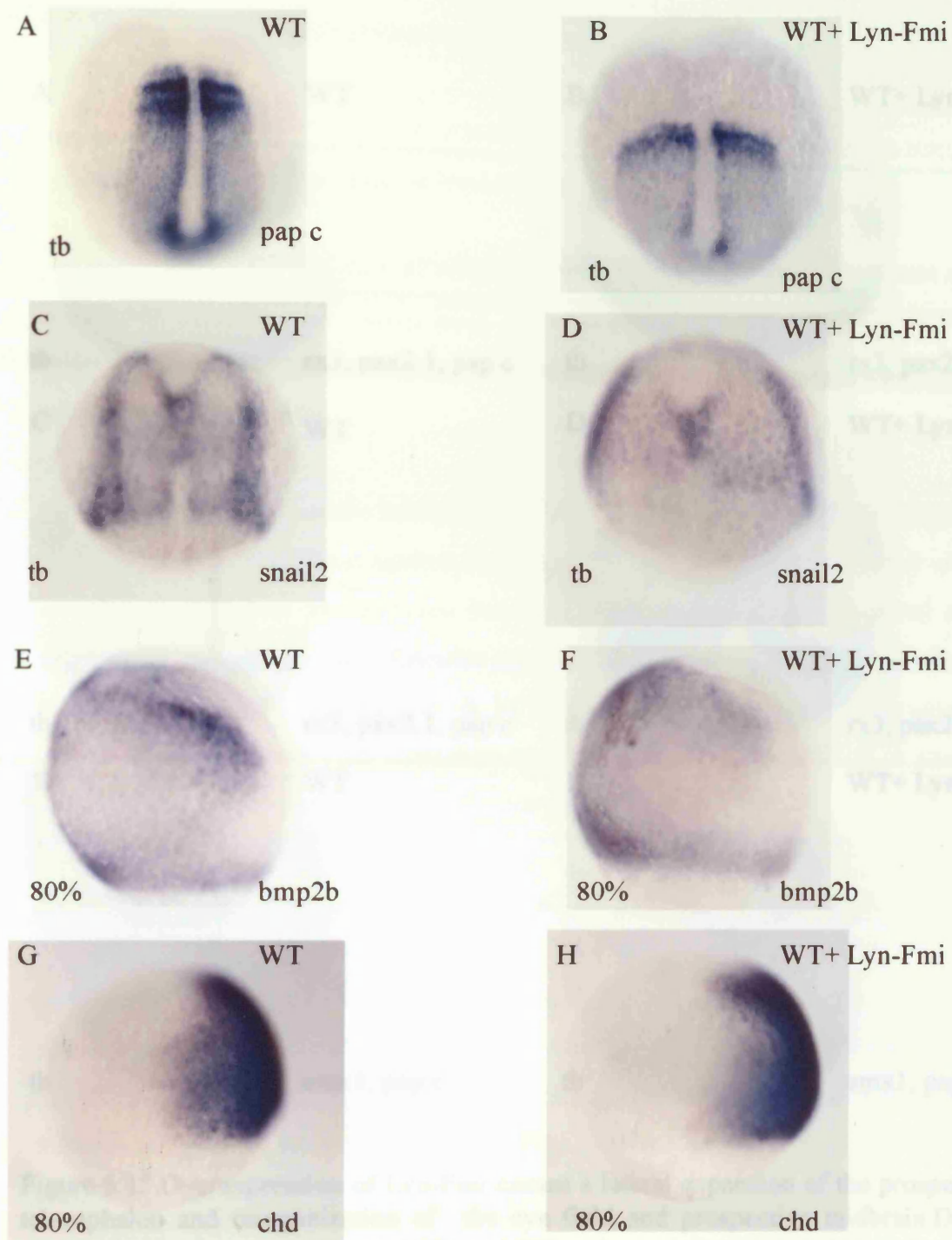


Figure 5.14. Wild type injected embryos with Lyn-Fmi have a lateral expansion of the head and presomitic mesoderm without affecting the D-V patterning. (A-D) Dorsal views of tailbud-stage wildtype (WT) and WT embryos injected with 100pg Lyn-Fmi RNA. (E-H) Lateral views of 80% epiboly wild-type (WT) and WT embryos injected with Lyn-Fmi embryos. Anterior is up and genes analysed are indicated bottom right.

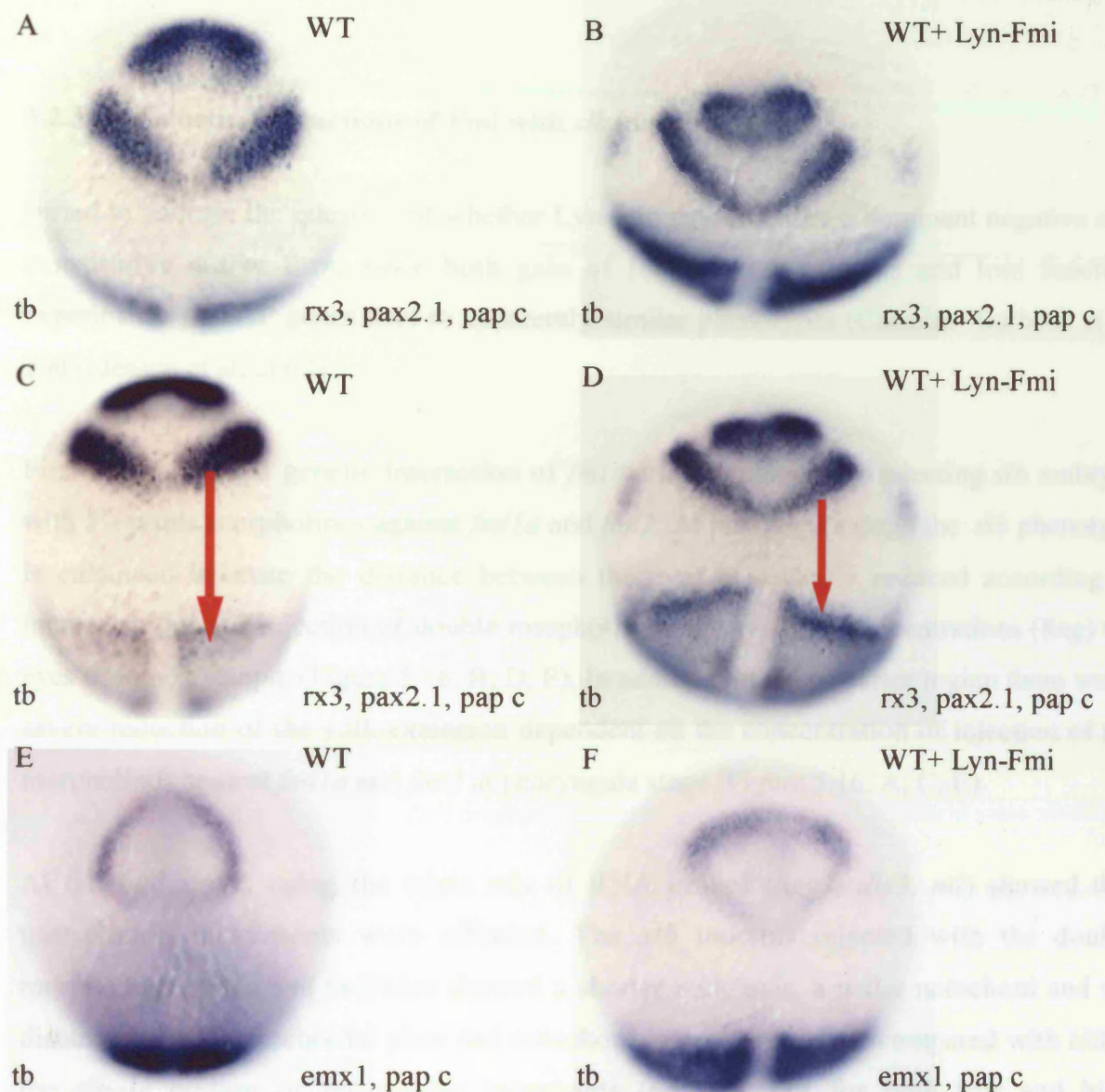


Figure 5.15. Overexpression of Lyn-Fmi causes a lateral expansion of the prospective telecephalon and reorganization of the eye field and prospective midbrain. Dorsal views of tailbud-stage wildtype (WT) and WT embryos injected with 100 pg Lyn-Fmi RNA (A-D) and animal views (E, F). Anterior is up and genes analysed are indicated bottom right. Arrows show the reduction in the body length along the of the anterior-posterior axis.

5.2.3.2.1. Genetic interactions of Fmi with *slb* mutants

I tried to address the question of whether Lyn-Fmi acts as either a dominant negative or a constitutive active form since both gain of function experiments and loss function experiments of PCP genes lead to apparently similar phenotypes (Carreira- Barbosa et al, 2003; Jessen et al, 2002).

First of all, I tested genetic interaction of *fmi* with *slb* mutants by injecting *slb* embryos with 5'-prime morpholinos against *fmi1a* and *fmi2*. At pharyngula stage the *slb* phenotype is enhanced because the distance between the eyes is severely reduced according to increasing dose of injection of double morpholinos. At very high concentrations (8ng) the eyes become cyclopic (Figure 5.16. B, D, F). In addition, in the posterior region there was a severe reduction of the yolk extension dependent on the concentration of injection of the morpholinos against *fmi1a* and *fmi2* at pharyngula stage (Figure 5.16. A, C, E).

At tail bud stage, using the triple mix of RNA probes (*hgg1*, *dlx3*, *ntl*) showed that gastrulation movements were affected. The *slb* mutants injected with the double morpholinos *fmi1a* and *fmi2* Mos showed a shorter body axis, a wider notochord and the distance between prechordal plate and notochord is severely reduce compared with either the single mutant or the double morphants (66%, n=114 for both low and high concentrations) (Figure 5.16. G, H, I, J, K, L). These results prove that Fmi is a positive regulator of the Wnt11 signaling pathway.

Secondly, I tested whether Lyn-Fmi overexpression in *slb* embryos leads to a similar phenotype of *slb* embryos injected with *fmi*-Mos. If Lyn-Fmi injection blocks the Wnt/PCP pathway thereby leading to a convergent extension phenotype, it might block both endogenous functions of Fmi1a and Fmi2, which act as positive regulators of the Wnt/PCP pathway. I injected with Lyn-Fmi RNA at high and low doses in *slb* mutants. By doing this experiment I detected an enhanced *slb* phenotype at pharyngula stage: a shorter embryonic axis and complete cyclopia (Figure 5.17. A, B, C, D, E, F). At tail bud stage more than 50% (n=67) of *slb* embryos injected with Lyn-Fmi also showed more defective CE movements

as compared to *slb* embryos, with the consequence that the prechordal plate remained posteriorly located beneath the neural plate and distance between prechordal plate and the notochord is severely reduced (50%, n=67) (Fig. 5.17.G, H, I, J). This result indicated that Fmi might function as positive regulator in the Wnt/PCP pathway or in parallel to this pathway. Taken together, these results suggest that Lyn-Fmi acts as a dominant negative form of Fmi.

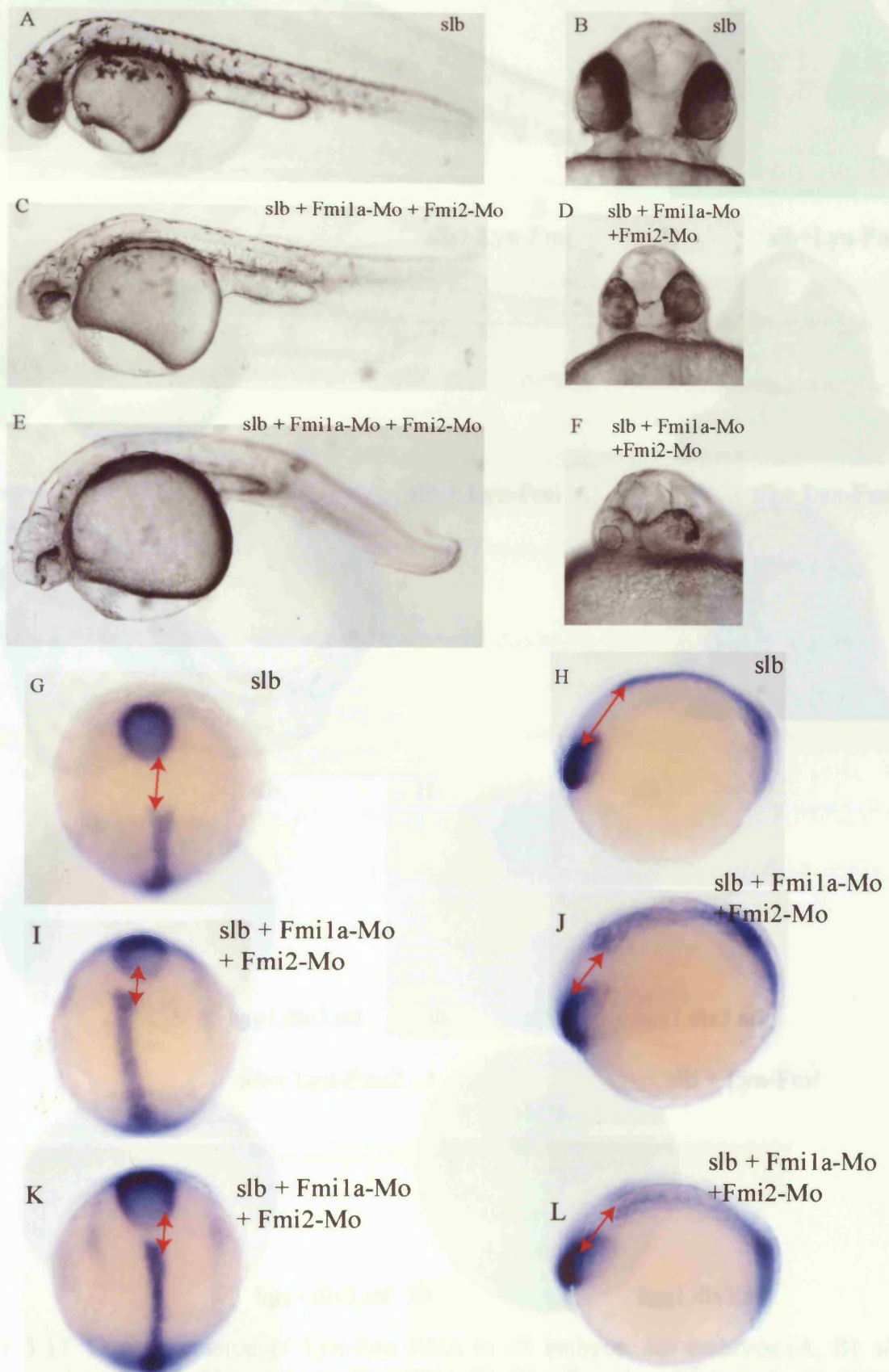


Figure 5.16. Genetic interactions of *fmi* with *slb* mutants. *slb* mutant embryos (A, B), *slb* embryos injected with 4ng of the combination of Mos against Fmi1a+Fmi2 (C, D), *slb* embryos injected with 8ng of the combination of Mos against Fmi1a+Fmi2 (E, F). Lateral views where anterior is left (A, C, E) and frontal views of the head region (B, D, F). *slb* embryos at tail bud stage (G, H), and *slb* embryos injected with the combination of Mos against Fmi1a+Fmi2 (4ng) (I, J) *slb* embryos injected with the combination of Mos against Fmi1a+Fmi2 (8ng) (K, L). Dorsal views where anterior is up (A, C, E, G, I, K) and lateral views (B, D, F, H, J, L). Expression of *dlx3* stains for the anterior edge of neural plate (np) and *hgg1* stains the polster (po) and *ntl* stains the notochord (no). Arrows indicate the distance between the polster and the notochord.

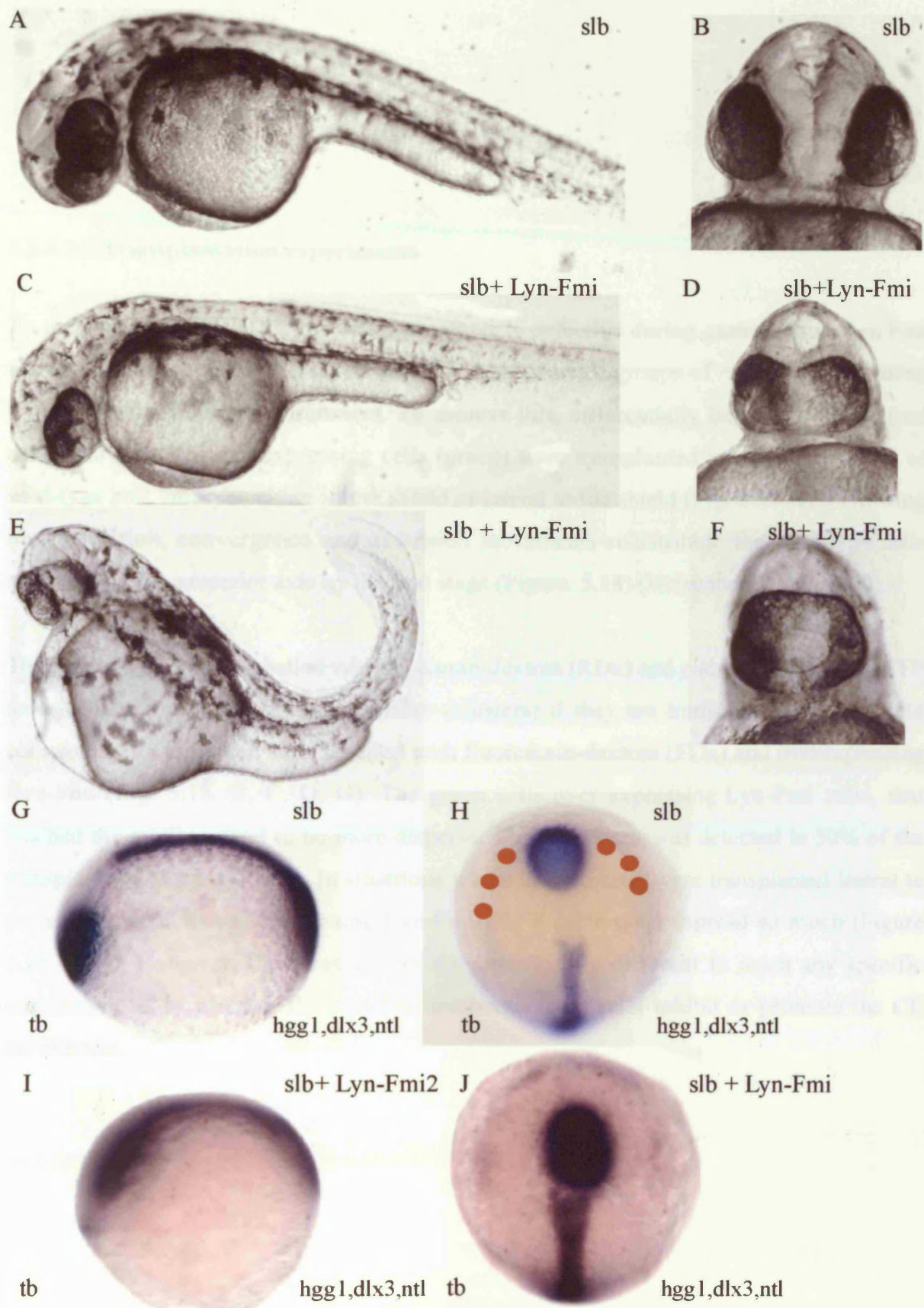


Figure 5.17. Overexpression of Lyn-Fmi RNA in *slb* embryos. *Slb* embryos (A, B), *slb* embryos injected with 50 pg of Lyn-Fmi RNA (C, D), *slb* embryos injected with 100pg of Lyn-Fmi RNA (E, F) at pharyngula stage. Lateral views where anterior is left (A, C, E,) and frontal views of the head region (B, D, F). At tail bud stage *slb* embryos lateral and dorsal views (G,H) and *slb* embryos injected with Lyn-Fmi RNA (100pg). Lateral and dorsal views(I, J). In dorsal views anterior is up and in lateral views anterior is left. Genes analysed are indicated bottom right. Dots mark the edge of neural plate. 150

5.2.3.2. Transplantation experiments

To understand which aspect of cell movements is defective during gastrulation when Fmi activity is compromised, I assayed the behaviour of small groups of cells over-expressing Lyn-Fmi in a wildtype environment. To achieve this, differentially labelled wildtype (red cells) and Lyn-Fmi overexpressing cells (green) were transplanted into the germ rings of wild-type host embryos either in the shield or lateral to the shield (Fig. 5.18.A). Following transplantation, convergence and extension movements redistribute the wild-type cells along the antero-posterior axis by tail bud stage (Figure. 5.18) (Heisenberg et al., 2000).

The red wild type cells labelled with rhodamin-dextran (RDx) and overexpressing Lyn-CFP tend to have a more cohesive behaviour (clusters) if they are transplanted to the shield compared with the green cells labelled with fluorescein-dextran (FDx) and overexpressing Lyn-Fmi (Fig. 5.18. B, C, D, G). The green cells over expressing Lyn-Fmi cells, that reached the midline, tend to be more disperse. This behaviour was detected in 50% of the transplanted embryos (n=55). In situations where labeled cells were transplanted lateral to the shield, the cells overexpressing Lyn-Fmi-EGFP seem not to spread so much (Figure 5.18. E, F). However, these results are not significantly different to reach any specific conclusion, as to whether the Lyn-Fmi overexpressing cells inhibit or promote the CE movements.

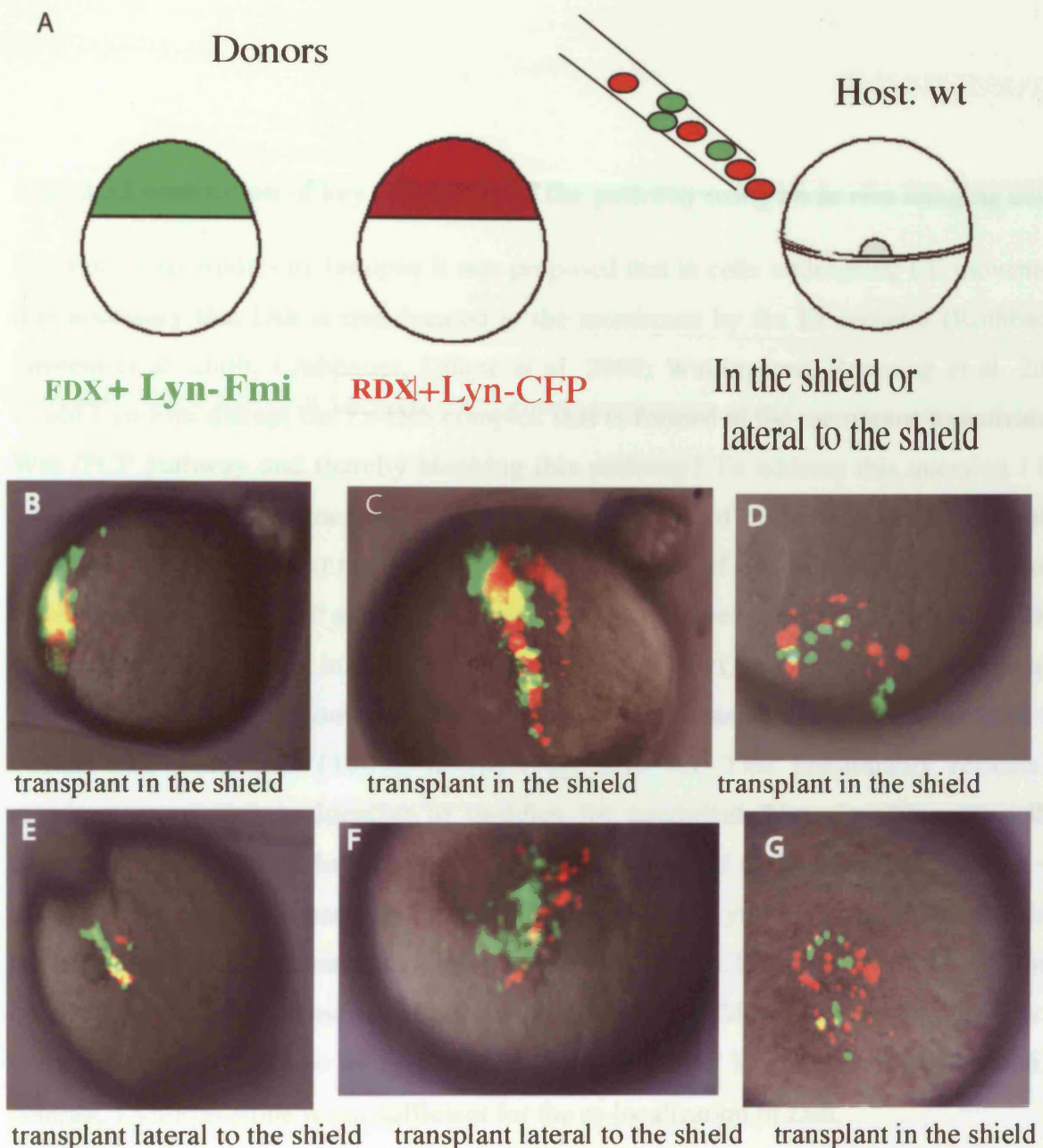
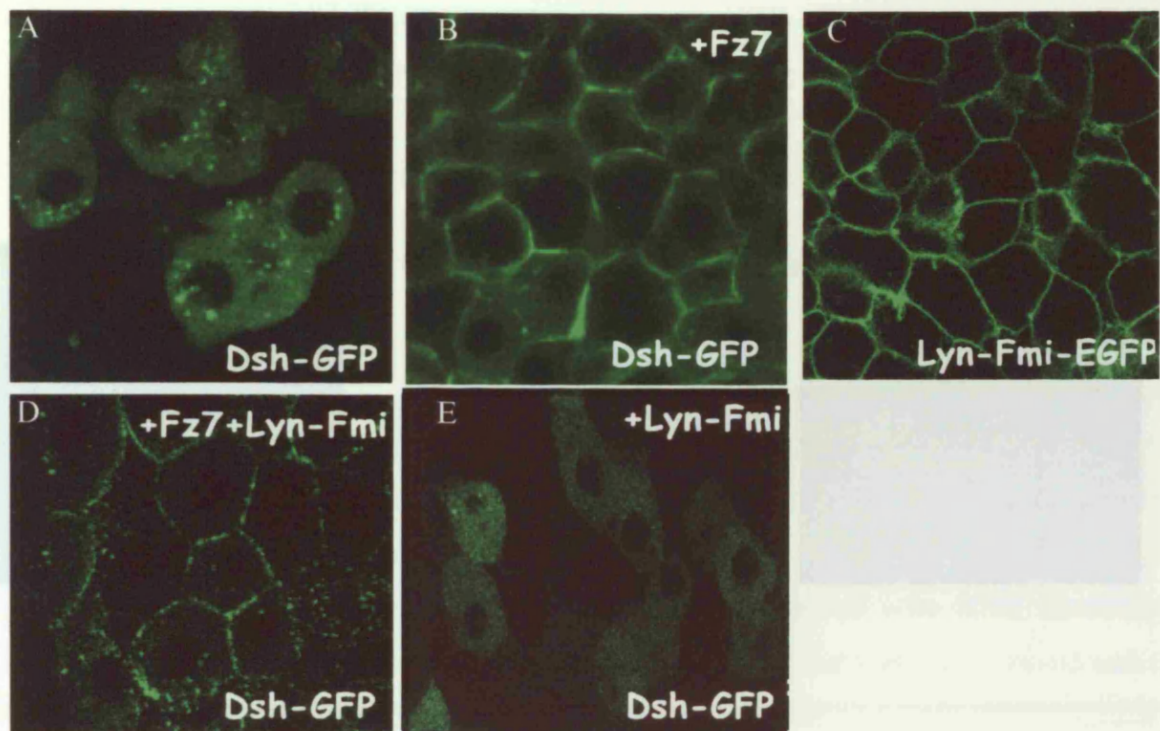


Figure 5.18. Analysis of cell behaviour of cells expressing Lyn-Fmi in gastrulating embryos. (A) Schematic of the experiment. Cells from embryos that received 100pg Lyn-Fmi RNA and fluorescein-dextran (FDx) and cells from embryos that received rhodamin-dextran (RDx) and 100pgLyn-CFP RNA were transplanted simultaneously into the germ rings of wild-type shield-stage hosts, in the shield or lateral to the shield. (B) Lateral view of a living tailbud-stage host embryo with dorsal to the top and (E) dorsal view of a living, tailbud-stage host embryo where the cells were transplanted lateral to the shield. (C, D, F, G) Animal views of living tailbud-stage host embryos. When the transplanted cells were in the shield the wild type cells (red) may be more clustered compared to Lyn-Fmi expressing cells (green) (A,B,C,G). When the transplant was lateral to the shield the Lyn-Fmi expressing cells (green) had a more clustered behaviour (E,F). This cell behaviour analysis was done at x20 magnification.

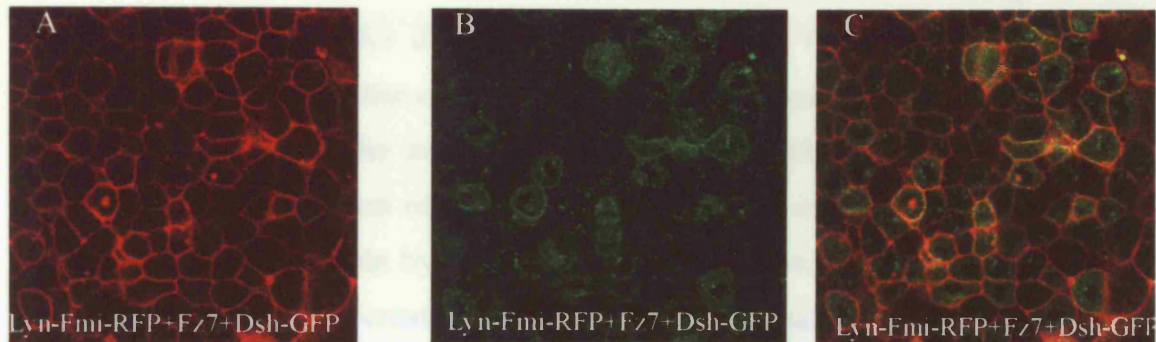
5.2.3.2.3. Localization of key regulators of the pathway using an *in vivo* imaging assay

From previous studies in *Xenopus* it was proposed that in cells undergoing CE movements, it is necessary that Dsh is translocated to the membrane by the Fz receptor (Rothbacher, Laurent et al. 2000; Umbhauer, Djiane et al. 2000; Wallingford, Rowling et al. 2000). Could Lyn-Fmi disrupt the Fz-Dsh complex that is formed at the membrane to activate the Wnt /PCP pathway and thereby blocking this pathway? To address this question I have established an assay to measure subcellular localisation of proteins in the living embryo that is presumably a direct read-out for the establishment of CE. In this assay, I co-injected RNA encoding Dsh-GFP and Fz7 at one cell stage, followed by confocal analysis of living embryos at early gastrula in zebrafish (Figure 5.19). When Dsh-GFP is expressed in animal pole blastomeres, it predominantly localises to the cytoplasm, sometimes associated with vesicle-like structures (100%, $n=10$) (Fig. 5.19 A). This presumably reflects the requirement of Dsh to localise to vesicles for canonical Wnt signalling (Capelluto, Kutateladze et al. 2002). In response to Fz7, Dsh is targeted to the membrane (90%, $n=30$) (Fig. 5.19.B), but this is partially inhibited by injection of Lyn-Fmi because Dsh remains at the membrane in a punctuated fashion (70%, $n=26$) (Fig. 5.19.D). In a control experiment of co-injection, with same previous conditions of Dsh-GFP and Lyn-Fmi, Dsh is not recruited to the membrane by Lyn-Fmi (5.19.E). Dsh-GFP localizes in the cytoplasm. By contrast, Lyn-Fmi alone is not sufficient for the re-localization of Dsh.

This punctuated localisation of Dsh caused by Lyn-Fmi raises the question as to whether Lyn-Fmi and the complex Fz/Dsh co-localize or they are mutually exclusive. To answer this I did the same kind of imaging of animal pole cells of embryos at 40% epiboly that had been injected with RNA encoding Dsh-GFP, Fz7 RNA and Lyn-Fmi-RFP RNA. Firstly, I detected the red channel that enables the visualization of Lyn-Fmi-RFP and it localizes only at the membrane as would be expected (Figure 5.20.A.). The green channel enables the visualization of Dsh-GFP and it localizes in the cytoplasm and in the membrane in a punctuated manner (Figure 5.20.B). The overlay of the two channels in the same region of the embryo shows, that Lyn-Fmi-RFP and Dsh-Fz7 complex co-localize (yellow regions in the membrane) (Figure 5.20.C).



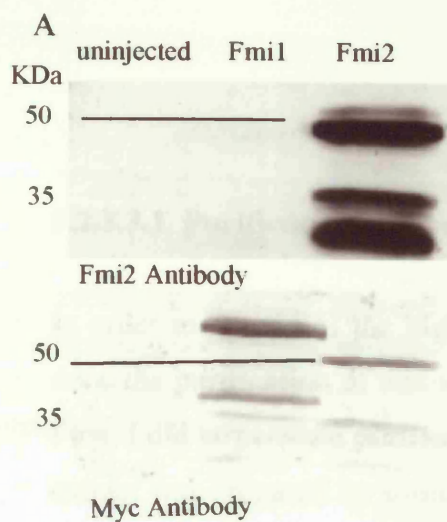
5.19. Lyn-Fmi partially inhibits Fz7-dependent membrane localisation of Dsh. Confocal images of animal pole cells of embryos at 40% epiboly. Embryos were injected with 200 pg RNA encoding Dsh-GFP (A) and 200 pg RNA encoding Dsh-GFP and 50 pg fz7 RNA (B). Dsh preferentially localises to vesicles (A) but relocates to the membrane in the presence of Fz7 (B). (C) The embryo was injected with 100 pg RNA encoding Lyn-Fmi tagged with EGFP. Lyn-Fmi localises to the membrane. (D) The embryo was injected with 200 pg RNA encoding Dsh-GFP, 50 pg fz7RNA and 100 pg Lyn-Fmi RNA. The Fz7-induced membrane localisation of Dsh is partially inhibited by Lyn-Fmi. (E) Injection of 100 pg Lyn-Fmi RNA and 200 pg RNA encoding Dsh-GFP. Lyn-Fmi alone does not recruit Dsh to the membrane.



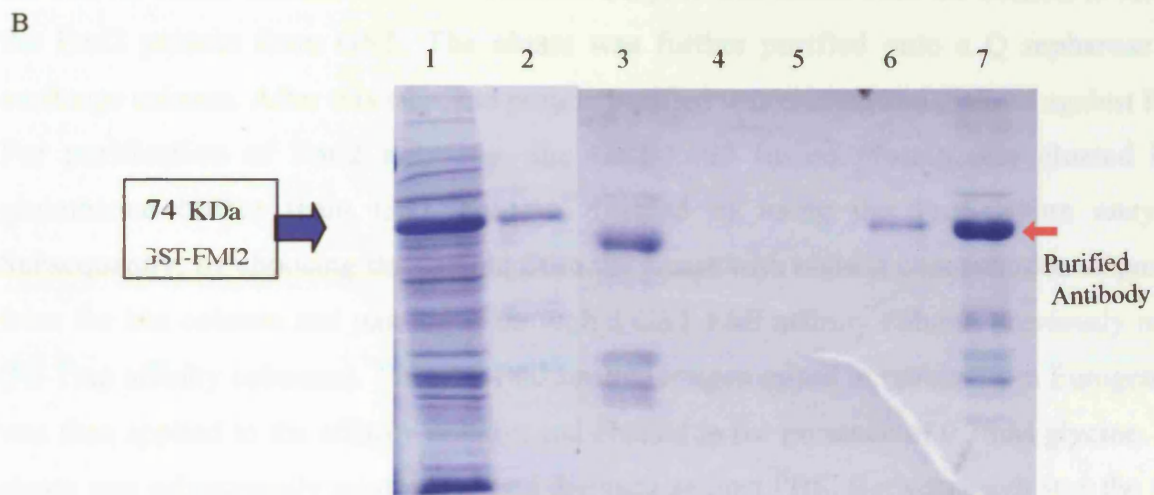
5. 20. Lyn-Fmi co-localizes with Dsh-GFP in the presence of Fz7. Different channels (red, green) of the same stack (A,B) and overlay of A and B images (C). Confocal images of animal pole cells of embryos at 40% epiboly. Embryos were injected with 200 pg RNA encoding Dsh-GFP, 50 pg Fz7RNA and 100 pg Lyn-Fmi-RFP RNA. (A) At the red channel enables the visualization of Lyn-Fmi-RFP and it localizes only at the membrane. (B) The green channel enables the visualization of Dsh-GFP and it localizes in the cytoplasm and at the membrane with a punctuated pattern. (C) The overlay of the two channels of the same region of the embryo show that Lyn-Fmi-RFP and Dsh-GFP co-localize (yellow regions at the membrane), indicating that Lyn-Fmi may form a complex with Fz7 and Dsh in this context.

5.2.3.3. Localization of Fmi protein

In *Drosophila*, sub-cellular polarised localisation of proteins acting in the PCP pathway provides a read-out for activity of the pathway (Axelrod, 2001; Strutt, 2001, Tree et al., 2002). Therefore, I hypothesized that sub cellular localisation of Flamingo protein might provide us with a clue for directional indications with respect to the direction of cells undergoing CE. To visualise endogenous Fmi, a polyclonal antibody was raised against the cytoplasmic region of the zebrafish Flamingo 2 in rabbits. The antigen was prepared initially by the production of Fmi-GST fusion protein in *Escherichia coli*, followed by purification of Fmi protein by cleavage of Fmi-GST protein and then the purified protein was injected in rabbits to create an antibody. In a preliminary assay by western blot analysis of extracts from animal caps of *Xenopus* embryos injected with RNA encoding the intracellular of *fmi1a* or *fmi2*, the specificity of the Fmi2 antibody was proved and there was no cross reaction with Fmi proteins (Figure.5.21A).



5.21. Specificity and purification of Fmi2 Antibody (A) Western blot analysis using Fmi2 antibody. Extracts from animal caps of *Xenopus* embryos injected with RNAs encoding the intracellular domain Fmi1 or Fmi2 tagged with the myc epitope were subjected to SDS-PAGE and Western blotting with Fmi2 Ab. The membrane was, then reacted with Myc antibody. Proving that the antibody is specific to Fmi2 because a pair of bands (proteins) a 50KDa, which is the expected size of the Flamingo 2 protein from the calculated amino acid residue, and another band of 35 kDa, which could be cleaved form the protein.



5.21.(B) SDS-PAGE gel from the protein purification

1. Crude extract E.coli (+) induce with IPTG
2. Eluate from GST column
3. Eluate from affinity (GST-FMI) column after applying the serum and dialysis
- 4 and 5. Recovery from ion exchange and affinity and desalting columns
6. Eluate from ion exchange column, showing sample less concentrated
7. Eluate from ion exchange column, showing sample more concentrated

Purification of GST-Fmi

Purification of the antibody

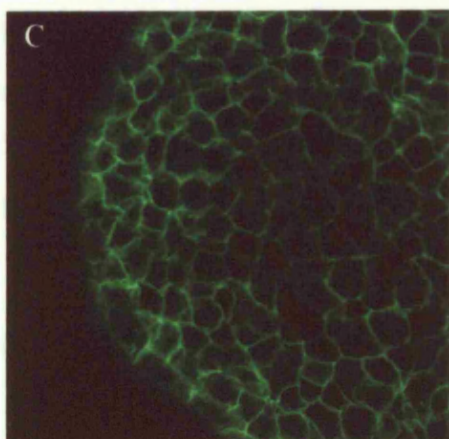


Figure 5.21.(C) Animal pole view of a zebrafish fixed embryo at 60% of epiboly injected with Lyn-Fmi2 RNA at one cell stage and stained with Fmi2 Antibody. It is clear that the protein is localised at the membrane of the cells.

5.2.3.3.1. Purification and refinement of Fmi antibody

In order to get rid of the high background in whole-mount Fmi antibody staining I have done the purification of this antibody through a series of production and purification steps. First, I did large-scale purification, in *E.coli* cells after IPTG induction and then the protein extract was prepared by sonication in PBS containing complete protease inhibitor cocktail. The extract was applied onto a GST column that had been equilibrated. After washing with the correct buffer extensively a ProScission enzyme was added onto the column to release the Fmi2 protein from GST. The eluate was further purified onto a Q sepharose ion exchange column. After this step, the protein purified was eluted and dialysed against PBS. For purification of Fmi2 antibody, the GST-Fmi2 fusion protein was eluted in a glutathione buffer from GST column, instead of using the ProScission enzyme. Subsequently, by choosing the sample from the eluate with highest concentration of protein from the last column and passing it through a GST-FMI affinity column previously made (Hi-Trap affinity columns). The anti-Fmi serum (antigen raised in rabbits from Eurogentec) was then applied to the affinity column and eluted in the presence of 0.3mM glycine. The eluate was subsequently neutralised and dialysed against PBS. Between each step the O.D (optical density) of the different samples was measured and all the proteins sizes were checked in SDS page gels. (for a more detailed description see Chapter 2 section 2.2.7) (Figure 5.21. B).

During this Ph.D. project I have been optimising the protocol and conditions for antibody Fmi 2 staining (see Chapter2 section 2.2.8.2). I could visualize a reasonable antibody staining in embryos injected with Lyn-Fmi2 RNA using confocal microscopy (Figure 5.21.C.) However, it was not sensitive enough to recognise endogenous protein in the gastrula embryos.

5.2.3.3.2.Possible localization of Fmi

An important question that I was trying to answer during this work was where Fmi protein localizes in gastrulating zebrafish embryos. One of the approaches to possibly solve this

was to visualize the protein localization by confocal analysis of living embryos at early gastrula that were injected with tagged DNA constructs of a full-length of Fmi2-Venus, Lyn-Fmi2-Venus or Δ N-Fmi2-Venus, which lacks the extracellular domain except the signal sequence of the protein (Venus is a YFP derivative) (Figure 5.22. A, B, C, D). Fmi-Venus localizes at the membrane particularly in the tips of long filopodia (Figure 5.22. A, B), while Lyn-Fmi-Venus localizes uniformly at the membrane (Figure 5.22. C). In contrast, Δ N-Fmi-Venus localizes only in the cytoplasm (Figure 5.22. D).

Western blot analysis was done with extracts from the embryos injected with DNAs encoding Fmi2-Venus or Lyn-Fmi2-Venus using a GFP antibody. The GFP antibody detected a band of 75 KDa from Fmi2-Venus and a band of 56 KDa from Lyn-Fmi2-Venus construct. The 75 KDa band corresponds to the transmembrane region plus the cytoplasmic tail of Flamingo, raising the possibility that this could be a cleaved form of Fmi protein (Figure 5.22.E). In addition to confirm this, the second western blot analysis was done with extracts from zebrafish embryos injected with same DNAs constructs using the Fmi2 antibody which recognizes the intracellular domain (Figure 5.22.E). The Fmi2 antibody detected the same bands of 75KDa and 56KDa for Fmi2-Venus and Lyn-Fmi2-Venus, respectively (Figure 5.22F). Taken together, these results suggest that Fmi may function in the formation of filipodia and that its ability to induce the cellular processes may correlate with a cleaved form of Fmi.

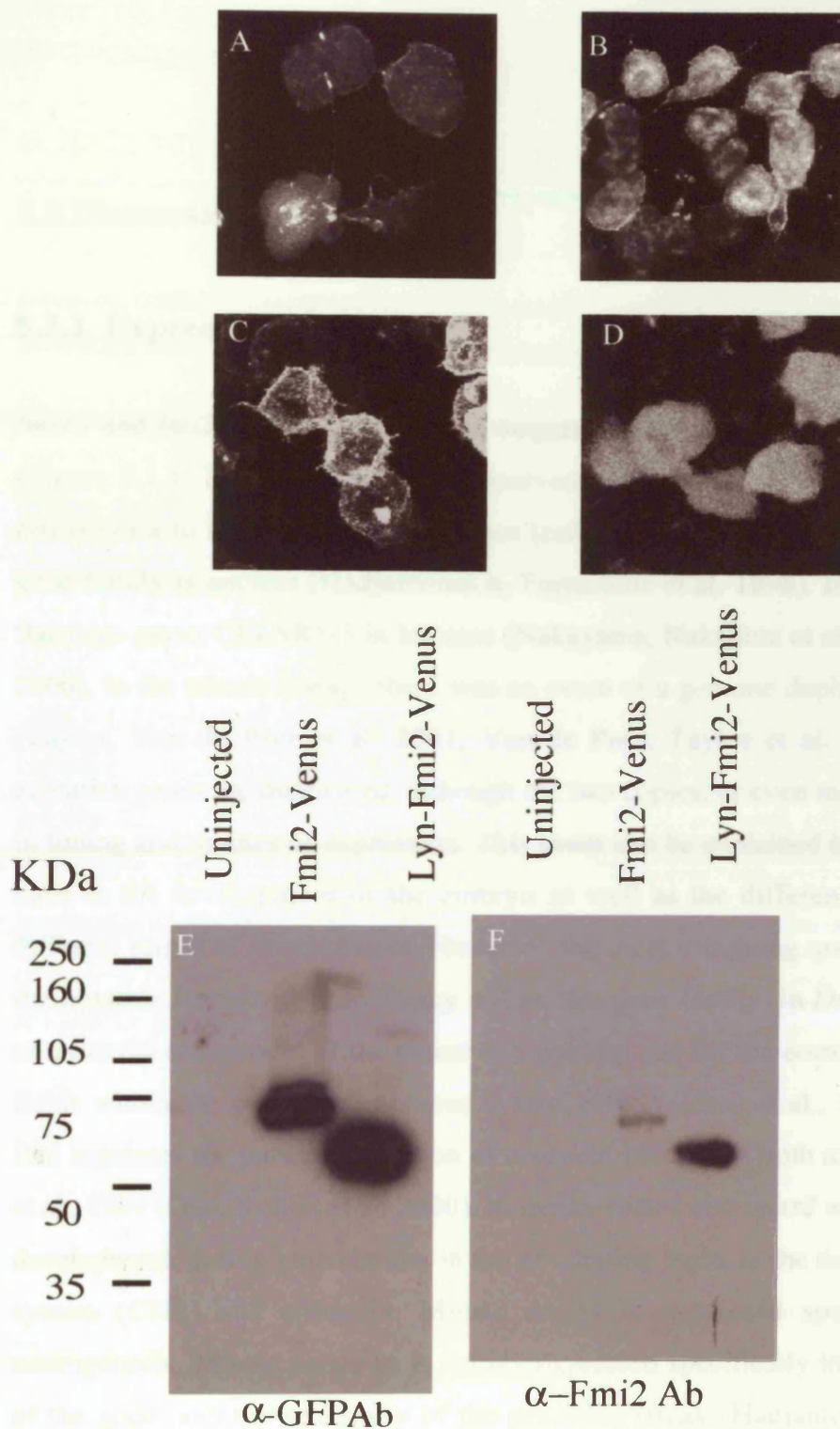


Figure 5.22. Possible localization of Fmi protein. A-D. Confocal images of animal pole cells of embryos at 60% epiboly. Embryos were injected with 20pg DNA encoding Fmi2-Venus (A,B), 20pg DNA encoding Lyn-Fmi2-Venus(C) and 20pg DNA encoding ΔN-Fmi2-Venus (D). (E)Western-blot analysis using a GFP antibody. The samples were extracted from embryos injected with 100 pg DNA encoding Fmi2-Venus or 100pg DNA encoding Lyn-Fmi2-Venus.It detects a band of 75 KDa which corresponds to the trans-membrane domain plus the cytoplasmic tail of Fmi protein and a 56 KDa band which is the expected size of the intracellular domain plus the Lyn cassette calculated from the amino acid residues.(F)The same blot using the Fmi2 antibody.

5.3. Discussion

5.3.1. Expression patterns

fmi1a and *fmi2* have a high degree sequence homology with *fmi* genes across species (Figure 5.1.). The *fmi* genes are conserved across species from *Caenorhabditis elegans*, *Drosophila* to three paralogs in mouse (*celsr1-3*). These data suggest that origin of this gene family is ancient (Hadjantonakis, Formstone et al. 1998). In addition there are three flamingo genes CELSR1-3 in humans (Nakayama, Nakajima et al. 1998; Wu and Maniatis 2000). In the teleost lineage there was an event of a genome duplication early in evolution (Taylor, Van de Peer et al. 2001; Van de Peer, Taylor et al. 2001), eventually some zebrafish genes are duplicated, although the two copies, or even more, are usually divergent in timing and/or sites of expression. This event can be explained by the different roles they have in the development of the embryo as well as the different functions they have in different stages of development. However, the most intriguing question is to know what is the possible functional redundancy within this gene family. In *Drosophila* the *fmi* gene is an essential component of the planar cell polarity and for the correct formation of dendritic fields within the peripheral nervous system (PNS) (Chae et al., 1999, Usui et al., 1999). Fmi regulates the pattern formation of neuronal process of both axons and dendrites (Usui et al., 1999 (Gao, Kohwi et al. 2000). In mouse *celsr1* and *celsr2* are expressed during early development, during gastrulation, in the developing brain, in the developing central nervous system (CNS) and epithelia. Mouse *celsr3* is expressed specifically during active neurogenesis. Mouse *celsr1* is mainly expressed specifically in the brain in the vicinity of the node, anterior extremity of the primitive streak (Hadjantonakis, Formstone et al. 1998). *celsr2* is expressed in the anterior neural ectoderm and *celsr3* starts to be expressed during somitogenesis (Formstone and Little 2001; Shima, Copeland et al. 2002). Each of the *celsr* genes is expressed prominently in the developing brain with a specific pattern, suggesting that they serve distinct functions in the CNS, playing a very important role in brain development. It is speculated that Celsr1 is implicated in nerve cell proliferation and Celsr3 is implicated in nerve cell differentiation and Celsr 2 may have a less specific role in the development of the nervous system (Shima, Copeland et al. 2002; Tissir, De-Backer et

al. 2002). Additionally, mouse *celsr 1-3* are involved in the PCP formation in the inner ear and they are expressed in the hair cells, mainly in the stereocilia (Shima, Copeland et al. 2002). Furthermore, *celsr1* and *celsr2* are detected in early gastrulation events, which correlate with the pattern of expression in *fmi1a* and *fmi2* and a possible role of those genes in regulating convergent extension movements. In addition, the pattern of expression of *fmi1a* and *fmi2* during gastrulation in zebrafish is similar to their orthologues in other vertebrates (expression in the shield and presumptive notochord) (Figure 5.2.; figure 5.3; Figure 5.4; Figure 5.5 and Figure 5.6). The zebrafish *fmi* genes might have roles in regulating convergent extension movements due to the dorsal expression of these genes.

In all vertebrates examined, *fmi* genes are consistently expressed very early in embryogenesis and subsequently in the developing nervous system. In mammals, the identification of mouse mutants of *Celsr 1*, *spin cycle* and *crash*, provides the first evidence for the function of Flamingo genes family in planar cell polarity in mammals. The expression pattern of this gene is correlated with neural tube defects. It further supports the involvement of planar cell polarity pathway in vertebrates that might control convergent extension movements at early stages and also neurulation at late stages of embryogenesis (Curtin et al., 2003). It is also interesting that two other mouse mutants that have severe neural tube defects (NTD) phenotypes are also involved in the vertebrate PCP pathway, the *Lpp1/Ltap* or *strabismus* mutant (Murdoch et al., 2001; Kibar et al., 2001) and the double knockout *dishevelled 1 & 2* (Hamblet et al., 2002), reinforcing the idea that normal convergent extension is essential for neural tube closure.

5.3.2. Loss of function- Morpholino approach

Firstly, the result obtained with the splice morpholinos suggest that *fmi1a* and *fmi2* genes are functionally redundant in regulating CE movements. At pharyngula stage, they have a typically curly down tail phenotype and at tail bud stage the embryos have a slightly posteriorly located prechordal plate (*hgg1*), wider neural plate (*dlx3*), a wider notochord (*ntl*), epiboly defects in the posterior region and laterally expanded presomitic mesoderm (*papc*) (Figures 5.6 and 5.7). These morpholinos weakly affect the CE movements. Similarly, the combination of the 5' prime morpholinos against *fmi1a* and *fmi2* led to a

weak CE phenotype even at higher concentration (Figure 5.10). These results suggest that the third *fmi* gene exposed during gastrulation may compensate the function of *fmi1a* and *fmi2* in regulating CE. Indeed, analyse of the combination of 5'- prime morpholinos, Mo *fmi1a* and Mo *fmi1b*, at pharyngula stage led to a weak phenotype of inhibition of gastrulation movements (Figure 5.8). At tail bud stage the embryos had epiboly defects in the posterior region and the presomitic mesoderm was affected (*papc*). In addition, the prechordal plate was posteriorly mis-positioned, the notochord and neural plate were wider as compared with wild type embryos (Figure 5.9). Taken together, these results indicate that three *fmi* genes are functionally redundant in regulating CE.

To test whether three *fmi* genes are functionally redundant, I also abrogated the functions of the three genes during gastrulation by injecting maternal-zygotic (MZ) *off-road (ord)/fmi2* mutants with *fmi1a+fmi1b* 5'-prime morpholinos. Surprisingly, the mutants with compromised Fmi function exhibited epiboly defects whereas the dorso-ventral patterning remained unaffected (Figure 5.12.). Associated with epiboly defects, the *fmi* triple mutant/morphants showed weakly defective CE movements (Figure 5.12.). Probably these defects are due primarily to disrupted epiboly movements and consequently CE movements are weakly affected as seen in epiboly mutants such as *half baked*, *avalanche*, *lawine*, and *weg* (Kane and Adams, 2002).

5.3.3. Dominant negative approach

The dominant negative approach is based on the prediction that a truncated form of the protein may block a function of endogenous protein to complement the morpholino approach. Fmi appears to have two distinct functions an extra-cellular function involved in cell adhesion (Usui et al., 1999) and other functions that are probably related to signalling (Shima, Kengaku et al. 2004). Therefore, to try to block the signalling function of Fmi I have made a construct in which the intracellular domain of Fmi is fused to a membrane target signal of Lyn to generate Lyn-Fmi.

Injection of Lyn-Fmi2 RNA in wild type embryos at high doses leads to a shorter body axis, dorsal flexure at the posterior region with fused eyes at pharyngula stage (Figure.

5.13). This phenotype resembles the *slb* (*wnt11*);*ppt* (*wnt5*) double mutant, which arises from severely disturbed CE movements during gastrulation. This construct could be a putative dominant negative form of Fmi by blocking the non-canonical/Wnt11/PCP pathway through a possible signalling function of Fmi. To support this idea, the injected wild type embryos with high dosage of Lyn-Fmi2 resemble *slb;ppt* double mutants indicating that these embryos have defects in CE movements by inhibiting the Wnt/PCP pathway (Figure 5.13., Figure 5.14, Figure 5.15) (Kilian et al, 2003; Carreira- Barbosa et al.,2003).

It remains to be addressed if Lyn-Fmi acts as a constitutive active form or as a putative dominant negative form of Fmi as gain of function and loss of function of the PCP genes in zebrafish leads to similar defective phenotypes (Carreira- Barbosa et al., 2003; Jessen et al, 2002). To address this, first of all, I overexpressed Lyn-Fmi in *slb* mutants. I detected an enhanced *slb* phenotype at pharyngula stage and especially at tail bud stage, the prechordal plate is severe displaced caudally in the *slb*^{-/-} embryo injected with Lyn-Fmi (Fig. 5.17.).

Secondly, I injected *slb* embryos with *fmi* Mos to see if abrogation of Fmi leads to an enhancement of the *slb* phenotype. As enhanced by Lyn-Fmi, injection of *fmi* Mos enhanced the *slb* phenotype at pharyngula stage because the distance between the eyes is severely reduced according to the increasing dose of the double morpholinos. Also, in the posterior region of these embryos there was a severe reduction of the yolk extension dependent on the concentration of the morpholinos (Figure 5.16.). At tail bud stage, the *slb* mutants injected with the double morpholinos against *fmi1a* and *fmi2* show a shorter body axis, a wider notochord and the distance between the prechordal plate and notochord is severely reduced compared with either the single mutants (Figure 5.16.).

These results indicate that Fmi might function in the Wnt/PCP pathway or in parallel to this pathway as a positive modulator. Although Lyn-Fmi appears to be a dominant negative form of Fmi in regulating gastrulation, it might even work as a context-dependent positive or negative modulator of Fz/PCP signalling, rather than just a downstream/upstream component of the pathway. Therefore, it will be important to examine if Lyn-Fmi can block caudal migration of facial motoneurons or if Lyn-Fmi can enhance a defective neuronal

migration in *ord/fmi2* mutants, as these mutants show a partially defective migration of facial motor neurons (Hitoshi Okamoto personal communications).

To understand mechanisms by which Lyn-Fmi negatively regulates the Wnt/PCP pathway I tried to analyse Lyn-Fmi interactions with other key regulators of the Wnt/PCP pathway using the *in vivo*-imaging assay (section 5.2.3.2.3 of this chapter). I showed that Lyn-Fmi partially inhibits Fz7-dependent membrane localisation of Dsh and that Lyn-Fmi does not recruit Dsh to the membrane by itself (Figure 5.19). Furthermore, the membrane localization of Lyn-Fmi is not mutually exclusive of Dsh-Fz7 complex localization, but rather it is co-localized with Fz7/Dsh (Figure 5.20.). These data support the idea that Lyn-Fmi somehow interacts directly or indirectly with the Dsh-Fz complex and thereby inhibits the Wnt/PCP pathway. However, the assay developed here is not sufficient to conclude this. In the future, it will be important to establish a direct-read out of CE movements in the embryo such as a Dsh-GFP transgenic line generated to visualise its localisation in cells undergoing CE movements.

5.3.4. Possible mechanism of action of Fmi protein

In order to better understand the function of Flamingo during gastrulation, I tried to look into the subcellular localisation of Flamingo protein that might correlate with the direction of cells undergoing convergent extension. As a first approach, a polyclonal antibody was raised against the cytoplasmic region of zebrafish Flamingo 2. In spite of the fact that the Fmi2 antibody specifically recognises Fmi2, but not Fmi1a (Figure 5.21), it was not good enough to visualise endogenous protein in the embryo.

As an alternative approach, I did confocal analysis of living embryos that had been injected with a DNA construct in which a full-length Fmi was tagged with Venus, an YFP derivative. In a preliminary experiment, Fmi-Venus localizes at the tips of long filopodia in the pre-gastrula embryo (Figure 5.21). The following step will be to examine the localisation of Fmi-Venus in cells undergoing CE. To do this, it might be necessary to generate a transgenic line in which Fmi-Venus is expressed under the control of an

inducible promoter, such as a heat shock promoter, in *ord/fmi2* embryos to avoid any gain of function consequences.

Additionally, to try to answer how Fmi activity mediates cell behaviour during gastrulation movements, using the *in vivo* imaging assay, I observed that Fmi2-Venus induces long filopodia as compared with Lyn-Fmi2-Venus, the negative control. These results suggest that the function of Fmi might act as, driving force of gastrulation movements or to react to a polarity cue for CE movements (Figure 5.22).

To explore this working hypothesis I performed a western blot analysis of zebrafish embryos injected with DNA encoding Fmi2-Venus or Lyn-Fmi2-Venus. It showed that the GFP antibody detects a band of 75 KDa with Fmi-Venus which corresponds to the transmembrane region plus the cytoplasmic tail of the Flamingo protein calculated from amino acid residues and therefore it might be a cleaved form of Fmi protein (Figure 5.22.). This result suggests that the cleaved form of Fmi could act as a receptor or co-receptor in response to directional cues still to be identified. This is supported by recent data showing that an N-terminal truncated form of Fmi may act as a signalling receptor during dentrite process outgrowth in mammalian neurons (Shima, Kengaku et al. 2004). Taking into account with the observation that Δ N-Fmi-Venus is not found at the membrane (Figure 5.22), Fmi could be initially presented at the membrane as a full-length and then cleaved to function as putative signalling receptor. In the future, it will be interesting to examine if the ability of Fmi to induce long processes is correlated with a cleaved form of Fmi that might act as signalling receptor independent of cell adhesion activity.

Finally, one of the most puzzling questions about Fmi is how distinct are its two possible functions; cell adhesion and signalling. I found that triple *fmi* mutant/morphants exhibited a more defective epiboly whereas embryos expressing Lyn-Fmi showed a severely defective CE during gastrulation. One interpretation for these contradictory results is that a dosage effect of Fmi is more sensitive to epiboly, when the cell adhesion function would be more required, while Lyn-Fmi might preferentially block a signalling function of Fmi, rather than its cell adhesion function. This hypothesis could be in part supported by observations that E-cadherins morphant embryos and *half baked* mutant embryos exhibit a defective epiboly movement (Babb and Marrs 2004; Kane, McFarland et al. 2005) and this defect is primarily

due to defective cell adhesion function (Montero, Carvalho et al. 2005). To complement my approach, it will be important to examine if overexpression of another mutant form of Fmi, which only has the extracellular domain including cadherin repeats without the 7 TM and the cytoplasmic domains, leads to any defects in epiboly or/and CE during gastrulation. Furthermore, it will be also intriguing to access cell adhesion activity of cells with compromised Fmi function in the cell aggregation assays as done in Montero et al., 2005.

5.4. Summary

In this chapter, I describe the cloning of zebrafish flamingo (*fmi*) genes and the characterisation of the expression pattern of the *fmi* genes during zebrafish embryogenesis, especially during gastrulation. To examine possible roles of *fmi* genes during zebrafish gastrulation, I have used various approaches: a morpholino approach, a dominant negative approach with an *in vivo* imaging assay, transplantation assays, co-localization tests and different studies of protein localization. *fmi* genes are required for proper gastrulation movements and may act together with Wnt/Fz/Dsh in regulating CE but in a context-dependent manner. Taken together all the results, Fmi appears to have two functions: cell adhesion and signalling. Future research in this field will involve to study the mechanisms by which Fmi regulates epiboly and CE and to understand how its functions is related to different forms of Fmi in time and in space during gastrulation.

Addendum

The regions of zebrafish *fmi1a* and *fmi2* that were used as probes for *in situ* hybridisations analyses correspond to the C-terminus region of flamingo gene as seen in Figure 5.1. In more detail the riboprobe generated for zebrafish *fmi1a* comprises the laminin A globular domains, cysteine rich regions, 7 transmembrane domains and the cytoplasmic tail, which is 3730 base pairs long. The riboprobe for zebrafish *fmi2* comprises the cysteine regions, the 7 transmembrane domains and the cytoplasmic tail that is 3844 base pairs long.

Additionally, *fmi1a* and *fmi2* probes used for *in situ* hybridisation studies in this chapter might contain regions of sufficient sequence identity to potentially cause cross-hybridisation between them although all the washes used in screening the zebrafish gastrula libraries were done with high stringency. By using Blast analysis of the two sequences I have obtained results of 73 to 74% of identity within the 7 transmembrane domain comprising sequences of 150 to 280 nucleotides, which is relatively high identity. The cross-hybridisation between riboprobes might be a concern in my studies due to the similarities of the expression patterns at early gastrulation stages. To overcome this problem a more detail analysis should be done at later stages (24 hours post fertilization).

The expression pattern for *fmi1b* was study in detail by ours collaborators from Hitoshi Okamoto lab, at early stage of gastrulation and later stages. The same team of collaborators has been able to prove using Ensemble database centre during the execution of this thesis that *fmi1a* and *fmi1b* are both orthologues of Fmi1 because they belong to distinct linkage groups or chromosomes; respectively *fmi1a* belongs to chromosome 25 and *fmi1b* to chromosome 8.

To determine the efficiency of gene knockdown by morpholinos additional controls should have been done like for example injection at one cell stage of control morpholinos for 5 prime morpholinos that for example include 4 nucleotides mismatches and confirm if they gave the same phenotype. Also for splice morpholinos experiments, control RT-PCR reactions should have been performed in order to assess and quantify the effectiveness of splicing inhibition.

CHAPTER 6

General Discussion and future directions

In this thesis I have first analyzed briefly functions of Wnt5 and Wnt11 ligands and of Fz2 and Fz7 receptors in regulating convergent extension (CE) movements in zebrafish. I showed that Ppt/Wnt5 is required for regulating CE movements in posterior mesendodermal and ectodermal regions while its function in the anterior mesendoderm is largely redundant to that of Slb/Wnt11. I also described preliminary experiments about the specificity of the Fz2 and Fz7 receptors to Wnt5 and Wnt11 ligands. Based on gene expression analyses, loss of function and gain of function assays the interactions between these Wnt ligands and Fz receptors works in a time-concentration-place dependent manner.

Furthermore, I described the isolation and functional characterisation of the zebrafish homologue of *Drosophila prickles* (*pk1*) during gastrulation. I demonstrated that zebrafish *pk1* functions together with Slb/Wnt11 and Ppt/Wnt5 to regulate CE movements from several experiments. Firstly, abrogation of Pk1 function by morpholino leads to defective convergent extension movements, enhances the *silberblick* (*slb/wnt11*) and (*pipetail/wnt5*) phenotypes and suppresses the ability of Wnt11 to rescue the *slb* phenotype. Secondly, gain-of-function of Pk1 also inhibits convergent extension movements and enhances the *slb* phenotype. Thirdly, consistent with the results in flies (Tree et al., 2002), I found that Pk1 can destabilise Dsh and thereby block the ability of Fz to target Dsh to the cell membrane by down-regulating levels of Dsh protein. These results show that Pk1 acts downstream of the non-canonical Wnt11/Wnt5 pathway to regulate convergent extension cell movements, but it is unlikely to simply be a linear component of this pathway.

With regard to co-localization or differential localization of Dsh, although I observed that Pk1 inhibits Fz-mediated membrane localization of Dsh in static zebrafish animal pole cells, other groups described that Dsh and Pk colocalise to the membrane in the presence of Fz7 in static *Xenopus* animal pole cells (Veeman et al., 2003; Takeuchi et al, 2003). To

solve this discrepancy, it will be important to visualize localizations of endogenous PCP proteins in cells undergoing CE.

Finally, I described the isolation of zebrafish flamingo (*fmi*) genes and the characterisation of the expression pattern of the *fmi* genes during zebrafish embryogenesis, especially during gastrulation. In order to examine possible functions of *fmi* genes during zebrafish gastrulation, I have done this using various approaches: a morpholino approach, a dominant negative approach with an *in vivo* imaging assay, transplantation assays, co-localization tests and different studies of protein localization. Firstly, abrogation of Flamingo function by the combination of *fmi1a* and *fmi2* morpholinos leads to defective convergent extension movements, enhances the *silberblick slb/wnt11* phenotypes and the *ord/fmi2* mutants defective epiboly phenotypes. The dominant negative approach with a mutant form of Fmi, Lyn-Fmi, leads me to conclude that possibly Fmi is involved in the regulation of CE movements by modulating the non-canonical Wnt pathway in a direct or indirect way. Analyses of Fmi protein based on over-expression of full-length Fmi fused with Venus suggest that Fmi could be cleaved to be functional during gastrulation but it is necessary to have the transmembrane domain to still be operative in gastrulation and it might have a function in the formation of filipodia during this stage of development in response to putative directional cues. Nevertheless, Fmi might act as a context-dependent positive or negative modulator of the non-canonical Wnt /PCP signalling, rather than just a downstream/upstream component of the pathway, as does Pk. My data support the idea that Fmi might have two distinct functions: cell adhesion function mediated by the extracellular domain of cadherin repeats and signalling function mediated by the seven-pass transmembrane and intracellular domains. These possible roles are consistent with recent data by (Shima et al, 2004). Future research will be necessary to study more extensively how Lyn-Fmi specifically blocks its signalling functions through the modulation of the Wnt/PCP pathway.

Also, it will be important to understand mechanisms by which Fmi can regulate different gastrulation movements such as epiboly and CE with respect to its cell adhesion and signaling functions.

6.1. Differences and similarities between the vertebrate system and the PCP in *Drosophila*

Genetic data in zebrafish and functional analyses in *Xenopus* strongly support the idea that there are several resemblances between the Wnt/Wg signaling pathways controlling gastrulation movements in vertebrates and those controlling PCP in *Drosophila*. However, regardless of the similarities between these pathways, there are also considerable divergences in both molecular and cellular contexts with respect to their outcomes.

One of the major differences is that the vertebrate non-canonical pathway includes Wnt ligands, such as Silberblick (Wnt11) and Pipetail (Wnt5), whereas no Wnt ligand is known to be involved in *Drosophila* PCP signaling (review in Tree et al., 2002). It is very difficult to prove a negative result and this is a dramatic difference in the way of the two pathways function. Also, there is not enough evidence that the Wnt proteins implicated in vertebrate CE act instructively as directional cues but rather they could have a more permissive role (discussed in section 6.3 of this chapter).

In zebrafish, several mutants of the Wnt/PCP pathway, which have defects in CE movements during gastrulation, have been characterized (Heisenberg et al., 2000; Rauch et al., 1997, Kilian et al., 2003, Darken et al., 2002; Goto and Keller, 2002; Jessen et al., 2002; Park and Moon, 2002; Veeman et al., 2003). Nonetheless, in the majority of the cases studied, the precise cellular mechanism that gives rise to these phenotypes is not fully understood. It has been speculated that the defects in CE movements in these mutants are due to a failure of epiblast and hypoblast cells to elongate along their medio-lateral axes, which is thought to be essential for medio-lateral cell intercalation behavior. It is still unknown as to whether the lack of medio-lateral cell elongation is just a secondary event of these cells not being able to move dorsally and intercalate or if the Wnt/PCP pathway directly controls the orientation of these cells and cell movement. Moreover, it is not clear if we can fully compare medio-lateral elongation of cells during vertebrate gastrulation and the polarization of *Drosophila* wing cells. As mentioned previously, the formation of a wing hair at the distal location in the cell is guided by the asymmetric localization of key regulators of PCP pathway along the cell proximal-distal axis. However, asymmetric membrane localization of the homologous proteins in epiblast and hypoblast cells

undergoing CE movements has not yet been observed. One possible explanation for this could be that the arrangement of the tissues in which the Wnt-Fz/PCP pathway works is different between *Drosophila* and vertebrates: a single plane versus a three-dimensional plane for orientation of cells. While wing cells are organized in an epithelium with no space between single cells, gastrulating cells in *Xenopus* and zebrafish look more loosely associated and show massive movements in relation to each other and on the substrate to which they attach (Keller et al., 2000; Glickman et al. 2003). Even though several regulators of the PCP pathway are conserved between *Drosophila* and vertebrates, the roles of these regulators in *Drosophila* PCP and vertebrate gastrulation could be quite different because in vertebrates there is a dynamic cellular assembly that exhibits both epithelial and mesenchymal features. Embryos are dynamic three-dimensional structures with several layers of tissues and with extensive movements, making the analysis very difficult to perform studies of PCP protein localization as already done in *Drosophila*. Also, the PCP pathway regulates the polarity of different structures: the trichomes of the wing, bristles on the body, and the ommatidia of the compound eye; but always the structure is unipolar. On the other hand, the non-canonical Wnt pathway in vertebrate gastrulation involves both unipolar and bipolar cell morphologies (reviewed in Keller, 2002; Myers et al., 2002; Wallingford et al., 2002).

One of the most important data is that the loss of function of Dsh, Vang/Stbm and Fmi/Stan homologues results in neural tube closure defects in mouse. Neural tube closure in vertebrate embryos requires proper CE movements of the neuroectoderm (Wallingford and Harland, 2001; Goto and Keller, 2002). This indicates that these genes function in a conserved pathway regulating CE in mammals (Kibar et al., 2001; Murdoch et al., 2001; Hamblet et al., 2002; Curtin et al., 2003). The mouse homologues of Vang/Stbm and Fmi/Stan are also necessary for proper polarity of sensory hair cells in the ear (Curtin et al., 2003; Montcouquiol et al., 2003). The roles and connections of the vertebrate homologues of the core PCP genes are not completely understood.

6.2. Fundamental characteristics of the function of the PCP proteins

This thesis proves that some genes that have been discovered to regulate cell polarisation during PCP in *Drosophila* are conserved in the pathway that regulates convergent extension during vertebrate gastrulation. The big task now is to find out if there is also a conserved mechanism of cell polarisation acting in both the PCP and the non canonical Wnt pathway in vertebrates. If this assumption is true, the main interest is to understand how broadly this is observed in nature. So far, little is known about how the core PCP proteins function together to translate a polarity signal into a three-dimensional plane of mesenchymal cells in vertebrates. Furthermore, it is also not clear if the same proteins act together in all contexts even in the same organism (Adler, 2002). Still there is necessity to characterize protein-protein interactions of these regulators and to reveal when they occur *in vivo* in polarising cells in different tissues, as well as to improve the understand of the long-range signals that control cell polarity in relation to the axes of the tissue, and the downstream effectors, such as potential transcription factors, that conduct to alterations in cell structure and movement.

Despite the fact that PCP genes are required for proper cell movements and morphology during gastrulation (Heisenberg and Tada, 2002), it is still doubtful how these genes function during gastrulation. They might either instructively establish the pattern of cellular rearrangements within the embryo or they might act permissively by allowing cells to interpret any patterning cues. My preferable interpretation is that the PCP genes permissively act during gastrulation as the *slb* phenotype can be rescued with ubiquitous over-expression of *wnt11* or Δ N-Dsh, which specifically activates the non-canonical pathway (Heisenberg et al., 2000). Even though these roles are not always easy to distinguish, as the cellular output might look very similar, they execute different functions. If a gene is involved in instructively patterning morphogenetic movements, the gene product itself must confer the patterning information that regulates cell movement and morphology during gastrulation. On the contrary, genes that function permissively only have the ability to translate a patterning signal but are not needed to give any patterning information themselves. More specific experiments, such as specific misexpression of

candidate genes, will help to make a distinction between these different functional possibilities. For example, different aspects of the non-canonical Wnt pathway have been involved with neuronal morphogenesis and neuronal migration. *Strabismus/trilobite* and *Prickle1* are necessary for the proper migration of hindbrain facial motor neurons (Jessen et al., 2002, Carreira-Barbosa et al., 2003). In addition, *Fmi* has a role in dendritic and axonal outgrowth, which is probably independent of the Wnt/Fz/Dsh pathway (Gao et al., 2000; Shima et al. 2004). Wnt/Fz/Dsh-dependent and independent activities of *Fmi*, *Stbm* and *Pk* suggest that PCP genes may regulate the behaviour of large populations of cells in a Wnt/PCP-dependent way, while they may respond to directional cues to migration or process outgrowth of small groups of cells via a mechanism independent of the non canonical Wnt pathway.

6.3. Remaining and arising questions

The place within the gastrula where the key regulators of the Wnt non-canonical pathway are necessary has not yet been established for most of the genes that regulate convergent extension movements (Heisenberg and Tada 2002). Even though the expression pattern of the majority of these genes has been established during gastrulation, this has provided only a comprehensive picture about the distribution of RNAs coding for those gene products. In contrast, the endogenous localization of the protein for almost these genes is yet unknown, especially in zebrafish. Studies in *Drosophila* have shown that the asymmetric localization of PCP proteins, for example, is the crucial step in polarizing cells within the wing epithelium (Strutt, 2002). The production of functional antibodies directed against genes with a morphogenetic function during vertebrate gastrulation will be necessary to visualize the intra- and intercellular distribution of those proteins. Furthermore, the generation of transgenic lines in zebrafish carrying GFP-tagged PCP proteins will allow us to visualize polarized localization of those proteins in the living embryo. These approaches will help to obtain details about the mechanisms by which these genes function during gastrulation.

One of the main challenges is to identify the complete array of direct and indirect outputs by which a gene can utilize on the co-ordination of gastrulation movements. These genes functions might be cell autonomous and non-autonomous and might depend on the

interaction between populations of cells in different germ layers. Studies in *Xenopus* have shown that mesodermal cells are necessary for the correct polarization and movement of ectodermal cells during gastrulation, suggesting that the cellular interactions between the germ layers are important (Elul and Keller R, 2000). Similarly, in zebrafish, the YSL appears to provide a substrate for the movement of hypoblast (mesendodermal) and epiblast (ectodermal) cells during gastrulation (D'Amico and Cooper, 2001; Ulrich et al., 2003). It was also shown that the movement of yolk syncytial cell nuclei during gastrulation is correlated with the CE movements seen in the overlying hypoblast and epiblast cell layers during gastrulation, suggesting that cell movements are coordinated between the yolk cell and germ layers (D'Amico and Cooper, 2001). Tissue specific manipulation of cellular movement and morphology plus the analysis of its effects on other tissues during gastrulation will be required to obtain information about the interaction between different cellular populations during gastrulation.

Given that, the PCP proteins act in a permissive way, what are the directional cues that inform cells where to move. So far, none of the secreted molecules has yet been identified. Zebrafish are ideally suited for forward genetics to search for new molecules. Consequently, it would be feasible to perform enhancer/suppressor screens using sensitized genetic backgrounds such as *slb/wnt11* and *ord/fmi2* taking advantage of the fact that those homozygous mutants are viable.

How fast all those questions can be answered will depend on the development or adaptation of new techniques. As many of these techniques are already available (although not necessarily in the gastrulation field), one can expect significant progress in understanding the molecular and cellular mechanisms that regulate zebrafish gastrulation movements in the near future.

Bibliography

Adler, P. N. (2002). "Planar signaling and morphogenesis in *Drosophila*." Dev Cell 2(5): 525-35.

Adler, P. N., J. Charlton and J. Liu (1998). "Mutations in the cadherin superfamily member gene *dachsous* cause a tissue polarity phenotype by altering frizzled signaling." Development 125(5): 959-68.

Adler, P. N., R. E. Krasnow and J. Liu (1997). "Tissue polarity points from cells that have higher Frizzled levels towards cells that have lower Frizzled levels." Curr Biol 7(12): 940-9.

Adler, P. N. and H. Lee (2001). "Frizzled signaling and cell-cell interactions in planar polarity." Curr Opin Cell Biol 13(5): 635-40.

Adler, P. N., J. Taylor and J. Charlton (2000). "The domineering non-autonomy of frizzled and van Gogh clones in the *Drosophila* wing is a consequence of a disruption in local signaling." Mech Dev 96(2): 197-207.

Amsterdam, A., S. Burgess, G. Golling, W. Chen, Z. Sun, K. Townsend, S. Farrington, M. Haldi and N. Hopkins (1999). "A large-scale insertional mutagenesis screen in zebrafish." Genes Dev 13(20): 2713-24.

Ataliotis, P., K. Symes, M. M. Chou, L. Ho and M. Mercola (1995). "PDGF signalling is required for gastrulation of *Xenopus laevis*." Development 121(9): 3099-110.

Axelrod, J. D. (2001). "Unipolar membrane association of Dishevelled mediates Frizzled planar cell polarity signaling." Genes Dev 15(10): 1182-7.

Axelrod, J. D. and H. McNeill (2002). "Coupling planar cell polarity signaling to morphogenesis." ScientificWorldJournal 2: 434-54.

Axelrod, J. D., J. R. Miller, J. M. Shulman, R. T. Moon and N. Perrimon (1998). "Differential recruitment of Dishevelled provides signaling specificity in the planar cell polarity and Wingless signaling pathways." Genes Dev 12(16): 2610-22.

Babb, S. G. and J. A. Marrs (2004). "E-cadherin regulates cell movements and tissue formation in early zebrafish embryos." Dev Dyn 230(2): 263-77.

Bakkers, J., C. Kramer, J. Pothof, N. E. Quaedvlieg, H. P. Spaink and M. Hammerschmidt (2004). "Has2 is required upstream of Rac1 to govern dorsal migration of lateral cells during zebrafish gastrulation." Development 131(3): 525-37.

Barth, K. A. and S. W. Wilson (1995). "Expression of zebrafish nk2.2 is influenced by sonic hedgehog/vertebrate hedgehog-1 and demarcates a zone of neuronal differentiation in the embryonic forebrain." Development 121(6): 1755-68.

Bastock, R., H. Strutt and D. Strutt (2003). "Strabismus is asymmetrically localised and binds to Prickle and Dishevelled during Drosophila planar polarity patterning." Development 130(13): 3007-14.

Baumann, M. and K. Sander (1984). "Bipartite axiation follows incomplete epiboly in zebrafish embryos treated with chemical teratogens." J Exp Zool 230(3): 363-76.

Bilder, D., M. Li and N. Perrimon (2000). "Cooperative regulation of cell polarity and growth by Drosophila tumor suppressors." Science 289(5476): 113-6.

Boutros, M. and M. Mlodzik (1999). "Dishevelled: at the crossroads of divergent intracellular signaling pathways." Mech Dev 83(1-2): 27-37.

Boutros, M., N. Paricio, D. I. Strutt and M. Mlodzik (1998). "Dishevelled activates JNK and discriminates between JNK pathways in planar polarity and wingless signaling." Cell 94(1): 109-18.

Brenner, S. (1974). "The genetics of *Caenorhabditis elegans*." Genetics 77(1): 71-94.

Brodsky, M. H. and H. Steller (1996). "Positional information along the dorsal-ventral axis of the *Drosophila* eye: graded expression of the four-jointed gene." Dev Biol 173(2): 428-46.

Cadigan, K. M. and R. Nusse (1997). "Wnt signaling: a common theme in animal development." Genes Dev 11(24): 3286-305.

Capelluto, D. G., T. G. Kutateladze, R. Habas, C. V. Finkielstein, X. He and M. Overduin (2002). "The DIX domain targets dishevelled to actin stress fibres and vesicular membranes." Nature 419(6908): 726-9.

Carmany-Rampey, A. and A. F. Schier (2001). "Single-cell internalization during zebrafish gastrulation." Curr Biol 11(16): 1261-5.

Carreira-Barbosa, F., M. L. Concha, M. Takeuchi, N. Ueno, S. W. Wilson and M. Tada (2003). "Prickle 1 regulates cell movements during gastrulation and neuronal migration in zebrafish." Development 130(17): 4037-46.

Casal, J., G. Struhl and P. A. Lawrence (2002). "Developmental compartments and planar polarity in *Drosophila*." Curr Biol 12(14): 1189-98.

Chae, J., M. J. Kim, J. H. Goo, S. Collier, D. Gubb, J. Charlton, P. N. Adler and W. J. Park (1999). "The *Drosophila* tissue polarity gene starry night encodes a member of the protocadherin family." Development 126(23): 5421-9.

Challa, A. K., C. E. Beattie and M. A. Seeger (2001). "Identification and characterization of roundabout orthologs in zebrafish." Mech Dev 101(1-2): 249-53.

Chen, S. and D. Kimelman (2000). "The role of the yolk syncytial layer in germ layer patterning in zebrafish." Development 127(21): 4681-9.

Cheng, J. C., A. L. Miller and S. E. Webb (2004). "Organization and function of microfilaments during late epiboly in zebrafish embryos." Dev Dyn 231(2): 313-23.

Choi, S. C. and J. K. Han (2002). "Xenopus Cdc42 regulates convergent extension movements during gastrulation through Wnt/Ca²⁺ signaling pathway." Dev Biol 244(2): 342-57.

Cohen, E. D., M. C. Mariol, R. M. Wallace, J. Weyers, Y. G. Kamberov, J. Pradel and E. L. Wilder (2002). "DWnt4 regulates cell movement and focal adhesion kinase during *Drosophila* ovarian morphogenesis." Dev Cell 2(4): 437-48.

Comer, F. I. and C. A. Parent (2002). "PI 3-kinases and PTEN: how opposites chemoattract." Cell 109(5): 541-4.

Concha, M. L. and R. J. Adams (1998). "Oriented cell divisions and cellular morphogenesis in the zebrafish gastrula and neurula: a time-lapse analysis." Development 125(6): 983-94.

Conway, G., A. Margoliath, S. Wong-Madden, R. J. Roberts and W. Gilbert (1997). "Jak1 kinase is required for cell migrations and anterior specification in zebrafish embryos." Proc Natl Acad Sci U S A 94(7): 3082-7.

Cooper, M. T. and S. J. Bray (1999). "Frizzled regulation of Notch signalling polarizes cell fate in the *Drosophila* eye." Nature 397(6719): 526-30.

Curtin, J. A., E. Quint, V. Tsipouri, R. M. Arkell, B. Cattanch, A. J. Copp, D. J. Henderson, N. Spurr, P. Stanier, E. M. Fisher, P. M. Nolan, K. P. Steel, S. D. Brown, I. C. Gray and J. N. Murdoch (2003). "Mutation of *Celsr1* disrupts planar polarity of inner ear hair cells and causes severe neural tube defects in the mouse." Curr Biol 13(13): 1129-33.

D'Amico, L. A. and M. S. Cooper (1997). "Spatially distinct domains of cell behavior in the zebrafish organizer region." Biochem Cell Biol 75(5): 563-77.

D'Amico, L. A. and M. S. Cooper (2001). "Morphogenetic domains in the yolk syncytial layer of axiating zebrafish embryos." Dev Dyn 222(4): 611-24.

Dabdoub, A., M. J. Donohue, A. Brennan, V. Wolf, M. Montcouquiol, D. A. Sassoon, J. C. Hseih, J. S. Rubin, P. C. Salinas and M. W. Kelley (2003). "Wnt signaling mediates reorientation of outer hair cell stereociliary bundles in the mammalian cochlea." Development 130(11): 2375-84.

Darken, R. S., A. M. Scola, A. S. Rakeman, G. Das, M. Mlodzik and P. A. Wilson (2002). "The planar polarity gene strabismus regulates convergent extension movements in *Xenopus*." Embo J 21(5): 976-85.

Davidson, G., B. Mao, I. del Barco Barrantes and C. Niehrs (2002). "Kremen proteins interact with Dickkopf1 to regulate anteroposterior CNS patterning." Development 129(24): 5587-96.

Djiane, A., J. Riou, M. Umbhauer, J. Boucaut and D. Shi (2000). "Role of frizzled 7 in the regulation of convergent extension movements during gastrulation in *Xenopus laevis*." Development 127(14): 3091-100.

Domingo, C. and R. Keller (2000). "Cells remain competent to respond to mesoderm-inducing signals present during gastrulation in *Xenopus laevis*." Dev Biol 225(1): 226-40.

Draper, B. W., P. A. Morcos and C. B. Kimmel (2001). "Inhibition of zebrafish *fgf8* pre-mRNA splicing with morpholino oligos: a quantifiable method for gene knockdown." Genesis 30(3): 154-6.

Driever, W., L. Solnica-Krezel, A. F. Schier, S. C. Neuhauss, J. Malicki, D. L. Stemple, D. Y. Stainier, F. Zwartkruis, S. Abdelilah, Z. Rangini, J. Belak and C. Boggs (1996). "A genetic screen for mutations affecting embryogenesis in zebrafish." Development 123: 37-46.

Eaton, S. (1997). "Planar polarization of Drosophila and vertebrate epithelia." Curr Opin Cell Biol 9(6): 860-6.

El-Messaoudi, S. and A. Renucci (2001). "Expression pattern of the frizzled 7 gene during zebrafish embryonic development." Mech Dev 102(1-2): 231-4.

Elul, T. and R. Keller (2000). "Monopolar protrusive activity: a new morphogenic cell behavior in the neural plate dependent on vertical interactions with the mesoderm in Xenopus." Dev Biol 224(1): 3-19.

Elul, T., M. A. Koehl and R. Keller (1997). "Cellular mechanism underlying neural convergent extension in Xenopus laevis embryos." Dev Biol 191(2): 243-58.

Fanto, M., L. Clayton, J. Meredith, K. Hardiman, B. Charroux, S. Kerridge and H. McNeill (2003). "The tumor-suppressor and cell adhesion molecule Fat controls planar polarity via physical interactions with Atrophin, a transcriptional co-repressor." Development 130(4): 763-74.

Fanto, M. and H. McNeill (2004). "Planar polarity from flies to vertebrates." J Cell Sci 117(Pt 4): 527-33.

Fanto, M. and M. Mlodzik (1999). "Asymmetric Notch activation specifies photoreceptors R3 and R4 and planar polarity in the Drosophila eye." Nature 397(6719): 523-6.

Farber, S. A., M. Pack, S. Y. Ho, I. D. Johnson, D. S. Wagner, R. Dosch, M. C. Mullins, H. S. Hendrickson, E. K. Hendrickson and M. E. Halpern (2001). "Genetic analysis of digestive physiology using fluorescent phospholipid reporters." Science 292(5520): 1385-8.

Feiguin, F., M. Hannus, M. Mlodzik and S. Eaton (2001). "The ankyrin repeat protein Diego mediates Frizzled-dependent planar polarization." Dev Cell 1(1): 93-101.

Fink, R. D. and M. S. Cooper (1996). "Apical membrane turnover is accelerated near cell-cell contacts in an embryonic epithelium." Dev Biol 174(2): 180-9.

Formstone, C. J. and P. F. Little (2001). "The flamingo-related mouse Celsr family (Celsr1-3) genes exhibit distinct patterns of expression during embryonic development." Mech Dev 109(1): 91-4.

Formstone, C. J. and P. F. Little (2001). "The flamingo-related mouse Celsr family (Celsr1-3) genes exhibit distinct patterns of expression during embryonic development." Mech Dev 109(1): 91-4.

Formstone, C. J. and I. Mason (2005). "Expression of the Celsr/flamingo homologue, c-fmil, in the early avian embryo indicates a conserved role in neural tube closure and additional roles in asymmetry and somitogenesis." Dev Dyn 232(2): 408-13.

Gao, F. B., M. Kohwi, J. E. Brenman, L. Y. Jan and Y. N. Jan (2000). "Control of dendritic field formation in Drosophila: the roles of flamingo and competition between homologous neurons." Neuron 28(1): 91-101.

Gilland, E., A. L. Miller, E. Karplus, R. Baker and S. E. Webb (1999). "Imaging of multicellular large-scale rhythmic calcium waves during zebrafish gastrulation." Proc Natl Acad Sci U S A 96(1): 157-61.

Glickman, N. S., C. B. Kimmel, M. A. Jones and R. J. Adams (2003). "Shaping the zebrafish notochord." Development 130(5): 873-87.

Glickman, N. S. and D. Yelon (2002). "Cardiac development in zebrafish: coordination of form and function." Semin Cell Dev Biol 13(6): 507-13.

Goto, T. and R. Keller (2002). "The planar cell polarity gene strabismus regulates convergence and extension and neural fold closure in Xenopus." Dev Biol 247(1): 165-81.

Gubb, D. and A. Garcia-Bellido (1982). "A genetic analysis of the determination of cuticular polarity during development in Drosophila melanogaster." J Embryol Exp Morphol 68: 37-57.

Gubb, D., C. Green, D. Huen, D. Coulson, G. Johnson, D. Tree, S. Collier and J. Roote (1999). "The balance between isoforms of the prickle LIM domain protein is critical for planar polarity in *Drosophila* imaginal discs." Genes Dev 13(17): 2315-27.

Habas, R., I. B. Dawid and X. He (2003). "Coactivation of Rac and Rho by Wnt/Frizzled signaling is required for vertebrate gastrulation." Genes Dev 17(2): 295-309.

Habas, R., Y. Kato and X. He (2001). "Wnt/Frizzled activation of Rho regulates vertebrate gastrulation and requires a novel Formin homology protein Daam1." Cell 107(7): 843-54.

Hadjantonakis, A. K., C. J. Formstone and P. F. Little (1998). "mCelsr1 is an evolutionarily conserved seven-pass transmembrane receptor and is expressed during mouse embryonic development." Mech Dev 78(1-2): 91-5.

Haffter, P. and C. Nusslein-Volhard (1996). "Large scale genetics in a small vertebrate, the zebrafish." Int J Dev Biol 40(1): 221-7.

Hall, A. and C. D. Nobes (2000). "Rho GTPases: molecular switches that control the organization and dynamics of the actin cytoskeleton." Philos Trans R Soc Lond B Biol Sci 355(1399): 965-70.

Hamblet, N. S., N. Lijam, P. Ruiz-Lozano, J. Wang, Y. Yang, Z. Luo, L. Mei, K. R. Chien, D. J. Sussman and A. Wynshaw-Boris (2002). "Dishevelled 2 is essential for cardiac outflow tract development, somite segmentation and neural tube closure." Development 129(24): 5827-38.

Hammerschmidt, M., F. Pelegri, M. C. Mullins, D. A. Kane, M. Brand, F. J. van Eeden, M. Furutani-Seiki, M. Granato, P. Haffter, C. P. Heisenberg, Y. J. Jiang, R. N. Kelsh, J. Odenthal, R. M. Warga and C. Nusslein-Volhard (1996). "Mutations affecting morphogenesis during gastrulation and tail formation in the zebrafish, *Danio rerio*." Development 123: 143-51.

Hannus, M., F. Feiguin, C. P. Heisenberg and S. Eaton (2002). "Planar cell polarization requires Widerborst, a B' regulatory subunit of protein phosphatase 2A." Development 129(14): 3493-503.

Hay, E. D. (1995). "An overview of epithelio-mesenchymal transformation." Acta Anat (Basel) 154(1): 8-20.

He, X., J. P. Saint-Jeannet, Y. Wang, J. Nathans, I. Dawid and H. Varmus (1997). "A member of the Frizzled protein family mediating axis induction by Wnt-5A." Science 275(5306): 1652-4.

Heisenberg, C. P., M. Brand, Y. J. Jiang, R. M. Warga, D. Beuchle, F. J. van Eeden, M. Furutani-Seiki, M. Granato, P. Haffter, M. Hammerschmidt, D. A. Kane, R. N. Kelsh, M. C. Mullins, J. Odenthal and C. Nusslein-Volhard (1996). "Genes involved in forebrain development in the zebrafish, *Danio rerio*." Development 123: 191-203.

Heisenberg, C. P., C. Houart, M. Take-Uchi, G. J. Rauch, N. Young, P. Coutinho, I. Masai, L. Caneparo, M. L. Concha, R. Geisler, T. C. Dale, S. W. Wilson and D. L. Stemple (2001). "A mutation in the Gsk3-binding domain of zebrafish Masterblind/Axin1 leads to a fate transformation of telencephalon and eyes to diencephalon." Genes Dev 15(11): 1427-34.

Heisenberg, C. P. and C. Nusslein-Volhard (1997). "The function of silberblick in the positioning of the eye anlage in the zebrafish embryo." Dev Biol 184(1): 85-94.

Heisenberg, C. P. and M. Tada (2002). "Zebrafish gastrulation movements: bridging cell and developmental biology." Semin Cell Dev Biol 13(6): 471-9.

Heisenberg, C. P., M. Tada, G. J. Rauch, L. Saude, M. L. Concha, R. Geisler, D. L. Stemple, J. C. Smith and S. W. Wilson (2000). "Silberblick/Wnt11 mediates convergent extension movements during zebrafish gastrulation." Nature 405(6782): 76-81.

Ho, L., K. Symes, C. Yordan, L. J. Gudas and M. Mercola (1994). "Localization of PDGF A and PDGFR alpha mRNA in *Xenopus* embryos suggests signalling from neural ectoderm and pharyngeal endoderm to neural crest cells." Mech Dev 48(3): 165-74.

Ho, R. K. and D. A. Kane (1990). "Cell-autonomous action of zebrafish *spt-1* mutation in specific mesodermal precursors." Nature 348(6303): 728-30.

Ho, R. K. and D. A. Kane (1990). "Cell-autonomous action of zebrafish *spt-1* mutation in specific mesodermal precursors." Nature 348(6303): 728-30.

Hou, S. X., Z. Zheng, X. Chen and N. Perrimon (2002). "The Jak/STAT pathway in model organisms: emerging roles in cell movement." Dev Cell 3(6): 765-78.

Houart, C., L. Caneparo, C. Heisenberg, K. Barth, M. Take-Uchi and S. Wilson (2002). "Establishment of the telencephalon during gastrulation by local antagonism of Wnt signaling." Neuron 35(2): 255-65.

Huelsken, J. and W. Birchmeier (2001). "New aspects of Wnt signaling pathways in higher vertebrates." Curr Opin Genet Dev 11(5): 547-53.

Hukriede, N. A., T. E. Tsang, R. Habas, P. L. Khoo, K. Steiner, D. L. Weeks, P. P. Tam and I. B. Dawid (2003). "Conserved requirement of *Lim1* function for cell movements during gastrulation." Dev Cell 4(1): 83-94.

Ibrahim, H. and R. Winklbauer (2001). "Mechanisms of mesendoderm internalization in the *Xenopus* gastrula: lessons from the ventral side." Dev Biol 240(1): 108-22.

Iijima, M., Y. E. Huang and P. Devreotes (2002). "Temporal and spatial regulation of chemotaxis." Dev Cell 3(4): 469-78.

Inoue, T., H. S. Oz, D. Wiland, S. Gharib, R. Deshpande, R. J. Hill, W. S. Katz and P. W. Sternberg (2004). "*C. elegans* LIN-18 is a Ryk ortholog and functions in parallel to LIN-17/Frizzled in Wnt signaling." Cell 118(6): 795-806.

Jessen, J. R., J. Topczewski, S. Bingham, D. S. Sepich, F. Marlow, A. Chandrasekhar and L. Solnica-Krezel (2002). "Zebrafish trilobite identifies new roles for Strabismus in gastrulation and neuronal movements." Nat Cell Biol 4(8): 610-5.

Joubin, K. and C. D. Stern (1999). "Molecular interactions continuously define the organizer during the cell movements of gastrulation." Cell 98(5): 559-71.

Kane, D. and R. Adams (2002). "Life at the edge: epiboly and involution in the zebrafish." Results Probl Cell Differ 40: 117-35.

Kane, D. A., M. Hammerschmidt, M. C. Mullins, H. M. Maischein, M. Brand, F. J. van Eeden, M. Furutani-Seiki, M. Granato, P. Haffter, C. P. Heisenberg, Y. J. Jiang, R. N. Kelsh, J. Odenthal, R. M. Warga and C. Nusslein-Volhard (1996). "The zebrafish epiboly mutants." Development 123: 47-55.

Kane, D. A., K. N. McFarland and R. M. Warga (2005). "Mutations in half baked/E-cadherin block cell behaviors that are necessary for teleost epiboly." Development 132(5): 1105-1116.

Keller, R. (2002). "Shaping the vertebrate body plan by polarized embryonic cell movements." Science 298(5600): 1950-4.

Keller, R., M. S. Cooper, M. Danilchik, P. Tibbetts and P. A. Wilson (1989). "Cell intercalation during notochord development in *Xenopus laevis*." J Exp Zool 251(2): 134-54.

Keller, R. and M. Danilchik (1988). "Regional expression, pattern and timing of convergence and extension during gastrulation of *Xenopus laevis*." Development 103(1): 193-209.

Keller, R., L. Davidson, A. Edlund, T. Elul, M. Ezin, D. Shook and P. Skoglund (2000). "Mechanisms of convergence and extension by cell intercalation." Philos Trans R Soc Lond B Biol Sci 355(1399): 897-922.

Keller, R., L. A. Davidson and D. R. Shook (2003). "How we are shaped: the biomechanics of gastrulation." Differentiation 71(3): 171-205.

Keller, R., J. Shih and A. Sater (1992). "The cellular basis of the convergence and extension of the *Xenopus* neural plate." Dev Dyn 193(3): 199-217.

Keller, R., J. Shih, A. K. Sater and C. Moreno (1992). "Planar induction of convergence and extension of the neural plate by the organizer of *Xenopus*." Dev Dyn 193(3): 218-34.

Keller, R. and P. Tibbetts (1989). "Mediolateral cell intercalation in the dorsal, axial mesoderm of *Xenopus laevis*." Dev Biol 131(2): 539-49.

Keller, R. E. (1980). "The cellular basis of epiboly: an SEM study of deep-cell rearrangement during gastrulation in *Xenopus laevis*." J Embryol Exp Morphol 60: 201-34.

Keller, R. E., M. Danilchik, R. Gimlich and J. Shih (1985). "The function and mechanism of convergent extension during gastrulation of *Xenopus laevis*." J Embryol Exp Morphol 89 Suppl: 185-209.

Keller, R. E. and J. P. Trinkaus (1987). "Rearrangement of enveloping layer cells without disruption of the epithelial permeability barrier as a factor in *Fundulus* epiboly." Dev Biol 120(1): 12-24.

Kibar, Z., K. J. Vogan, N. Groulx, M. J. Justice, D. A. Underhill and P. Gros (2001). "Ltap, a mammalian homolog of *Drosophila* Strabismus/Van Gogh, is altered in the mouse neural tube mutant Loop-tail." Nat Genet 28(3): 251-5.

Kilian, B., H. Mansukoski, F. C. Barbosa, F. Ulrich, M. Tada and C. P. Heisenberg (2003). "The role of Ppt/Wnt5 in regulating cell shape and movement during zebrafish gastrulation." Mech Dev 120(4): 467-76.

Kim, C. H., T. Oda, M. Itoh, D. Jiang, K. B. Artinger, S. C. Chandrasekharappa, W. Driever and A. B. Chitnis (2000). "Repressor activity of Headless/Tcf3 is essential for vertebrate head formation." Nature 407(6806): 913-6.

Kim, S. H., A. Yamamoto, T. Bouwmeester, E. Agius and E. M. Robertis (1998). "The role of paraxial protocadherin in selective adhesion and cell movements of the mesoderm during *Xenopus* gastrulation." Development 125(23): 4681-90.

Kimelman, D. and K. J. Griffin (2000). "Vertebrate mesendoderm induction and patterning." Curr Opin Genet Dev 10(4): 350-6.

Kimmel, C. B., W. W. Ballard, S. R. Kimmel, B. Ullmann and T. F. Schilling (1995). "Stages of embryonic development of the zebrafish." Dev Dyn 203(3): 253-310.

Kimmel, C. B., R. M. Warga and D. A. Kane (1994). "Cell cycles and clonal strings during formation of the zebrafish central nervous system." Development 120(2): 265-76.

Kimmel, C. B., R. M. Warga and T. F. Schilling (1990). "Origin and organization of the zebrafish fate map." Development 108(4): 581-94.

Kinoshita, N., H. Iioka, A. Miyakoshi and N. Ueno (2003). "PKC delta is essential for Dishevelled function in a noncanonical Wnt pathway that regulates *Xenopus* convergent extension movements." Genes Dev 17(13): 1663-76.

Knapik, E. W., A. Goodman, M. Ekker, M. Chevrette, J. Delgado, S. Neuhauss, N. Shimoda, W. Driever, M. C. Fishman and H. J. Jacob (1998). "A microsatellite genetic linkage map for zebrafish (*Danio rerio*)." Nat Genet 18(4): 338-43.

Kominami, T. and H. Takata (2004). "Gastrulation in the sea urchin embryo: a model system for analyzing the morphogenesis of a monolayered epithelium." Dev Growth Differ 46(4): 309-26.

Krasnow, R. E., L. L. Wong and P. N. Adler (1995). "Dishevelled is a component of the frizzled signaling pathway in *Drosophila*." Development 121(12): 4095-102.

Krylova, O., J. Herreros, K. E. Cleverley, E. Ehler, J. P. Henriquez, S. M. Hughes and P. C. Salinas (2002). "WNT-3, expressed by motoneurons, regulates terminal arborization of neurotrophin-3-responsive spinal sensory neurons." Neuron 35(6): 1043-56.

Kuhl, M., L. C. Sheldahl, C. C. Malbon and R. T. Moon (2000). "Ca(2+)/calmodulin-dependent protein kinase II is stimulated by Wnt and Frizzled homologs and promotes ventral cell fates in *Xenopus*." J Biol Chem 275(17): 12701-11.

Kuhl, M., L. C. Sheldahl, M. Park, J. R. Miller and R. T. Moon (2000). "The Wnt/Ca²⁺ pathway: a new vertebrate Wnt signaling pathway takes shape." Trends Genet 16(7): 279-83.

Kuroda, S., T. Satoh and A. Shinagawa (2001). "Involvement of a urethane-sensitive system in timing the onset of gastrulation in *Xenopus laevis* embryos." Dev Growth Differ 43(4): 401-13.

Lawson, K. A., J. J. Meneses and R. A. Pedersen (1991). "Clonal analysis of epiblast fate during germ layer formation in the mouse embryo." Development 113(3): 891-911.

Lee, J. S., R. Ray and C. B. Chien (2001). "Cloning and expression of three zebrafish roundabout homologs suggest roles in axon guidance and cell migration." Dev Dyn 221(2): 216-30.

Lee, J. Y. and B. Goldstein (2003). "Mechanisms of cell positioning during *C. elegans* gastrulation." Development 130(2): 307-20.

Lele, Z., J. Bakkers and M. Hammerschmidt (2001). "Morpholino phenocopies of the swirl, snailhouse, somitabun, minifin, silberblick, and pipetail mutations." Genesis 30(3): 190-4.

Lewis, J. and A. Davies (2002). "Planar cell polarity in the inner ear: how do hair cells acquire their oriented structure?" J Neurobiol 53(2): 190-201.

Li, L., H. Yuan, W. Xie, J. Mao, A. M. Caruso, A. McMahon, D. J. Sussman and D. Wu (1999). "Dishevelled proteins lead to two signaling pathways. Regulation of LEF-1 and c-Jun N-terminal kinase in mammalian cells." J Biol Chem 274(1): 129-34.

Liu, L., S. W. Chong, N. V. Balasubramanian, V. Korzh and R. Ge (2002). "Platelet-derived growth factor receptor alpha (pdgfr-alpha) gene in zebrafish embryonic development." Mech Dev 116(1-2): 227-30.

Liu, L., V. Korzh, N. V. Balasubramanian, M. Ekker and R. Ge (2002). "Platelet-derived growth factor A (pdgf-a) expression during zebrafish embryonic development." Dev Genes Evol 212(6): 298-301.

Logan, C. Y. and R. Nusse (2004). "The Wnt signaling pathway in development and disease." Annu Rev Cell Dev Biol 20: 781-810.

Marlow, F., J. Topczewski, D. Sepich and L. Solnica-Krezel (2002). "Zebrafish Rho kinase 2 acts downstream of Wnt11 to mediate cell polarity and effective convergence and extension movements." Curr Biol 12(11): 876-84.

Marlow, F., F. Zwartkruis, J. Malicki, S. C. Neuhauss, L. Abbas, M. Weaver, W. Driever and L. Solnica-Krezel (1998). "Functional interactions of genes mediating convergent extension, knypek and trilobite, during the partitioning of the eye primordium in zebrafish." Dev Biol 203(2): 382-99.

Marsden, M. and D. W. DeSimone (2001). "Regulation of cell polarity, radial intercalation and epiboly in *Xenopus*: novel roles for integrin and fibronectin." Development 128(18): 3635-47.

Medina, A., W. Reintsch and H. Steinbeisser (2000). "Xenopus frizzled 7 can act in canonical and non-canonical Wnt signaling pathways: implications on early patterning and morphogenesis." Mech Dev 92(2): 227-37.

Miller, J. R., A. M. Hocking, J. D. Brown and R. T. Moon (1999). "Mechanism and function of signal transduction by the Wnt/beta-catenin and Wnt/Ca²⁺ pathways." Oncogene 18(55): 7860-72.

Miyagi, C., S. Yamashita, Y. Ohba, H. Yoshizaki, M. Matsuda and T. Hirano (2004). "STAT3 noncell-autonomously controls planar cell polarity during zebrafish convergence and extension." J Cell Biol 166(7): 975-81.

Mlodzik, M. (2002). "Planar cell polarization: do the same mechanisms regulate Drosophila tissue polarity and vertebrate gastrulation?" Trends Genet 18(11): 564-71.

Montcouquiol, M., R. A. Rachel, P. J. Lanford, N. G. Copeland, N. A. Jenkins and M. W. Kelley (2003). "Identification of Vangl2 and Scrib1 as planar polarity genes in mammals." Nature 423(6936): 173-7.

Montero, J. A., L. Carvalho, M. Wilsch-Brauninger, B. Kilian, C. Mustafa and C. P. Heisenberg (2005). "Shield formation at the onset of zebrafish gastrulation." Development.

Montero, J. A. and C. P. Heisenberg (2003). "Adhesive crosstalk in gastrulation." Dev Cell 5(2): 190-1.

Montero, J. A. and C. P. Heisenberg (2004). "Gastrulation dynamics: cells move into focus." Trends Cell Biol 14(11): 620-7.

Montero, J. A., B. Kilian, J. Chan, P. E. Bayliss and C. P. Heisenberg (2003). "Phosphoinositide 3-kinase is required for process outgrowth and cell polarization of gastrulating mesendodermal cells." Curr Biol 13(15): 1279-89.

Morgan, R., A. M. El-Kadi and C. Theokli (2003). "Flamingo, a cadherin-type receptor involved in the Drosophila planar polarity pathway, can block signaling via the canonical wnt pathway in Xenopus laevis." Int J Dev Biol 47(4): 245-52.

Moriguchi, T., K. Kawachi, S. Kamakura, N. Masuyama, H. Yamanaka, K. Matsumoto, A. Kikuchi and E. Nishida (1999). "Distinct domains of mouse dishevelled are responsible for the c-Jun N-terminal kinase/stress-activated protein kinase activation and the axis formation in vertebrates." J Biol Chem 274(43): 30957-62.

Mullins, M. C., M. Hammerschmidt, D. A. Kane, J. Odenthal, M. Brand, F. J. van Eeden, M. Furutani-Seiki, M. Granato, P. Haffter, C. P. Heisenberg, Y. J. Jiang, R. N. Kelsh and C. Nusslein-Volhard (1996). "Genes establishing dorsoventral pattern formation in the zebrafish embryo: the ventral specifying genes." Development 123: 81-93.

Mullins, M. C., M. Hammerschmidt, D. A. Kane, J. Odenthal, M. Brand, F. J. van Eeden, M. Furutani-Seiki, M. Granato, P. Haffter, C. P. Heisenberg, Y. J. Jiang, R. N. Kelsh and C. Nusslein-Volhard (1996). "Genes establishing dorsoventral pattern formation in the zebrafish embryo: the ventral specifying genes." Development 123: 81-93.

Munro, E. M. and G. M. Odell (2002). "Polarized basolateral cell motility underlies invagination and convergent extension of the ascidian notochord." Development 129(1): 13-24.

Murdoch, B., K. Chadwick, M. Martin, F. Shojaei, K. V. Shah, L. Gallacher, R. T. Moon and M. Bhatia (2003). "Wnt-5A augments repopulating capacity and primitive hematopoietic development of human blood stem cells in vivo." Proc Natl Acad Sci U S A 100(6): 3422-7.

Murdoch, J. N., R. A. Rachel, S. Shah, F. Beermann, P. Stanier, C. A. Mason and A. J. Copp (2001). "Circletail, a new mouse mutant with severe neural tube defects: chromosomal localization and interaction with the loop-tail mutation." Genomics 78(1-2): 55-63.

Myers, D. C., D. S. Sepich and L. Solnica-Krezel (2002). "Convergence and extension in vertebrate gastrulae: cell movements according to or in search of identity?" Trends Genet 18(9): 447-55.

Nakayama, M., D. Nakajima, T. Nagase, N. Nomura, N. Seki and O. Ohara (1998). "Identification of high-molecular-weight proteins with multiple EGF-like motifs by motif-trap screening." Genomics 51(1): 27-34.

Nance J, P. J. (2002). "Cell polarity and gastrulation in *C. elegans*." Development Jan;129(2):387-97. 129(2): 387-97.

Nasevicius, A. and S. C. Ekker (2000). "Effective targeted gene 'knockdown' in zebrafish." Nat Genet 26(2): 216-20.

Nasevicius, A., T. M. Hyatt, S. B. Hermanson and S. C. Ekker (2000). "Sequence, expression, and location of zebrafish frizzled 10." Mech Dev 92(2): 311-4.

Nusslein-Volhard, C. a. W., E. (1980). "Mutations affecting segment number and polarity in *Drosophila*." Nature 287: 795-801.

Oates, A. C., P. Wollberg, S. J. Pratt, B. H. Paw, S. L. Johnson, R. K. Ho, J. H. Postlethwait, L. I. Zon and A. F. Wilks (1999). "Zebrafish stat3 is expressed in restricted tissues during embryogenesis and stat1 rescues cytokine signaling in a STAT1-deficient human cell line." Dev Dyn 215(4): 352-70.

Oishi, I., H. Suzuki, N. Onishi, R. Takada, S. Kani, B. Ohkawara, I. Koshida, K. Suzuki, G. Yamada, G. C. Schwabe, S. Mundlos, H. Shibuya, S. Takada and Y. Minami (2003). "The receptor tyrosine kinase Ror2 is involved in non-canonical Wnt5a/JNK signalling pathway." Genes Cells 8(7): 645-54.

Orr-Urtreger, A., M. T. Bedford, M. S. Do, L. Eisenbach and P. Lonai (1992). "Developmental expression of the alpha receptor for platelet-derived growth factor, which is deleted in the embryonic lethal Patch mutation." Development 115(1): 289-303.

Orr-Urtreger, A. and P. Lonai (1992). "Platelet-derived growth factor-A and its receptor are expressed in separate, but adjacent cell layers of the mouse embryo." Development 115(4): 1045-58.

Pandur, P., D. Maurus and M. Kuhl (2002). "Increasingly complex: new players enter the Wnt signaling network." Bioessays 24(10): 881-4.

Park, M. and R. T. Moon (2002). "The planar cell-polarity gene *stbm* regulates cell behaviour and cell fate in vertebrate embryos." Nat Cell Biol 4(1): 20-5.

Patton, E. E. and L. I. Zon (2001). "The art and design of genetic screens: zebrafish." Nat Rev Genet 2(12): 956-66.

Penzo-Mendez, A., M. Umbhauer, A. Djiane, J. C. Boucaut and J. F. Riou (2003). "Activation of Gbetagamma signaling downstream of Wnt-11/Xfz7 regulates Cdc42 activity during *Xenopus* gastrulation." Dev Biol 257(2): 302-14.

Perez-Moreno, M., C. Jamora and E. Fuchs (2003). "Sticky business: orchestrating cellular signals at adherens junctions." Cell 112(4): 535-48.

Postlethwait, J. H. and W. S. Talbot (1997). "Zebrafish genomics: from mutants to genes." Trends Genet 13(5): 183-90.

Psychoyos, D. and C. D. Stern (1996). "Fates and migratory routes of primitive streak cells in the chick embryo." Development 122(5): 1523-34.

Rajagopalan, S., E. Nicolas, V. Vivancos, J. Berger and B. J. Dickson (2000). "Crossing the midline: roles and regulation of Robo receptors." Neuron 28(3): 767-77.

Rauch, G. J., M. Hammerschmidt, P. Blader, H. E. Schauerte, U. Strahle, P. W. Ingham, A. P. McMahon and P. Haffter (1997). "Wnt5 is required for tail formation in the zebrafish embryo." Cold Spring Harb Symp Quant Biol 62: 227-34.

Rawls, A. S., J. B. Guinto and T. Wolff (2002). "The cadherins fat and dachsous regulate dorsal/ventral signaling in the Drosophila eye." Curr Biol 12(12): 1021-6.

Rawls, A. S. and T. Wolff (2003). "Strabismus requires Flamingo and Prickle function to regulate tissue polarity in the Drosophila eye." Development 130(9): 1877-87.

Rothbacher, U., M. N. Laurent, M. A. Deardorff, P. S. Klein, K. W. Cho and S. E. Fraser (2000). "Dishevelled phosphorylation, subcellular localization and multimerization regulate its role in early embryogenesis." Embo J 19(5): 1010-22.

Sambrook, J. (1989). "Molecular cloning: A laborator Manual." Cold Spring Harbor Laboratory Press, New York 2nd edition.

Sausedo, R. A. and G. C. Schoenwolf (1993). "Cell behaviors underlying notochord formation and extension in avian embryos: quantitative and immunocytochemical studies." Anat Rec 237(1): 58-70.

Sausedo, R. A. and G. C. Schoenwolf (1994). "Quantitative analyses of cell behaviors underlying notochord formation and extension in mouse embryos." Anat Rec 239(1): 103-12.

Schier, A. F. (2001). "Axis formation and patterning in zebrafish." Curr Opin Genet Dev 11(4): 393-404.

Schwarz-Romond, T., C. Asbrand, J. Bakkers, M. Kuhl, H. J. Schaeffer, J. Huelsken, J. Behrens, M. Hammerschmidt and W. Birchmeier (2002). "The ankyrin repeat protein Diversin recruits Casein kinase Iepsilon to the beta-catenin degradation complex and acts in both canonical Wnt and Wnt/JNK signaling." Genes Dev 16(16): 2073-84.

Sepich, D. S., D. C. Myers, R. Short, J. Topczewski, F. Marlow and L. Solnica-Krezel (2000). "Role of the zebrafish trilobite locus in gastrulation movements of convergence and extension." Genesis 27(4): 159-73.

Shanmugalingam, S., C. Houart, A. Picker, F. Reifers, R. Macdonald, A. Barth, K. Griffin, M. Brand and S. W. Wilson (2000). "Ace/Fgf8 is required for forebrain commissure formation and patterning of the telencephalon." Development 127(12): 2549-61.

SHAO JUN DU, S. M. P., JAN L. CHRISTIAN, L. LYNN MCGREW, and A. R. T. MOON (1995). "Identification of Distinct Classes and Functional Domains of Wnts through Expression of Wild-Type and Chimeric Proteins in Xenopus Embryos." 15,(5): 2625-2634.

Sheldahl, L. C., M. Park, C. C. Malbon and R. T. Moon (1999). "Protein kinase C is differentially stimulated by Wnt and Frizzled homologs in a G-protein-dependent manner." Curr Biol 9(13): 695-8.

Sheldahl, L. C., D. C. Slusarski, P. Pandur, J. R. Miller, M. Kuhl and R. T. Moon (2003). "Dishevelled activates Ca²⁺ flux, PKC, and CamKII in vertebrate embryos." J Cell Biol 161(4): 769-77.

Shih, J. and S. E. Fraser (1995). "Distribution of tissue progenitors within the shield region of the zebrafish gastrula." Development 121(9): 2755-65.

Shih, J. and R. Keller (1992). "Patterns of cell motility in the organizer and dorsal mesoderm of *Xenopus laevis*." Development 116(4): 915-30.

Shih, J. and R. Keller (1992). "Cell motility driving mediolateral intercalation in explants of *Xenopus laevis*." Development 116(4): 901-14.

Shima, Y., N. G. Copeland, D. J. Gilbert, N. A. Jenkins, O. Chisaka, M. Takeichi and T. Uemura (2002). "Differential expression of the seven-pass transmembrane cadherin genes *Celsr1-3* and distribution of the *Celsr2* protein during mouse development." Dev Dyn 223(3): 321-32.

Shima, Y., M. Kengaku, T. Hirano, M. Takeichi and T. Uemura (2004). "Regulation of dendritic maintenance and growth by a mammalian 7-pass transmembrane cadherin." Dev Cell 7(2): 205-16.

Shimada, Y., T. Usui, S. Yanagawa, M. Takeichi and T. Uemura (2001). "Asymmetric colocalization of Flamingo, a seven-pass transmembrane cadherin, and Dishevelled in planar cell polarization." Curr Biol 11(11): 859-63.

Simpson, J. H., T. Kidd, K. S. Bland and C. S. Goodman (2000). "Short-range and long-range guidance by slit and its Robo receptors. Robo and Robo2 play distinct roles in midline guidance." Neuron 28(3): 753-66.

Slusarski, D. C., V. G. Corces and R. T. Moon (1997). "Interaction of Wnt and a Frizzled homologue triggers G-protein-linked phosphatidylinositol signalling." Nature 390(6658): 410-3.

Slusarski, D. C., J. Yang-Snyder, W. B. Busa and R. T. Moon (1997). "Modulation of embryonic intracellular Ca²⁺ signaling by Wnt-5A." Dev Biol 182(1): 114-20.

Small, J. V. and I. Kaverina (2003). "Microtubules meet substrate adhesions to arrange cell polarity." Curr Opin Cell Biol 15(1): 40-7.

Smith, J. L., G. C. Schoenwolf and J. Quan (1994). "Quantitative analyses of neuroepithelial cell shapes during bending of the mouse neural plate." J Comp Neurol 342(1): 144-51.

Solnica-Krezel, L. and M. S. Cooper (2002). "Cellular and genetic mechanisms of convergence and extension." Results Probl Cell Differ 40: 136-65.

Solnica-Krezel, L. and W. Driever (1994). "Microtubule arrays of the zebrafish yolk cell: organization and function during epiboly." Development 120(9): 2443-55.

Solnica-Krezel, L., D. L. Stemple, E. Mountcastle-Shah, Z. Rangini, S. C. Neuhauss, J. Malicki, A. F. Schier, D. Y. Stainier, F. Zwartkruis, S. Abdelilah and W. Driever (1996). "Mutations affecting cell fates and cellular rearrangements during gastrulation in zebrafish." Development 123: 67-80.

Strahle, U. and S. Jesuthasan (1993). "Ultraviolet irradiation impairs epiboly in zebrafish embryos: evidence for a microtubule-dependent mechanism of epiboly." Development 119(3): 909-19.

Strutt, D. (2003). "Frizzled signalling and cell polarisation in Drosophila and vertebrates." Development 130(19): 4501-13.

Strutt, D., R. Johnson, K. Cooper and S. Bray (2002). "Asymmetric localization of frizzled and the determination of notch-dependent cell fate in the Drosophila eye." Curr Biol 12(10): 813-24.

Strutt, D. I. (2001). "Asymmetric localization of frizzled and the establishment of cell polarity in the Drosophila wing." Mol Cell 7(2): 367-75.

Strutt, D. I., U. Weber and M. Mlodzik (1997). "The role of RhoA in tissue polarity and Frizzled signalling." Nature 387(6630): 292-5.

Strutt, H. and D. Strutt (1999). "Polarity determination in the Drosophila eye." Curr Opin Genet Dev 9(4): 442-6.

Strutt, H. and D. Strutt (2002). "Nonautonomous planar polarity patterning in Drosophila: dishevelled-independent functions of frizzled." Dev Cell 3(6): 851-63.

Sumanas, S. and S. C. Ekker (2001). "Xenopus frizzled-5: a frizzled family member expressed exclusively in the neural retina of the developing eye." Mech Dev 103(1-2): 133-6.

Sumanas, S. and S. C. Ekker (2001). "Xenopus frizzled-7 morphant displays defects in dorsoventral patterning and convergent extension movements during gastrulation." Genesis 30(3): 119-22.

Sumanas, S., H. J. Kim, S. Hermanson and S. C. Ekker (2001). "Zebrafish frizzled-2 morphant displays defects in body axis elongation." Genesis 30(3): 114-8.

Sumanas, S., H. J. Kim, S. B. Hermanson and S. C. Ekker (2002). "Lateral line, nervous system, and maternal expression of Frizzled 7a during zebrafish embryogenesis." Mech Dev 115(1-2): 107-11.

Sumanas, S., P. Strege, J. Heasman and S. C. Ekker (2000). "The putative wnt receptor Xenopus frizzled-7 functions upstream of beta-catenin in vertebrate dorsoventral mesoderm patterning." Development 127(9): 1981-90.

Symes, K. and M. Mercola (1996). "Embryonic mesoderm cells spread in response to platelet-derived growth factor and signaling by phosphatidylinositol 3-kinase." Proc Natl Acad Sci U S A 93(18): 9641-4.

Tada, M. and M. L. Concha (2001). "Vertebrate gastrulation: calcium waves orchestrate cell movements." Curr Biol 11(12): R470-2.

Tada, M., M. L. Concha and C. P. Heisenberg (2002). "Non-canonical Wnt signalling and regulation of gastrulation movements." Semin Cell Dev Biol 13(3): 251-60.

Tada, M. and J. C. Smith (2000). "Xwnt11 is a target of Xenopus Brachyury: regulation of gastrulation movements via Dishevelled, but not through the canonical Wnt pathway." Development 127(10): 2227-38.

Takeichi, M., S. Nakagawa, S. Aono, T. Usui and T. Uemura (2000). "Patterning of cell assemblies regulated by adhesion receptors of the cadherin superfamily." Philos Trans R Soc Lond B Biol Sci 355(1399): 885-90.

Takeuchi, M., J. Nakabayashi, T. Sakaguchi, T. S. Yamamoto, H. Takahashi, H. Takeda and N. Ueno (2003). "The prickle-related gene in vertebrates is essential for gastrulation cell movements." Curr Biol 13(8): 674-9.

Tamai, K., M. Semenov, Y. Kato, R. Spokony, C. Liu, Y. Katsuyama, F. Hess, J. P. Saint-Jeannet and X. He (2000). "LDL-receptor-related proteins in Wnt signal transduction." Nature 407(6803): 530-5.

Taylor, J., N. Abramova, J. Charlton and P. N. Adler (1998). "Van Gogh: a new *Drosophila* tissue polarity gene." Genetics 150(1): 199-210.

Taylor, J. S., Y. Van de Peer, I. Braasch and A. Meyer (2001). "Comparative genomics provides evidence for an ancient genome duplication event in fish." Philos Trans R Soc Lond B Biol Sci 356(1414): 1661-79.

Theisen, H., J. Purcell, M. Bennett, D. Kansagara, A. Syed and J. L. Marsh (1994). "dishevelled is required during wingless signaling to establish both cell polarity and cell identity." Development 120(2): 347-60.

Tissir, F., O. De-Backer, A. M. Goffinet and C. Lambert de Rouvroit (2002). "Developmental expression profiles of Celsr (Flamingo) genes in the mouse." Mech Dev 112(1-2): 157-60.

Tomlinson, A. and G. Struhl (1999). "Decoding vectorial information from a gradient: sequential roles of the receptors Frizzled and Notch in establishing planar polarity in the *Drosophila* eye." Development 126(24): 5725-38.

Topczewski, J., D. S. Sepich, D. C. Myers, C. Walker, A. Amores, Z. Lele, M. Hammerschmidt, J. Postlethwait and L. Solnica-Krezel (2001). "The zebrafish glypican knypek controls cell polarity during gastrulation movements of convergent extension." Dev Cell 1(2): 251-64.

Torres, M. A., J. A. Yang-Snyder, S. M. Purcell, A. A. DeMarais, L. L. McGrew and R. T. Moon (1996). "Activities of the Wnt-1 class of secreted signaling factors are antagonized by the Wnt-5A class and by a dominant negative cadherin in early *Xenopus* development." J Cell Biol 133(5): 1123-37.

Tree DR, M. D., Axelrod JD. (2002). "A three-tiered mechanism for regulation of planar cell polarity." Semin Cell Dev Biol. 2002 Jun;13(3):217-24. 13(3): 217-24.

Trinkaus, J. P. (1996). "Ingression during early gastrulation of fundulus." Dev Biol 177(1): 356-70.

Trinkaus, J. P., M. Trinkaus and R. D. Fink (1992). "On the convergent cell movements of gastrulation in *Fundulus*." J Exp Zool 261(1): 40-61.

Uemura, T. and Y. Shimada (2003). "Breaking cellular symmetry along planar axes in *Drosophila* and vertebrates." J Biochem (Tokyo) 134(5): 625-30.

Ueno, N. and N. D. Greene (2003). "Planar cell polarity genes and neural tube closure." Birth Defects Res C Embryo Today 69(4): 318-24.

Ulrich, F., M. L. Concha, P. J. Heid, E. Voss, S. Witzel, H. Roehl, M. Tada, S. W. Wilson, R. J. Adams, D. R. Soll and C. P. Heisenberg (2003). "Slb/Wnt11 controls hypoblast cell migration and morphogenesis at the onset of zebrafish gastrulation." Development 130(22): 5375-84.

Umbhauer, M., A. Djiane, C. Goisset, A. Penzo-Mendez, J. F. Riou, J. C. Boucaut and D. L. Shi (2000). "The C-terminal cytoplasmic Lys-thr-X-X-X-Trp motif in frizzled receptors mediates Wnt/beta-catenin signalling." Embo J 19(18): 4944-54.

Unterseher, F., J. A. Hefele, K. Giehl, E. M. De Robertis, D. Wedlich and A. Schambony (2004). "Paraxial protocadherin coordinates cell polarity during convergent extension via Rho A and JNK." Embo J 23(16): 3259-69.

Usui, T., Y. Shima, Y. Shimada, S. Hirano, R. W. Burgess, T. L. Schwarz, M. Takeichi and T. Uemura (1999). "Flamingo, a seven-pass transmembrane cadherin, regulates planar cell polarity under the control of Frizzled." Cell 98(5): 585-95.

Van de Peer, Y., J. S. Taylor, I. Braasch and A. Meyer (2001). "The ghost of selection past: rates of evolution and functional divergence of anciently duplicated genes." J Mol Evol 53(4-5): 436-46.

Veeman, M. T., J. D. Axelrod and R. T. Moon (2003). "A second canon. Functions and mechanisms of beta-catenin-independent Wnt signaling." Dev Cell 5(3): 367-77.

Veeman, M. T., D. C. Slusarski, A. Kaykas, S. H. Louie and R. T. Moon (2003). "Zebrafish prickles, a modulator of noncanonical Wnt/Fz signaling, regulates gastrulation movements." Curr Biol 13(8): 680-5.

Villano, J. L. and F. N. Katz (1995). "four-jointed is required for intermediate growth in the proximal-distal axis in Drosophila." Development 121(9): 2767-77.

Vinson, C. R. and P. N. Adler (1987). "Directional non-cell autonomy and the transmission of polarity information by the frizzled gene of Drosophila." Nature 329(6139): 549-51.

Vinson, C. R., S. Conover and P. N. Adler (1989). "A Drosophila tissue polarity locus encodes a protein containing seven potential transmembrane domains." Nature 338(6212): 263-4.

Wallingford, J. B., A. J. Ewald, R. M. Harland and S. E. Fraser (2001). "Calcium signaling during convergent extension in Xenopus." Curr Biol 11(9): 652-61.

Wallingford, J. B., S. E. Fraser and R. M. Harland (2002). "Convergent extension: the molecular control of polarized cell movement during embryonic development." Dev Cell 2(6): 695-706.

Wallingford, J. B. and R. M. Harland (2001). "Xenopus Dishevelled signaling regulates both neural and mesodermal convergent extension: parallel forces elongating the body axis." Development 128(13): 2581-92.

Wallingford, J. B., B. A. Rowling, K. M. Vogeli, U. Rothbacher, S. E. Fraser and R. M. Harland (2000). "Dishevelled controls cell polarity during Xenopus gastrulation." Nature 405(6782): 81-5.

Wallingford, J. B., K. M. Vogeli and R. M. Harland (2001). "Regulation of convergent extension in Xenopus by Wnt5a and Frizzled-8 is independent of the canonical Wnt pathway." Int J Dev Biol 45(1): 225-7.

Wang, B., D. J. Lim, J. Han, Y. S. Kim, C. B. Basbaum and J. D. Li (2002). "Novel cytoplasmic proteins of nontypeable Haemophilus influenzae up-regulate human MUC5AC mucin transcription via a positive p38 mitogen-activated protein kinase pathway and a negative phosphoinositide 3-kinase-Akt pathway." J Biol Chem 277(2): 949-57.

Warga, R. M. and C. B. Kimmel (1990). "Cell movements during epiboly and gastrulation in zebrafish." Development 108(4): 569-80.

Weber, U., N. Paricio and M. Mlodzik (2000). "Jun mediates Frizzled-induced R3/R4 cell fate distinction and planar polarity determination in the Drosophila eye." Development 127(16): 3619-29.

Wedlich, D. (2002). "The polarising role of cell adhesion molecules in early development." Curr Opin Cell Biol 14(5): 563-8.

Wehrli, M., S. T. Dougan, K. Caldwell, L. O'Keefe, S. Schwartz, D. Vaizel-Ohayon, E. Schejter, A. Tomlinson and S. DiNardo (2000). "arrow encodes an LDL-receptor-related protein essential for Wingless signalling." Nature 407(6803): 527-30.

Weiner, O. D., P. O. Nielsen, G. D. Prestwich, M. W. Kirschner, L. C. Cantley and H. R. Bourne (2002). "A PtdInsP(3)- and Rho GTPase-mediated positive feedback loop regulates neutrophil polarity." Nat Cell Biol 4(7): 509-13.

Westerfield, M. (1993). "The Zebrafish Book: A guide for laboratory use of zebrafish".

Westfall, T. A., R. Brimeyer, J. Twedt, J. Gladon, A. Olberding, M. Furutani-Seiki and D. C. Slusarski (2003). "Wnt-5/pipetail functions in vertebrate axis formation as a negative regulator of Wnt/beta-catenin activity." J Cell Biol 162(5): 889-98.

Westfall, T. A., B. Hjertos and D. C. Slusarski (2003). "Requirement for intracellular calcium modulation in zebrafish dorsal-ventral patterning." Dev Biol 259(2): 380-91.

Wilson, P. and R. Keller (1991). "Cell rearrangement during gastrulation of *Xenopus*: direct observation of cultured explants." Development 112(1): 289-300.

Wilson, P. A., G. Oster and R. Keller (1989). "Cell rearrangement and segmentation in *Xenopus*: direct observation of cultured explants." Development 105(1): 155-66.

Winklbauer, R., A. Medina, R. K. Swain and H. Steinbeisser (2001). "Frizzled-7 signalling controls tissue separation during *Xenopus* gastrulation." Nature 413(6858): 856-60.

Winter, C. G., B. Wang, A. Ballew, A. Royou, R. Karess, J. D. Axelrod and L. Luo (2001). "*Drosophila* Rho-associated kinase (Drok) links Frizzled-mediated planar cell polarity signaling to the actin cytoskeleton." Cell 105(1): 81-91.

Wodarz, A. and R. Nusse (1998). "Mechanisms of Wnt signaling in development." Annu Rev Cell Dev Biol 14: 59-88.

Wolff, T. and G. M. Rubin (1998). "Strabismus, a novel gene that regulates tissue polarity and cell fate decisions in *Drosophila*." Development 125(6): 1149-59.

- Wong, G. T., B. J. Gavin and A. P. McMahon (1994). "Differential transformation of mammary epithelial cells by Wnt genes." Mol Cell Biol 14(9): 6278-86.
- Wu, Q. and T. Maniatis (2000). "Large exons encoding multiple ectodomains are a characteristic feature of protocadherin genes." Proc Natl Acad Sci U S A 97(7): 3124-9.
- Wunnenberg-Stapleton, K., I. L. Blitz, C. Hashimoto and K. W. Cho (1999). "Involvement of the small GTPases XRhoA and XRnd1 in cell adhesion and head formation in early *Xenopus* development." Development 126(23): 5339-51.
- Yamamoto, A., S. L. Amacher, S. H. Kim, D. Geissert, C. B. Kimmel and E. M. De Robertis (1998). "Zebrafish paraxial protocadherin is a downstream target of spadetail involved in morphogenesis of gastrula mesoderm." Development 125(17): 3389-97.
- Yamanaka, H., T. Moriguchi, N. Masuyama, M. Kusakabe, H. Hanafusa, R. Takada, S. Takada and E. Nishida (2002). "JNK functions in the non-canonical Wnt pathway to regulate convergent extension movements in vertebrates." EMBO Rep 3(1): 69-75.
- Yamashita, S., C. Miyagi, A. Carmany-Rampey, T. Shimizu, R. Fujii, A. F. Schier and T. Hirano (2002). "Stat3 Controls Cell Movements during Zebrafish Gastrulation." Dev Cell 2(3): 363-75.
- Yamashita, S., C. Miyagi, T. Fukada, N. Kagara, Y. S. Che and T. Hirano (2004). "Zinc transporter LIVI controls epithelial-mesenchymal transition in zebrafish gastrula organizer." Nature 429(6989): 298-302.
- Yan, D., J. B. Wallingford, T. Q. Sun, A. M. Nelson, C. Sakanaka, C. Reinhard, R. M. Harland, W. J. Fantl and L. T. Williams (2001). "Cell autonomous regulation of multiple Dishevelled-dependent pathways by mammalian Nkd." Proc Natl Acad Sci U S A 98(7): 3802-7.

Yeo, S. Y., M. H. Little, T. Yamada, T. Miyashita, M. C. Halloran, J. Y. Kuwada, T. L. Huh and H. Okamoto (2001). "Overexpression of a slit homologue impairs convergent extension of the mesoderm and causes cyclopia in embryonic zebrafish." Dev Biol 230(1): 1-17.

Yoshikawa, S., R. D. McKinnon, M. Kokel and J. B. Thomas (2003). "Wnt-mediated axon guidance via the Drosophila Derailed receptor." Nature 422(6932): 583-8.

Zalik, S. E., E. Lewandowski, Z. Kam and B. Geiger (1999). "Cell adhesion and the actin cytoskeleton of the enveloping layer in the zebrafish embryo during epiboly." Biochem Cell Biol 77(6): 527-42.

Zeidler, M. P., N. Perrimon and D. I. Strutt (1999). "The four-jointed gene is required in the Drosophila eye for ommatidial polarity specification." Curr Biol 9(23): 1363-72.

Zeidler, M. P., N. Perrimon and D. I. Strutt (2000). "Multiple roles for four-jointed in planar polarity and limb patterning." Dev Biol 228(2): 181-96.

Zheng, L., J. Zhang and R. W. Carthew (1995). "frizzled regulates mirror-symmetric pattern formation in the Drosophila eye." Development 121(9): 3045-55.